INFORMATION TO USERS

This manuscript has been reproduced from the microfilm master. UMI films the text directly from the original or copy submitted. Thus, some thesis and dissertation copies are in typewriter face, while others may be from any type of computer printer.

The quality of this reproduction is dependent upon the quality of the copy submitted. Broken or indistinct print, colored or poor quality illustrations and photographs, print bleedthrough, substandard margins, and improper alignment can adversely affect reproduction.

In the unlikely event that the author did not send UMI a complete manuscript and there are missing pages, these will be noted. Also, if unauthorized copyright material had to be removed, a note will indicate the deletion.

Oversize materials (e.g., maps, drawings, charts) are reproduced by sectioning the original, beginning at the upper left-hand corner and continuing from left to right in equal sections with small overlaps. Each original is also photographed in one exposure and is included in reduced form at the back of the book.

Photographs included in the original manuscript have been reproduced xerographically in this copy. Higher quality 6" x 9" black and white photographic prints are available for any photographs or illustrations appearing in this copy for an additional charge. Contact UMI directly to order.

UMI

A Bell & Howell Information Company
300 North Zeeb Road, Ann Arbor MI 48106-1346 USA
313/761-4700 800/521-0600

Expression of the mRNA Encoding VGF, a Neural-Specific Peptide Precursor, in the Developing and Adult Rat Central Nervous Systems, and its Modulation in Response to Changes in Neuronal Electrical Activity, Seizure, and Lesion

by

Susan Elizabeth Snyder

A dissertation submitted to the Graduate Faculty in Biomedical Sciences
in partial fulfillment of the requirements for the degree of Doctor of Philosophy,
The City University of New York

1996

UMI Number: 9630509

UMI
300 North Zeeb Road
Ann Arbor, MI 48103

This manuscript has been read and accepted by the Graduate Faculty in Biomedical Sciences in satisfaction of the dissertation requirement for the degree of Doctor of Philosophy.

4/26/96
Date

J. L. Roberts
James L. Roberts, Ph.D.,
Chair of Examining Committee

4/26/96
Date

Terry Ann Krulwich, Ph.D.,
Executive Officer

4/26/96
Date

Stephen R. J. Salton, M.D., Ph.D.,
Thesis Advisor

Mariann Blum, Ph.D.
Victor A. Friedrich, Jr., Ph.D.
John E. Pintar, Ph.D.
James L. Roberts, Ph.D.
Stephen R. J. Salton, M.D., Ph.D.

Supervisory Committee

The City University of New York

Abstract

Expression of the mRNA Encoding VGF, a Neural-Specific Peptide Precursor,
in the Developing and Adult Rat Central Nervous Systems, and its Modulation
in Response to Changes in Neuronal Electrical Activity, Seizure, and Lesion

by

Susan Elizabeth Snyder

Advisor: Stephen R. J. Salton, M.D., Ph.D.

VGF is the non-acronymous name of a peptide precursor expressed by neurons and neuroendocrine cells, whose transcription and secretion are rapidly induced by neurotrophins and by depolarization. To gain insight into the possible functions and regulation of VGF *in vivo*, this study characterizes the distribution of VGF mRNA in the developing and mature rat central nervous system, compares it to the distributions of mRNAs encoding the Trk neurotrophin receptors, and describes its modulation in response to perturbation of neuronal electrical activity, seizure, and lesion.

VGF expression was first detectable at embryonic day 11.5 in the primordia of cranial, sympathetic, and dorsal root ganglia, and its distribution expanded throughout development to include significant expression throughout the brain and spinal cord of the adult rat. VGF mRNA levels are particularly high during critical developmental periods in many regions of the nervous system. Significant overlap between VGF and various *trk* mRNAs was observed, and though no *trk* mRNA exclusively colocalized with VGF message, good correlation was found between the distributions of the VGF and *trk*B kinase mRNAs, implying that activation of TrkB may account for much VGF expression.

Furthermore, we have shown that VGF mRNA is regulated in the CNS by manipulations affecting neuronal activity and by lesion. Inhibition of retinal electrical activity during the visual critical period rapidly repressed VGF mRNA in the lateral geniculate. In the adult, kainate-induced seizures up-regulated VGF in dentate granule cells, hippocampal pyramidal cells, and cortex within hours. Direct cortical lesion produced rapid, complex changes in VGF expression, including strong induction in ipsilateral cortex, and deep repression in the deafferented ipsilateral striatum. Days later, following normalization of cortical VGF expression, we observed delayed induction of VGF mRNA in a striatal region where compensatory cortical sprouting occurs. Taken together these observations strongly suggest that in addition to a likely role in the mediation of neurotrophin effects, VGF or the peptides derived from it may also play a critical role in the synaptogenesis and synaptic reorganization which often result from changing afferent input during development and in the adult, in both physiological and pathological conditions.

To my mother,
Ruth Lewit Snyder,
with love

Acknowledgments

My deepest thanks must go to my dissertation advisor and mentor, Steven R. J. Salton. It has been a pleasure to be his first official student. Steve has an amazing wealth of knowledge, bench hands he still keeps in peak condition, and he's consistently sweet, kind, easy-going, supportive and fun. In short, he's pretty much an angel of an advisor—and so I second the motion that he really deserved that Pew. Thanks x 10^6 for everything Steve—I could *never* have done it without you.

My profuse gratitude is also richly deserved by the following people:

— Victor Friedrich, for his invaluable advice and tireless support on all fronts, without which I would never have been able to complete this degree, and for his genuine sweetness, brilliant sense of humor, and sparkling enthusiasm for science and life which have greatly enriched mine during these years;

— Jim Roberts, for his caring, steady support, encouragement and guidance through all of my ups and downs, and for his incredible barbeques;

— Mariann Blum, John Pintar, Kevin Kelley, and Klaudiusz Weiss for serving on my advisory committees and for their helpful feedback and friendly support throughout this project;

— Randy Streck, who taught me how to do *in situ* hybridization, the backbone of my entire thesis project;

— Henri Tiedge who taught me how to dip slides, helped me troubleshoot my protocols when nothing was working, provided stimulating late-night conversation in the lab, and took me Rollerblading to get some fresh air;

— Patrick Hof for tirelessly helping me with neuroanatomy, making important new papers magically appear on my desk before the library even had the journals, his masterful impressions, and warm support.

I heartily thank Paul Isackson, Karl Murray, Tom McNeill, and Cheng Heng-Wei, our collaborators, for their generous gifts of the seized and lesioned brains described in Chapter 5, and for critical reading of the manuscript resulting from my work on their animals.

I also owe much to several people who have served as role models and mentors *extraordinaire*, and have been my sources of inspiration for many years: Bob Desnick who kindled my interest in science and medicine; Ivan Lieberburg who breathed life into that spark; and Kurt Hirschhorn for showing me the brilliance with which one can burn, and being an unwavering source of professional and personal support and advice. I owe a particular debt of thanks to Terry Krulwich for her steady example, and for helping me to burn my candle at both ends without raging out of control or burning out altogether.

Many thanks to my dear friends Diana Casper, Yasodha Natkunam, and Josina Reddy, and to Anne Wang for helpful discussions, moral support, warm hugs, and being generally wonderful. Also to Konstantinos Andrikopoulos, Jen Coleman, Shari Dermer, Jesse Eisler, Greg Elder, Tony Geraci, Seung Hahm, John LaPolla, Li Ji, Dominique Lorang, Esther Nimchinsky, Phil San Filippo, Cyndi Shannon Weickert, Steve Siegel, Peter Werner, and Tracy Yeo, for contributing fun, understanding, and relative sanity to life in lab. To all other past and present members of the Salton Lab and Fishberg Center who contributed in a positive way to the Fishberg atmosphere, many thanks. And to my "siblings" in all of this pleasure and pain—Josh Berman, Tony deBeus, Waldo Feng, David Friedland, Yasodha Natkunam, and Dave Naylor—my deepest appreciation for years of camaraderie, heartiest congratulations on all of your successes, and most sincere wishes for happy and productive futures for you all.

To Jason Banfelder, whose support, encouragement, hugs, laughter, and unconditional love got me through the homestretch, and who finally gets bragging rights.

To my parents, Ruth and Clif Snyder, who each gave me the best of themselves, as well as every opportunity and all the love any child could ever want.

To my big brothers, Rob and Jon Snyder, and Andy Beim, and my sister-in-law Sharon, who have stood by me through it all, and my wonderful new family: my stepmother, Ruth Dorner Snyder; and my new siblings, Dan Dorner, Lisa Black, and Michael Dorner, and their families, for their warmth and love.

And finally, to the memories of two Marthas—Lehman and Graham—exceptional women who profoundly and irreversibly influenced my life and work with the extraordinary wisdom of their words and actions, and the simple beauty of all they created.

Thank you all so much.

I must also heartily thank the Upjohn Company—for without innumerable doses of their product, Dramamine® (Non-Drowsy Formula), to get me through dipping slides in total darkness and many hours of microscopy, these projects could absolutely never have been completed.

This work was funded by grants from the National Institutes of Health (GM 41227 & AG 10676), The Dysautonomia Foundation and The American Paralysis Association, and Pew Memorial Trust Scholar and Irma T. Hirschl Career Scientist Awards to Stephen R. J. Salton, M.D., Ph.D.

...I believe that we learn by practice. Whether it means to learn to dance by practicing dancing or to learn to live by practicing living, the principles are the same. In each it is the performance of a dedicated precise set of acts, physical or intellectual, from which comes shape of achievement, a sense of one's being, a satisfaction of spirit.

— Martha Graham

Format of Dissertation

This dissertation was prepared in accordance with the guidelines of The City University of New York. The paper begins with a general introduction, ends with general conclusions, and includes chapter-specific introductions and discussions as appropriate. To avoid redundancy the "Methods and Materials" and "References" have been consolidated.

Some of the data in Chapters 4 and 5 have been presented in preliminary form at the 22nd and 25th Annual Meetings of the Society for Neuroscience, and Chapter 5 contains results which have been submitted to **The Journal of Neuroscience.**

Table of Contents

List of Figures

Abbreviations

1-10	layers of the spinal cord gray matter
3v	third ventricle
4v	fourth ventricle
α	α-motor neuron
AAs	amino acids
Acc. #	Accession number
Ad	adrenal
AD	anterodorsal nucleus of the thalamus
ADP	anterodorsal preoptic nucleus of the hypothalamus
aFGF	acidic fibroblast growth factor
Ah	Ammon's horn
AHN	anterior hypothalamic nuclei
Ah ne	Ammon's horn neuroepithelium
Am	amygdala
AM	anteromedial nucleus of the thalamus
ANOVA	analysis of variance
AntThal	anterior thalamic nuclei
AOB	accessory olfactory bulb
AON	anterior olfactory nucleus
APN	anterior pretectal nucleus
aPont ne	anterior pontine neuro-epithelium
ARH	arcuate nucleus
AV	anteroventral nucleus of the thalamus
AVP	anteroventral preoptic nucleus of the hypothalamus
AVPV	anteroventral periventricular nucleus of the hypothalamus
BDNF	brain-derived neurotrophic factor
bFGF	basic fibroblast growth factor
BG	basal ganglia
Br	bronchus
bs	brainstem
BSA	bovine serum albumin
BST	basal nucleus of the stria terminalis
Cb	cerebellum
CDF	cholinergic differentiation factor
Cb Cx	cerebellar cortex
Cb n	deep cerebellar nuclei
CL	centrolateral nucleus of the thalamus
CM	centromedian nucleus of the thalamus
CNS	central nervous system
CNTF	ciliary neurotrophic factor
CPu	caudoputamen
CREB	cAMP response element binding protein
ctz	cortical transitory zone
Cx	cortex
d	dorsal
dcs	dorsal corticospinal tract
DEPC-dH$_2$O	diethylpyrocarbonate-treated deionized water
Derm	dermis
dh	dorsal horn
dH$_2$O	deionized water
DG	dentate gyrus
Di	diencephalon
dLGN	dorsal lateral geniculate nucleus of the thalamus
dmH	dorsomedial hypothalamus
DNA	deoxyribonucleic acid
DNase	deoxyribonuclease
d.p.i.	dots per inch
DRG	dorsal root ganglion
Drk	nucleus of Darkschewitsch
dtg	dorsal tegmentum
DTT	dithiothreitol
E#	embryonic day #
ec	external capsule
EDTA	ethylenediaminetetraacetic acid
EGF	epidermal growth factor
EGL	external germinal layer
Ent Cx	entorhinal cortex
Epi	epidermis
EPL	external plexiform layer
Es	esophagus
E-W	Edinger-Westphal nuclei
fb	forebrain
FF	fields of Forel

FN	fastigial nucleus
Fr Cx	frontal cortex
fx	fornix
GaCL	ganglion cell layer
GAP-43	growth associated protein-43
GCL	granule cell layer
Gl	glandular portion of the stomach
Glom	glomerular layer
GP	globus pallidus
Gr	nucleus gracilis
GrL	granular layer
GT	germinal trigone
H	hypothalamus
hdb	horizontal limb of the nucleus of the diagonal band
hi	hilus
Hippo	hippocampus
HPLC-dH_2O	high performance liquid chromatography -grade water
hsDNA	herring sperm DNA
IAM	interanteromedial nucleus of the thalamus
IC	inferior colliculus
ic	internal capsule
ica	internal carotid artery
IGF-I	insulin-like growth factor I
IGF-II	insulin-like growth factor II
igl	intergeniculate leaflet
IGL	internal granular layer
III	oculomotor nuclei
IL-6	interleukin-6
INL	inner nuclear layer
IO	inferior olive
i.p.	intraperitoneal
IPL	internal plexiform layer
IPN	interpeduncular nucleus
IS	inner segments of photoreceptors
IV	trochlear nuclei
IXi	inferior ganglion of the glosso-pharyngeal nerve
IXs	superior ganglion of the glosso-pharyngeal nerve
izh	intermediate zone of the hippocampus
K	kidney
kb	kilobase(s)
kD	kiloDalton(s)
L	liver
LA	left atrium
LCer	lateral cervical nucleus
LD	latero-dorsal nucleus of the thalamus
lf	lateral funiculus
LP	lateral posterior nucleus of the thalamus
LS	lateral septum
LSp	lateral spinal nucleus
LV	lateral ventricle
LVh	left ventricle of the heart
Mb	midbrain
Md	medulla
MD	mediodorsal nucleus of the thalamus
MDF	muscle-derived differentiation factor
Me	mesencephalon
MGN	medial geniculate nucleus
mh	medial habenula
Mi	mitral cell layer
Mol	molecular layer
MRN	mesencephalic reticular nucleus
mRNA	messenger RNA
MS	medial septum
mVe	medial vestibular nucleus
nAc	nucleus accumbens
nbM	nucleus basalis magnocellularis
ne	neuroepithelium
NGF	nerve growth factor
NILE	NGF-inducible large external glycoprotein
non-Gl	non-glandular portion of the stomach
nt	neural tube
NT-3	neurotrophin-3
NT-4/5	neurotrophin-4/5
NT-6	neurotrophin-6
ntSol	nucleus of the tractus solitarius
ntz	nuclear transitory zone
nVII	facial nucleus
nX	vagal nucleus
nXII	hypoglossal nucleus
o/i Cx	orbital and insular cortex

ob	olfactory bulb
Oc Cx	occipital cortex
OlfN	olfactory nerve layer
olf ne	neuroepithelium of the olfactory bulb
olf svz	subventricular zone of the olfactory bulb
olf v	olfactory bulb portion of the lateral ventricle
ONL	outer nuclear layer
OT	olfactory tubercle
Otic	otic ganglion
P#	postnatal day #
$p75^{NTR}$	the p75 neurotrophin receptor
Pa	pancreas
pa	pars anterior
PaG	periaqueductal gray
PAGE	polyacrylamide gel electrophoresis
Par Cx	parietal cortex
ParaS	parasubiculum
PBS	phosphate buffered saline
pd	pars distalis
PF	parafascicular nucleus of the thalamus
PH	posterior hypothalamus
pi	pars intermedia
pig	pigment epithelium
Pir Cx	piriform cortex
pit	pituitary
Pkj	Purkinje cells
PMCo	posteromedial cortical amygdaloid nucleus
pn	pars nervosa
PNS	peripheral nervous system
pnV	principal nucleus of the trigeminal
Po	pons
Po n	pontine nuclei
POA	preoptic area
PoT	posterior thalamic nucleus
PP	peripeduncular nucleus
PPN	pedunculopontine nucleus
PPT	posterior pretectal nucleus
PR	perireuniens nucleus of the thalamus
Prep	nucleus prepositus
PreS	presubiculum
PreT	pretectum
PS	parastrial nucleus of the hypothalamus
PSCH	suprachiasmatic preoptic nucleus of the hypothalamus
pt	pars tuberalis
PT	the paratenial nucleus of the thalamus
PVi	intermediate periventricular nucleus of the hypothalamus
pvn	paraventricular nucleus of the thalamus
PVp	posterior periventricular nucleus of the hypothalamus
PVP	polyvinylpyrrolidine
PVpo	preoptic periventricular nucleus of the hypothalamus
R	retina
RA	right atrium
Re	reuniens nucleus of the thalamus
Rf	reticular formation
Rh	rhomboid nucleus of the thalamus
RNA	ribonucleic acid
RNase	ribonuclease
Rp	Rathke's pouch
RR	retrorubral fields
RS	retrosplenial cortex
Rt	reticular thalamic nucleus
S	septum
SC	superior colliculus
SCG	superior cervical ganglion
SCN	suprachiasmatic nucleus
SDS	sodium dodecyl sulfate
SEM	standard error of the mean
SEZ	subependymal zone
sfo	subfornical organ
sg	stratum granulosum
SI	substantia innominata
slm	stratum lacunosum-moleculare
slu	stratum lucidum
SM	submedial (gelatinosus) nucleus of the thalamus
SmI	small intestine
SN	substantia nigra

so	stratum oriens
SO	superior olive
SON	supraoptic nucleus
sp	stratum pyramidale
SpC	spinal cord
SPF	subparafascicular nucleus
spV	spinal trigeminal nucleus
spVe	spinal vestibular nucleus
sr	stratum radiatum
SRE	serum response element
SSC	sodium citrate solution
St	stomach
STN	subthalamic nucleus
Str	striatum
Sub	subiculum
SubM	submandibular gland
Symp	sympathetic chain/ganglion
Te	telencephalon
Te Cx	temporal cortex
Th	thalamus
TNF	tumor necrosis factor
To	tongue
TriG	trigeminal ganglion
tRNA	transfer RNA
TSH-β	thyroid stimulating hormone-β
TTX	tetrodotoxin
V	trigeminal ganglion
v	ventral
VAL	ventral antero-lateral complex of the thalamus
vdb	vertical limb of the nucleus of the diagonal band
Vert	vertebrae
vf	ventral funiculus
VGF	the non-acronymous arbitrary name of the gene product discussed herein
vh	ventral horn
VI	abducens nucleus
VII	facial ganglion
VIII	vestibulocochlear ganglion
Vit	vitreous
vLGN	ventral lateral geniculate nucleus of the thalamus
VM	ventromedial nucleus of the thalamus
vmH	ventromedial hypothalamus
VPL	ventroposterolateral nucleus of the thalamus
VPM	ventroposteromedial nucleus of the thalamus
vz	ventricular zone
wm	white matter
X	vagal ganglion
X-XIs	superior ganglion of the vagus-cranial accessory ganglion complex
Xi	inferior ganglion of the vagus nerve
XI n	cranial accessory nerve
Xs	superior ganglion of the vagus nerve
ZI	zona incerta

Chapter 1: Introduction

The neurotrophins and their receptors

Early in embryogenesis a small group of cells separates itself from the dorsal edge of the forming neural tube. This region, the neural crest, gives rise to a number of mature cell types including melanocytes, some facial bones, a subset of sensory neurons, and a common progenitor cell from which are derived both the sympathetic neurons and the cells of the adrenal medulla (Landis and Patterson 1981). It has been shown both *in vivo* and *in vitro* that the fate chosen by these sympathoadrenal stem cells depends upon the environmental cues to which they are exposed (LeDouarin 1980). Exposure of these progenitors to glucocorticoids produces differentiated adrenal chromaffin cells, whereas nerve growth factor (NGF) promotes neuronal differentiation (Aloe and Levi-Montalcini 1979; Doupe *et al.* 1985).

NGF was discovered over forty years ago when Rita Levi-Montalcini, working with Viktor Hamburger, noticed that a soluble factor produced by a mouse sarcoma was extremely effective at promoting the outgrowth of neuronal processes from sensory and sympathetic ganglia both *in vivo* and in explant culture (Levi-Montalcini and Hamburger 1951; Levi-Montalcini *et al.* 1954). In the years that followed, NGF was purified and shown in numerous studies to be essential for the normal development and maintenance of sympathetic and most neural crest-derived sensory neurons (Levi-Montalcini and Angeletti 1963; Chun and Patterson 1977a,b,c; Greene 1977a,b). A dramatic illustration of this requirement is the near-total loss of the dorsal root and sympathetic chain ganglia produced by treatment of developing animals with antisera raised against NGF (Levi-Montalcini and Booker 1960; Levi-Montalcini and Angeletti 1966; Gorin and Johnson 1979; Johnson *et al.* 1980). Recent work has further substantiated these classic studies with the finding that mice with homozygous null mutations of the NGF gene also have massively reduced numbers of sympathetic and sensory neurons, resulting in particularly severe phenotypic deficits in nociception and thermoception (Crowley *et al.* 1994). A secondary phenotype including fur loss, cutaneous ulceration, loss of digits, and corneal opacification then results from the animals' inability to detect and thereby evade noxious stimuli.

Since the discovery of NGF, a large body of work has supported a concept known as the Neurotrophic Theory—that the normal formation and maintenance of the nervous system in general is highly dependent upon the competition among neurons for limited supplies of NGF and other related target-derived neurotrophic factors which allow them to evade normal developmental cell death, and which support neuronal differentiation and process outgrowth. These neurotrophic growth factors exert their effects by binding to specific cell surface receptors. In the case of NGF, there are two known types of receptors: a tyrosine kinase receptor known as Trk or TrkA, was identified as a major receptor for NGF in 1991 (Kaplan *et al.* 1991a,b; Klein *et al.* 1991a), and alone is sufficient to transduce an NGF signal into the cell and produce a physiological response (Ip *et al.* 1993); the other receptor, identified earlier, is the p75 neurotrophin receptor ($p75^{NTR}$), often referred to as the low-affinity receptor. This name is misleading, however, as recent experiments have shown that when $p75^{NTR}$ is co-expressed with TrkA, the two molecules physically interact, forming high-affinity NGF binding sites by increasing the association rate of NGF and TrkA (Chao and Hempstead 1995; Wolf *et al.* 1995).

The Trk receptors each contain cell adhesion-related leucine-rich motifs and immunoglobulin-like domains extracellularly, a single transmembrane domain, and a pair of intracellular tyrosine kinase domains. Their activation is dependent upon ligand-mediated receptor oligomerization and auto-phosphorylation of intracellular tyrosine residues (Schlessinger and Ullrich 1992). The subsequent binding of SH2 domains of specific cytoplasmic enzymes and adaptor molecules to the phosphotyrosine residues initiates a cascade of signaling events including the Ras-Raf pathway, leading to the prolonged activation of MAP kinase (Heumann 1994).

Data are rapidly accumulating which suggest that the participation of the second receptor, $p75^{NTR}$, is not limited to modulation of the ligand-binding affinity and dose responsiveness of Trk, but may itself be an effector molecule, activating its own second messenger pathways. Several lines of evidence point to a role for $p75^{NTR}$ in regulating neuronal survival: it is part of the tumor necrosis factor (TNF) receptor family and shares with these proteins a domain known to be involved in cell death; it appears to actively induce apoptosis when not bound by a ligand (Rabizadeh *et al.* 1993); like the TNF receptor, it is able to activate sphingomyelinase thus increasing intracellular ceramide, which in turn is able to activate a specific kinase that leads to activation of the transcription factor NFκB (Dubrowsky *et al.* 1994); and finally, recent work by Brugg *et al.* (1996) has shown that ceramide causes apoptotic cell death in mature cultured mesencephalic dopamine neurons in a dose-dependent fashion. Recently, work in cultured cells lines has suggested that neurotrophin-activated Trk can inhibit neurotrophin-activated $p75^{NTR}$-induced sphingomyelin hydrolysis, introducing another layer of regulation of neurotrophin effects on the cell (Dubrowsky *et al.* 1995).

NGF and its receptors are present not only in the peripheral nervous system (PNS) but also in discrete populations of cells in the brain at critical times during neurogenesis and in the adult, and thus most likely play an important role in the normal development and function of portions of the central nervous system (CNS) as well as the PNS. A primary central role of NGF is in the septohippocampal system where NGF receptors are found on cells of the cholinergic nuclei of the basal forebrain, and NGF is produced by their target cells in the pyramidal layer of the hippocampus. The septal cells respond vigorously to NGF *in vitro* (Knüsel *et al.* 1990), and NGF can prevent the loss of these neurons following axotomy (Koliatsos *et al.* 1990, 1991; Tuszynski *et al.* 1990). Cholinergic neurons in the striatum respond to NGF as well (Johnston *et al.* 1987).

In the past decade, it has been shown that unlike the majority of neural crest-derived sensory neurons, those derived from ectodermal placodes (such as the cells of the petrosal and nodose ganglia) do not require NGF for their development or maintenance. However, many of the placode-derived sensory neurons are supported by a closely related protein, brain-derived neurotrophic factor (BDNF) (Lindsay *et al.* 1985). BDNF is also able to support or promote the differentiation of many of the neural crest-derived neurons which are not responsive to NGF, such as those of the mesencephalic nucleus of the trigeminal nerve (Davies *et al.* 1986), as well as neurons of the vestibular and spiral ganglia (Ernfors *et al.* 1994a; Zheng *et al.* 1995), motor neurons (Yan *et al.* 1993), cerebellar granule cells (Gao *et al.* 1995), cholinergic neurons of the basal forebrain, mesencephalic dopamine neurons (Knüsel *et al.* 1991), retinal ganglion cells (Johnson *et al.* 1986), striatal calbindin-positive and GABAergic neurons (Ventimiglia *et al.* 1995), and a subset of dorsal root ganglion (DRG) neurons among others. Mice homozygous for a null mutation in the BDNF gene experience a loss of sensory neurons responsive to tactile stimuli, and a number of neurochemical changes in their brains (Ernfors *et al.* 1994a; Jones *et al.* 1994).

Neurotrophin-3 (NT-3), another member of this family of growth factors known as the neurotrophins, has been shown to exert trophic effects on cells of the trigeminal mesencephalic nucleus, noradrenergic neurons of the locus coeruleus, motor neurons, calbindin-expressing hippocampal neurons, striatal calbindin-positive and GABAergic neurons, proprioceptive neurons of the dorsal root ganglia, nodose, and developing sympathetic ganglia (Hohn *et al.* 1990; Maisonpierre *et al.* 1990; Hyman *et al.* 1991; Arenas and Persson 1994; Ventimiglia *et al.* 1995). Mice with a targeted disruption of the NT-3 gene lack proprioceptive afferents and show severe neurological dysfunction (Ernfors *et al.* 1994b; Tessarollo *et al.* 1994).

Neurotrophin-4 was discovered in *Xenopus* ovaries (Hallböök *et al.* 1991), and later shown to be the frog homologue of mammalian neurotrophin-5 (Berkemeier *et al.* 1991). This factor, now commonly referred to as NT-4/5, has been shown to support sensory and sympathetic neurons, motor neurons, spiral ganglion neurons, mesencephalic dopamine neurons, striatal calbindin-positive and GABAergic neurons, and cerebellar granule cells in culture, and seems to be required for the development of nodose and petrosal neurons *in vivo,* as null mutants have deficits in these ganglia (Hynes *et al.* 1994; Koliatsos *et al.* 1994; Conover *et al.* 1995; Gao *et al.* 1995; Ventimiglia *et al.* 1995; Zheng *et al.* 1995).

Additionally, in 1994 another member of this family was discovered in zebrafish and named neurotrophin-6 (Gotz *et al.* 1994). It is somewhat different from the other neurotrophins in that it is found bound to heparin-binding molecules on the cell surface and/or extracellular matrix. It has weak but NGF-like trophic actions on chick sensory and sympathetic neurons and is expressed in the embryonic cerebellar homologue and some adult tissues. Other details of its effects and distribution remain unknown. It seems likely that like the other four neurotrophins, it may have distinct effects in the nervous system.

Like NGF, these other neurotrophins exert their effects through two cell surface receptors: a Trk tyrosine kinase receptor and $p75^{NTR}$. As NGF binds the TrkA receptor, so BDNF and NT-3 bind the related tyrosine kinase receptors TrkB and TrkC, respectively (Klein *et al.* 1991b; Lamballe *et al.* 1991; Soppet *et al.* 1991; Squinto *et al.* 1991). Under certain conditions, such as in the absence of the $p75^{NTR}$, NT-3 is also able to bind to TrkA and TrkB, although with lower affinity than do NGF and BDNF (Ip *et al.* 1993). The primary tyrosine kinase receptor for NT-4/5 seems to be TrkB, although it too can bind TrkA under some circumstances (Berkemeier *et al.* 1991; Klein *et al.* 1992). Additionally, there exist truncated variants of Trks B and C which lack the intracellular tyrosine kinase signaling domains. Little information is available regarding the possible functions of these isoforms, although roles in dominant negative inhibition of Trk signaling, neurotrophin presentation, and cell adhesion have been proposed (Jelsma and Aguayo 1994). Lastly, all four of these neurotrophins bind the $p75^{NTR}$ with similar affinities. Nothing, however, is yet known about the binding properties of NT-6.

As might be predicted from the overlapping ligand-binding properties of the Trk receptors, mice lacking these receptors tend to exhibit somewhat more severe phenotypes than mice lacking the neurotrophins themselves, in which remaining neurotrophins may be able to partially compensate for the loss of other factors. For example, the TrkB knockout mouse suffers not only a sensory deficit like the BDNF mutant, but also has motor neuron loss, which is not seen in NT-4/5 or combined BDNF/NT-4/5 knockout mice (Klein*et al.* 1993; Conover *et al.* 1995; Liu *et al.* 1995). Thus it appears that another neurotrophin, perhaps NT-3, is able to support the TrkB expressing motor neurons in the absence of these factors, while disruption of the receptor gene itself renders BDNF, NT-4/5, and the compensatory factor ineffectual. Yet the phenotypes of the TrkB and TrkC null mutants are quite mild with respect to the brain; they produce no gross neuroanatomical brain defects and few obvious neurochemical ones (Klein *et al.* 1993, 1994). While TrkA expression in the brain is primarily restricted to basal forebrain and striatal cholinergic neurons, TrkB and TrkC exhibit widespread patterns of expression, so perhaps, though important to many neuronal populations, they may be able to compensate for one another to some extent. Interestingly, homozygous p75^{NTR} null mutants display a loss of sensory neurons and specific portions of the sympathetic innervation, reflecting their decreased sensitivity to neurotrophins and perhaps abnormal neurotrophin/Trk specificity (Lee *et al.* 1992, 1994a,b; Chao 1994). They also exhibit specific deficits in the retrograde transport of the TrkB-binding neurotrophins (Curtis *et al.* 1995).

As understanding of the remarkable effects neurotrophins exert on nervous system development has increased, great interest has arisen in the possibility that these substances may play a pivotal role not only in the etiology and possible treatments of developmental disorders of the nervous system, but also in neurodegenerative disease, and in traumatic, toxic, and ischemic injury. Indeed, many studies have shown neuroprotective and neuroregenerative effects of exogenously applied neurotrophins in experimental injury, excitotoxic, and ischemic paradigms (Lindvall *et al.* 1994). Moreover, recent evidence implies that endogenous neurotrophins may normally subserve these functions. For example, cell populations particularly resistant to excitotoxic and ischemic damage, such as dentate granule cells, tend to express much higher basal levels of neurotrophins and their receptors, and respond to such insults with more substantial changes in the levels of these substances than do more vulnerable neurons (Lindvall *et al.* 1994). Furthermore, mild ischemia or seizure, which induce neurotrophin and Trk up-regulation, can protect neurons against a subsequent ischemic or epileptogenic stimulus which without such "pretreatment" would otherwise have proven fatal to the cell. In another example, NT-3 in the locus coeruleus, an area of the brain thought to be involved in mood disorders, is induced by stress and repressed by anti-depressant therapy (Smith *et al.* 1995).

In addition to their roles in the differentiation and survival of neurons, and recovery from injury, neurotrophins may also participate in the normal physiology of adult brain. Interestingly, the BDNF gene has recently been shown to be directly inducible by estrogen, implying that normal hormonal variation may dramatically affect neurotrophin function (Sohrabji *et al.* 1995). Furthermore, many studies have demonstrated the regulation of neurotrophins, particularly induction of NGF and BDNF, and reduction of NT-3, by seizure activity (Gall and Lauterborn 1992). Several recent studies have shown that not only pathological but physiologic neuronal activity can regulate Trks and neurotrophins (Castrén *et al.* 1992; Kesslak *et al.* 1995; Neeper *et al.* 1995), and conversely that neurotrophins, acting through their Trk receptors, can dramatically regulate synaptic activity (Kim *et al.* 1994; Frostig *et al.* 1995; Kang and Schuman 1995; Levine *et al.* 1995; Patterson *et al.* 1995). Moreover, neurotrophins can affect axonal and dendritic branching and synaptic reorganization in the adult nervous system. Funakoshi *et al.* (1995) found that NT-4/5 is up-regulated in muscle by muscular activity, and that intramuscular injection of NT-3 causes motor nerve sprouting.

PC12 cells as a model system for growth factor-inducible neuronal differentiation

As discussed earlier, adrenal medullary chromaffin cells and sympathetic neurons both arise from a common neural crest-derived precursor. The primary similarity between the two differentiated cell types is that they are both catecholaminergic. Mature chromaffin cells are unable to respond to NGF, whereas sympathetic neurons are not only responsive to NGF but are dependent upon it. Since these neurons require NGF for survival, controlled *in vitro* study of their responses to NGF is quite difficult.

Pheochromocytomas are catecholamine-secreting slow-growing tumors of the adrenal medulla which, though they demonstrate a fairly atypical histology with large irregular nuclei, are rarely ever malignant. Like the chromaffin cells from which they are derived, these tumor cells do not require NGF for their survival.

In 1976, however, Lloyd Greene and Arthur Tischler established in culture a clonal rat pheochromocytoma cell line designated PC12, which has since become the most widely used model system for studying the mechanism of NGF action and the program of gene expression triggered during neuronal differentiation. It consists of chromaffin-like cells which stop dividing and differentiate dramatically when treated with NGF, taking on a sympathetic neuron-like phenotype (Greene and Tischler 1976). Despite the fact that they are a transformed cell line, using PC12 cells has several advantages over studying primary sympathetic or chromaffin cultures. First, they are a relatively homogenous population and can be grown in bulk, facilitating biochemical studies. Furthermore, they have not been exposed to NGF and do not require it for survival, thus very early events in NGF induction can be evaluated, and better control experiments can be performed. Within just minutes after NGF is added to the culture, aggregation and activation of the TrkA tyrosine kinase causes an intracellular cascade of increased protein phosphorylation and second messenger activation as described above, leading to increased membrane ruffling, and a strong though transient induction of a number of immediate early genes encoding transcription factors, including *c-fos, c-jun, c-myc, NGF-IA,* and *NGF-IB* (Greenberg *et al.* 1985; Leonard *et al.* 1987; Milbrandt 1987; Wu *et al.*

1989). Then, beginning a few hours later, a number of neuronal structural and functional proteins (delayed-response genes) are induced, including peripherin (Leonard *et al.* 1988), neurofilament subunits (Lindenbaum *et al.* 1988), MAP 1 (Drubin *et al.* 1985), the NGF-inducible large external glycoprotein (NILE) (Salton *et al.* 1983a,b), ornithine decarboxylase (Feinstein *et al.* 1985), and GAP-43 (Basi *et al.* 1987). Over a period of days, if NGF treatment is continued, the neuronal phenotype develops—the cells extend neurites, make small clear and dense-core vesicles, and become electrically excitable, able to generate sodium-based action potentials.

A number of other factors can produce similar, though not identical, differentiation of PC12 cells. For example, basic fibroblast growth factor (bFGF) produces neurite outgrowth, though to a lesser extent than treatment with NGF, and many of the same gene products are induced (Togari *et al.* 1985; Rydel and Greene 1987). Interleukin-6 (IL-6) also differentiates PC12 cells, with similar extensive neurite outgrowth, immediate early gene induction, and induction of excitability. The effect, however, is delayed and the cells do not remain viable longer than two weeks in culture (Satoh *et al.* 1988). In contrast, several other factors including epidermal growth factor (EGF), activate tyrosine kinase receptors, induce many of the same immediate early genes and increase protein phosphorylation, yet produce no phenotypic differentiation of PC12 cells (Greenberg *et al.* 1985; Milbrandt 1987; Wu *et al.* 1989). So the rapid induction of these early genes and effects is clearly not specific to the neurotrophic factor treatments. Therefore, these gene products and related events, though important for growth factor function in general, can not be solely responsible for eliciting neuronal differentiation in this system. To truly understand what makes a PC12 cell differentiate into a neuron, it would be necessary to discover what it is that these neurotrophic factor-induced transcription pathways are doing differently from those induced by non-neurotrophic growth factors. A few years ago, it was found that prolonged Ras and ERK (extracellular signal-related kinase, a.k.a. MAP kinase) activation seems to be somewhat specific to the NGF signaling pathway (Qiu and Green 1992). Very recently, a neurotrophin-specific cAMP response element-binding protein (CREB) kinase was identified that produces sustained activation, via phosphorylation, of the transcription factor CREB, which occurs only briefly in response to non-neurotrophin receptor activation (Bonni *et al.* 1995). This sustained activity of phospho-CREB seems to cooperate with other transcription factors to selectively induce expression of neurotrophin-specific sets of delayed response genes, which would then result in the development of a neuronal phenotype.

VGF, a neuronal gene product rapidly and selectively induced by NGF in PC12 cells

Several years ago, in an effort to elucidate the unique mechanism by which NGF exerts its effects, subtractive screening of a PC12 cell library was performed in our laboratory (Salton 1991) in a search for clones rapidly and selectively induced by NGF as compared to EGF. The screening paradigm was designed so as to minimize the number of extraneous positive clones obtained and to eliminate those clones containing previously described NGF+EGF-inducible genes. One gene isolated in the lab by this method, NGF33.1, was found to be "VGF", a nervous system-specific gene so named by Levi *et al.* in 1985 when they cloned its cDNA from plate <u>V</u> of an N<u>GF</u> induced PC12 cell library. This identity was discovered by alignment of the published predicted amino acid sequence of VGF with that predicted from our cDNA clone NGF33.1 (GenBank Acc. # M60525), which revealed ten long stretches of amino acid identity interrupted by shorter stretches of dissimilarity (see Figure 1). Since the nucleotide sequence of the original VGF isolate has never been published or entered into the databases, the clones cannot be directly compared at this level. However, the discrepancies in the predicted protein sequences of VGF and NGF33.1 can be almost completely resolved by allowing a number of shifts in the reading frame due to multiple single-base deletions and insertions. Low-stringency Southern blots performed by both groups suggest that there is only a single copy of each gene in the genome, which argues that these genes are identical, since two genes so similar yet unique would have obligatorily cross-hybridized (Levi *et al.* 1985; Salton 1991). These results also argue that there are no other highly related genes in the rat genome. Thus we are confident that our clone and VGF are one and the same.

VGF mRNA induction

By northern blot, both laboratories have demonstrated the rapid 10-50 fold induction of an approximately 2.7 kb VGF mRNA transcript in NGF-treated PC12 cells. This induction is maximal by 5-6 hours of NGF treatment, returns to basal levels by 48 hours, and is partially protein synthesis-dependent (Levi *et al.* 1985; Salton 1991; Baybis and Salton 1992; Possenti *et al.* 1992). Similarly, quantitative RNase protection analysis performed in our laboratory showed a 15-30 fold induction of VGF mRNA with 3-6 hours of NGF, and further, 7-fold stimulation by bFGF, only a 2-5 fold increase with EGF or serum stimulation, 2-fold induction by insulin, and no effect of treatment with retinoic acid (Salton 1991; Salton *et al.* 1991). Protection assays studying the effects of a number of second messenger pathway activators showed a 7-fold induction of VGF mRNA levels by phorbol ester treatment, and 1.5-fold induction by 8-bromo-cAMP. Additionally, KCl-induced depolarization of the cells produced a 5-fold induction. No one treatment produced levels comparable to those in NGF-treated cells (Salton 1991). Recently, however, it has been shown that VGF is fully inducible by BDNF and NT-3 in primary cortical neuronal culture (Bonni *et al.* 1995).

The VGF gene

The sequence of the rat VGF gene (GenBank Acc. # M60522) and its predicted amino acid sequence are shown in Figure 1 (Salton *et al.* 1991). The transcription start site as determined by primer extension is unusual in that it requires polymerase initiation at a pyrimidine. However, the presence of a standard TATAAA box at -24 relative to this site provides further evidence that this is the genuine start of transcription. There are two small introns, 261 and 124 nucleotides long respectively, located within the 700 base 5'-untranslated portion of the transcript. The ribosome binding site does not conform to the most common consensus, however, the sequence surrounding the putative site does not preclude binding and initiation. Levi *et al.* (1985) also predict this ATG to be the translation start site, and all but one of the first 154 amino acids are predicted identically by both groups. The uninterrupted coding sequence is then followed by an approximately 450 nucleotide 3'-untranslated region containing a known message destabilization sequence (ATTTA), and a consensus polyadenylation signal (AATAAA) 3005 bases from the cap site.

Besides the -24 TATAAA box, the VGF promoter region contains a CCAAT box at -133 which lies embedded in an unknown element with dyad symmetry (-138[TCCAATCATTGGA]-126), four GC boxes (SP-1 sites; at -62, -99, -253, -605), two AP-2 sites (at -39 and -252), an E-box at -44 (consensus sequence for the binding of the USF family of transcription factors), a cAMP-response element (CRE) at -71, an NGFI-A binding site at -6, two NFκB sites within intron A, and a serum response element (SRE) at -511. The recently described

REST binding site that has been shown to be responsible for silencing the transcription of several neuron-specific genes in non-neuronal cells is not found (Chong *et al.* 1995). The CREB binding site (CRE) and the CCAAT box have both been shown to be particularly important for VGF induction by neurotrophins; both are necessary, but neither alone is sufficient (Hawley *et al.* 1992; Bonni *et al.* 1995; D'Arcangelo *et al.* 1996). Control of VGF regulation by these elements occurs even in the absence of protein synthesis. The transcription factor CREB is stored in cytoplasmic pools in an unphosphorylated form. It is then phosphorylated by a specific kinase activated in the intracellular second messenger cascade upon binding of a Trk receptor by its neurotrophin. Phosphorylated CREB is then able to enter the nucleus, bind to CREs, and participate in the transcriptional induction of the VGF gene. The NGFI-A site is not required for expression or induction, but its presence approximately doubles the level of induction (D'Arcangelo *et al.* 1996). It is the enhancement of VGF induction by this element which is responsible for the protein synthesis-dependent aspect of neurotrophin-induced VGF transcription.

The VGF protein and VGF-derived peptides

As predicted by Salton (1991), the VGF protein should contain 617 amino acids with a molecular mass of 68,000. There is a potential sulfation site near the C-terminus of the protein, but there appear to be no phosphorylation or glycosylation sites. The protein is largely hydrophilic with the exception of a distinctly hydrophobic N-terminus which may be a signal peptide. Possenti *et al.* (1989) point out that an appropriate cleavage site exists just after one stretch of hydrophobic residues. In the same paper, they present a careful series of studies showing that the VGF protein is found in vesicles in NGF-treated PC12 cells and is secreted through both the constitutive and regulated pathways. By immunoprecipitation and by *in vitro* translation of selected VGF mRNA, they visualized a protein product with an apparent molecular weight of 90 kD on an SDS-PAGE gel. This is substantially larger than either group's protein sequence predicts. Levi *et al.* (1985) speculated that this aberrant electrophoretic mobility may be due to the unusually high proline content of the protein. Often they also visualized a second band at 75 kD, the proportion of which increased with time after induction, and which they speculated may be due to cleavage of the protein. Indeed, a number of putative dibasic proteolytic cleavage sites which could be recognized by subtilisin class proteases such as PC1 and PC2 do appear in the sequence (at AAs 178-179, 283-284, 311-312, 373-374, 421-422, 431-433, 483-488, 564-566, 586-587, and 597-598; see Figure 1), implying that the protein may be processed into smaller, potentially bioactive peptides.

Recently, Trani *et al.* (1995) showed western blots of PC12 cell extracts using more sensitive antisera raised to non-overlapping regions of the VGF polypeptide (amino acids 4-240 and 609-617). Both antisera recognize the same two bands described above, however, upon treatment of the PC12 cells with NGF for 48 hours, the N-terminal antiserum$_{4\text{-}240}$ additionally recognizes a band with an apparent molecular weight of 50 kD, while the carboxy-terminal antiserum$_{609\text{-}617}$ recognizes several smaller peptides as well (Trani *et al.* 1995). Thus, peptides exist which are cleaved from the C-terminal domain of the VGF protein, and at least in this cell line, induction toward a neuronal phenotype not only causes increased transcription and translation of VGF, but specific endoproteolytic processing into smaller neuropeptides as well. Moreover, region-specific processing in the brain occurs, such that all regions contain the two high-molecular weight forms, but most regions also contain large amounts of the 20 and 18 kD forms (except olfactory bulb and pons), while a 10 kD form is strongly expressed in cortex, thalamus and pons, but not elsewhere. The smaller species found in NGF-treated PC12 cells are somewhat larger than these, and may represent incomplete or different processing in these cells. Although significant amounts of the high-molecular weight forms of VGF are found in adrenal chromaffin cells, no processing was detected in adrenal medullary extracts. GH3 cells (somatotrophs) express but do not process VGF, while AtT20 (corticotrophs), GT1-7 hypothalamic, and MTC medullary thyroid carcinoma cells do produce the smaller cleavage products. Isolated cerebellar granule cells gradually express full-length somatically-localized VGF and then begin to process it into peptides localized in the neuronal processes as the cells mature in culture. These VGF-derived peptides are also preferentially secreted upon depolarization, whereas the larger species are retained.

Moreover, another laboratory has serendipitously isolated from bovine posterior pituitary a peptide (peptide V) which appears to consist precisely of the extreme carboxy-terminal 30 amino acids of the VGF polypeptide (Liu *et al.* 1994)—a fragment which could clearly be generated by cleavage of the dibasic site at AAs 586-587 (see Figure 1).

Although the VGF protein has no substantial sequence similarity to any known proteins, weak homology exists between small portions of VGF and areas in several cytoskeletal proteins including neurofilament-L, neurofilament-M, troponin, tropomyosin, and MAP 2. The significance of these mild similarities is unknown. More importantly, VGF is quite proline rich, which taken together with its many potential proteolytic cleavage sites and putative sulfation site, implies a similarity to a group of proteins also located in dense-core vesicles of the nervous system and neurosecretory cells such as those of the adrenal medulla, known as the chromogranins and secretogranins (CG/SGs; Winkler and Fischer-Colbrie 1992). Like VGF, the CG/SGs undergo tissue-specific cleavage, and it is the lower-molecular weight species which are found in neuronal processes. Many functions have been attributed to these proteins, including roles in vesicular packaging and maintenance. Recently, however, a number of CG/SG-derived peptides have been isolated, and several have been shown to have biological activities. Some seem to inhibit or promote release of co-stored hormones, at least one has monocyte-chemoattractive properties and causes dopamine release from rat striatal slices, and another demonstrates some neurotrophic properties (Winkler and Fischer-Colbrie 1992; Saria *et al.* 1993).

Anatomical localization of VGF

mRNA distribution

VGF message has been found only in the central and peripheral nervous systems, and in neuroendocrine or neurosecretory cells. VGF mRNA was not detected in adult rat adrenal, heart, kidney, liver, lung, placenta, skeletal muscle, spleen (Salton *et al.* 1991), or uterus (Levi *et al.* 1985) by northern analysis. Nor is it found in GH3 (somatotrophs), HTC (hepatoma), or FRTL5 (thyroid) cells (Levi *et al.* 1985). Initial studies in our laboratory demonstrated that VGF mRNA is widely expressed in the rat nervous system including cortex, cerebellum, spinal cord, and sympathetic ganglia. Highest levels were seen in developing animals—particularly, postnatal day 10 (P10) brain, cerebellum, and superior cervical ganglia (SCGs), while slightly lower levels were seen in P10 cortex, P6 cortex and cerebellum, P4 brain, adult brain, and P2 spinal cord (Salton *et al.* 1991). Additionally, another group found VGF message in the postnatal hypothalamus, adult olfactory bulb, hippocampus, cortex, cerebellum, and hypothalamus—with highest levels in the cortex and lowest in the hypothalamus (van den Pol *et al.* 1994).

One study claimed to find, but never showed, VGF mRNA expression by *in situ* hybridization in the adult rat brain in the hippocampal formation (highest in CA1, CA2, and subiculum); in the suprachiasmatic and arcuate nuclei and many neurons of the lateral hypothalamus; in cortical, medial, and central amygdaloid nuclei; in the paraventricular, laterodorsal, mediodorsal, and ventral posteromedial thalamic nuclei; and the layer V pyramidal cells of frontal and parietal cortex (no data shown, Mahata *et al.* 1993a). The authors state that the temporal cortex, substantia nigra, ventral tegmental area, and reticular thalamic nucleus did not express significant levels of VGF mRNA.

Polypeptide distribution

Most of the early work done on the VGF polypeptide has focused on its role in the hypothalamus and pituitary. Initially, a detailed immunohistochemical study of VGF in the hypothalamus was performed (van den Pol *et al.* 1989), and the most intense staining was seen in the neurons of the central and caudal portions of the dorsomedial region of the suprachiasmatic nucleus (SCN) and their projection areas. Weaker staining was noted particularly in the paraventricular and supraoptic nuclei, as well as the arcuate nucleus. Even lower levels are found in the amygdala, cortex, globus pallidus, hippocampus, posterior pituitary, and thalamus. By electron microscopy, a particular concentration of staining in boutons making dendritic or somatic synapses is seen. No immunoreactivity is seen in glia at any level. In P4 animals, immunostaining not seen in adults is observed in the dorsal lateral geniculate and several other thalamic nuclei. Staining with a monoclonal antibody which seems to bind some part of the NGF/NGF receptor complex, although it is unclear exactly which receptor and in what way (Chandler *et al.* 1984) shows little overlap with VGF reactivity in the adult hypothalamus. VGF has, however, been colocalized with vasopressin, oxytocin, and vasoactive intestinal peptide (VIP) in hypothalamic magnocellular neurons.

More recently, VGF polypeptide has been identified in neurons in adult brain and in neurosecretory cells in the adrenal medulla and pituitary (Ferri *et al.* 1992; van den Pol *et al.* 1994). In the rat brain, van den Pol *et al.* (1994) detected immunoreactivity in the olfactory tubercle, septum, striatum, amygdala, hippocampus, thalamus, and cortex, with the highest levels of immunostaining in the medial hypothalamus—despite finding in the same study that the hypothalamus displays the lowest level of mRNA expression. Expression of VGF protein can also be detected at varying levels in the trigeminal, dorsal root, and sympathetic ganglia, adrenal medulla, and spinal cord (Ferri *et al.* 1992). Immunoreactive nerve fibers are found in all organs but are particularly abundant in the intestine. In the pituitary, low levels of VGF immunostaining are seen in occasional anterior pituitary lactotrophs in males, and gonadotrophs and a few lactotrophs in females (Ferri 1995).

Regulation of VGF by physiologic stimuli

Several studies demonstrating the regulation of VGF by various physiologic stimuli have appeared since the onset of this work. In the adult hypothalamus, 5-fold induction of VGF mRNA occurs in the parvocellular neurons of the paraventricular nucleus 2 weeks after adrenalectomy (Mahata *et al.* 1993c), and in a ventral subpopulation of the magnocellular paraventricular neurons 10 days after a specific lesion of septohippocampal cholinergic neurons by the toxin ethylcholine aziridinium (AF64A; Mahata *et al.* 1993a). VGF mRNA is also induced in magnocellular neurons of the paraventricular and supraoptic nuclei in response to osmotic stress (Mahata *et al.* 1993b), which correlates with earlier findings of increased VGF immunostaining of magnocellular vasopressin neurons in vasopressin-deficient Brattleboro rats (van den Pol *et al.* 1989).

Studies to date outside of the hypothalamus are quite limited. In anterior pituitary gonadotrophs and lactotrophs, VGF levels vary dramatically during the estrous cycle (2-3 fold in whole pituitary by RNase protection assay), while in both males and females gonadectomy causes induction of VGF mRNA (3-fold in whole pituitary RNA in males and 2-fold in females) and increased immunostaining in the hypertrophic gonadotrophs (Ferri 1995). Cysteamine-induced, vagus nerve-dependent duodenal ulceration is associated with 2-fold induction of VGF mRNA (at 12 hours after treatment) in stomach-projecting preganglionic parasympathetic neurons of the nucleus of the tractus solitarius and the dorsal motor nucleus of the vagus, centers of autonomic control of the gut, which project directly to and receive afferent input from the gut (Kanemasa *et al.* 1995).

Summary and Overview

In summary, VGF is a neuron- and neuroendocrine-specific gene that is rapidly and selectively induced by the neurotrophins (NGF, BDNF, and NT-3). Its expression in the nervous system displays distinct regional heterogeneity and is developmentally regulated—notably peaking at times when the majority of the differentiation, migration, and synaptogenesis are occurring in a given region. Additionally, VGF is processed in a cell-type specific fashion, and secreted in response to neurotrophins and depolarization. Therefore, given the vital roles of neurotrophins in normal development, injury, and the adult, it is likely that VGF may be involved in intercellular signaling, growth cone guidance, and/or synaptic organization.

Much could potentially be learned from a detailed description of VGF expression in the brain, but previous localization work had been either gross RNA analysis, or immunohistochemistry focused solely on the hypothalamus (van den Pol *et al.* 1989; Levi *et al.* 1991; Salton 1991; Salton *et al.* 1991). I, therefore, proposed to determine more precisely the anatomical expression pattern of VGF throughout the adult central nervous system. In light of the knowledge that VGF was secreted from PC12 cells, and the then unconfirmed possibility that the VGF polypeptide might be cleaved into smaller peptides, both of which might account for the fact that previous studies seemed to find much less VGF immunoreactivity than one would expect from the RNA data, I chose to study the distribution of the mRNA encoding VGF by *in situ* hybridization. Since mRNA transcripts remain in the cells which synthesize them, and are rarely transported out of the cell soma, this method had the potential to be more sensitive than immunohistochemistry while providing more anatomical detail than RNA analysis of regional homogenates. Using this method, I have investigated the anatomical distribution of VGF message in the adult rat CNS. The resulting data are presented in Chapter 3 of this dissertation.

In order to further elucidate the possible roles of VGF during ontogeny, I also sought to determine the precise spatiotemporal expression pattern of VGF in the developing animal. At the onset of this endeavor, virtually all developmental studies had used either northern or RNase protection analysis to examine VGF expression at the regional level. The only exception which existed was a single mention of VGF immunoreactivity in the thalamus, suprachiasmatic nucleus and hippocampal interneurons of a P4 rat brain (van den Pol *et al.* 1989). I have, therefore, used the same technique to examine the ontogeny of VGF expression in the embryonic and neonatal rat. The results of this developmental *in situ* hybridization study are presented in Chapter 4.

Thirdly, bearing in mind the NGF-inducibility of VGF, and the possibility that other neurotrophins might also affect its expression, I wanted to be able to compare the expression pattern of VGF with those of the neurotrophin receptors. While ample *in situ* and immunohistochemical information existed in the literature, much of it focused on such different regions and developmental ages that comparison among these data was quite difficult. As a result, I included in my developmental and adult experiments sections which I hybridized with Trk-specific probes, so that they might be more readily compared with my VGF data. This comparison is presented in Chapter 5.

While there were several studies which examined the response of VGF expression to external stimuli in cultured cell lines, no experimental manipulations had been attempted in the intact animal. Considering my own preliminary data showing high levels of VGF message in the dorsal lateral geniculate nucleus (dLGN) in P5 brain (Snyder *et al.* 1992), immunohistochemical localization of VGF polypeptide in the dLGN one day earlier (van den Pol *et al.* 1989), and a study which demonstrated that the abnormal geniculocortical development caused by monocular deprivation during the postnatal development of the visual system could be averted by concomitant NGF treatment (Maffei *et al.* 1992), I examined the effect of this experimental *in vivo* perturbation of neurotrophin-dependent development on VGF expression in the dLGN. The results of these experiments are also presented in Chapter 5.

Lastly, during the course of my work, several opportunities for collaborative further studies of *in vivo* manipulation on VGF expression arose. In collaboration with Drs. Thomas McNeill and Cheng Heng-Wei at the University of Southern California, I examined the effect of their unilateral cortical lesion paradigm on VGF mRNA levels in lesioned adult brains they kindly provided. I also studied the effect of kainic acid-induced seizures on VGF expression in adult brain in seized tissue generously provided to us by Dr. Paul Isackson and Karl Murray of The Mayo Clinic in Jacksonville, Florida. These data are also presented in Chapter 5.

Figure 1: The VGF gene [adapted from Salton *et al.* (1991)].
The sequence of the VGF gene including 1557 bases of the 5′-untranslated and 459 bases of the 3′-untranslated regions is shown. The sequence is numbered with respect to the presumptive transcription start site at position 1.
The TATAAA, SP-1, CCAAT, AP-2, E-box (USF), NGFI-A, and CREB elements are *underlined*. The SRE, having dyad symmetry, is identified at -511 by the *arrows*. The dyad symmetry element surrounding the CCAAT box is highlighted with a *dotted overline*. Consensus splice site dinucleotides are *double underlined*. Consensus 3' polyadenylation (AATAAA) and mRNA destabilization (ATTTA) sequences are *underlined*.

The predicted amino acid sequence of the VGF polypeptide is shown above the gene sequence and numbered in *italics* with respect to the initial methionine. *Underlined* amino acids are identical to the deduced amino acid sequence of the VGF cDNA clone (Levi *et al.* 1985). Dibasic residues, putative endoproteolytic cleavage sites, are indicated by *overbrackets* (╓─╖).

```
-853 AAGCTTAAGGGTGTGGGAGAGTTGGATTAAAAGGGGGCACAACAGGGACCCCTTATCAACC
-792  ACAGCAAAGTCCGCTGGCCAGAAGGGCAGACACACCTTTTTTCCCCACCCCCTTCAGAAC
-732  TGGTTTGAACAGACAGGACCCAGAGGCACACGTATCGTCAATCTTTCCCTTTTCTCTTCC
-672  GACTAGGACCCTTTCCAAGGTGATTACCCAAACCGCAAGATCCACCCATCTGCGCTGACC
        SP1
-612  CTGGGCGGGGCATCCCACACCGCAGATCCACCCCCTCTTCCTCTCAGGTTCAAGTCGTCCT
            →                 →  SRE   ←            ←
-552  TGGGCGTGCTCCCTATAGACCATACTGTGGCGGAGTAGGGAGGCAGGCCCCTTCCCCGGC
-492  TTTCAATCCCTTACCGTCCCCCCATCCAGTACTGATCTTTTACTGGCGCCCAATTAGATG
-432  CTGGCGGTGCCCTCTTCCTATTCTGCTCAGCAACGCGGGCTCCGCGCCTCAAGAGCTTTG
-372  TAACCCACCCTCCCGCCTTCTGGCTCCTCTGTACCCACCCTTCCATTCATTTTTCCATTC
                                                               SP1*
-312  ATTCATTCATCCTTTTCTCCTCGTCCCTCCTTCATTCATTCATAGCCCCCTGCCCCGCCC
-252  GCCTAGACATTTCATTCATTCATTCATTCATTCATTTCCCCGGAGCTCCGCTAGCTCACGC
                                                                CCAAT
-192  CCCTCTAGCCGAGGGCCCTACTGCGCAGGTGCAGGCCGGGAGCGACGCTTATCCTCCAAT
                                       SP1*                    CREB
-132  TATTGGACTTCCACAGTCCACCAGGCACCCGGCCCGCTTCCCCATGAATGAACATTGACGT
          SP1
 -72  CAATGGGGCGGGGGCGAGACCACGTGACCCCGCGCGCTCCCCTTTATAAAGCAGCGGTGGC
      NGFI-A          1→
 -12  GCGGGGGCCTGTC CAGCGTGCTGAAGCCGGAGCGAGAGCGCTGTTGCTGACCCAGCTGAG
  48  CCCAGCTCCTAGGACGCCAGCCCTCGACCATCTTTCATACTCCAGCCACGGAACGGAGCC
 108  AGGGCAGACGGGTCCGGATTTTCCCCCTGCCCCGACCCTCCTCTCCACCTCCCGCCGTCG
                     INTRON A →
 168  TGACACCGGCTG GTAAATACTCCGCTGTCCATCCCTCTAACCCTCTTCACTCGTGGCG
 227  TGAAAGGAGGATTTTCTTTCCTTATGGGGTATTGAGAGCATAGCGGTGTGCCCCCGGGAA
 287  GGGTCTTTGGTAAACGGGGAGTCTCTGCTTCTCTGTCGCTGATGAAGTCGCCCACGCACC
 347  ATCCGGGGAGTCCTGTGGGGAGGGAACAGATCCCCCCTCCCACTTATCATTGCTGCTTAG
 407  TACACGGGCGCTGGCTGAGAGATGACTTTGGGAAG GGGGCGACAGGAGGCACTGGGTAC
 466  CCAGAACGAGGATTGCGAGCGTTCTCTGACCATTTGCACGACCCCAGAGATTGCCACATC
                                         INTRON B →
 526  TTTCTTGTTCTCTGCTAAACGTTTCTCTTCGG GTAAGGTTAGAGAAATGAGGGAAACCC
 585  CGGATTTCCTGCTTAAAGGTGGGGGGAGGGAATCGAGAAATAGAAAGAGGGAAATTCTTA
 645  TAGAAATCCTCTATTTCTCTGGTTTCTTCTGTTTTTCAG TCTCTGGCAGCCCGTTGGTC
   1  METLysThrPheThrLeuProAlaSerValLeuPheCysPheLeuLeuLeuIleArgGly
 704  ATGAAAACCTTCACGTTGCCAGCATCCGTCCTCTTCTGCTTCCTTCTACTCATCCGGGGG
  21  LeuGlyAlaAlaProProGlyArgSerAspValTyrProProProLeuGlySerGluHis
 764  TTGGGAGCAGCACCCCCCGGGCGCTCCGATGTTTATCCTCCTCCCCTCGGCTCTGAGCAT
  41  AsnGlyGlnValAlaGluAspAlaValSerArgProLysAspAspSerValProGluVal
 824  AATGGGCAGGTAGCTGAGGACGCAGTGTCCCGGCCAAAGGATGACAGCGTCCCAGAGGTC
  61  ArgAlaAlaArgAsnSerGluProGlnAspGlnGlyGluLeuPheGlnGlyValAspPro
 884  CGAGCGGCTCGGAATTCCGAGCCTCAGGACCAGGGAGAGCTCTTCCAGGGCGTGGATCCC
  81  ArgAlaLeuAlaAlaValLeuLeuGlnAlaLeuAspArgProAlaSerProProAlaVal
 944  CGGGCGCTGGCCGCGGTACTGTTGCAGGCACTGGACCGTCCGGCCTCGCCCCCGGCTGTC
 101  ProAlaGlySerGlnGlnGlyThrProGluGluAlaAlaGluAlaLeuLeuThrGluSer
1004  CCGGCAGGTTCCCAGCAGGGAACACCCGAAGAAGCAGCAGAAGCTCTGCTGACCGAGTCC
 121  ValArgSerGlnThrHisSerLeuProAlaSerGluIleGlnAlaSerAlaValAlaPro
1064  GTGCGCAGTCAGACCCATAGCCTCCCGGCATCAGAAATCCAAGCGTCCGCTGTGGCGCCC
 141  ProArgProGlnThrGlnAspAsnAspProGluAlaAspAspArgSerGluGluLeuGlu
1124  CCTCGCCCTCAGACTCAGGACAACGATCCCGAGGCAGACGACCGCTCAGAAGAGCTGGAG
 161  AlaLeuAlaSerLeuLeuGlnGluLeuArgAspPheSerProSerAsnAlaLysArgGln
1184  GCACTAGCATCCTTGCTCCAAGAACTTCGAGATTTCAGTCCGAGTAATGCTAAGCGCCAG
 181  GlnGluThrAlaAlaAlaGluThrGluThrArgThrHisThrLeuThrArgValAsnLeu
1244  CAAGAGACGGCGGCAGCAGAGACTGAAACCCGCACGCACACGCTGACCCGAGTCAATCTG

 201  GluSerProGlyProGluArgValTrpArgAlaSerTrpGlyGluPheGlnAlaArgVal
1304  GAGAGCCCCGGGCCAGAGCGCGTATGGCGCGCTTCCTGGGGAGAGTTCCAGGCGCGCGTC
 221  ProGluArgAlaProLeuProProSerValProSerGlnPheGlnAlaArgMETSerGlu
1364  CCGGAGCGTGCTCCTCTGCCGCCCTCGGTCCCTTCTCAATTCCAGGCTCGAATGTCCGAA
 241  AsnValProLeuProGluThrHisGlnPheGlyGluGlyValSerSerProLysThrHis
1424  AACGTTCCCCTTCCCGAAACCCATCAGTTCGGGGAAGGAGTGTCCTCCCCTAAAACACAT
 261  LeuGlyGluThrLeuThrProLeuSerLysAlaTyrGlnSerLeuSerAlaProPhePro
1484  CTTGGTGAGACTTTGACACCCTTATCCAAGGCGTACCAAAGTCTAAGTGCCCCCTTCCCC
 281  LysValArgArgLeuGluGlySerPheLeuGlyGlySerGluAlaGlyGluArgLeuLeu
1544  AAGGTGCGTCGGCTCGAGGGCTCATTCCTGGGCGGTTCCGAGGCAGGAGAGCGCCTGCTT
 301  GlnGlnGlyLeuAlaGlnValGluAlaGlyArgArgGlnAlaGluAlaThrArgGlnAla
1604  CAACAAGGGTTAGCTCAGGTAGAGGCAGGGAGGAGGCAGGCGGAGGCCACCCGGCAGGCC
 321  AlaAlaGlnGluGluArgLeuAlaAspLeuAlaSerAspLeuLeuLeuGlnTyrLeuLeu
1664  GCAGCGCAAGAAGAGCGGCTGGCCGATCTCGCCTCCGACCTGCTGCTCCAGTATTTGCTG
 341  GlnGlyGlyAlaArgGlnArgAspLeuGlyGlyArgGlyLeuGlnGluThrGlnGlnGlu
1724  CAGGGCGGCGCCCGGCAGCGCGATCTCGGGGGTCGCGGGCTGCAGGAGACGCAGCAAGAG
 361  ArgGluAsnGluArgGluGluGluAlaGluGlnGluArgArgGlyGlyGlyGluAspGlu
1784  CGGGAGAACGAGAGGGAGGAGGAGGCGGAGCAGGAGAGACGCGGTGGTGGGGAGGACGAG
 381  ValGlyGluGluAspGluGluAlaAlaGluAlaGluAlaGluAlaGluGluAlaGluArg
1844  GTGGGGGAAGAGGATGAGGAGGCGGCAGAGGCGGAGGCGGAGGCAGAGGAGGCGGAGAGG
 401  AlaArgGlnAsnAlaLeuLeuPheAlaGluGluGluAspGlyGluAlaGlyAlaGluAsp
1904  GCGCGGCAGAACGCGCTCCTGTTCGCCGAGGAGGAGGACGGGGAAGCCGGAGCCGAGGAC
 421  LysArgSerGlnGluGluAlaProGlyHisArgArgLysAspAlaGluGlyThrGluGlu
1964  AAGCGCTCCCAGGAGGAGGCGCCAGGCCATCGGCGGAAGGATGCTGAGGGGACAGAGGAG
 441  GlyGlyGluGluAspAspAspAspGluGluMETAspProGlnThrIleAspSerLeuIle
2024  GGCGGGGAGGAGGATGACGACGACGAAGAGATGGATCCGCAGACGATCGATAGTCTCATT
 461  GluLeuSerThrLysLeuHisLeuProAlaAspAspValValSerIleIleGluGluVal
2084  GAACTGTCCACCAAACTCCACCTGCCAGCAGACGATGTGGTCAGCATCATCGAAGAGGTG
 481  GluGluLysArgLysArgLysLysAsnAlaProProGluProValProProProArgAla
2144  GAGGAGAAACGGAAGCGGAAGAAGAACGCCCCTCCCGAGCCGGTGCCGCCCCCCAGGGCT
 501  AlaProAlaProThrHisValArgSerProGlnProProProProAlaProAlaArgAsp
2204  GCCCCAGCCCCGACCCATGTCCGCTCCCCGCAGCCCCCACCTCCCGCCCCGGCCCCGGGAT
 521  GluLeuProAspTrpAsnGluValLeuProProTrpAspArgGluGluAspGluValPhe
2264  GAGTTGCCGGACTGGAACGAAGTACTCCCACCCTGGGATCGGGAGGAGGATGAGGTGTTT
 541  ProProGlyProTyrHisProPheProAsnTyrIleArgProArgThrLeuGlnProPro
2324  CCCCCGGGGCCCTATCACCCCTTCCCAAACTACATTCGGCCGCGGACACTGCAGCCGCCC
 561  AlaSerSerArgArgArgHisPheHisHisAlaLeuProProAlaArgHisHisProAsp
2384  GCATCCTCCCGCCGCCGTCACTTCCATCACGCGTTGCCACCTGCGCGCCACCATCCCGAT
 581  LeuGluAlaGlnAlaArgArgAlaGlnGluGluAlaAspAlaGluGluArgArgLeuGln
2444  CTGGAGGCCCAGGCCAGGCGCGCGCAGGAGGAAGCGGACGCGGAGGAGCGCCGGCTGCAG
 601  GluGlnGluGluLeuGluAsnTyrIleGluHisValLeuLeuHisArgPro .
2504  GAGCAGGAGGAGCTGGAGAATTACATTGAGCACGTGCTGCTGCACCGCCCGTGACCCGCC
2564  CCTGCGCGCCCGCTCCCAACTGCGCGCGCCGCCACGCCCCCCCTCCGTGTCGCTCCTCCT
2624  CCCTCTCGGTGTTTGCATGCGCCCCGGCTCCGCCCCTCGGCTGCCGCCCGGCCCCGCCCC
2684  ACAAGGCCCCGCCCCGGGTTCTGTCAGGACCAGACCTGTCAGACTTCTTTGGGGTCTGAT
2744  CCTGGGGCCAGCCCAGGCGGGTGTGTGGTTTGTGCGAGTCCCCTTACACCCCCACTTCCT
2804  CCAGGGGCCTCGTCCCCATCTAGTTTCTCTAGCGACTTCCTGGTCCCAAACGGGGAAAAG
2864  CTGTTCTATTTAATCGTGTGAAGTGTCTGTCTCCCAGCCTTGGGGCCCCCGGAGCCTCCC
2924  TTCTCCAAATTGCTGTGAACTTACCCACATCTTGCCCTTCTGTTGTAAATACCCCTCACG
2984  GAGGAAATAGTTTTGCTAAGAAATAAAAGTGACTATTTT ATTAGGACTTTGTTTTCCAT
3043  TATTCACCCGTCCCCTTGGGCCTATCTGGCTTCAAGGGGC
```

Chapter 2: Methods and Materials

Animals and treatments

All animals were housed in climate-controlled rooms on a 12-hour light/dark cycle with free access to food and water. All developmental ages stated in this dissertation follow the convention which considers the day following the evening of conception to be embryonic day 0 (E0), and the day of birth to be postnatal day 0 (P0). For developmental studies, postnatal, adult, or timed-pregnant Sprague-Dawley rats (Charles River Laboratories, Wilmington, MA; Zivic-Miller Laboratories, Allison Park, PA) were killed by CO_2 narcosis, and rapidly dissected on ice. Brains or whole embryos were then embedded in OCT compound (Miles, Elkhart, IN), frozen in 2-methyl butane on dry ice powder, and stored at -20°C until sectioning.

For the monocular deprivation study (Chapter 5), postnatal day 23 Long-Evans hooded rat pups (Harlan Sprague-Dawley, Indianapolis, IN) were placed under ether anesthesia, and given 3 µl intravitreous injections of a 0.15mM solution of the sodium channel blocker tetrodotoxin (TTX; Sigma, St. Louis, MO) in 3.5mM citrate buffer (pH 4.8) or the same volume of buffer alone, into the right eye with a Hamilton 700 microsyringe (Hamilton, Reno, NV). The animals were returned to their mothers before being killed by CO_2 narcosis either 1, 6, 12, 24, or 48 hours after injection. The brains were rapidly removed on ice, and embedded in OCT as described above.

For seizure studies (Chapter 5), brains treated as follows by Karl Murray were obtained from the laboratory of Dr. Paul Isackson at the Mayo Clinic, Jacksonville, Florida. Adult male Sprague-Dawley rats, weighing 250-300 g, were injected intraperitoneally with 10 mg/kg kainic acid in phosphate-buffered saline (PBS), or an equivalent volume of PBS alone, and at either 1, 3, 6, 12, 24, or

48 hours after injection, were anesthetized with 50 mg i.p. sodium pentobarbital/kg (Abbott Laboratories, Chicago) and subjected to transcardiac perfusion with PBS followed by 4% paraformaldehyde in PBS (4% Para). The brains were removed, post-fixed 1-2 days at 4°C in 4% Para, cryoprotected in 20% sucrose/4% Para at 4°C overnight, frozen and embedded in OCT.

For the cortical lesion study (Chapter 5), brains treated as follows by Dr. Cheng Heng-Wei were obtained from the laboratory of Dr. Thomas McNeill at The Andrus Gerontology Center at The University of Southern California. Adult male Fischer-344 rats (Charles River Laboratories, Wilmington, MA) weighing 250-300 g, were anesthetized with 50 mg i.p. pentobarbital/kg and placed in a stereotax. Unilateral cortical lesions involving most of the frontal and part of the parietal cortex were made by aspiration with a fine-tipped glass pipette under a dissecting microscope (Figure 2). The wound cavity was gently filled with Gelfoam, and the overlying scalp sutured. Control rats were not lesioned. Rats were killed by decapitation 1, 3, 6, 12, or 24 hours, or 3 or 10 days after lesioning, and their brains were removed, frozen and embedded in OCT.

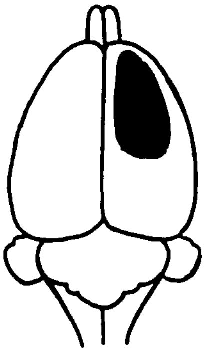

Figure 2: Schematic diagram of the extent of the unilateral cortical lesion. The lesion is shown as a *blackened region* on an outline of the dorsal view of an adult rat brain. Adapted from Swanson (1992).

For all embedded brains and embryos, 10 μm frozen sections were cut on a Bright-Hacker cryostat (Huntingdon, England), thaw-mounted onto Superfrost®/Plus slides (Fisher Scientific, Fairlawn, NJ), and stored at -20°C or -80°C.

Preparation of riboprobes

The VGF riboprobe was transcribed from a plasmid construct made by S. R. J. Salton and described previously, which contains a 304 base pair cDNA fragment corresponding to bases 1592-1896 of the 3′ end of the VGF coding region (Salton 1991). Plasmids constructed by S. R. J. Salton and J. Li and containing DNA fragments encoding portions of the extracellular domains of TrkA (bases 951-1305, Acc. #M85214), TrkB (bases 1601-1945, Acc. #M55291), TrkC (bases 951-1285, Acc. #L14445), and the carboxy-terminus of the catalytic form of the TrkB kinase (bases 3131-3360, Acc. #M55291), were used as templates for the transcription of the corresponding riboprobes (Snyder *et al.* 1996). Probes complementary to the regions encoding the Trk extracellular domains, will hybridize to mRNAs encoding both full-length and truncated forms of the Trks, however, the TrkB kinase probe will hybridize only to mRNA encoding full-length, catalytic forms of the receptor. Probe specificity had been previously determined by hybridization to northern blots onto which electrophoretically separated PC12 cell and rat brain total RNAs had been transferred (S. R. J. Salton, personal communication). These plasmid templates were then linearized by appropriate restriction enzyme digestion, and antisense- and control sense-strand riboprobes were transcribed from them using [^{35}S]-UTP (New England Nuclear, Boston, MA), Riboprobe® System II transcription buffers (Promega, Madison, WI), and either T_3 or T_7 RNA polymerase (Stratagene, La Jolla, CA). All riboprobes were purified by Sephadex G100 (Pharmacia, Piscataway, NJ) column chromatography, and stored at -80°C in 100mM dithiothreitol until use.

In situ hybridization

In situ hybridization was carried out essentially as described by Zheng and Pintar (1995). Slides were removed from the freezer directly into RNase-free

4% paraformaldehyde, 50mM NaCl, 100mM sodium phosphate (pH 7.2) fixative for 2-15 minutes, rinsed in diethylpyrocarbonate-treated deionized water (DEPC-dH_2O) and dehydrated through a graded ethanol series. Sections from the seizure study, which had been perfusion fixed, were treated with Proteinase K at 5 μg/ml in 0.1M Tris (pH 8), 50mM ethylenediaminetetraacetic acid (EDTA) for 30 minutes at 37°C and rinsed again before dehydration. After air drying, all slides were rehydrated in DEPC-dH_2O, followed by a 0.05M triethanolamine, 0.026M acetic acid solution for 2 minutes, then were acetylated for 10 minutes in 1 ml acetic anhydride rapidly mixed with 200 ml triethanolamine solution, rinsed, and dehydrated. Sections were prehybridized for 1-2 hours in 600mM NaCl, 10mM Tris (pH 7.5), 0.12% Ficoll, 0.12% bovine serum albumin (BSA), 0.12% polyvinylpyrrolidine (PVP), 1mM EDTA, 0.5 mg sheared denatured herring sperm DNA (hsDNA)/ml, 0.5 mg yeast total RNA/ml, 50 μg yeast tRNA/ml, 50% deionized formamide at room temperature, before hybridization overnight at 50°C in a humidified chamber in a similar buffer additionally containing 2.5×10^4 cpm of [^{35}S]-labeled riboprobe/μl, 10mM dithiothreitol (DTT), 0.1% sodium dodecyl sulfate (SDS), 10% dextran sulfate, and only 100 μg hsDNA/ml. The next day, slides were washed for 30 minutes in 1 x SSC (sodium citrate solution; Sambrook *et al.*, 1989), 10mM DTT, 50% deionized formamide at 50°C, then 30 minutes in 0.5 x SSC at room temperature. In each experiment, the appropriate *trk* or VGF sense-strand riboprobes were hybridized to adjacent sections in parallel with antisense probes. Following treatment with 0.1 mg ribonuclease A (RNase; Type IIA, Sigma)/ml in 0.5M NaCl, 10mM Tris (pH 7.5), 1mM EDTA for 30 minutes at room temperature, the slides were subjected to two 10 minute washes in the same buffer without RNase, and a final wash for 2 hours in 3.5 liters of 0.2 x SSC at 65-70°C. After dehydration through a graded ethanol series containing 300mM ammonium acetate, slides were air dried and exposed to Hyperfilm-βmax film (Amersham, Arlington Heights, IL) alongside [^{14}C]micro-scales (Amersham) for 2 days to 2 weeks. Films were developed in GBX developer (Eastman Kodak, Rochester, NY) diluted 1:5 with dH_2O, and fixed with Kodak Rapid Fix. Slides were then dipped in a 1:1 mixture of Kodak NTB2 emulsion and HPLC-grade water (HPLC-dH_2O) at 42°C in an acid-washed Coplin jar, allowed to dry for 2 hours, placed in light-tight boxes with desiccant capsules, and stored at 4°C for the duration of a 1-4 week exposure. Slides were allowed to come to room temperature before being developed for 3 minutes in Kodak D19 developer mixed 1:1 with dH_2O, rinsed for 25 seconds in dH_2O, fixed in Kodak Rapid Fix for 3.5 minutes, and rinsed in three changes of dH_2O. They were then counterstained with cresyl violet (Eastman Kodak, Rochester, NY), dehydrated, cleared in 2 changes of Polyclear (D-Limonene; Florida Chemical, Winter Haven, FL), coverslipped with DPX mountant (Fluka Chemicals, Ronkonkoma, NY), and when dry, cleaned with a razor blade and glass cleaner to remove excess emulsion from the reverse side.

Image preparation

Emulsion-dipped sections were visualized on a Stemi SV8 dissecting microscope (Zeiss, Germany) and a Microphot FX microscope (Nikon, Japan), and bright field and dark field photomicrographs were taken using Kodak Ektachrome 160T slide film. Structures were identified with the aid of several published atlases and texts of rodent development and adult neuroanatomy (Sherwood and Timiras 1970; Hebel and Stromberg 1986; Paxinos and Watson 1986; Jacobson 1991; Paxinos *et al.* 1991; Kaufman 1992; Schambra *et al.* 1992; Swanson 1992; Altman and Bayer 1995; Paxinos 1995). Ektachrome slides and film autoradiographs were scanned into a Power Macintosh computer (Apple, Cupertino, CA) using an ARCUS II flatbed scanner and Fotolook software (Agfa, Wilmington, MA). Composite figures were made using Photoshop (Adobe Systems, Mountain View, CA) on a Power Macintosh computer, and were printed on either a Phaser 440 dye-sublimation printer (Tektronix, Wilsonville, OR) or a 600 d.p.i. LaserWriter Pro (Apple, Cupertino, CA).

Image analysis

For the kainic acid seizure and unilateral cortical lesion studies, film autoradiographs were scanned into a Power Macintosh computer as described above, and autoradiographic densitometry analysis, standardized against [^{14}C]micro-scales, was performed using the public domain software NIH Image (National Institutes of Health, Bethesda, MD) obtained by anonymous file transfer over the Internet from zippy.nimh.nih.gov. Mean optical density readings for each brain region in each hemisphere at each timepoint were determined on autoradiograms corresponding to at least 7 and at least 4 coronal sections from each animal for the kainate seizure and cortical lesion studies respectively. Results were analyzed and charted using Microsoft Excel (Microsoft, Redmond, WA), SuperANOVA (Abacus Concepts, Berkeley, CA), and Canvas (Deneba Systems, Miami, FL) on a Power Macintosh 7100 computer. Two- or 3-factor analysis of variance (ANOVA) was performed on the kainate-seized (for brain region and time post-injection) and cortical-lesioned (for brain region, contralateral or ipsilateral hemisphere, and time post-lesion) data respectively. Fisher's Protected Least Significant Difference (Fisher's PLSD) tests were then used to identify where significant interactions had occurred.

Chapter 3: Distribution of VGF mRNA in the Adult Rat Central Nervous System

Introduction

Despite early northern analyses which demonstrated substantial VGF expression in whole rat brain RNA (van den Pol *et al.* 1989; Salton *et al.* 1991), detailed studies of VGF localization in the adult animal have largely been focused on the hypothalamus and pituitary (van den Pol *et al.* 1989; Mahata *et al.* 1993a,b,c; Okamura *et al.* 1994; Ferri 1995). The few exceptions, all published during the course of the present study, include: a description of VGF immunohistochemistry in spinal cord and peripheral neuronal and neuroendocrine tissues (Ferri *et al.* 1992); one study which claimed to find, but never showed, VGF mRNA expression by *in situ* hybridization in several regions of the adult rat brain (Mahata *et al.* 1993a); another which demonstrated VGF message in the cortex and dLGN by *in situ* hybridization, and described VGF immunoreactivity in a number of brain regions, of which the thalamus, hippocampus, and cortex were shown (Lombardo *et al.* 1995); and a recent detailed immunohistochemical study of VGF in the adult brain by van den Pol *et al.* (1994). In a preliminary RNase protection analysis of adult rat nervous tissues, I found the highest levels of VGF mRNA in brainstem, whole brain, and cortex (S. E. Snyder, unpublished results). Lower levels were observed in spinal cord, olfactory bulb, pituitary, cerebellum, and eyes. VGF mRNA was undetectable in sciatic nerve and testis. In the current study, I provide a thorough survey of VGF mRNA localization throughout the adult rat CNS as determined by *in situ* hybridization histochemistry.

Results

Specificity of VGF mRNA detection by *in situ* hybridization

Earlier work in our laboratory has shown by Southern analysis that there is most likely a sole VGF gene in the rat, and by northern analysis that our VGF probes recognize an approximately 2.7 kb mRNA band in nervous tissue but detect nothing in other organs (Salton 1991; Salton *et al.* 1991). Although alternative splicing of VGF RNA occurs (Hawley *et al.* 1992), both introns are upstream of the coding region, which is entirely contained in exon 3. Thus, the VGF riboprobe used in the current studies, which is derived from the 3′ end of the coding region, will hybridize to all possible VGF polypeptide-encoding RNAs.

The specificity of our VGF probe was clearly maintained in *in situ* hybridization to sections of rat tissue, both in its predilection for nervous tissues on a gross level, and in its restriction to neurons and neuroendocrine cells at the microscopic level. For example, in a representative parasagittal section from an E19.5 fetus (Figure 3A), strong VGF hybridization signal was observed in portions of the brain, spinal cord, and cranial and dorsal root ganglia. Although hybridization in the developing pancreas and epidermis (which contain endocrine and neural crest-derived elements), and myenteric plexus was also apparent at this stage, as was an extremely weak signal over the fetal liver, no appreciable signal was seen in skeletal or cardiac muscle, adipose tissue, the skeleton, vascular elements, or other organs. Panels B and B′ show parasagittal sections of an E13.5 embryo hybridized with VGF sense-strand control and antisense probes respectively, while panels C and C′ are comparable hybridizations to parasagittal sections of a P10 rat brain. In both cases, the sense probe produced no appreciable hybridization, while the antisense probe produced a characteristic VGF hybridization pattern, including the lack of signal in fiber tract regions such as the corpus callosum. The emulsion autoradiograph in panel D further demonstrates the neuronal specificity of VGF hybridization in the adult rat brain at high magnification. Clusters of silver grains indicative of VGF-specific hybridization were found exclusively over the large, lightly stained neuronal somata, while the smaller, darker glial cells and neuropil were unlabeled.

VGF mRNA expression in the CNS

The distribution of VGF mRNA in the adult rat CNS is shown in Figures 4-9. These data revealed a wide distribution of VGF mRNA expression, in at least a subset of neurons, throughout most structures at all levels of the brain, spinal cord, and retina studied. White matter, meninges, ependyma, choroid plexus, subependymal zones, blood vessels, and other neuron-sparse regions such as layer I of the cerebral cortex were essentially unlabeled.

Olfactory system

VGF mRNA expression was found in both the main and accessory olfactory bulbs (Figure 4A and B). The mitral cell layer and all but the outermost cells of the glomerular layer displayed strong labeling, as did some occasional cells in the external plexiform layer, particularly in the external half; while the granule cell layer was moderately labeled (Figure 6A and A′). The olfactory nerve layer and subependymal zone were virtually devoid of hybridization signal.

The pyramidal cell layer of all portions of the anterior olfactory nucleus (AON), particularly the external portion, also displayed very strong labeling (Figure 4B and C). The lateral olfactory tract like other white matter was unlabeled.

The induseum griseum (IG) and taenia tecta (TT) were moderately to strongly labeled (Figure 4D-G), and neurons of the cortical layer of the olfactory tubercle displayed a strong hybridization signal, particularly those situated more ventrolaterally (Figure 4E-I; Figure 5G).

Insofar as along with the AON, IG, and TT they constitute unimodal association cortex of the olfactory system, the expression of VGF mRNA in the piriform, periamygdaloid, transitional, and lateral entorhinal cortices (together the lateral olfactory cortex; de Olmos *et al.* 1978) will be mentioned here. Layer II of the piriform cortex exhibited quite strong VGF labeling in the adult brain rostral to the anterior commissure (Figure 4D-H, Figure 5E-G). The more caudal portions were labeled as well, but somewhat more moderately (Figure 4I-M). Deep to the piriform cortex, the endopiriform nucleus was also strongly labeled. Hybridization in the periamygdaloid and transitional areas, and the entorhinal cortex appeared very similar to that in the caudal piriform cortex; moderate labeling was seen throughout all layers but layer I (Figure 4N-R; Figure 5).

Cerebral cortex

The majority of the cerebral isocortex and transitional cortical areas including not only the frontal, parietal, temporal, and occipital cortices, but agranular insular, cingulate, retrosplenial, prelimbic, orbital, ectorhinal, and perirhinal cortices, and claustrum as well, displayed a fairly consistent VGF mRNA hybridization pattern throughout (Figure 4; Figure 5). The highest density of expression was seen in layer V where many cells were strongly labeled. Fewer, but still significant numbers of strongly labeled cells were found in layers II and VI, while many other neuronal somata in all cellular layers (II-VI) displayed weak to moderate labeling (Figure 6D). Only the rare cell in neuron-sparse layer I displayed detectable hybridization. Relative to the other motor and sensory cortices, VGF mRNA levels seemed to be somewhat lower in the visual cortical areas (Figure 4N-R).

Hippocampal formation

In Ammon's horn, cells of the pyramidal layer of CA1-3 were moderately to heavily labeled by the VGF riboprobe (Figure 4; Figure 5). The stratum pyramidale of CA2 seemed to exhibit the most intense hybridization, while that of CA1 and the lateral/ventral portion of CA3 also showed strong labeling (Figure 6E). In the pyramidal layer of the medial portion of CA3 (near and between the blades of the dentate gyrus) and the stratum granulosum of the dentate gyrus, most cells were only weakly labeled, although the occasional strongly labeled cell could be seen. Very strongly labeled cells were consistently found throughout the stratum oriens, the stratum lucidum of CA3, and the polymorph region of the dentate hilus, and rarely, in the dentate molecular layer (Figure 6E). Several of the strongly labeled dentate cells seemed to be aligned along deep surface of the granular layer, particularly along the suprapyramidal blade; these cells and those of the stratum oriens and stratum lucidum are likely to be either basket cells or another one of the poorly understood GABAergic and peptidergic hippocampal neuronal cell types.

As seen in Figure 4 and Figure 5, substantial VGF mRNA hybridization was also apparent in the subicular complex—the subiculum and presubiculum had the strongest labeling. The entire entorhinal cortex, as mentioned above, displayed VGF hybridization as well, with the most intense labeling in layer II. And again, the induseum griseum was fairly strongly labeled (Figure 4D-G).

Amygdala

Strongest VGF mRNA hybridization in this region was observed in the medial nucleus, particularly the anterodorsal portion (Figure 4K). The nucleus of the lateral olfactory tract and basolateral nucleus were also strongly labeled (Figure 4J). Most other amygdaloid nuclei displayed moderate or low levels of hybridization (Figure 4J-M).

Septal region

The septal region is seen in Figure 4E-I. Neurons with moderate to strong labeling were very common in the dorsal and ventral parts of the lateral septal nucleus (LSd, LSv); the intermediate portion, however, showed only a few moderately labeled cells. The medial septal nucleus contained many moderately labeled cells, but not as many as in the LSd and LSv. The nucleus of the diagonal band contained numerous highly labeled cells. In the posterior septal complex, both the septofimbrial and triangular septal nuclei displayed moderate labeling. Among the bed nuclei of the stria terminalis the dorsal nucleus was strongly labeled; the transverse contained a few strongly labeled cells; the interfasicular, principal, subcommissural, dorsomedial, and anteroventral nuclei were moderately labeled; and the remainder showed low levels of hybridization.

Basal ganglia

As seen in Figure 4E-K, moderate levels of VGF mRNA hybridization were observed throughout most of the caudoputamen, although the caudalmost portions hybridized somewhat less strongly than the main portion of the nucleus. The bulk of the globus pallidus remained essentially unlabeled. However, there were scattered strongly labeled cells near its ventromedial border, which might have been cells of the nucleus basalis magnocellularis (nbM) to the extent that it exists in the rat. The nucleus accumbens and ventral pallidum were moderately labeled, although the septal portion of the accumbens shell displayed quite strong hybridization. The substantia innominata was only very weakly labeled. However, a number of cells in the magnocellular preoptic nucleus displayed moderate labeling. The subependymal zone at the dorsomedial border of the caudoputamen was unlabeled.

Thalamus and epithalamus

All of the principal sensory relay nuclei of the thalamus expressed moderate or high levels of VGF mRNA (Figure 4K-Q). Specifically, the dorsal lateral geniculate (dLGN), medial geniculate (MGN), and ventroposteromedial (VPM) nuclei displayed very high levels of VGF hybridization; and the ventro-posterolateral (VPL) and the posterior complex (PoT) contained moderate to high labeling. The principal motor relay nuclei—the ventral antero-lateral complex (VAL) and the ventromedial nucleus (VM)—showed moderate to high VGF expression as well. Of the "association" nuclei: mediodorsal (MD) contained high labeling in its medial and lateral divisions and moderate labeling in its central division; the submedial (SM; gelatinosus) nucleus contained sparsely distributed moderately labeled cells, as did the perireuniens nucleus (PR); the paratenial nucleus (PT) was strongly labeled; the lateral posterior nucleus (LP) showed high levels of hybridization; and the laterodorsal nucleus (LD) exhibited low to moderate signal. In the anterior group, the anteroventral (AV), anteromedial (AM), and interanteromedial (IAM) nuclei were all strongly labeled, whereas the anterodorsal (AD) showed only low to moderate hybridization. Of the midline and intralaminar nuclei, the paraventricular (pvn), reuniens (Re), and rhomboid (Rh) nuclei were only weakly to moderately labeled; the centrolateral (CL) was weakly labeled; and the centromedian (CM) and parafascicular (PF) nuclei displayed moderate to high hybridization signal. In the ventral thalamus, the reticular nucleus (Rt) was extremely weakly labeled, while the zona incerta (ZI) and the fields of Forel (FF) contained sparsely scattered neurons expressing moderate levels of VGF mRNA. The ventral lateral geniculate (vLGN) and the intergeniculate leaflet (igl) contained a few neurons with low to moderate labeling. The subthalamic nucleus (STN) and the posterior portion of the subparafascicular nucleus (SPF) were moderately labeled, and the peripeduncular nucleus (PP) and the medial SPF were strongly labeled.

There was no VGF mRNA hybridization detectable in the medial habenula; in the lateral habenula only low levels of labeling were seen (Figure 4L-M).

Hypothalamus

Several regions of the ventral hypothalamus displayed very high levels of VGF mRNA hybridization (Figure 4I-N): the suprachiasmatic preoptic (PSCH), median preoptic, preoptic periventricular (PVpo), anteroventral periventricular (AVPV), supraoptic (SON), suprachiasmatic (SCN), arcuate (ARH), and posterior periventricular (PVp) nuclei especially. The anterodorsal and anteroventral preoptic (ADP, AVP), parastrial (PS), dorsomedial (dmH), ventromedial (vmH; dorsomedial part and a few cells in the ventrolateral part), posterior (PH), and the anterior and dorsal portions of the anterior hypothalamic (AHN) nuclei, and subparaventricular zone were moderately to strongly labeled. Other moderately labeled nuclei included: the parvicellular portions of the paraventricular nucleus (in the lateral posterior magnocellular portion labeling was very low); the intermediate periventricular nucleus (PVi); the medial preoptic area; and the medial part of the medial preoptic nucleus (the lateral part was weakly labeled). The lateral hypothalamic area generally displayed low to moderate labeling but also contained a number of scattered strongly labeled cells.

Labeling in the mammillary bodies was very low. No VGF mRNA was detectable in the medial mammillary nucleus, although weak labeling could be appreciated in the lateral mammillary nucleus. The supramammillary nucleus, however, showed moderate labeling in its lateral portions and strong labeling in its medial region, and the tuberomammillary nuclei were moderately to strongly labeled as well (Figure 4N).

Brainstem

In the pretectal area of the midbrain (Figure 4M-O), moderate VGF mRNA hybridization was observed in the posterior pretectal nucleus (PPT) and most other regions, with the exception of the anterior pretectal nucleus (APN) which was only weakly labeled.

Both the substantia nigra pars reticulata and pars compacta displayed moderate VGF mRNA labeling (Figure 4P). The ventral tegmental area and red nucleus were moderately labeled with a number of strongly labeled cells throughout. The interpeduncular nucleus (IPN) displayed moderate to high labeling which appeared highest in the central, apical, and dorsomedial subnuclei. The mesencephalic reticular nucleus (MRN) and pedunculopontine nucleus (PPN) were found to have low hybridization levels overall, yet they did contain a few moderately or strongly labeled cells. The retrorubral fields (RR) contained more such cells.

In the superior colliculus, the superficial gray was unlabeled, but the dorsal and intermediate gray had moderate to strong labeling which was strongest at the midline between the two colliculi (Figure 4P-R). The external nucleus of the inferior colliculus was strongly labeled as was the nucleus of the brachium of the inferior colliculus. Within the inferior colliculus itself there was strong patchy labeling throughout (Figure 4S).

The Edinger-Westphal (E-W), oculomotor (III), and trochlear (IV) nuclei labeled very robustly with the VGF probe. The nucleus of Darkschewitsch (Drk) labeled strongly, while the interstitial nucleus of Cajal exhibited low to moderate hybridization, and the abducens nucleus (VI) had very little signal. The periaqueductal gray labeled strongly, as did the suprageniculate nucleus, and the dorsal tegmental nucleus displayed moderate to high hybridization signal. The region of the locus coeruleus did not appear to be labeled. Several regions of the raphé contained moderate to high levels of VGF message, as did much of the brainstem reticular formation.

The pontine nuclei displayed intense VGF hybridization signal, and the tegmental reticular nucleus was strongly labeled as well. The medial accessory and principal inferior olives expressed moderate amounts of VGF message, as did the lateral reticular nucleus (Figure 4V-Y).

Although the principal sensory nucleus of the trigeminal was essentially unlabeled, the paratrigeminal nucleus was lightly labeled, and some of the other sensory trigeminal nuclei, such as most divisions of the oral part of the spinal trigeminal nucleus exhibited strong VGF mRNA hybridization. The motor nucleus of the trigeminal was quite highly labeled. The external cuneate nucleus displayed strong labeling as well (Figure 4Y).

The cochlear nuclei were moderately to strongly labeled, and the nucleus of the lateral lemniscus and the periolivary nuclei were strongly labeled. The nucleus of the trapezoid body, however, appeared unlabeled. The lateral vestibular nucleus contained very strongly labeled cells; while the superior and medial vestibular nuclei displayed moderate labeling. The nucleus prepositus was lightly to moderately labeled, as was the efferent vestibular nucleus.

The lateral portion of the nucleus tractus solitarius displayed occasional moderate labeling; the medial portion labeled only weakly. The dorsal motor nucleus of the vagus was not labeled. Portions of the parabrachial nucleus were moderately to strongly labeled, particularly the central lateral part and the Kölliker-Fuse subnucleus.

The facial nucleus (nVII) contained low to moderate hybridization signal. The vagal (nX) and hypoglossal (nXII) nuclei, however, were very strongly labeled. A few cells in the salivatory nuclei displayed moderate to high labeling, and the nucleus ambiguus was moderately labeled.

Cerebellum

Most of the granular layer of the cerebellar cortex was devoid of VGF labeling, however, sprinkled throughout were occasional cells robustly expressing VGF message (Figure 4U-Z; Figure 7A) often apparently, but not always, near the Purkinje cell layer. At higher magnification (Figure 7B), some cells strongly expressing VGF were clearly seen to be in the granular layer, and appeared to be larger than the surrounding granule cells (*white arrowheads*). A few smaller, more moderately labeled cells actually appeared to be in the Purkinje cell layer, between the Purkinje cell somata (*black arrowheads*). These neurons could all be Golgi cells which, though they generally reside in the granular layer can also be found in the Purkinje cell layer. On the other hand, given their location, those in the Purkinje cell layer could be candelabrum cells as well (Lainé and Axelrad 1994). As they are found in the cerebellar hemispheres as commonly as in the vermal areas, they are unlikely to be unipolar brush cells (Mugnaini and Floris 1994). Furthermore, the Purkinje cells themselves appeared to express very low levels of VGF mRNA as well. There were no labeled cells in the molecular layer.

Moderate to strong VGF mRNA hybridization was observed in all of the deep cerebellar nuclei (Figure 4V-Y). A higher magnification image of the fastigial nucleus is shown in Figure 7C and C′.

Spinal cord

At all levels of spinal cord examined, neurons throughout the extent of both the dorsal and ventral horns displayed robust VGF mRNA expression (Figure 8A-C). In the ventral horn, the large α-motor neurons were clearly and strongly labeled, as were a number of smaller neurons (probably small α- and γ-motor neurons) while glial profiles and capillaries were not (Figure 8D). White matter tracts, fasciculi, and nerve roots were unlabeled.

Retina

Figure 9 shows the distribution of VGF mRNA in the adult retina. While low levels of hybridization were appreciated over the inner segments of the photoreceptors and over the outer nuclear layer, the cells of the inner nuclear and ganglion cell layers displayed robust VGF expression.

VGF mRNA expression in the adrenal gland

Figure 10 shows the pattern of *in situ* hybridization obtained in the adrenal gland. The cells of the adrenal medulla displayed strong VGF mRNA expression, whereas no hybridization was detected in the adrenal cortex.

Figure 3: Specificity of the VGF probe in *in situ* hybridization analysis. Panel *A* is an inverted film autoradiograph showing the predominantly nervous system-specific VGF hybridization pattern obtained in a parasagittal section of an E19.5 rat fetus. Panels *B* and *B′* are near-adjacent parasagittal sections of an E13.5 embryo hybridized with the VGF sense-strand control and VGF antisense probes respectively. Panels C and *C′* are similar sense and antisense *in situs* in parasagittal sections of a P10 brain. The emulsion autoradiograph seen under bright field optics in Panel *D* demonstrates the neuronal specificity of VGF probe hybridization in adult brain: many neurons (large pale nuclei) show labeling, whereas glial cells (small dark nuclei) do not. Scale bars: *A-C,* 2 mm; *D,* 25 μm.

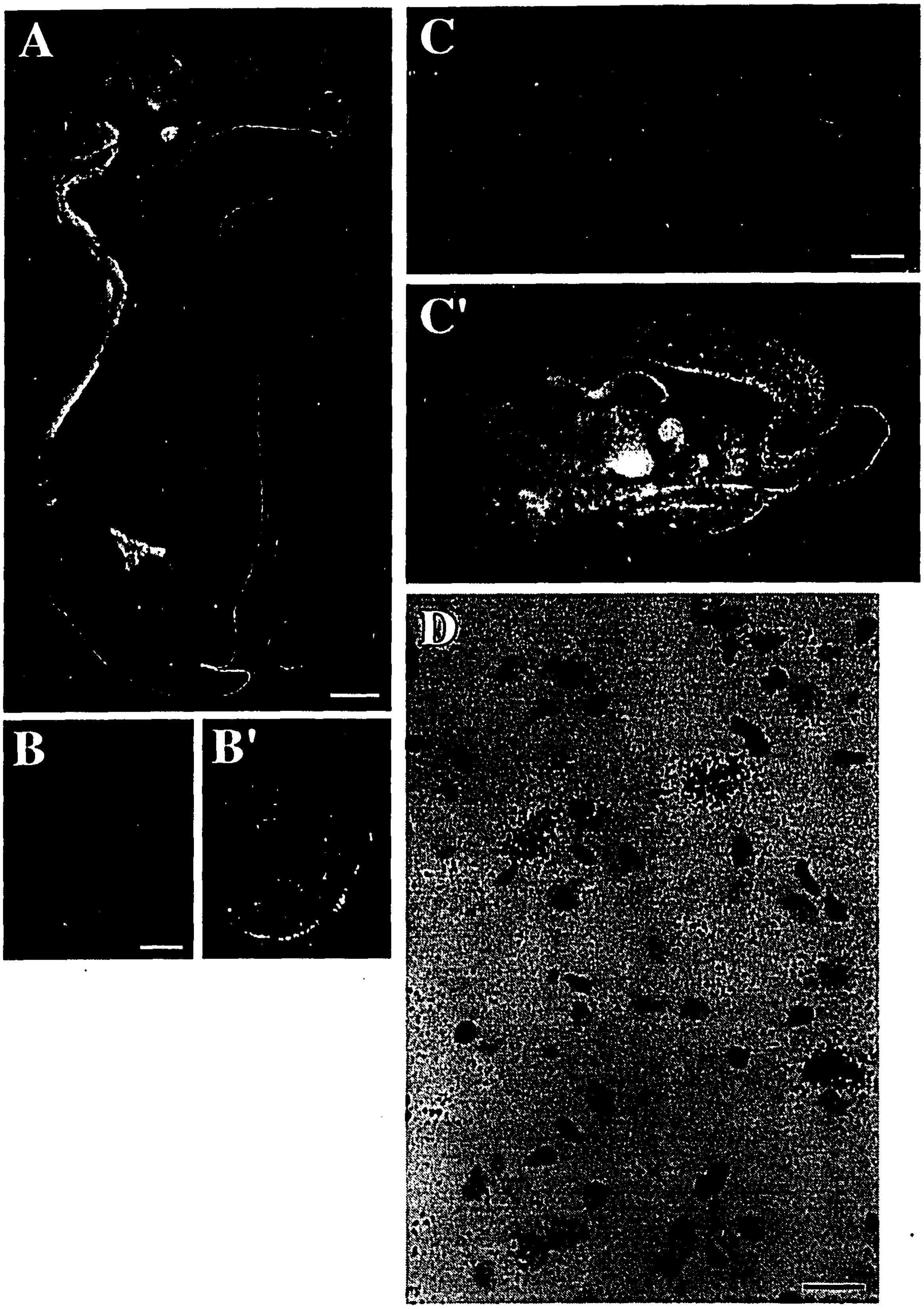
A
B
B'
C
C'
D

Figure 4: VGF mRNA expression in a series of coronal sections of the adult rat brain (female; multiparous) extending from the olfactory bulbs (rostral; *A*) to the medulla (caudal; *BB*). Low magnification inverse film and a few dark field emulsion (*A-D, G, S*) autoradiographs illustrating hybridization of the ^{35}S-labeled VGF riboprobe are shown. Areas displaying greater hybridization intensity corresponding to higher levels of mRNA appear bright against a dark background. Scale bars: *A-C,* 1 mm; *D-BB,* 2 mm.

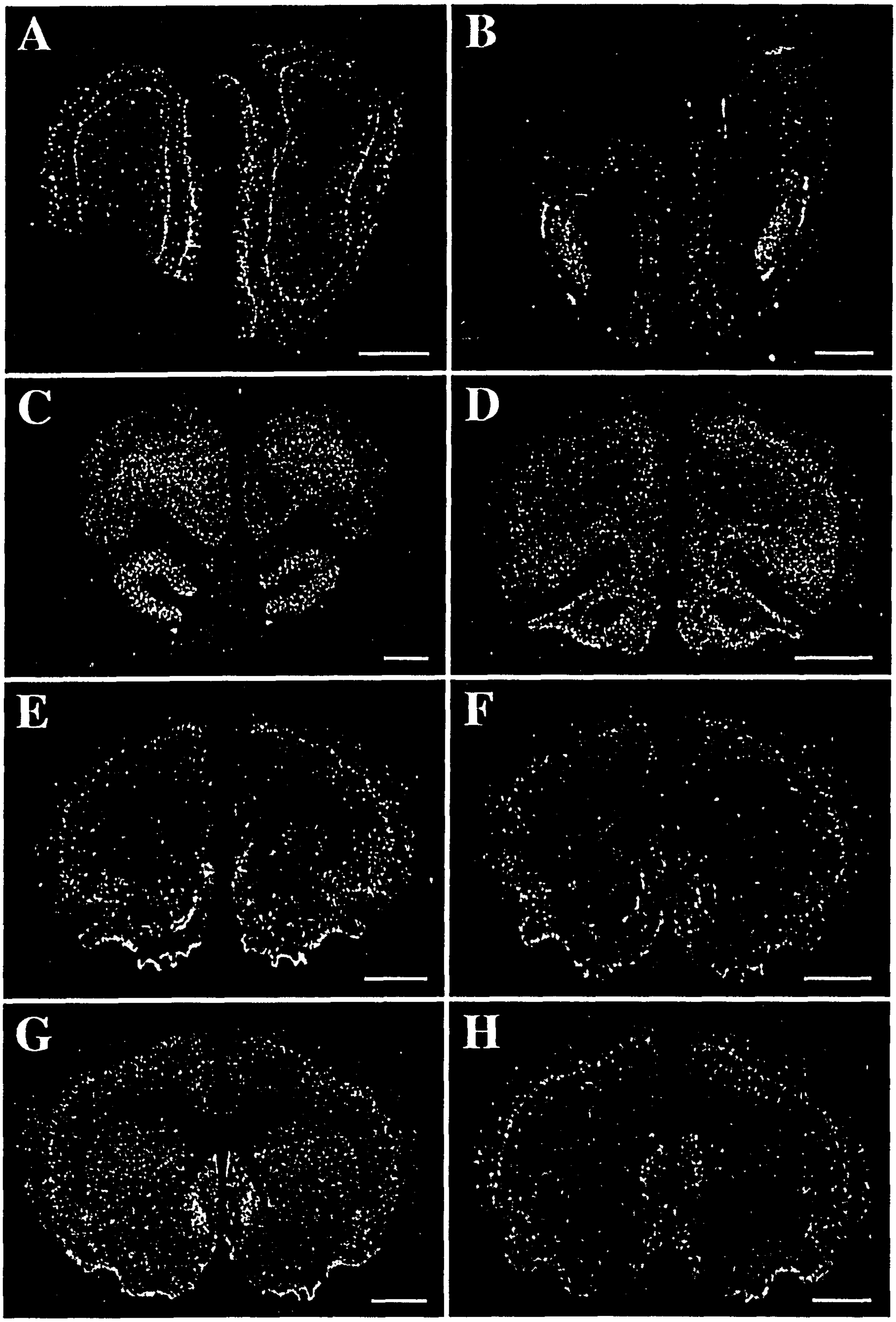
A
B
C
D
E
F
G
H

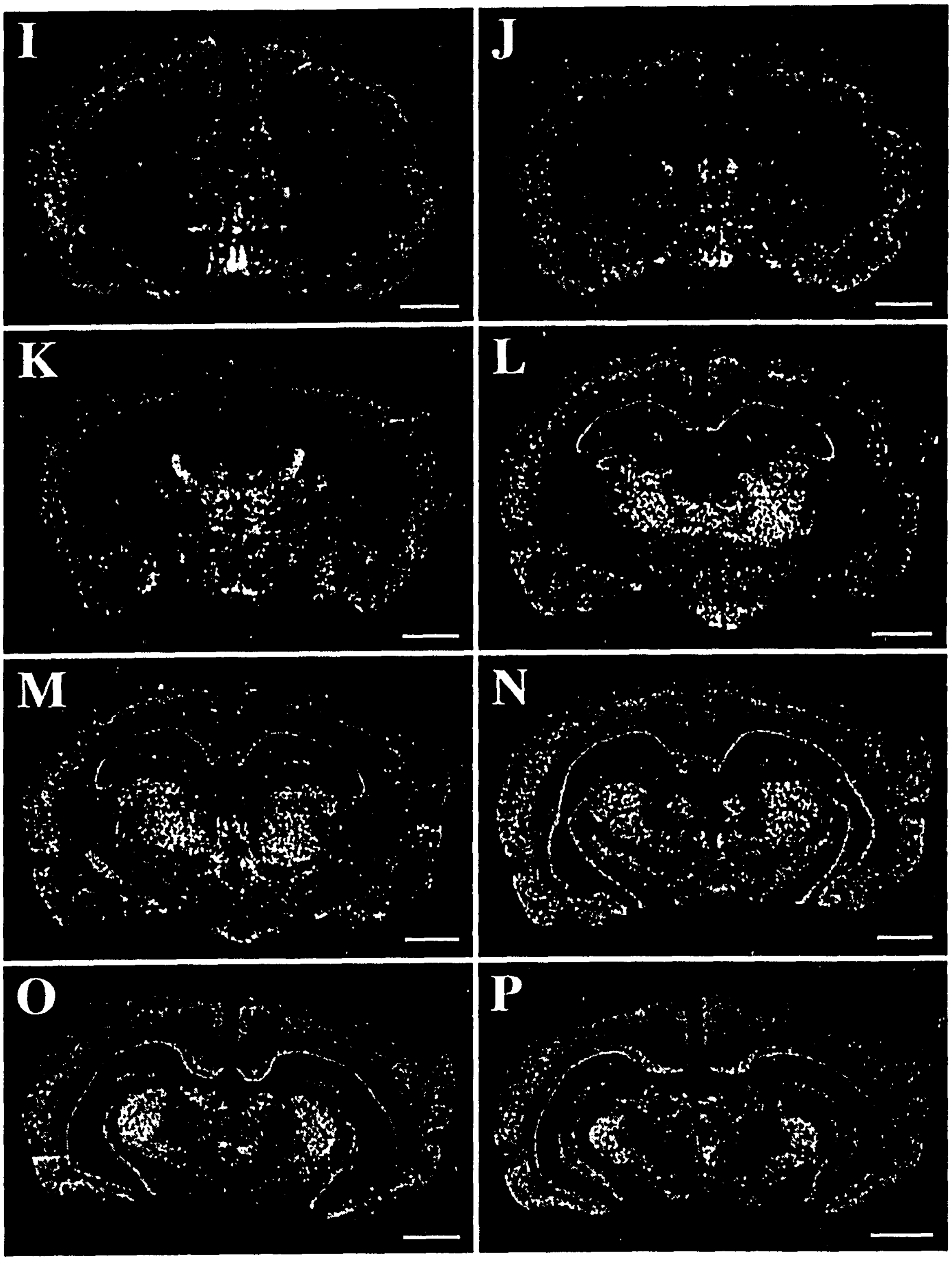
I
J
K
L
M
N
O
P

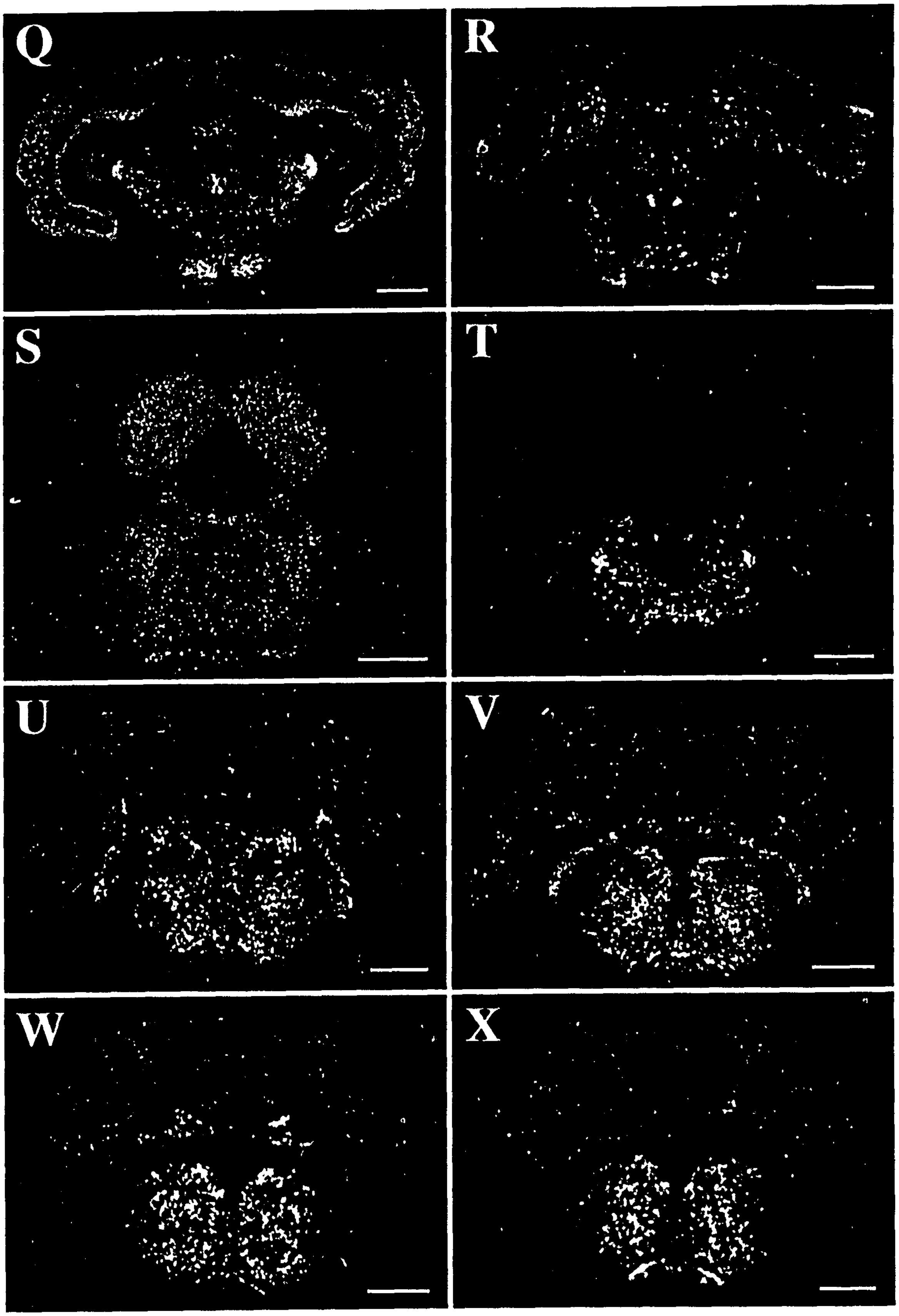
Q
R
S
T
U
V
W
X

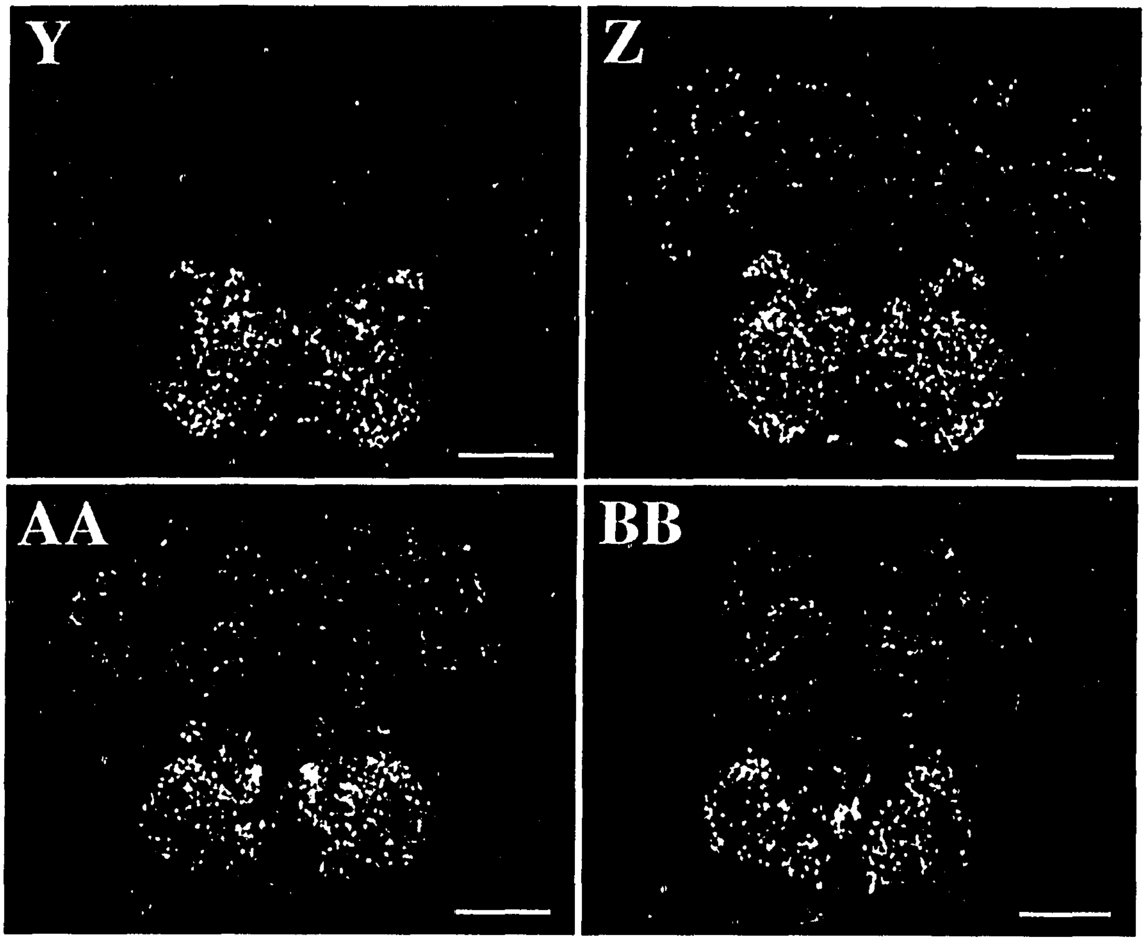
Y
Z
AA
BB

Figure 5: VGF mRNA expression in a series of horizontal sections of the adult rat brain (female; nulliparous) extending from dorsal (*A*) to ventral (*G*). The olfactory bulbs were somewhat damaged during the dissection. Low magnification inverse film autoradiographs are shown. Scale bars, 2 mm.

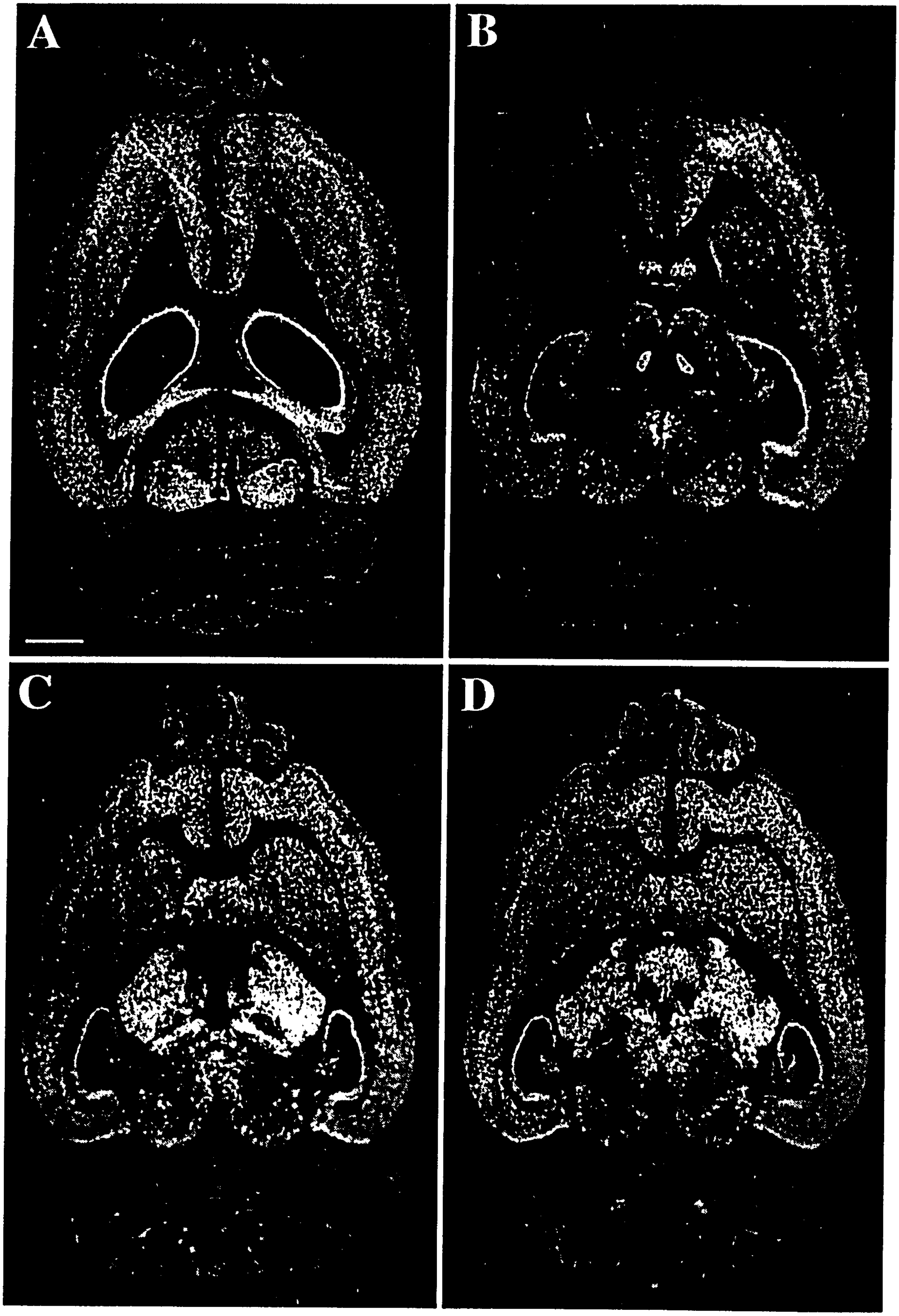
A
B
C
D

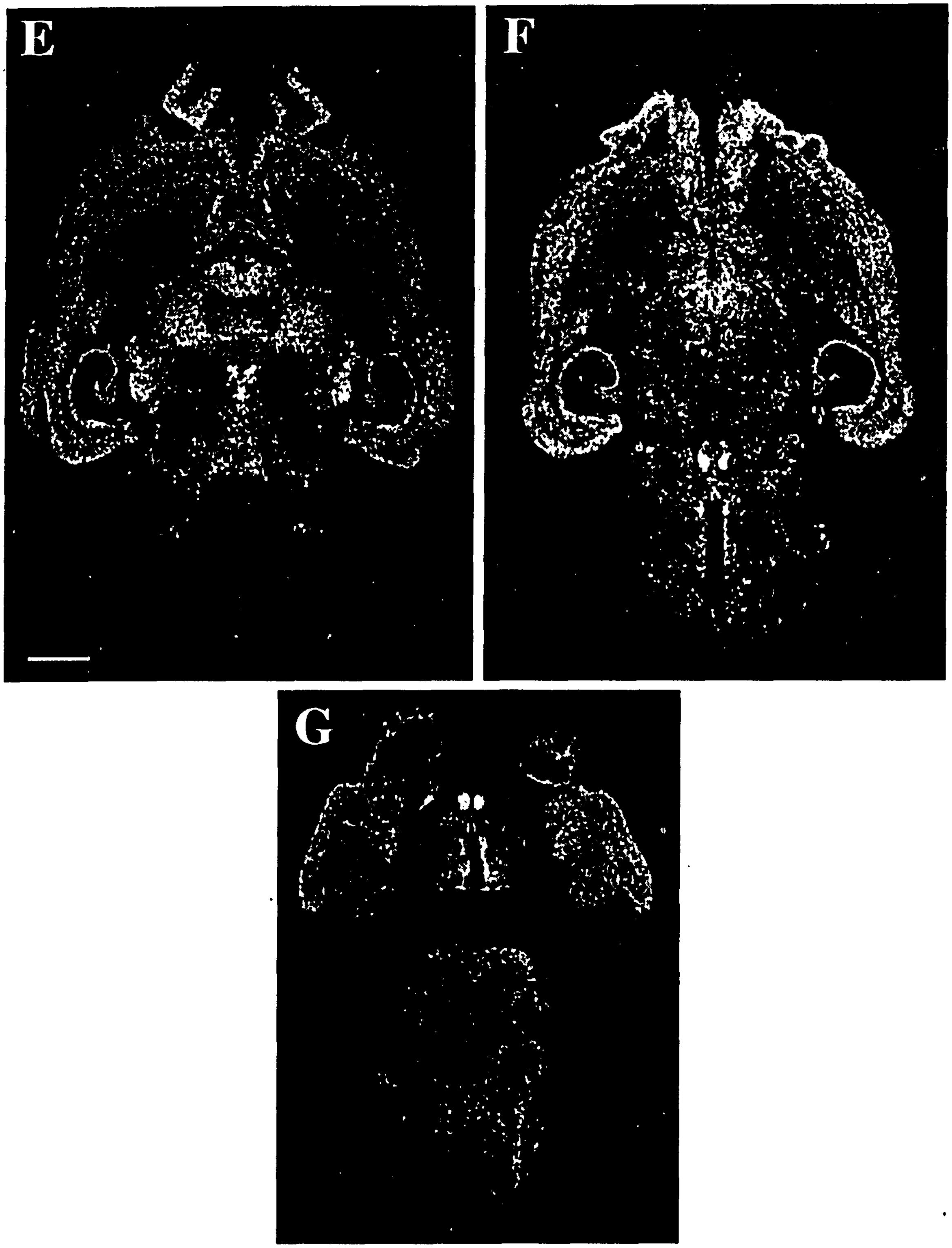
E
F
G

Figure 6: High magnification emulsion autoradiographs of VGF mRNA hybridization in selected regions of the adult rat brain. All but *A* are dark field photomicrographs. *A, A'*: Olfactory bulb, from a horizontal section, photographed under bright field (cresyl violet counterstain) and dark field optics respectively. *B*: Basal ganglia, from a horizontal section. *C*: Septal region, from a horizontal section *D*: Coronal section through the neocortex *E*: Coronal section through the dorsal hippocampus. Scale bars: *A*, 100 µm; *B*, 500 µm; *C*, 200 µm; *D*, 200 µm; *E*, 500 µm.

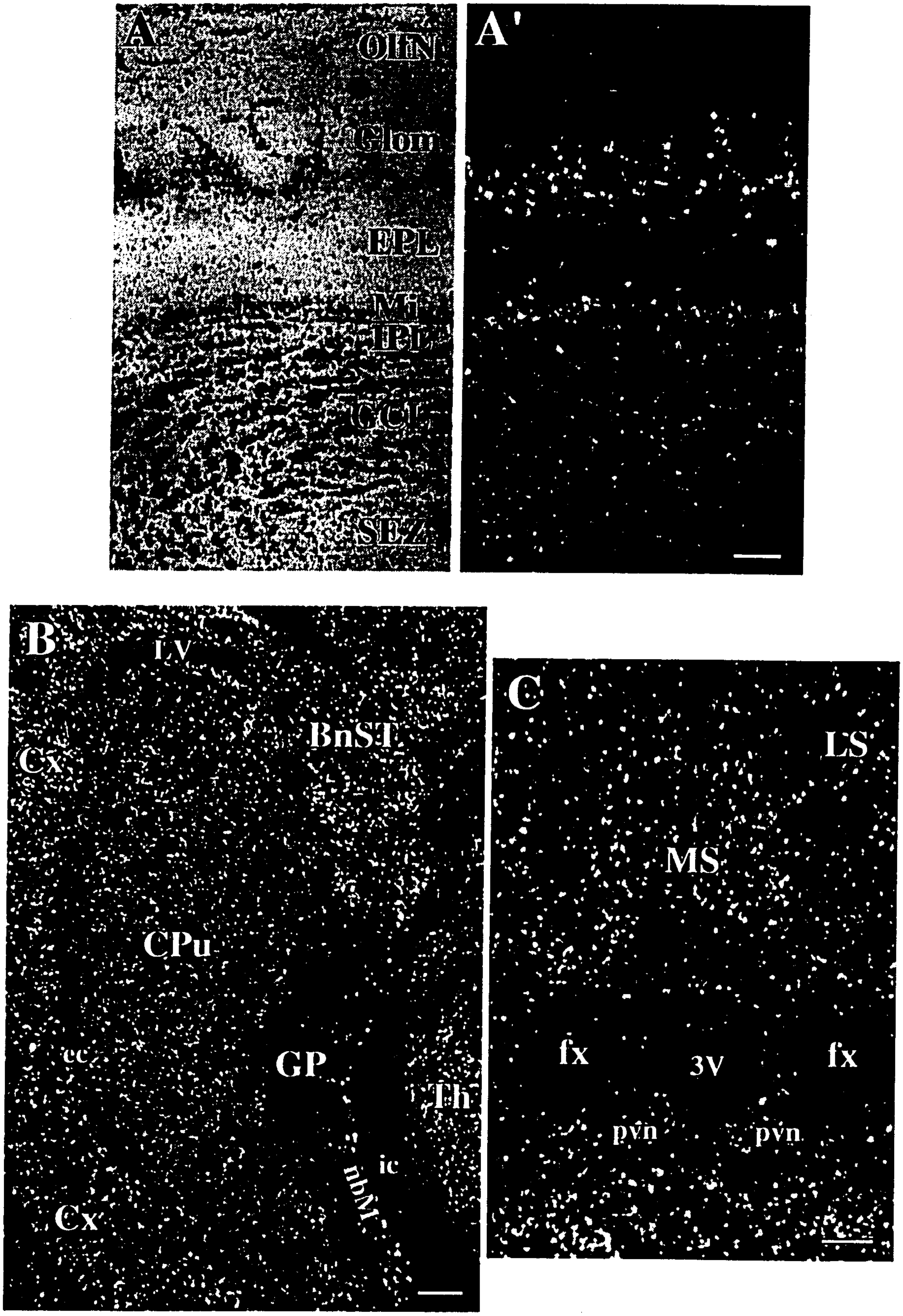
A
OlfN
Glom
EPL
Mi
IPL
GCL
SEZ
A'
B
LV
BnST
Cx
CPu
cc
GP
Th
ic
nbM
Cx
C
LS
MS
fx
3V
fx
pvn
pvn

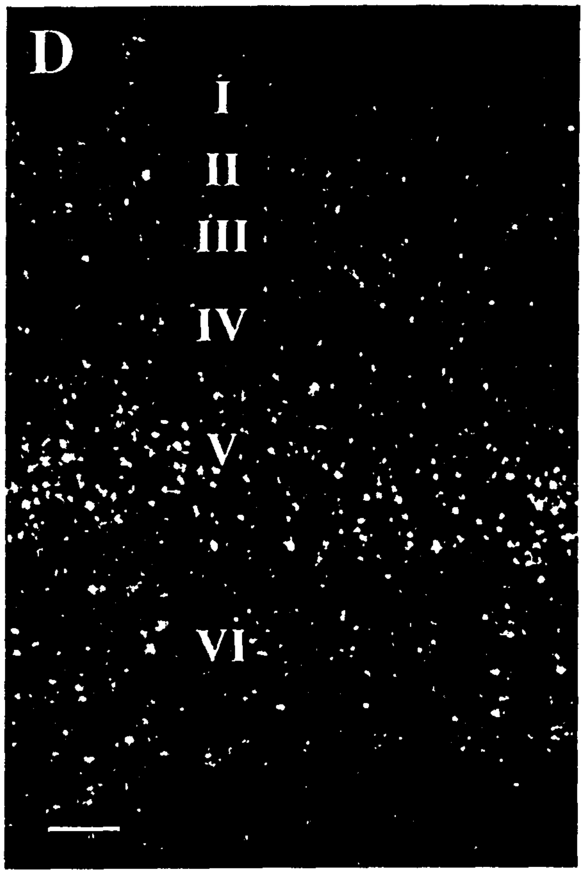
D
I
II
III
IV
V
VI

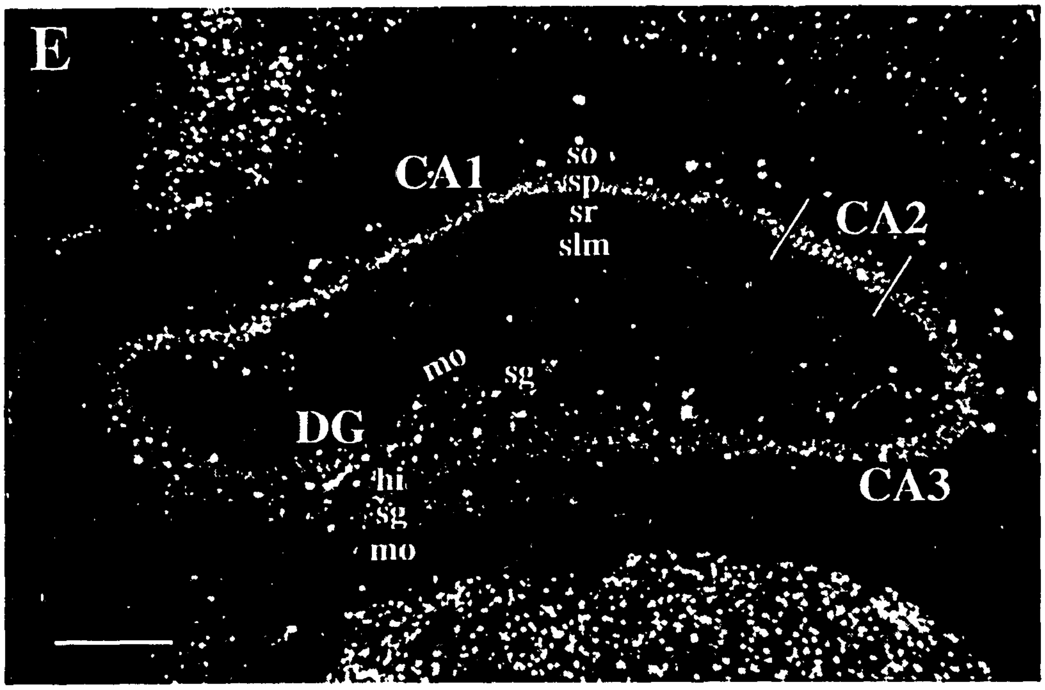
E
CA1
so
sp
sr
slm
CA2
mo
sg
DG
hi
sg
mo
CA3

Figure 7: High power emulsion autoradiographs of VGF mRNA hybridization in the adult cerebellum. A moderately high magnification dark field photomicrograph of one lobule is shown in *A*. *B* is a much higher magnification bright field photomicrograph showing VGF riboprobe hybridization (signal appears as small black grains) to a few cells in the granular layer (*Gr; white arrowheads*), and Purkinje layer (*Pkj; black arrowheads*) including low levels in the Purkinje cells themselves (*large pale cells in the Purkinje layer*). *C* and *C′* are bright and dark field images respectively, showing labeling of the fastigial nucleus (*FN*). Scale bars: *A*, 500 µm; *B*, 25 µm; *C & C′*, 100 µm.

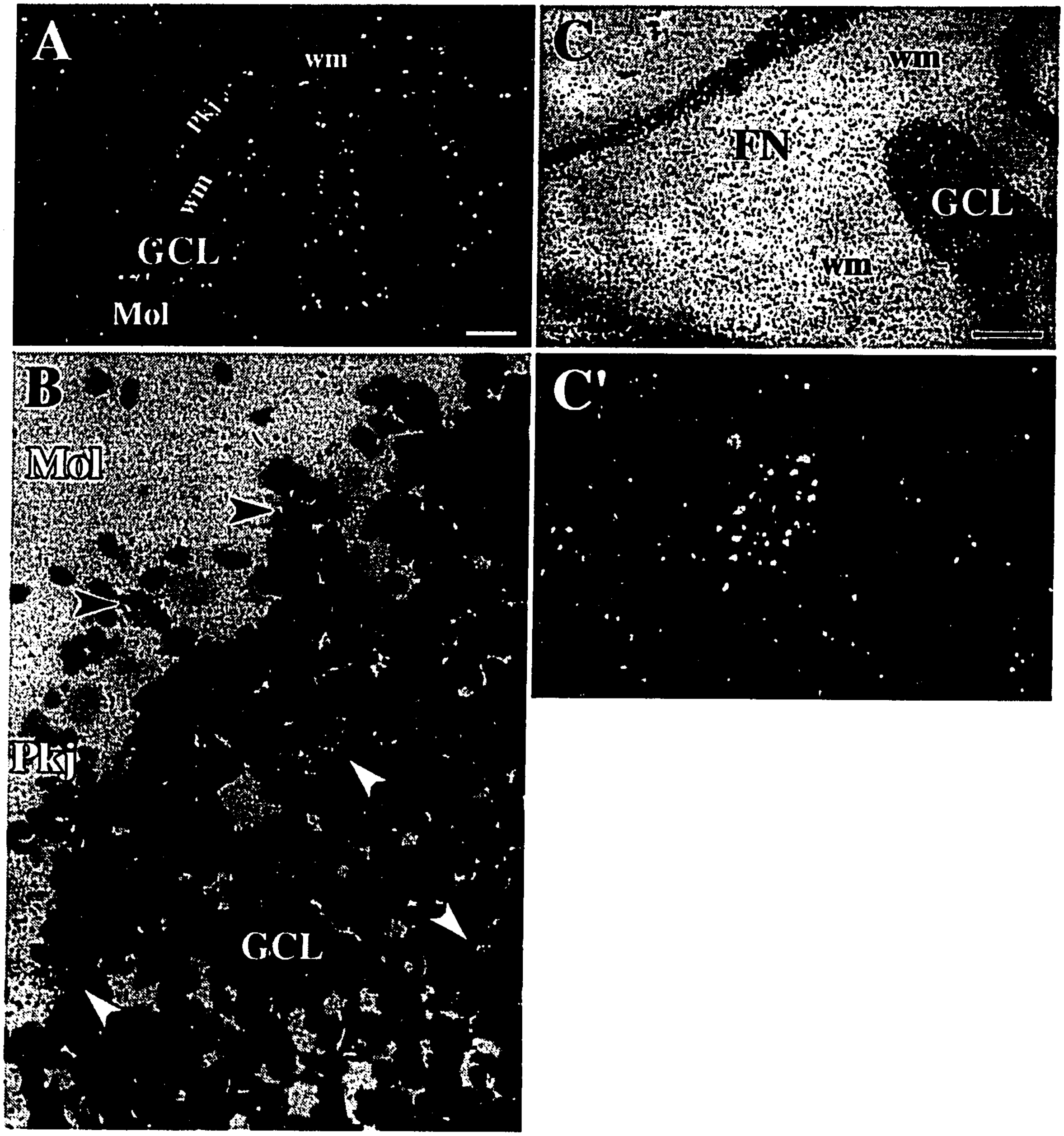
A
wm
Pkj
wm
GCL
Mol
C
wm
FN
GCL
wm
B
Mol
Pkj
GCL
C'

Figure 8: VGF mRNA expression in the adult spinal cord. *A*-C show dark field emulsion autoradiographs of transverse sections through the spinal cord at approximately the C5, L5, and sacral levels respectively. Strong hybridization over neurons of the ventral horn (*white arrowheads*) including a number of α-motor neurons (α) is shown at higher magnification in *D*. Note that glial profiles and a capillary traversing the field (*small black arrowheads*) are unlabeled.
Scale bars: *A-C*, 500 μm; *D*, 50 μm.

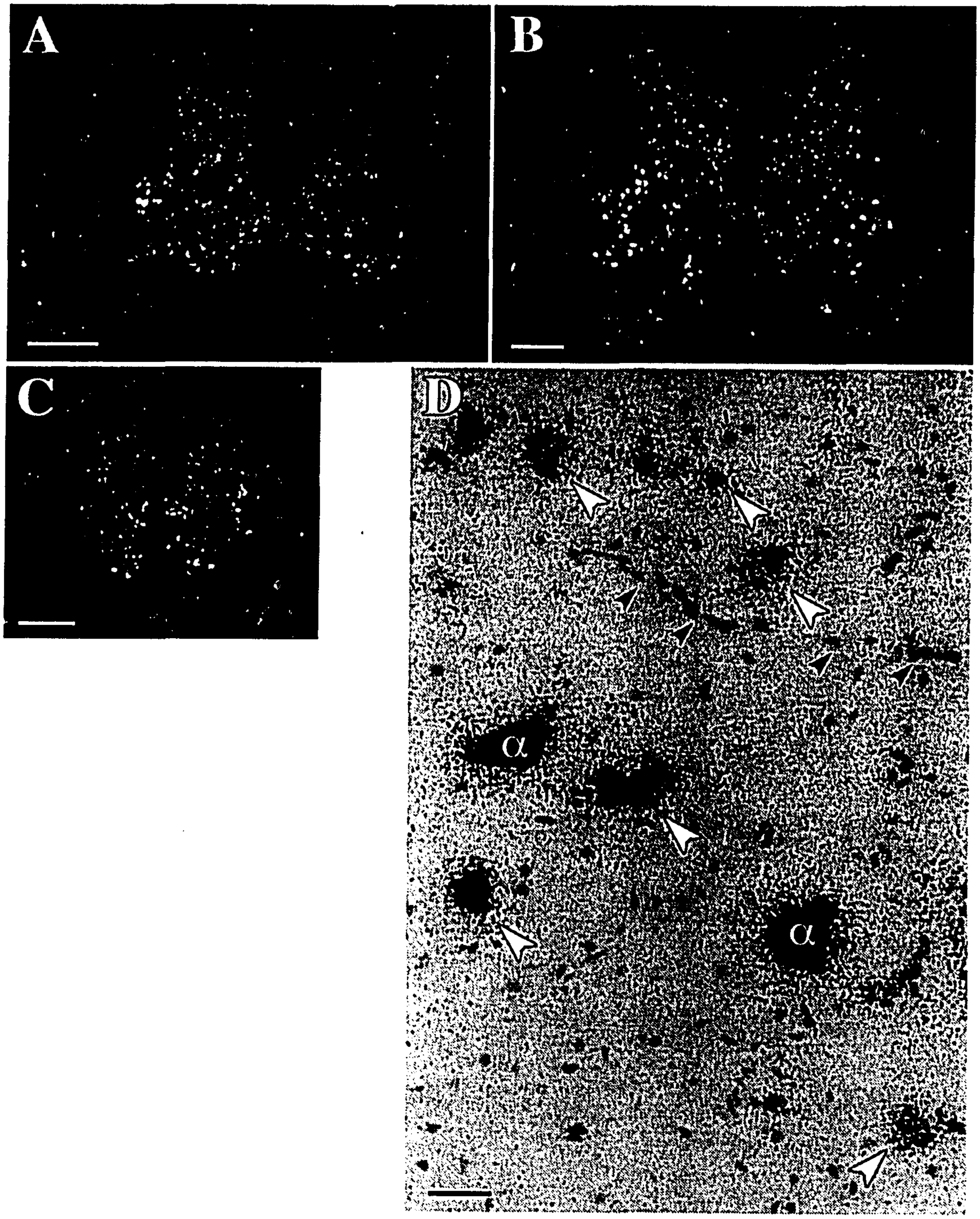
A
B
C
D
α
α

Figure 9: VGF mRNA expression in the adult retina. Bright field (*A*) and dark field (*B*) photomicrographs show strong hybridization in the inner nuclear (*INL*) and ganglion cell (*GaCL*) layers. Scale bar, 50 µm.

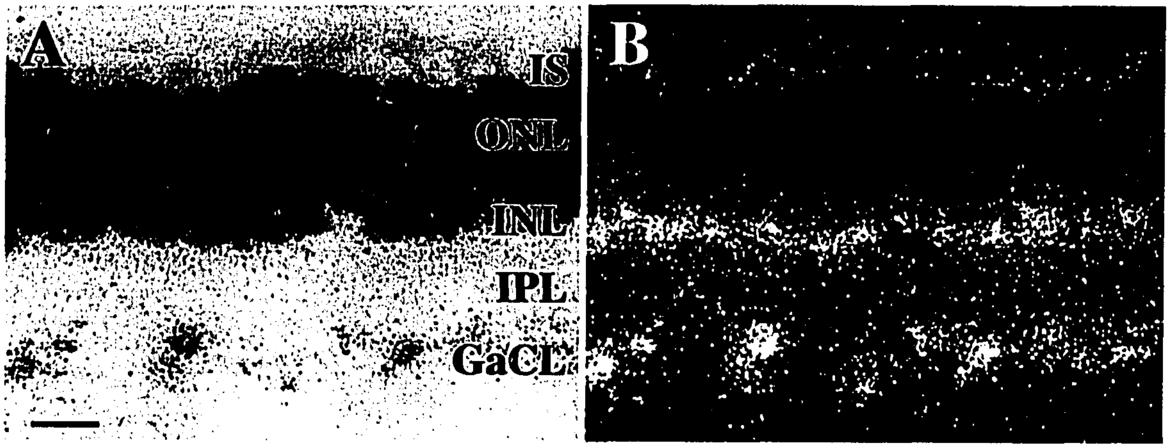
A
IS
ONL
INL
IPL
GaCL
B

Figure 10: VGF mRNA expression in the adult adrenal gland. A dark field emulsion autoradiograph demonstrating strong hybridization in the medulla (*Md*) but none in the cortex (*Cx*) is shown. Scale bar, 250 μm.

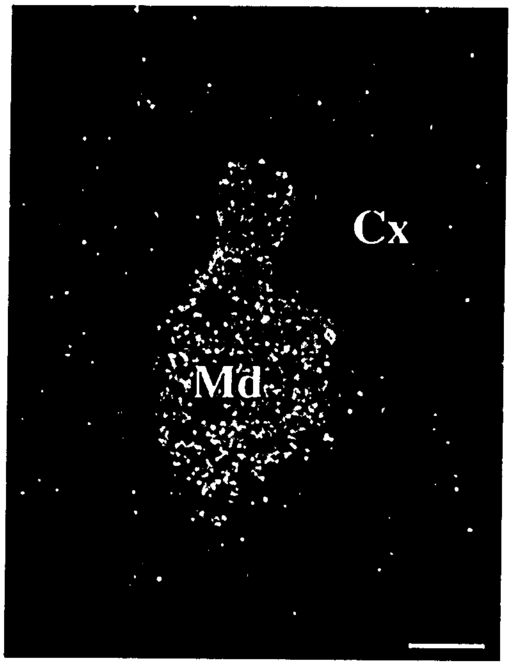
Cx
Md

Discussion

Consistent with previous northern and RNase protection analyses, immunohistochemical and *in situ* studies (van den Pol *et al.* 1989, 1994; Salton *et al.* 1991; Ferri *et al.* 1992; Mahata *et al.* 1993a; Lombardo *et al.* 1995), the current data show that VGF mRNA is expressed in many regions of the adult rat brain and spinal cord. Furthermore, and also in agreement with earlier work, VGF mRNA expression *in vivo* was found to be restricted to neuronal and neuroendocrine cell populations.

In contrast to earlier accounts of VGF *in situ* hybridization (van den Pol *et al.* 1989; Mahata *et al.* 1993a; Lombardo *et al.* 1995), which were not very comprehensive and/or actually showed little of the data which were discussed, I have conducted a detailed examination of VGF mRNA expression throughout the adult rat CNS. My data both confirm and extend the earlier studies, in that I observed VGF mRNA hybridization in all of the locations reported previously; but further, I have found the expression pattern to be much more extensive, including many neuronal populations throughout all levels of the brain and spinal cord, than has been previously described. Additionally, I have demonstrated for the first time, expression of VGF mRNA in the retina, where it is particularly abundant in the retinal ganglion cells and inner nuclear layer.

Furthermore, the distribution of VGF-like immunoreactivity reported in published immunohistochemical studies (Ferri *et al.* 1992; van den Pol *et al.* 1994; Lombardo *et al.* 1995) is also much more restricted than the mRNA distribution I have shown here—in most cases largely because the authors were not attempting to give an exhaustive account of VGF expression throughout the CNS. In their recent paper, van den Pol *et al.* (1994) did make an effort to describe VGF expression in the brain in detail—showing VGF-like immunoreactivity in the olfactory tubercle, septum, caudoputamen, supraoptic and paraventricular nuclei of the hypothalamus, central amygdala, paraventricular nucleus of the thalamus—yet the pattern they reported, even using colchicine to inhibit transport of proteins into neuronal processes, is only a subset of that described here, and showed little immunoreactivity in a number of brain regions where even their own northern analysis had detected high levels of VGF mRNA, such as olfactory bulb and cerebellum. While it is possible that this discrepancy may be due to variability in the rate of VGF transcription or translation, or in the stability of the RNA or protein, it seems that the restricted distribution of VGF reported in van den Pol's study is most likely due to their unfortunate use of antisera directed against AAs 80-340 and 443-580 of the VGF polypeptide. Recently, VGF in neurons has been shown to be processed into small peptides (Trani *et al.* 1995), most of which derive from the C-terminus of the VGF polypeptide and are detectable by antisera raised against AAs 572-617 or AAs 608-617 but not an anti-$VGF_{4\text{-}240}$ antiserum: these peptides would very likely not be detected by the anti-$VGF_{80\text{-}340}$, and could even be missed by the anti-$VGF_{443\text{-}580}$ antisera used by van den Pol *et al.* Despite this, particularly strong immunostaining was seen in the hypothalamus, implying that like peripheral neuroendocrine tissues such as the adrenal medulla (Trani *et al.* 1995), the neurosecretory cells of the hypothalamus may not process VGF into small peptides as do most neurons. Should this hypothesis prove to be correct, subsequent immunohistochemistry using more C-terminal antisera would be expected to yield a pattern of labeling more similar to that which I report here, and is eagerly awaited.

Although early studies in our laboratory did not detect VGF mRNA expression in whole adrenal gland homogenates (Salton *et al.* 1991)—perhaps due to degradation of the RNA by substances from the adrenal cortex, or perhaps due to lack of sensitivity of the assays—northern analysis of RNA from isolated adrenal medulla demonstrated that there are low levels of VGF mRNA expressed in that tissue (Ferri *et al.* 1992). In the same study, using anti-VGF_{80-340} and anti-$VGF_{443-558}$ sera, VGF-like immunoreactivity of varying intensity was observed in the outer portion of the adrenal medulla. While my data confirm this finding by demonstrating the anatomical localization of VGF mRNA in the adrenal medulla, I observed no particular predilection of the hybridization signal for the outer portion of the medulla. Recently, Laslop *et al.* (1994) have described data suggesting that VGF mRNA is synthesized not only by chromaffin cells but by the ganglion cells of the adrenal medulla as well, and that expression in both cell types is inducible by reserpine treatment, which is known to stimulate the adrenal medulla.

Furthermore, earlier studies in our laboratory have shown VGF mRNA expression in the adult SCG (Salton *et al.* 1991), and others have shown mRNA in the dorsal root and trigeminal ganglia, and immunoreactivity both there and in the coeliac ganglion, enteric plexuses, gut endocrine mucosal cells, and anterior pituitary, as well as immunostained nerve fibers scattered throughout many other organs (Ferri *et al.* 1992).

Despite the discovery of VGF as a uniquely NGF-inducible gene, and regardless of the fact that NGF induces VGF more potently than any other known stimulus, the distribution of VGF mRNA in the CNS as detailed in the current study and those described above, and in the PNS as shown by others, implies that something other than NGF must be responsible for the vast majority of VGF expression in the adult animal, since the distributions of NGF and its receptors are far more limited than that which we see for VGF. Induction by related neurotrophins and/or neuronal activity is likely to account for much of the remainder of the expression of this widespread neuronal peptide precursor.

Chapter 4: Distribution of VGF mRNA in the Developing Rat Nervous System

Introduction

Given that VGF gene expression is primarily neuronal, abundant during development, and highly neurotrophin-inducible, and that its protein product is secreted from the cell, it is likely that VGF plays a vital role in nervous system development (Possenti *et al.* 1989; Salton *et al.* 1991; Ferri *et al.* 1992). Determination of the time of onset of VGF expression and the characterization of the anatomical pattern of VGF expression during embryogenesis and throughout neural ontogeny should prove helpful in establishing the nature of this function. Yet previous studies from our laboratory and others describing the distribution of VGF during development were restricted to northern analysis, RNase protection assays, and limited observation of VGF immunoreactivity in P4 brain (van den Pol *et al.* 1989; Salton *et al.* 1991). While these studies showed that VGF message levels in the CNS peak during the first two weeks of postnatal life, they were unable to provide detailed resolution, and did not pinpoint the date of onset of VGF expression. Thus, I undertook an investigation of VGF in development. In this study, I describe the anatomical localization of VGF mRNA as determined by *in situ* hybridization from midgestation through the first week and a half of life in the rat.

Results

The distribution of VGF mRNA in the developing rat from the time of neural tube closure into the second week of life is shown in Figures 11 and 14-31. VGF mRNA expression overwhelmingly predominated in the central and peripheral nervous systems at all ages studied. Specific hybridization was first observed at midgestation in cranial and sensory ganglia, and gradually acquired a broad distribution throughout the central nervous system as well. This remarkably nervous system-specific pattern of VGF mRNA distribution at various stages of development is described in detail below.

Spatial and temporal distribution of VGF mRNA in the developing rat

To characterize the ontogenic expression pattern of the VGF gene, the regional and cellular localization of VGF mRNA was studied using *in situ* hybridization in rats from embryonic day 11.5 (E11.5) to postnatal day 10 (P10). In general, VGF expression first appeared in sensory ganglia, then in the spinal cord and a few restricted regions of the brain. Brain expression expanded gradually, with widespread labeling of neocortex appearing quite late in development. Areas containing predominantly dividing cells such as the ventricular and subventricular zones of the central nervous system were invariably devoid of VGF mRNA expression, as were the vast majority of non-neural tissues.

Embryonic day 11.5

VGF mRNA was undetectable in most sections of E11.5 embryos studied. However, as shown in Figure 11, hybridization was observed in regions containing neural crest-derived cells destined to become cranial, sympathetic and dorsal root ganglia, and over what appear to be migrating crest cells fated to become the enteric ganglia. Hybridization convincingly above background levels could not be detected in the neural tube. The notochord did not express detectable VGF mRNA at this or any subsequent stage of embryonic development.

High levels of VGF hybridization were also noted over occasional individual non-embryonic cells throughout the circumference of the uterine wall, and in a more dense cluster of cells in the thick bottom portion of the uterus (Figure 12).

Embryonic day 13.5

Maternal uterine labeling was also seen at E13.5 (Figure 13), the latest gestational age at which embryos were sectioned *in utero*. At this stage, the labeled cells were clearly aligned as a monolayer of cells which appeared to be just at the border between the maternal component of the decidual reaction and the trophoblast.

In the E13.5 embryo (shown in parasagittal section in Figure 14 and transverse section in Figure 15), strong VGF mRNA expression was seen in the developing DRGs, the ventrolateral mantle layer of the spinal cord, the anlage of the sympathetic chain and SCG, and in a number of developing cranial ganglia including the trigeminals (V), the facials (VII), the vestibulocochlear complex (VIII), the glossopharyngeals (IX), and the vagus-cranial accessory complex (X-XI). Moderate to high levels of VGF expression were found in several discrete cell populations in the ventral portion (basal plate) of the developing medulla including the facial nucleus, and low levels of hybridization were found in the outermost mantle layer of portions of the developing telencephalon and diencephalon. Occasional labeled cells were also found in the walls of the gut.

Embryonic day 15.5

By E15.5 (Figure 16), in addition to expression in the regions described above at E13.5, some localized areas of the brain contained cells which were expressing VGF message more strongly than before; in particular the basal forebrain, septal region, anterior and intermediate thalamus, hypothalamus, tegmentum, and anterior pons. Figure 17 shows at higher magnification VGF mRNA expression in several cranial ganglia (panels A and A′), DRGs (panel B), the spinal cord and sympathetic chain (panel C). In all of these ganglia the pattern of VGF hybridization appeared fairly uniform. Labeling was still strongly restricted to the ventral portion of the developing spinal cord. Furthermore, the portion of the developing pituitary corresponding to the future pars tuberalis displayed strong VGF mRNA expression (shown at higher magnification in Figure 17D and D′), as did a few cells in the region of the future pars anterior. In the developing retina, low levels of hybridization could be appreciated (data not shown). Strong hybridization signal was also seen in neural tissue surrounding the ducts of the submandibular gland—the presumptive submandibular ganglion. Labeling in the gut, in the stomach in particular, was now clearly seen to correspond to the location of the myenteric plexus (Figure 17E and E′). Moderate levels of hybridization were seen in the adrenal, low levels were found in the liver, and a few labeled cells were seen in the pancreatic primordium as well (shown at high power in Figure 17F and F′).

Embryonic day 17.5

By E17.5 (Figure 18) expression could now be identified in the developing olfactory bulbs, basal ganglia, preoptic area, amygdala, hippocampal formation, piriform cortex, and cerebellar anlage. Moreover, regions which were labeled at earlier stages such as the thalamus, hypothalamus, and brainstem exhibited stronger and somewhat more widespread hybridization than before. For example, labeling in a number of thalamic nuclei, including the dLGN, PoT, VP, and AV, was particularly intense. The outer layers of the cortical plate in some regions began to show very low levels of hybridization at this stage. In the spinal cord, labeling was no longer restricted to the ventrolateral mantle layer, but was now seen in the dorsal portion as well (shown at higher magnification in Figure 19B). Labeling in the retina at E17.5 was substantially higher than had been observed two days earlier (Figure 18D). This was also the case in the pancreas, in which hybridization was now grossly apparent (data not shown). Figure 19 shows at higher magnification VGF mRNA hybridization in several cranial ganglia (panels A and A′) and the myenteric plexus (panel C), which at this stage of development was clearly apparent not only in the stomach but throughout the small intestine. Lastly, portions of the epidermis began to show labeling for VGF mRNA at this time, and the vibrissal follicles were labeled as well.

Embryonic day 19.5

VGF mRNA expression the E19.5 fetus is shown in parasagittal section in Figure 20 and transverse section in Figure 21. While labeling could be newly seen in the olfactory tubercle, anterior olfactory nucleus, and entorhinal cortex among other areas, it should be noted that both the extent and intensity of VGF mRNA hybridization in previously labeled structures were substantially increased. For example, extremely low levels of hybridization seen in portions of the cortical plate at E17.5 had increased to moderate levels in the some areas, particularly the orbital and insular regions by this time. Hybridization in the cortical plate was found to be concentrated in cells in the outer half of the cortical plate proper (although some labeled cells could be seen in the deeper half) and in the subplate (Figure 22A and A′). In the olfactory bulb, labeling was seen throughout the inner plexiform layer, the granule cell layer, and the outermost portion of the subventricular zone (Figure 22B and B′). Furthermore, there was now VGF expression throughout the dorso-ventral extent of the spinal cord, particularly rostrally, although the ventral horn still demonstrated the most intense hybridization (Figure 22C-E′). The lateral cervical and lateral spinal nuclei were also clearly labeled.

Peripherally, the sympathetic, dorsal root, and cranial ganglia were still expressing large amounts of VGF mRNA at this stage (Figure 22F-G′). Furthermore, several parasympathetic ganglia, such as the sphenopalatine ganglion (Figure 22H and H′) were shown to express VGF mRNA in the E19.5 fetus. Very intense hybridization was observed in the region of the submandibular gland (Figure 22I_1 and I_2), which when underexposed could be shown to be labeling not of the gland itself nor of its ducts, but of clearly neural tissue which tended to be closely associated with the submandibular ducts—the parasympathetic submandibular ganglion (Figure 22I-I″). The cardiac ganglia were labeled as well (Figure 22J and J′).

The skin was also more clearly labeled at E19.5 than it had been earlier (Figure 21; Figure 22). Strong hybridization was seen throughout the entire epidermis, except the stratum corneum, in hair follicles (Figure 22K and K′), and in vibrissal follicles. In the abdomen (Figure 22L and L′), low VGF mRNA hybridization signal was still appreciable in the adrenal gland, while that in the pancreas had increased to quite high levels. In the gut, labeling of the myenteric plexus was strong throughout, including the esophagus, stomach, and bowel. Additionally, there was now also strong labeling of the esophageal mucosal layer. Mucosal labeling was also seen in the stomach, restricted to the fundus or non-glandular portion (Figure 21I; Figure 22M).

Day of birth (postnatal day 0)

The trend of expansion of the VGF expression pattern with increasing developmental age continued into the postnatal period—sections demonstrating the localization of VGF mRNA in the head of the newborn rat are shown in Figure 23 and Figure 24. Notably, expression had expanded further into the cortical regions, particularly the allocortices, while remaining low to nonexistent in most isocortical regions except the rostral frontal cortex. As a result, in many sections a dramatically high-contrast border occurs exactly at the rhinal fissure between the expressing and non-expressing cortex (Figure 24C-J, esp. panels C, F, H-J). A similar transition often occurs at the border between the cingulate or retrosplenial cortex and the adjacent parietal or occipital cortex.

VGF mRNA had also increased dramatically in the cerebellum by P0 (Figure 23A-E; Figure 24L). The deep nuclei in particular, were quite strongly labeled.

In the olfactory bulbs, the mitral cell layer was now found to label strongly with the VGF riboprobe (Figure 25A and A′), even more so than the internal granular layer. Cells in the deep part of the glomerular layer were also showing hybridization signal at this age.

The retina continued to express high levels of VGF mRNA which, as shown at higher magnification in Figure 25B, was predominantly found in the inner nuclear (neuroblastic) layer.

In the developing pituitary, VGF was clearly being expressed not only in the pars tuberalis (where it remained quite high), but more extensively in the pars anterior and also in the pars intermedia (Figure 25C and C′).

Postnatal day 5

As development continues into the first postnatal week, the pattern of

VGF mRNA expression begins to look more like that found in the adult brain, with moderate levels of VGF hybridization in many neurons throughout the diencephalon and brainstem, and particularly strong labeling in the principal thalamic relay nuclei and portions of the hypothalamus (Figure 26; Figure 27; Figure 28). The outstanding exceptions being the cerebellum which still labels more strongly than in the adult, and the neocortex which still labels less. The sharp demarcation at the rhinal fissure still exists, particularly more caudally between the perirhinal and the temporal and occipital cortices (Figure 26F-G). In the more rostral neocortex a striped VGF expression pattern with alternating radial bands of higher and lower hybridization can be seen (Figure 26C-D; Figure 27A-F). In the colliculi, VGF labeling was still quite low.

Postnatal day 10

P10 brains (Figure 29; Figure 30; Figure 31) approached the adult pattern of hybridization even more closely than did those taken at P5, in that for example, there was now somewhat broader expression in the isocortices. Labeling in the inferior colliculus increased dramatically at this age relative to surrounding structures. In the cerebellum, the development of which occurs predominantly postnatally, the pattern looks very different from that in the adult; there is strong VGF mRNA expression in the internal granule cell layer.

Ontogeny of VGF mRNA expression in selected structures

The cerebellum and hippocampus both have particularly characteristic and well understood adult cytoarchitecture and connectivity, and many details of their normal patterns of histogenesis, neurogenesis, migration, and synaptogenesis are well documented (Altman and Das 1965; Altman 1972a,b,c; Bayer and Altman 1974; Schlessinger *et al.* 1975, 1978; Bayer 1980a,b; Crespo *et al.* 1986; Altman and Bayer 1990a,b). In light of the availability of this information, detailed study of these regions with regard to the onset and/or intensity of VGF gene expression might help elucidate in which, if any, of these developmental processes VGF might participate.

Furthermore, since the pattern of VGF mRNA expression in the developing pituitary gland was somewhat unusual and unexpected, I will present it in greater detail here.

The cerebellum

Changes in the intensity and distribution of VGF mRNA hybridization in the developing rat cerebellum are illustrated in Figure 32. The earliest stage at which VGF mRNA labeling was detectable in the cerebellar anlage was E17.5 (panel A). Hybridization was apparent in the region containing developing Purkinje cells (Pkj), and in the nuclear transitory zone (ntz) where the cells destined to become the fastigial nucleus are located at this age. The germinal trigone (GT) and external germinal layer (EGL) were unlabeled, as was the cortical transitory zone (ctz) containing cells destined to become Purkinje neurons. A similar pattern was observed at E19.5 (panel B), except that the cells of the ntz had now migrated more ventrally to take up a more mature position as the fastigial nucleus.

By P0 (panel C), there was a much more diffuse pattern of labeling deep to (but not including) the EGL. In most regions only the Purkinje cell layer and deep nuclei displayed significant hybridization signal, but in a small region in the middle of the cerebellar hemisphere, what appeared to be the molecular layer was labeled as well (data not shown). The intensity of the Purkinje cell layer hybridization appeared to display some variability from lobule to lobule as well, and was weakest dorsally.

At P5 (panel D), there was moderate labeling of the IGL throughout the cerebellum, which was strongest in crus 1 of the ansiform lobule of the cerebellar hemispheres and in the most anterior and most posterior vermal lobules (2 and 9), and still weakest dorsally (vermal lobule 6 and the simple lobule of the cerebellar hemisphere). There was also low signal in the EGL which is clear on film autoradiographs but difficult to appreciate in dark field images of emulsion dipped sections, as the signal is obscured by the heavy cresyl violet counterstaining in this layer. The developing cerebellar nuclei continued to hybridize as well (not shown). Interestingly, one lobule—crus 1 of the ansiform lobule of the cerebellar hemispheres, which displayed higher IGL VGF mRNA hybridization levels than any other portion of the cerebellum studied—also showed strong labeling in what was either the Purkinje cell layer or the inner portion of the primitive molecular layer.

By P10 (panel E), a similar phenomenon was seen; a different small portion of cerebellar cortex, deeper and more medial to that seen at P5, was now displaying this unusual labeling. Other portions of the same layer also contained lower yet appreciable VGF mRNA hybridization at this stage. Hybridization in the IGL remained moderate throughout most of the cerebellum, but could be seen to be beginning to concentrate in a smaller number of cells.

Finally, by adulthood (panel F), the only grossly apparent labeling in the cerebellum was overwhelmingly restricted to the deep cerebellar nuclei and scattered cells, probably Golgi neurons, throughout the granule cell and Purkinje cell layers. As illustrated in Chapter 3 (Figure 7), the Purkinje cells themselves also express low levels of VGF in the adult. There was no labeling above background in the molecular layer.

The hippocampus

Expression of VGF during the development of the hippocampus is shown in Figure 33. Early in the genesis of the hippocampus (E17.5), strong VGF hybridization was observed only in the nacient stratum pyramidale of CA1 region of Ammon's horn (panel A). Low labeling was detectable in the intermediate zone of the same region. Hybridization was not detectable in the proliferating neuroepithelium.

By E19.5 (panel B), the region of VGF probe hybridization had expanded with the growing stratum pyramidale. Among these labeled cells, those located more caudally (toward the subiculum rather than the dentate) were distributed more diffusely. There were also some labeled cells which appeared not to be in the stratum pyramidale proper but were just outside of it. Weak hybridization was also seen in the region of the dentate gyrus primordium, in which the first granule cells are just being born at this stage.

By the day of birth, there was still labeling throughout the stratum pyramidale of Ammon's horn, however, it was now weaker in CA1 than in CA3. Furthermore, there were more strongly labeled cells outside of the pyramidal layer than before. There were still labeled cells in the hilar region of the dentate gyrus, and a subtle band of weakly labeled cells along the developing granule layer of the dorsal blade of the gyrus.

At P5 (panel D), labeling in all of the CA regions had declined to moderate levels and the labeling in the dentate had increased to moderate levels, such that the intensity of labeled cells throughout the hippocampus was now quite uniform. Furthermore it was now more clear that there were at least two populations of labeled cells in Ammon's horn; those in the pyramidal layer, and those in the molecular layers like the stratum oriens and stratum lucidum. In the dentate, there was a tight band of labeled cells in the dorsal blade and crest, and a more diffuse band of cells could be seen in the hilar region.

By P10 (panel E), the dentate hilar neurons, the non-pyramidal neurons of

Ammon's horn, and the neurons of the pyramidal layer of CA2 showed stronger hybridization. The remaining pyramidal neurons, now more mature and tightly packed, and dentate gyrus granule cells, including those in the developing ventral blade were more moderately labeled. This pattern was very similar to that seen in the adult (panel F).

The pituitary gland

The ontogeny of VGF mRNA expression from E15.5 to birth is illustrated in Figure 34. From the earliest stage studied at which VGF riboprobe hybridization was convincingly detectable, E15.5, very intense VGF mRNA expression was seen in the region of the developing pars tuberalis (A and A′). By E17.5 (B and B′), scattered cells in the pars distalis also displayed strong VGF labeling. This pattern was maintained at E19.5 (C and C′). By P0 (D and D′), however, expression levels in the pars tuberalis had declined somewhat to simply high rather than extremely intense as seen earlier. Furthermore, labeling was now detectable in the pars intermedia as well.

No VGF-specific labeling was seen in the pars nervosa at any stage of development studied.

Figure 11: Dark field emulsion autoradiographs showing VGF mRNA expression in parasagittal (*A*) and roughly transverse (*B*) sections of E11.5 rat embryos.
Arrows in *A* point to VGF hybridization signal in the primordia of the glossopharyngeal (IX) and vagal (X) ganglion complexes. *Arrowheads* in *B* point to VGF hybridization signal in what appear to be migrating neural crest cells. Abbreviations: *DRG,* dorsal root ganglion; *Me,* mesencephalon; *nt,* neural tube; *Symp,* sympathetic ganglion; *Te,* telencephalon. Scale bars: *A,* 500 µm; *B,* 250 µm.

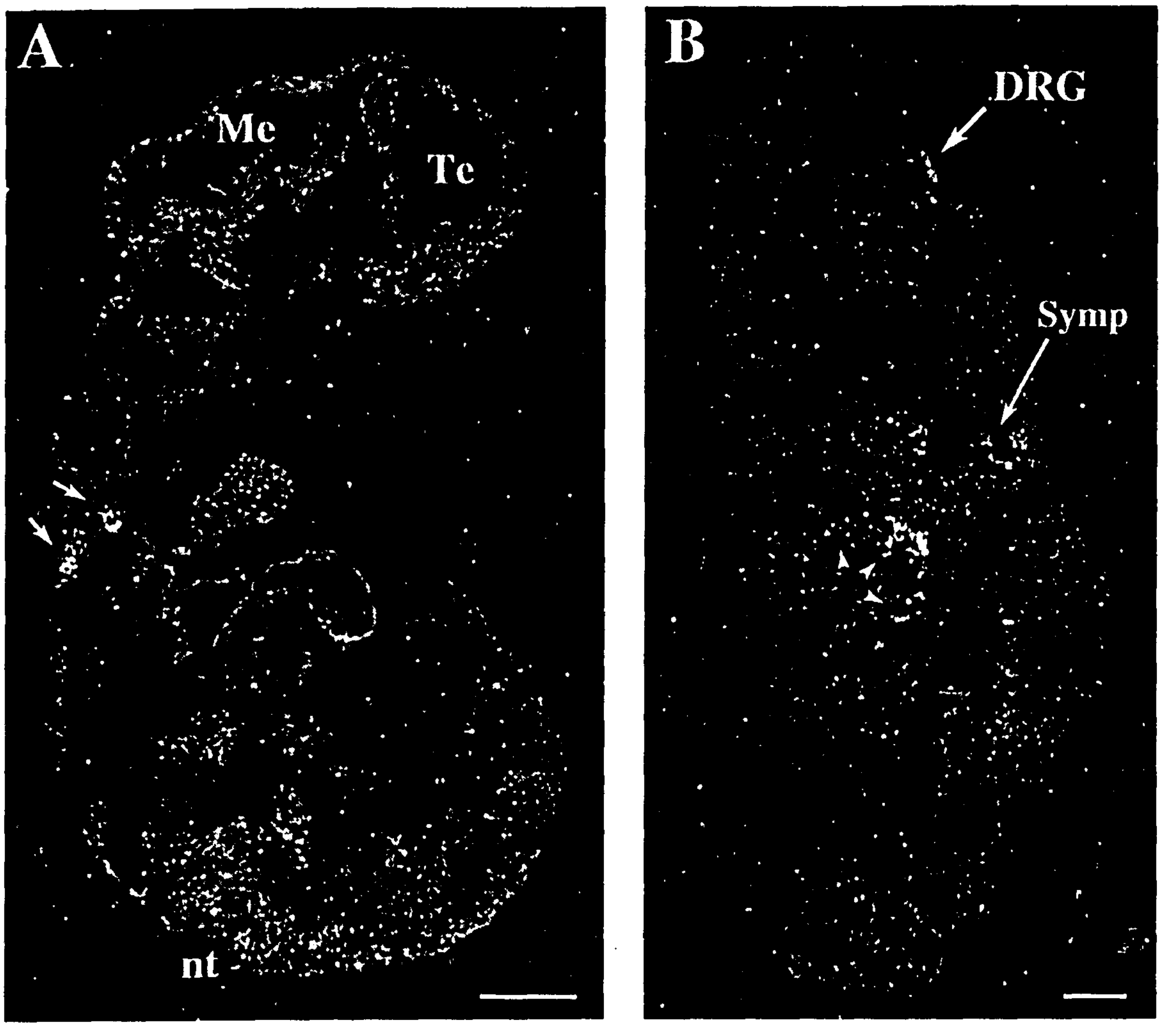
A
Mc
Te
nt
B
DRG
Symp

Figure 12: VGF mRNA expression in the gravid uterus at E11.5 shown in a low magnification dark field emulsion autoradiograph in *A*. Note the strong VGF mRNA hybridization to a subpopulation of cells in the uterine wall (*arrows*) at the region between the trophoblast and the maternal component of the decidual reaction. Several of these cells are shown in the higher magnification bright field emulsion autoradiograph in *B*. Scale bars: *A*, 1 mm; *B*, 80 μm.

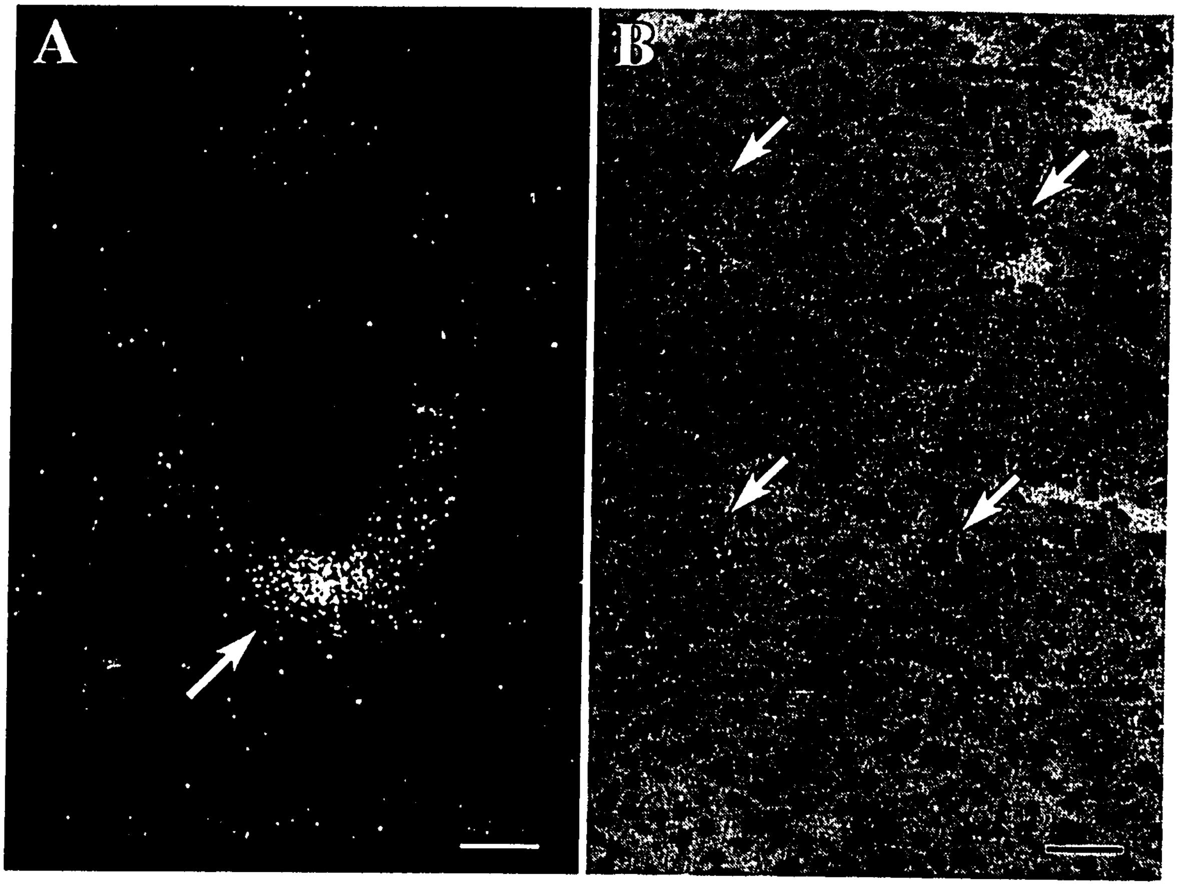
A
B

Figure 13: VGF mRNA expression in the gravid uterus at E13.5 shown in a low magnification dark field emulsion autoradiograph in *A* and *B*. Note the strong VGF mRNA hybridization to a subpopulation of cells in the uterine wall (*arrowheads*) now forming a monolayer between the trophoblast and the maternal component of the decidual reaction. Scale bars, 1 mm.

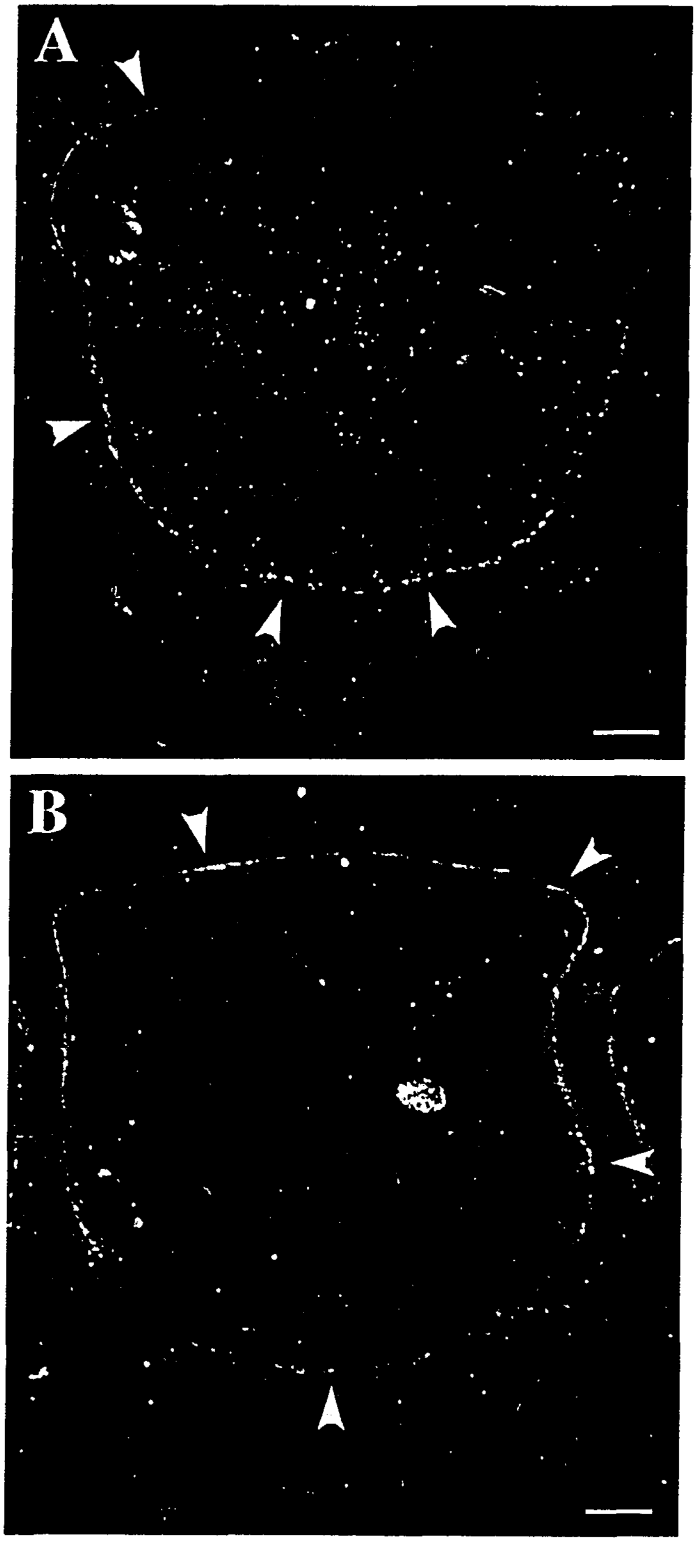
A
B

Figure 14: Dark field emulsion autoradiographs showing VGF mRNA expression in parasagittal sections of the E13.5 rat embryo.
For abbreviations see list p. xviii. Scale bars, 1 mm.

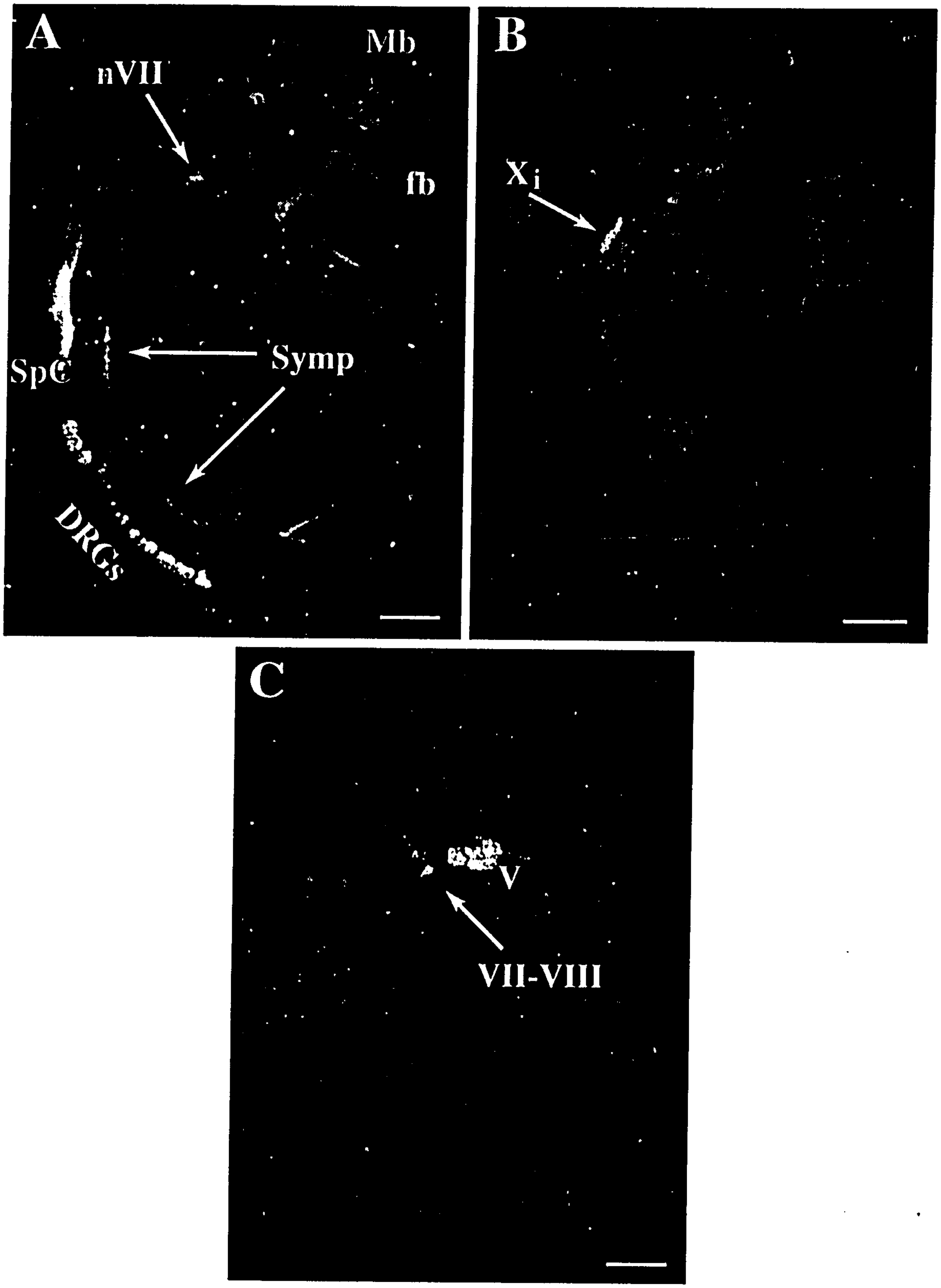
A
nVII
Mb
fb
SpC
Symp
DRGs
B
X_i
C
V
VII-VIII

Figure 15: Dark field emulsion autoradiographs showing VGF mRNA expression in transverse sections of the E13.5 rat embryo from a crown-to-rump series. Dorsal is up; ventral is down.

For abbreviations see list p. xviii. Scale bars, 500 µm.

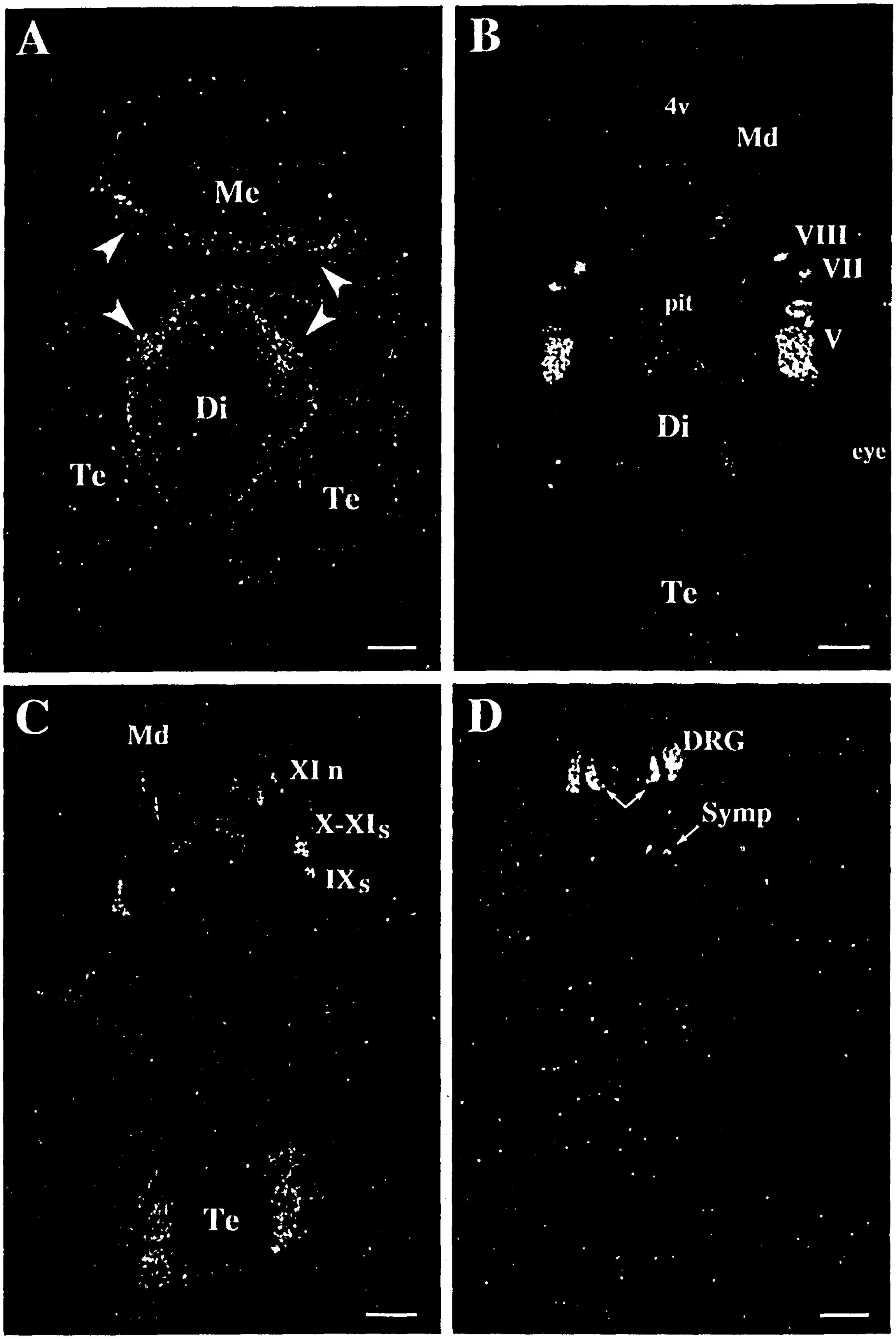
A
Mc
Di
Te
Te
B
4v
Md
VIII
VII
pit
V
Di
eye
Te
C
Md
XI n
X-XIs
IXs
Te
D
DRG
Symp

Figure 16: Dark field film autoradiographs showing VGF mRNA expression in parasagittal sections of the E15.5 rat embryo.

For abbreviations see list p. xviii. Scale bars, 1 mm.

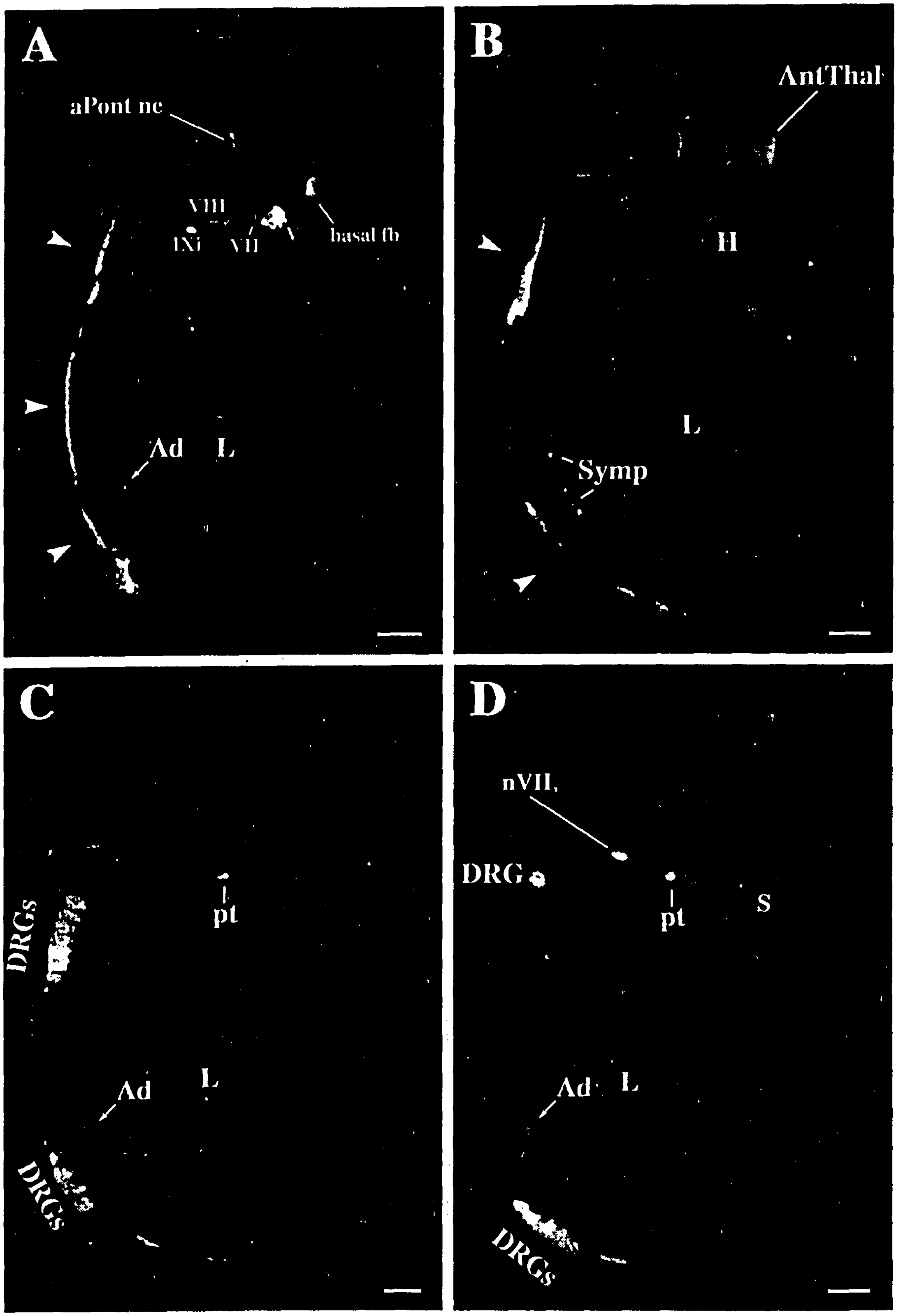
A
aPont nc
VIII
IXi
VII
V
basal fb
Ad
L
B
AntThal
H
L
Symp
C
DRGs
pt
Ad
L
DRGs
D
nVII
DRG
pt
S
Ad
L
DRGs

Figure 17: VGF mRNA expression in selected regions of the E15.5 embryo at higher magnification in parasagittal section. *A* & *A'*: cranial ganglia in bright and dark field emulsion autoradiographs respectively. *B*: dark field emulsion autoradiograph of DRGs. C: dark field emulsion autoradiograph of developing spinal cord and sympathetic chain (*arrowheads*). *D* & *D'*: the developing pituitary in bright and dark field. *E* & *E'*: the developing stomach and surrounding region in bright and dark field. *Arrowheads* highlight VGF mRNA hybridization in the developing enteric plexus. *F* & *F'*: the developing kidney and adrenal gland and surrounding region in bright and dark field.

For abbreviations see list p. xviii. Scale bars: *A-C'*, 200 μm; *D & D'*, 100 μm; *E-F'*, 200 μm.

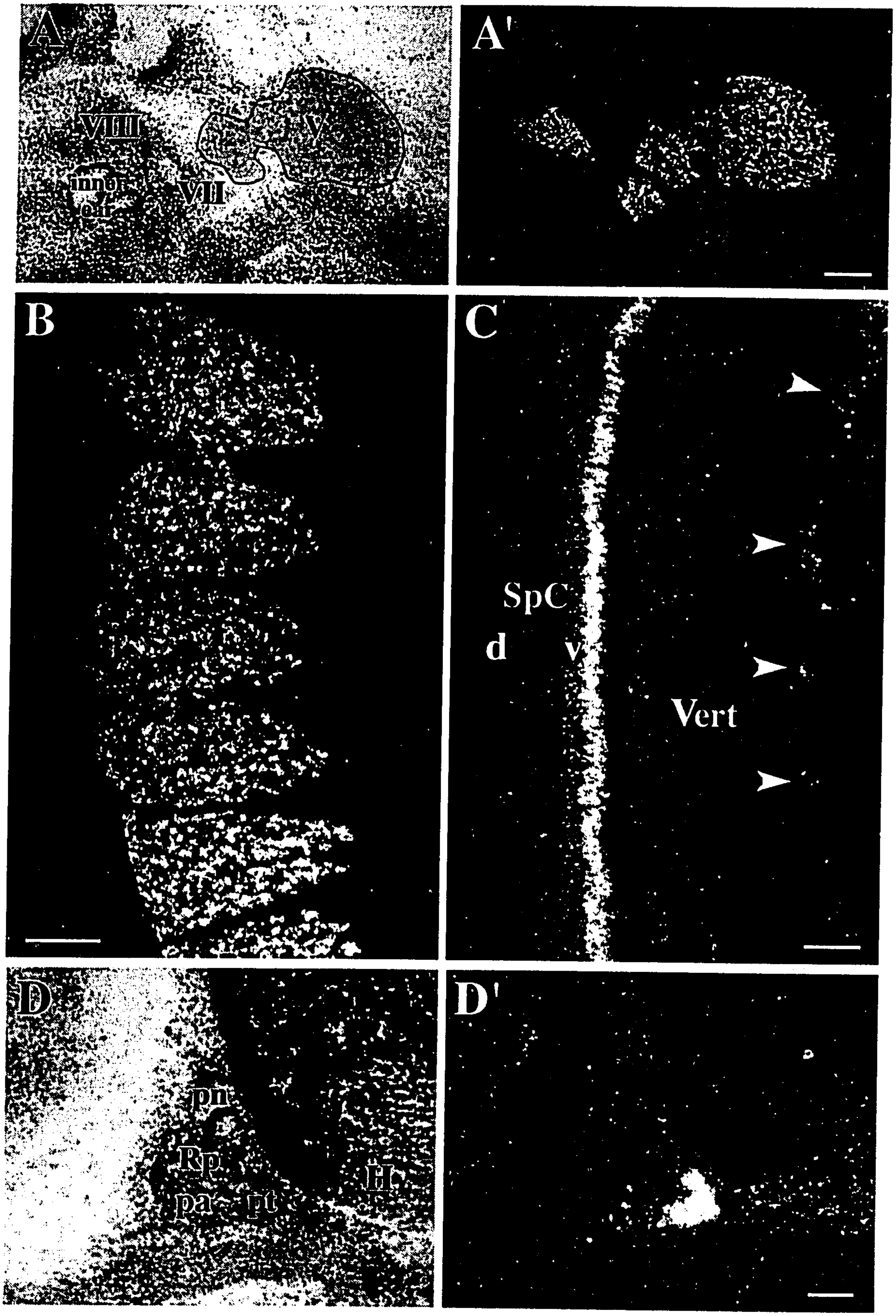
A
VIII
inner ear
VII
V
A'
B
C
SpC
d
v
Vert
D
pn
Rp
pa
pt
H
D'

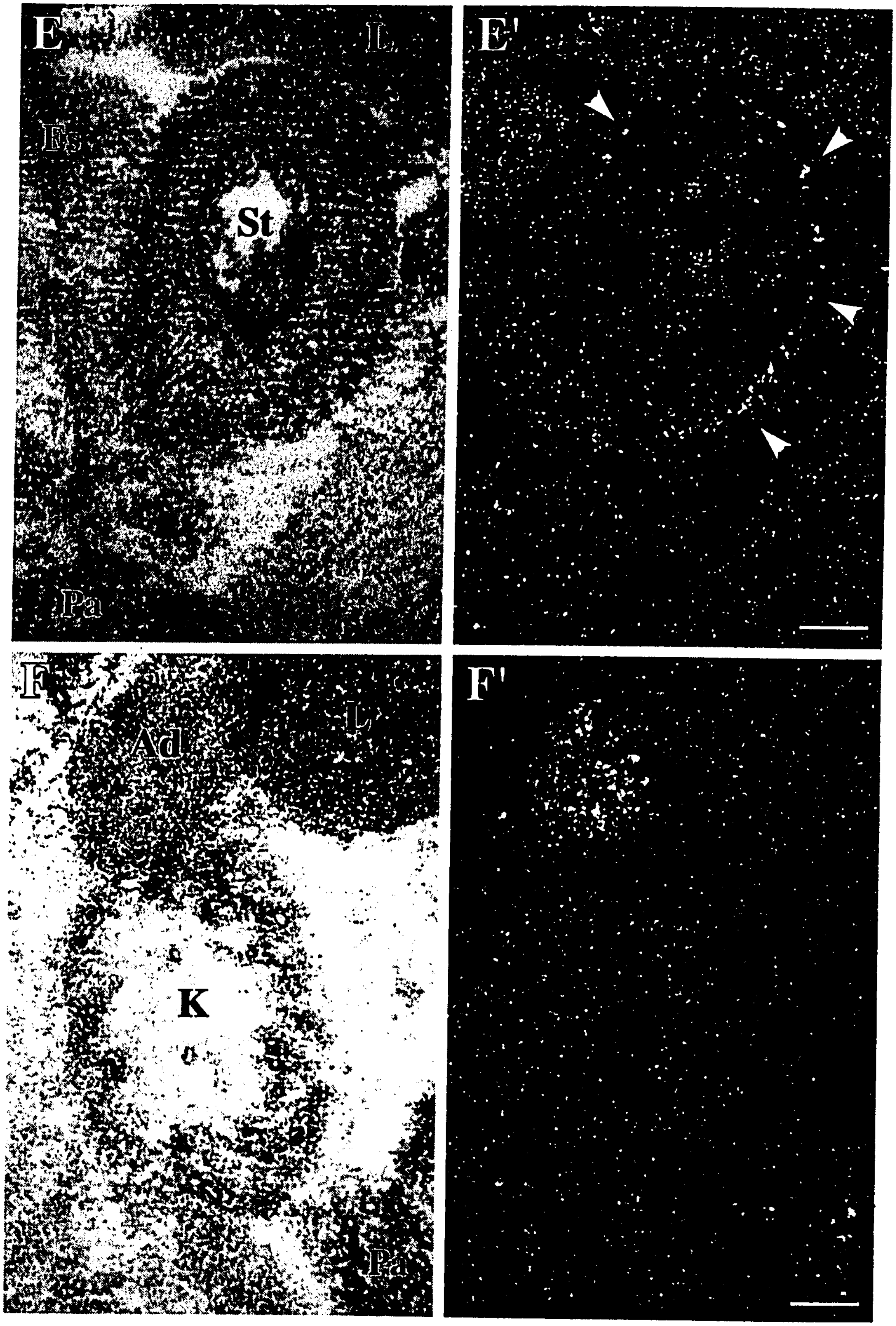
E
L
Es
St
Pa
E'
F
Ad
L
K
Pa
F'

Figure 18: Dark field film autoradiographs showing VGF mRNA expression in parasagittal sections of the E17.5 rat embryo.

For abbreviations see list p. xviii. Scale bars, 2 mm.

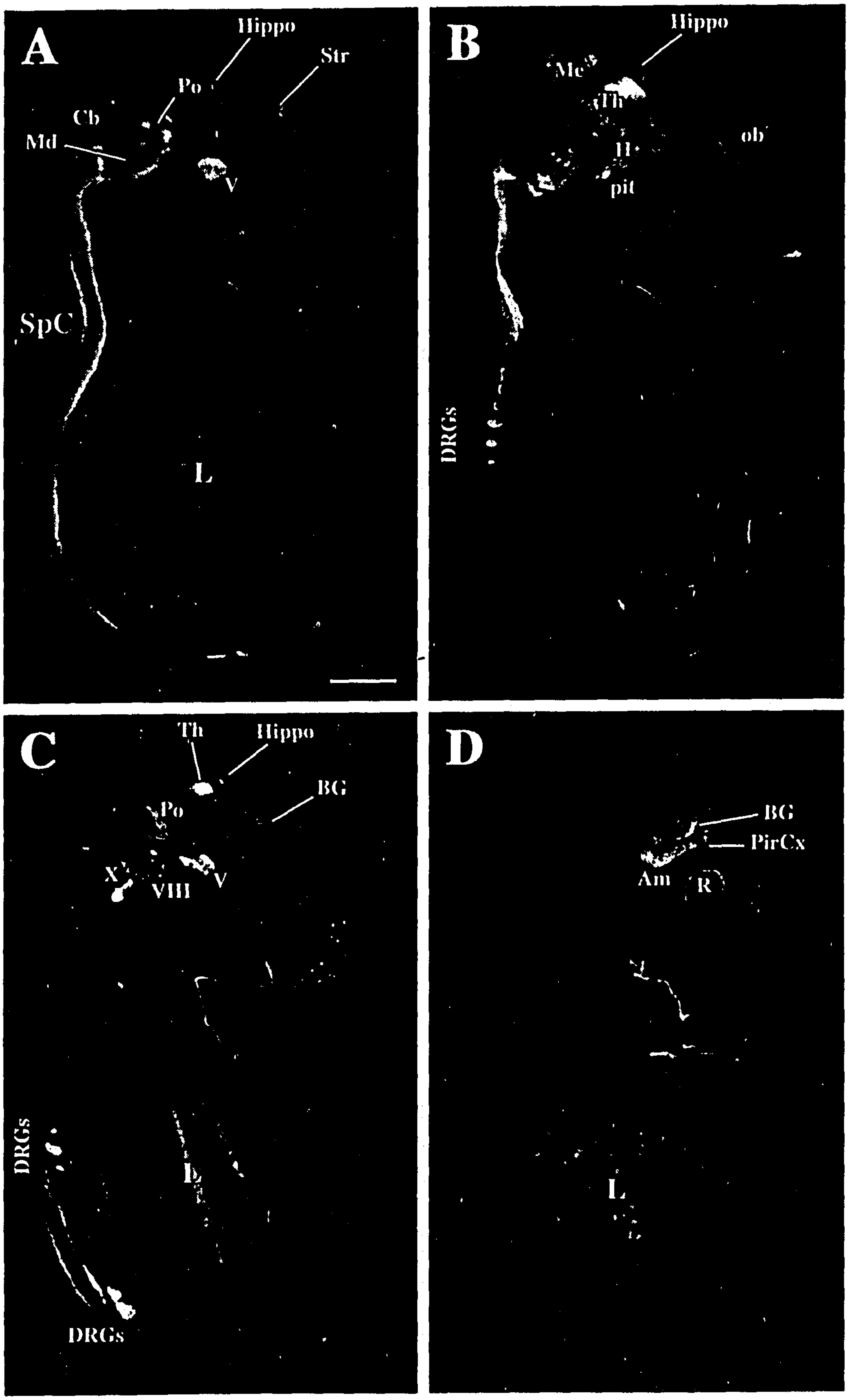
A
Hippo
Str
Po
Cb
Md
V
SpC
L
B
Hippo
Me
Th
ob
H
pit
DRGs
C
Th
Hippo
BG
Po
X
VIII
V
DRGs
L
DRGs
D
BG
PirCx
Am
R
L

Figure 19: VGF mRNA expression in selected regions of the E17.5 embryo at higher magnification in parasagittal section. *A* & *A'*: cranial ganglia in bright and dark field emulsion autoradiographs respectively. *B*: dark field emulsion autoradiograph of developing spinal cord, DRGs, and sympathetic ganglion. C: dark field emulsion autoradiograph of the developing stomach and surrounding bowel.

For abbreviations see list p. xviii. Scale bars: *A & A'*, 500 µm; *B*, 200 µm; *C*, 250 µm.

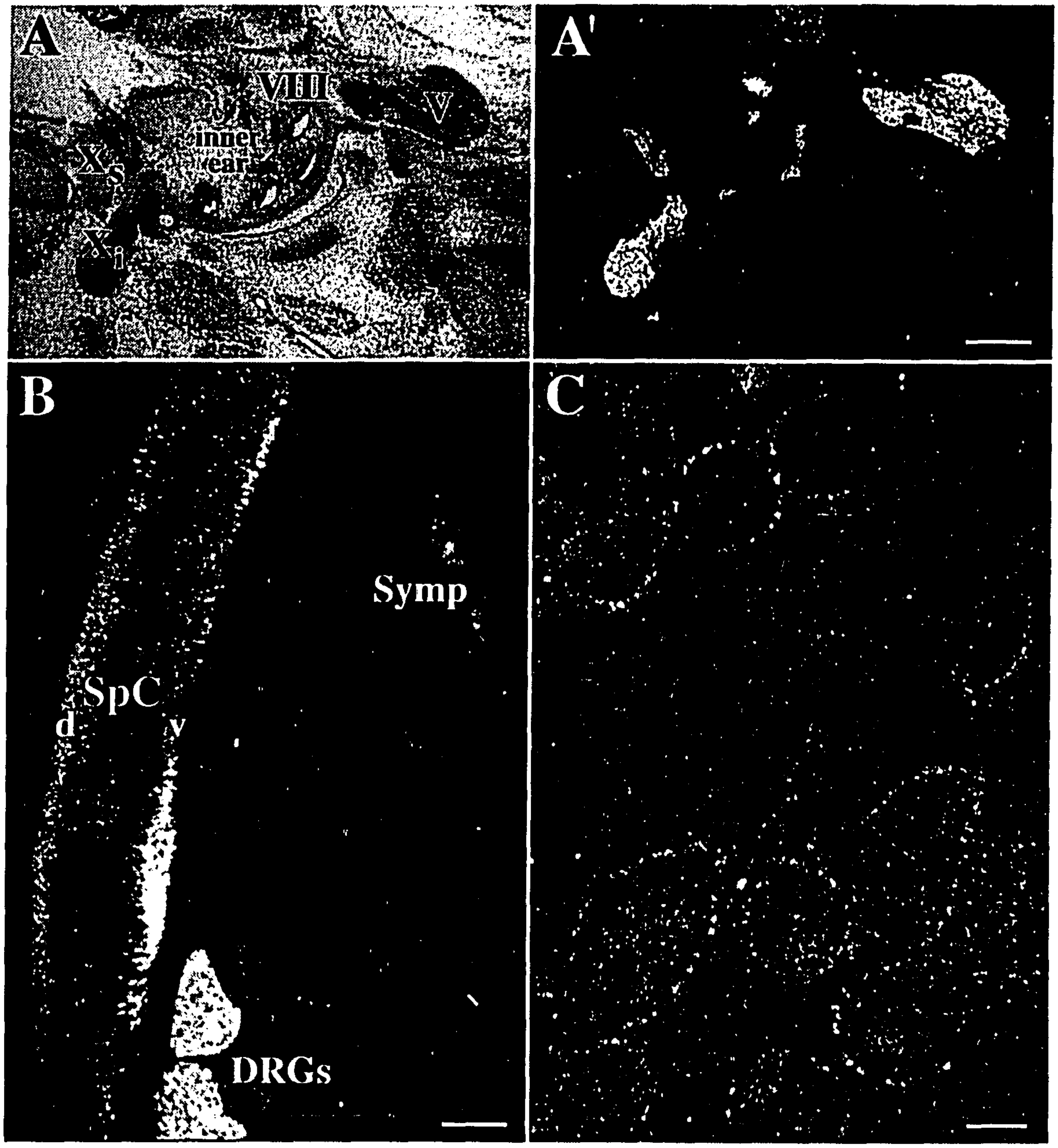
A
VIII
V
inner ear
X_s
X_i
A'
B
SpC
d
v
Symp
DRGs
C

Figure 20: Dark field film autoradiographs showing VGF mRNA expression in parasagittal sections of the E19.5 rat embryo.

For abbreviations see list p. xviii. Scale bars, 2 mm.

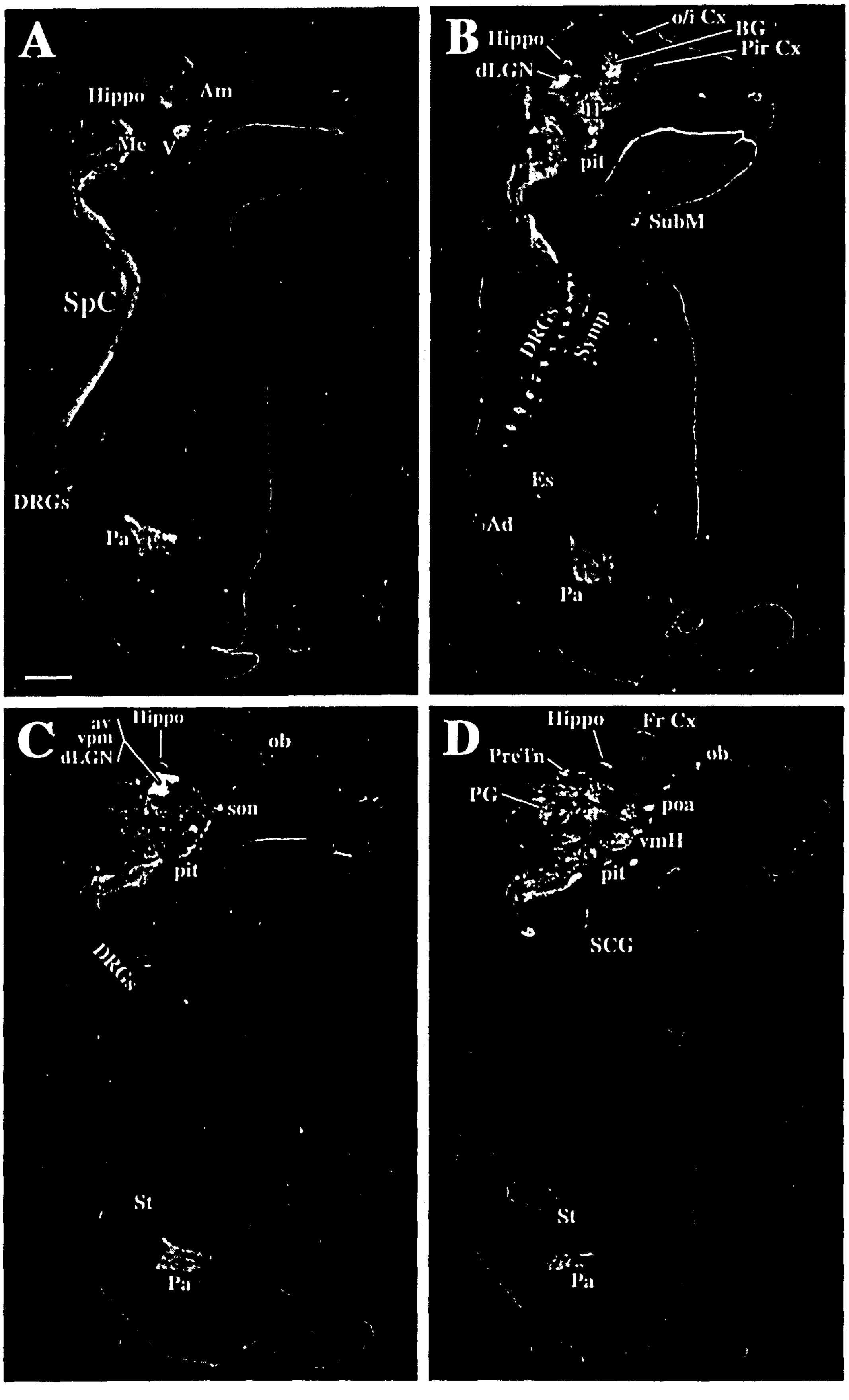
A
Hippo
Am
Mc
V
SpC
DRGs
Pa
B
Hippo
o/i Cx
BG
Pir Cx
dLGN
H
pit
SubM
DRGs
Symp
Es
Ad
Pa
C
av
vpm
dLGN
Hippo
ob
son
pit
DRGs
St
Pa
D
Hippo
Fr Cx
PreTn
ob
PG
poa
vmH
pit
SCG
St
Pa

Figure 21: Dark field emulsion autoradiographs (*A-I*) showing VGF mRNA expression in a crown-to-rump series of transverse sections of the E19.5 rat embryo.

For abbreviations see list p. xviii. Scale bars, 1 mm.

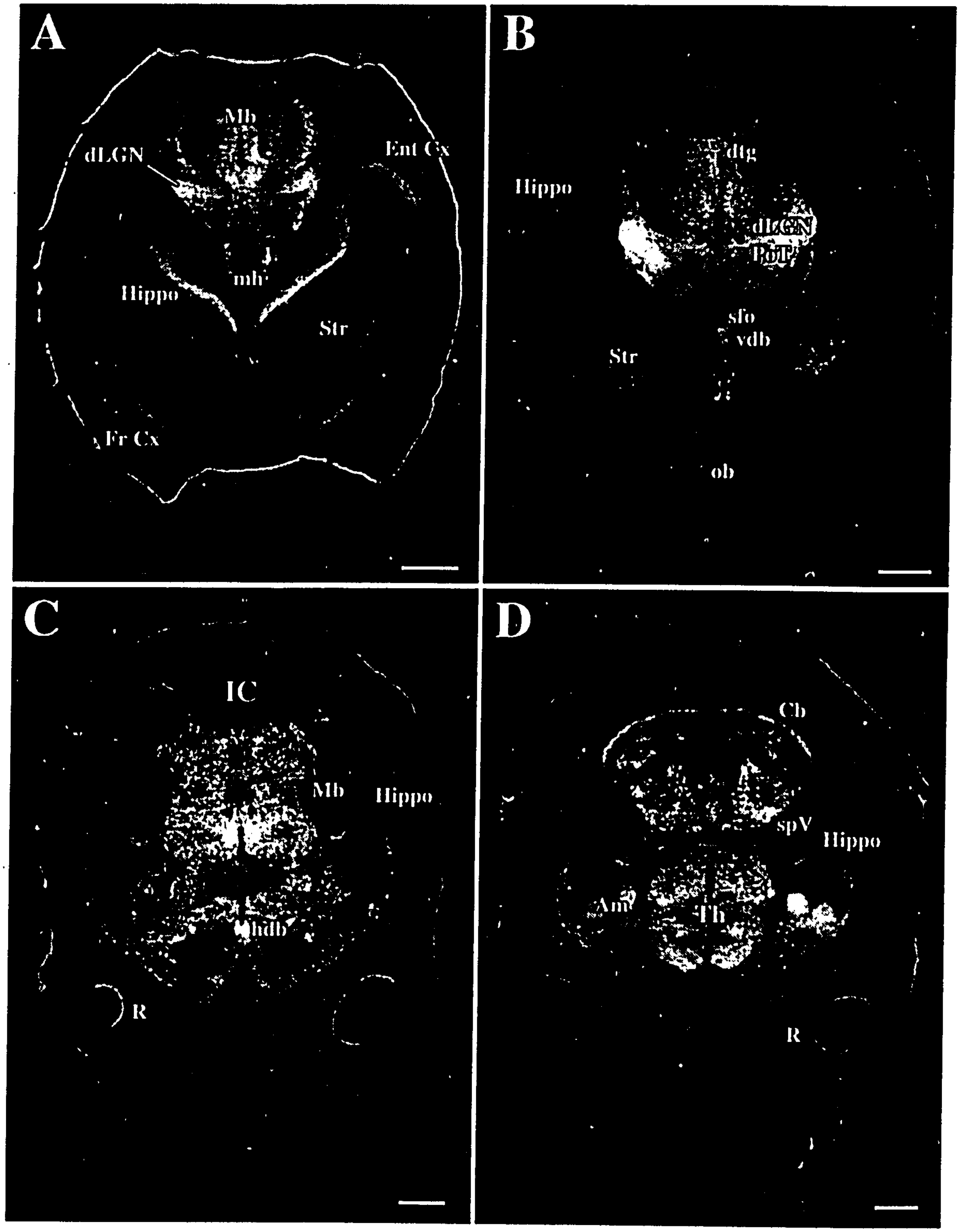
A
Mb
dLGN
Ent Cx
Hippo
mh
Str
Fr Cx
B
dtg
Hippo
dLGN
PoT
sfo
vdb
Str
ob
C
IC
Mb
Hippo
hdb
R
D
Cb
spV
Hippo
Am
Th
R

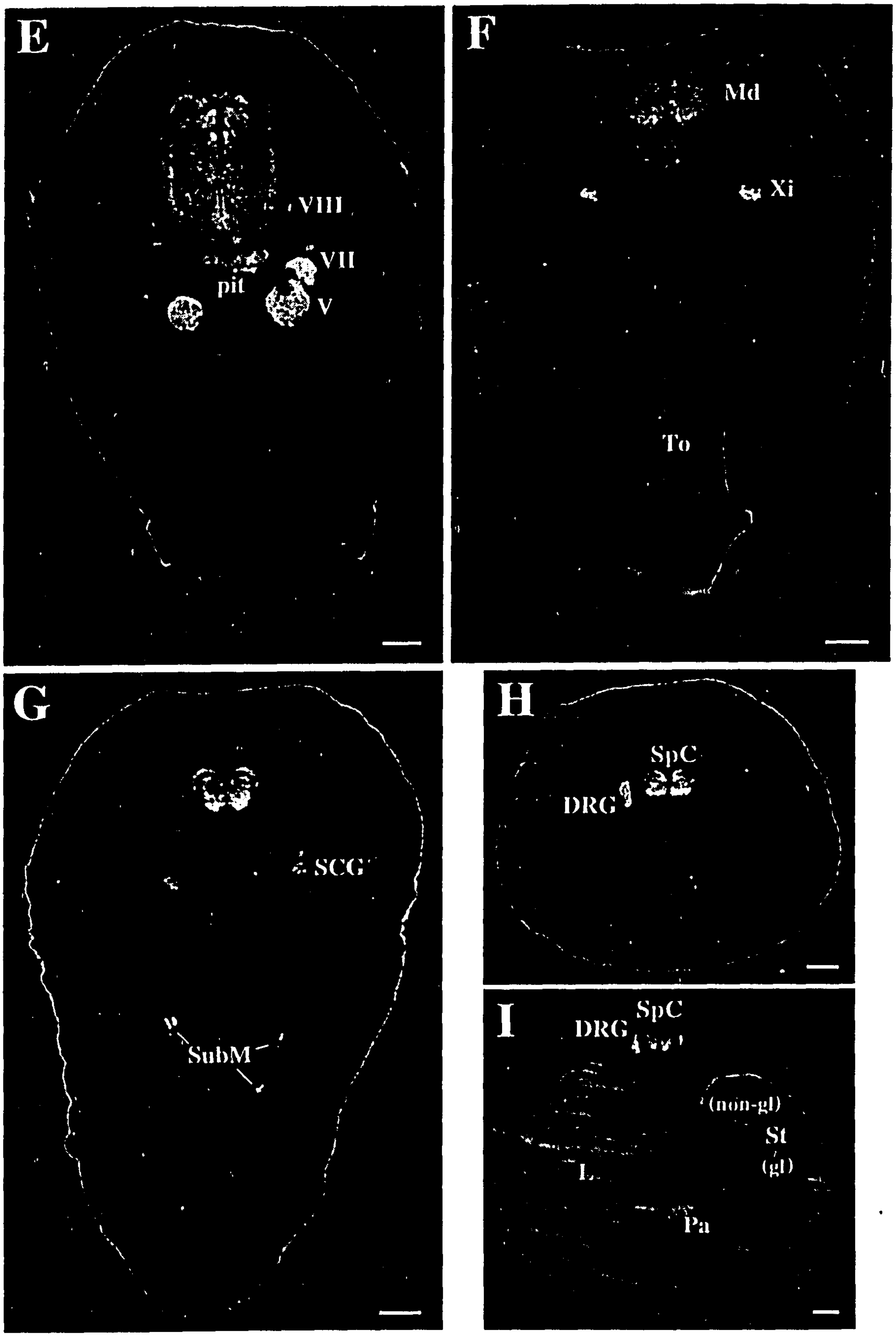
E
VIII
VII
pit
V
F
Md
Xi
To
G
SCG
SubM
H
SpC
DRG
I
DRG
SpC
(non-gl)
St
(gl)
L
Pa

Figure 22: VGF mRNA expression in selected regions of the E19.5 embryo at higher magnification. *A* & *A'*: parasagittal section through the cortical plate at a transition zone between VGF-expressing and non-expressing regions, in bright and dark field emulsion autoradiographs respectively. *B* & *B'*: olfactory bulb in parasagittal section, in bright and dark field. *C* & *C'*: bright and dark field images of developing spinal cord in transverse section. Cervical. *D* & *D'*: As in C. Lumbar enlargement. *E* & *E'*: As in C. Sacral. *F*: the developing dorsal root ganglia (*arrowheads*) and sympathetic chain (*arrows*) in parasagittal section; dark field. *G* & *G'*: cranial ganglia in parasagittal section; in bright and dark field. *H* & *H'*: sphenopalatine ganglion in parasagittal section; in bright and dark field. *I, I', I''*: (*I*) bright field photomicrograph of the submandibular gland in parasagittal section; the boxed region containing portions of the submandibular ganglion (*arrowheads*) is shown in *I'* & *I''* in bright and dark field. Note that this emulsion autoradiogram was intentionally underexposed in order to be able to visualize the cellular elements beneath the silver grains. I_1 and I_2 show at lower power, part of a transverse section, through the submandibular gland and ganglion of another embryo exposed for a more usual length of time to illustrate the very intense labeling of this parasympathetic ganglion. *J* & *J'*: cardiac ganglion in parasagittal section showing its location behind the heart in bright field in *J*; the boxed region is shown in dark field in *J'*. *K* & *K'*: skin in bright and dark field. *L* & *L'*: abdominal organs in parasagittal section in bright and dark field; *arrowheads* indicate the labeledmyenteric plexus. *M:* stomach in parasagittal section depicting mucosal hybridization in the non-glandular portion (*arrow*), but not the glandular portion. *Arrowheads* indicate the labeledmyenteric plexus.

For abbreviations see list p. xviii. Scale bars: *A & A'*, 200 µm; *B & B'*, 250 µm; *C-E'*, 200 µm; *F & F'*, 100 µm; *G-H'*, 250 µm; *I*, 200 µm; *I' & I''*, 50 µm; I_1-*K'*, 100 µm; *L-M'*, 500 µm.

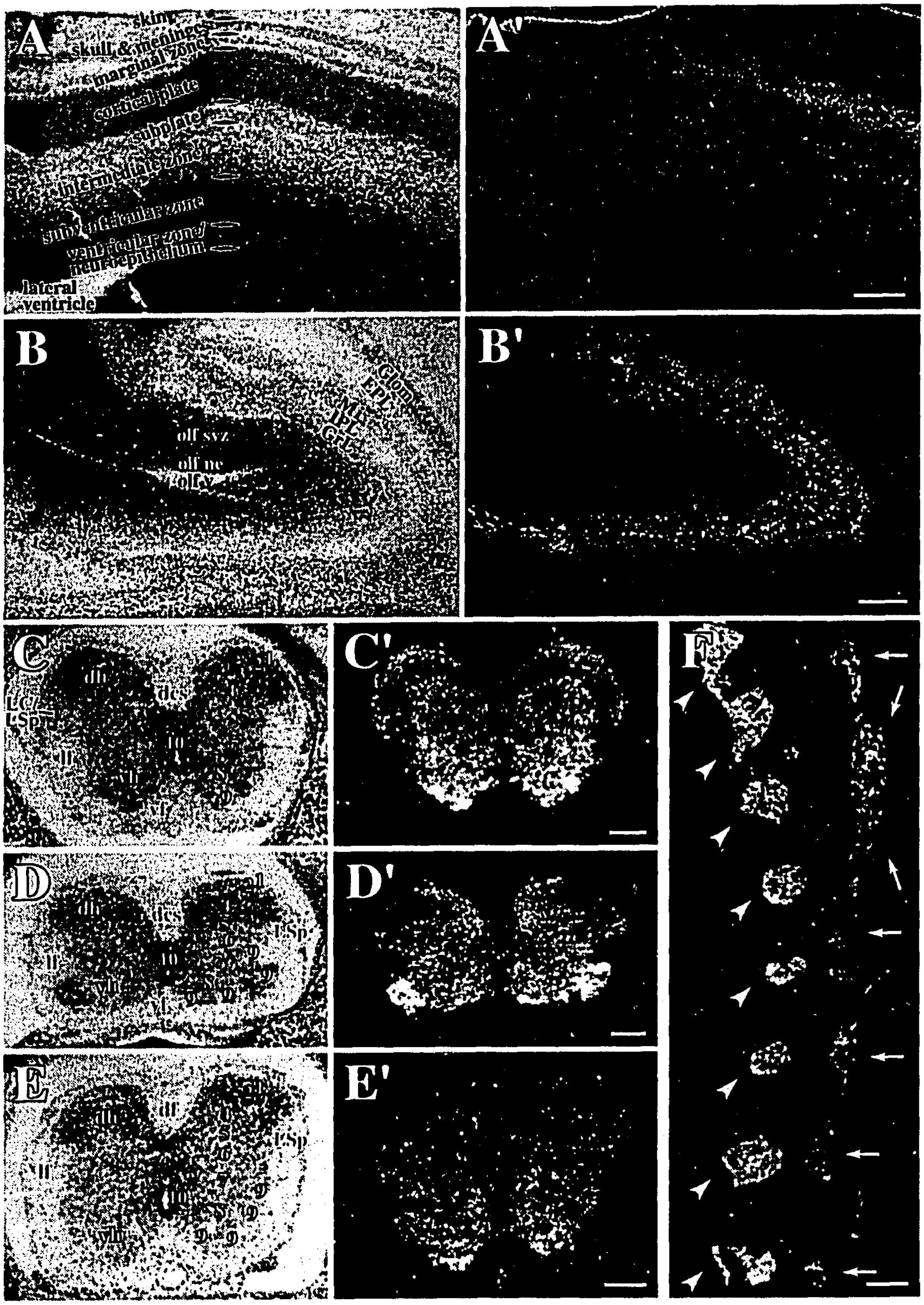
A
skin
skull & meninges
marginal zone
cortical plate
subplate
intermediate zone
subventricular zone
ventricular zone/
neuroepithelium
lateral
ventricle
A'
B
Glom
EPL
Mi
IPL
GL
olf svz
olf ne
olf v
B'
C
dh
dcs
LC/
LSp
lf
vh
vf
C'
D
dh
dcs
LSp
lf
vh
vf
D'
E
dh
df
LSp
lf
vh
E'
F

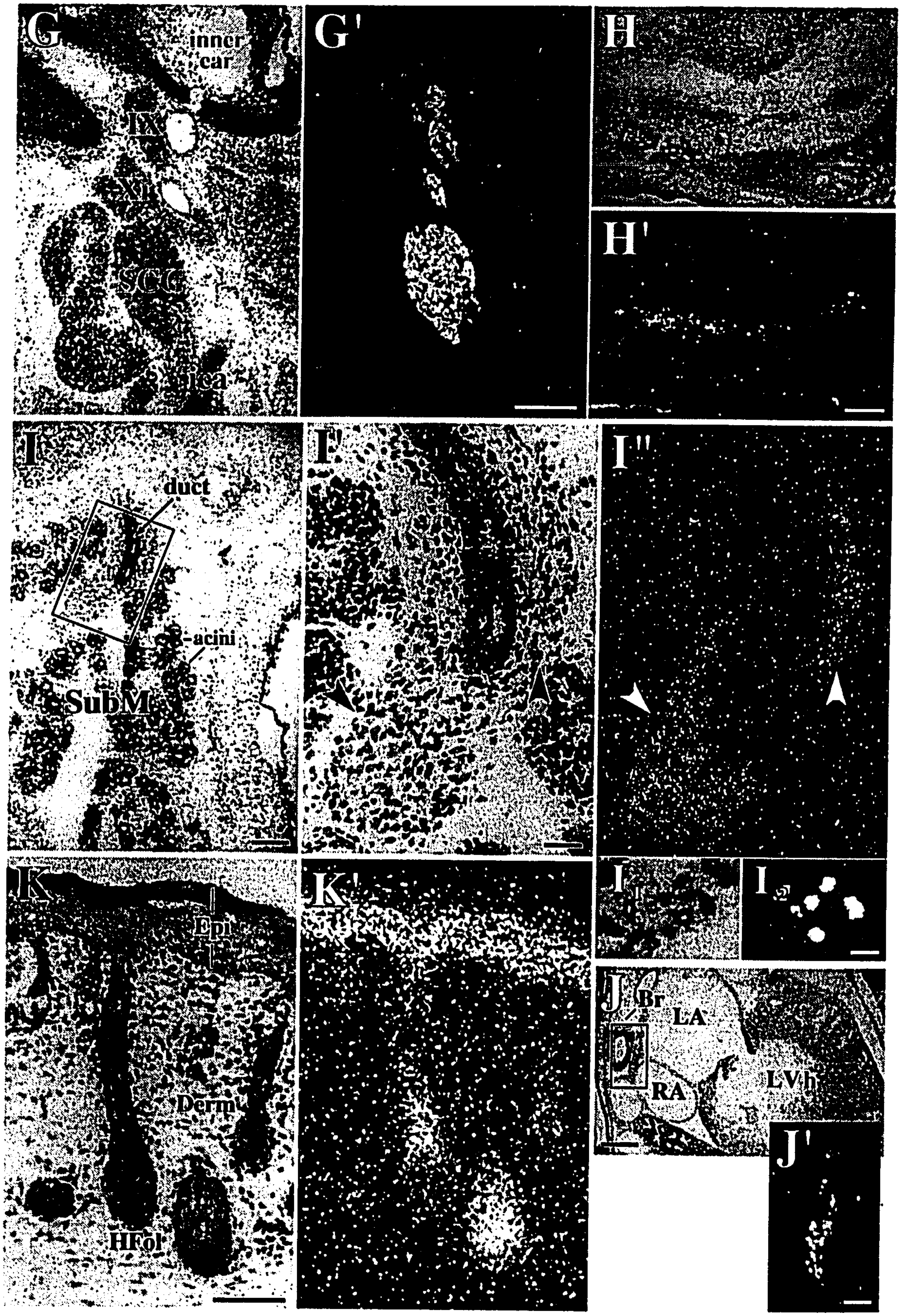
G
inner ear
IX
XI
SCG
ica
G'
H
H'
I
duct
acini
SubM
I'
I''
I_1
I_2
K
Epi
Derm
HFol
K'
J
Br
LA
RA
LVh
J'

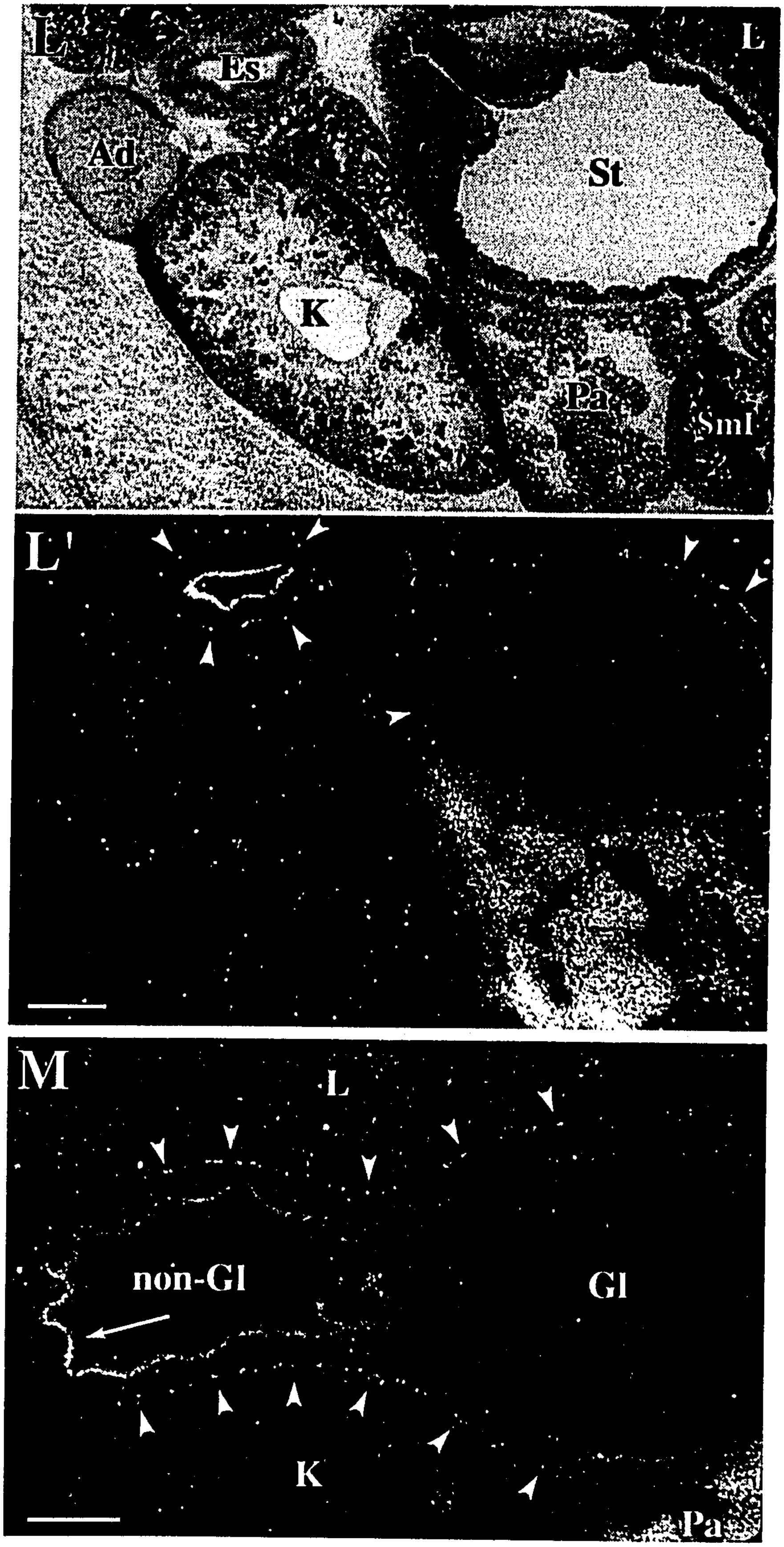
L
Es
L
Ad
St
K
Pa
Sml
L'
M
L
non-Gl
Gl
K
Pa

Figure 23: Dark field film and emulsion autoradiographs (*A*-*G*) showing VGF mRNA expression in parasagittal sections of the neonatal rat head.
For abbreviations see list p. xviii. Scale bars, 1 mm.

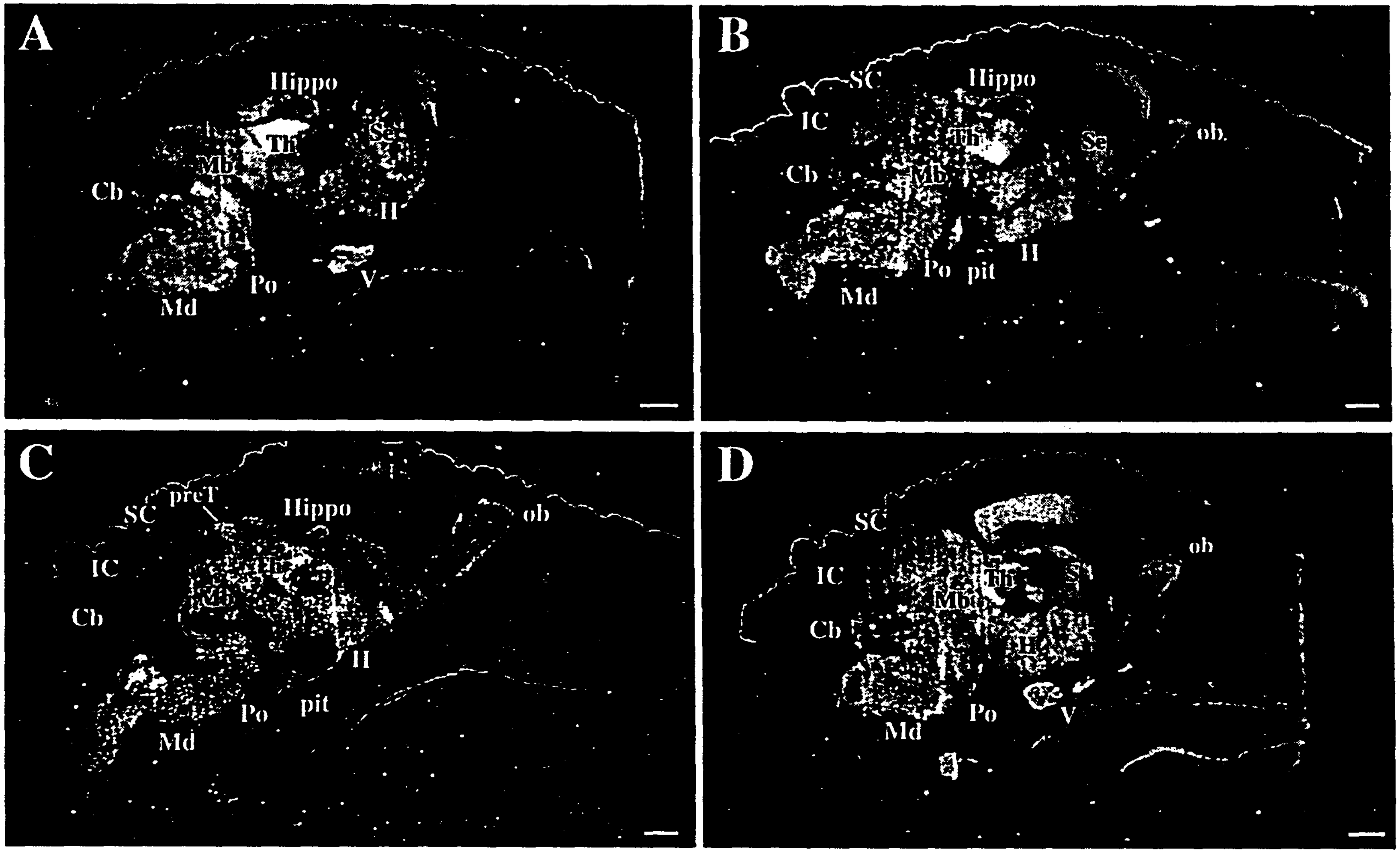
A
Hippo
Th
Se
Mb
Cb
H
Po
V
Md
B
SC
Hippo
IC
Th
Se
ob
Cb
Mb
H
Po
pit
Md
C
preT
SC
Hippo
ob
IC
Th
Mb
Cb
H
Po
pit
Md
D
SC
ob
IC
Th
Mb
Cb
H
Po
V
Md

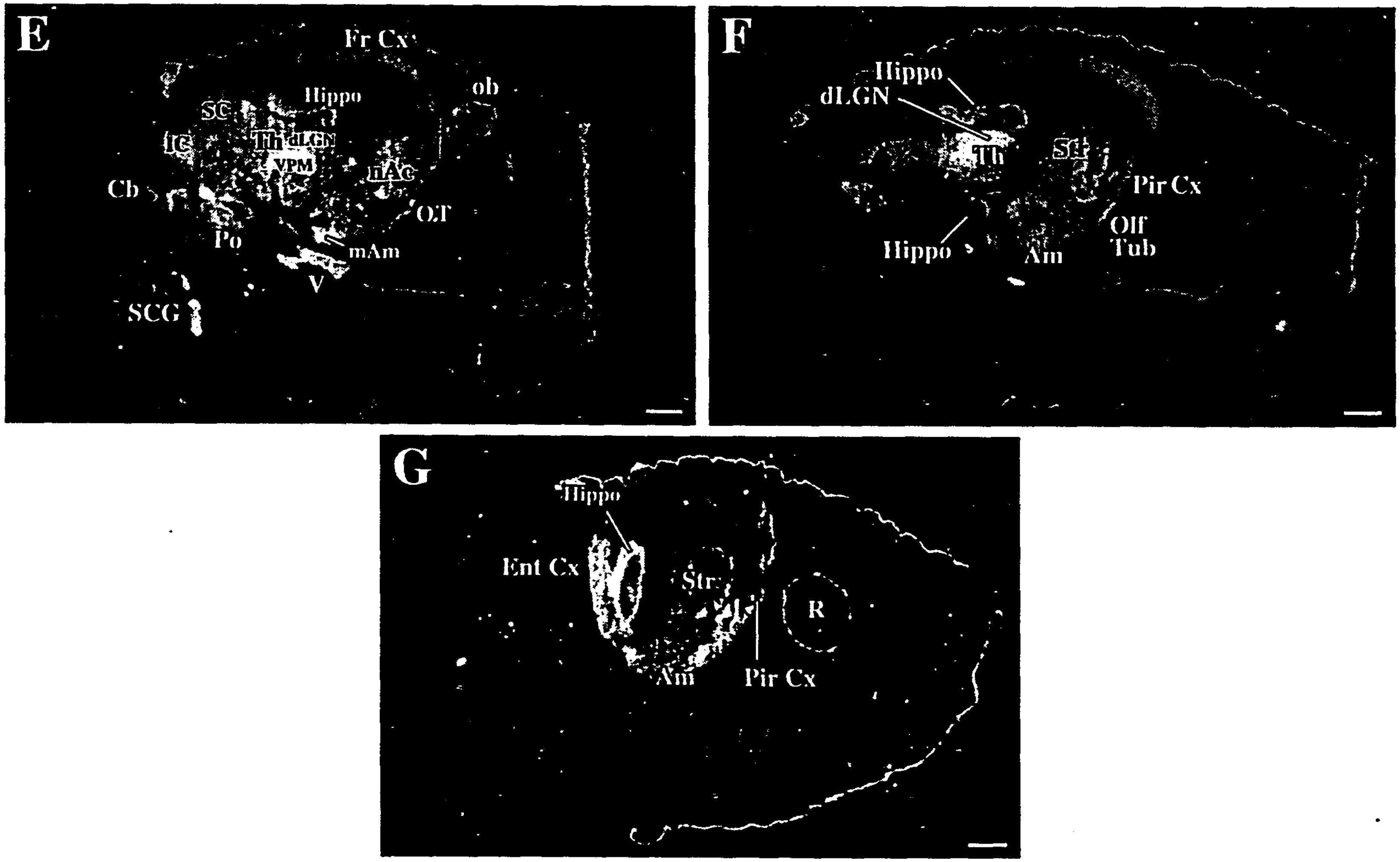
E
Fr Cx
ob
Hippo
SC
IC
Th
dLGN
VPM
nAc
Cb
OT
Po
mAm
V
SCG
F
Hippo
dLGN
Th
St
Pir Cx
Olf
Tub
Hippo
Am
G
Hippo
Ent Cx
Str
R
Am
Pir Cx

Figure 24: Dark field film and emulsion autoradiographs (*A-M*) showing VGF mRNA expression in a rostrocaudal series of coronal sections of the neonatal rat head.

For abbreviations see list p. xviii. Scale bars: *A-L,* 2 mm; *M,* 1 mm.

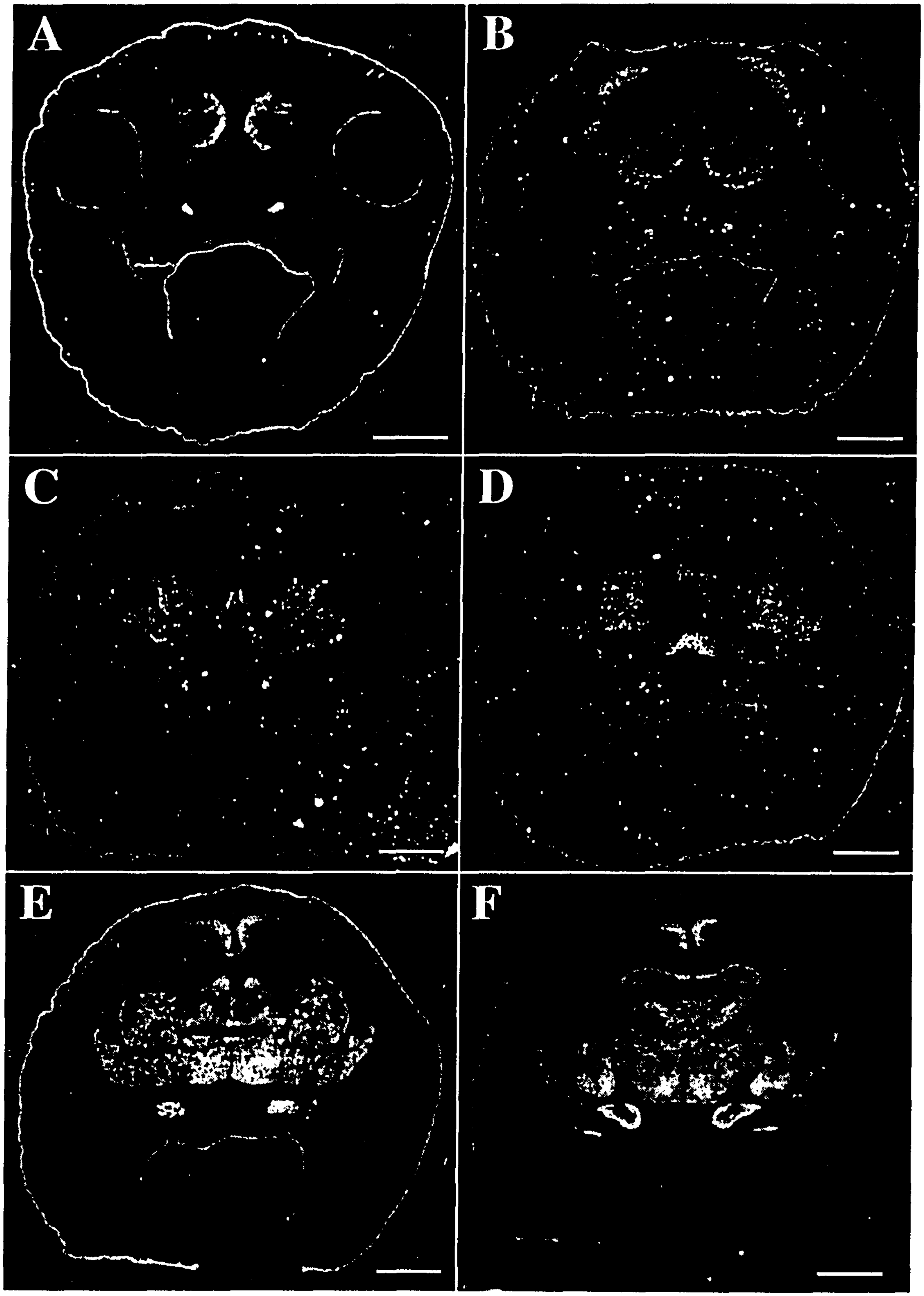
A
B
C
D
E
F

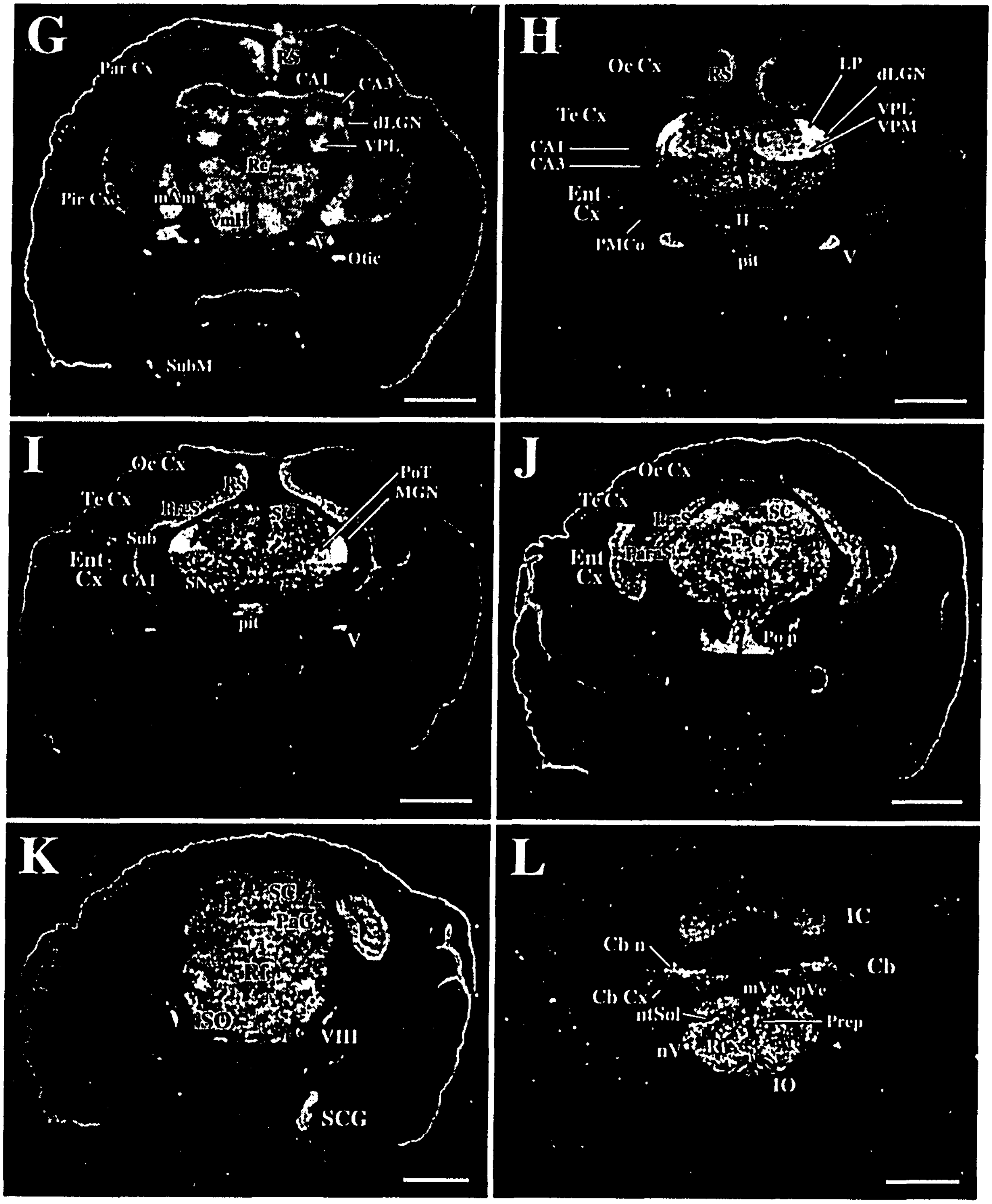
G
RS
Par Cx
CA1
CA3
dLGN
VPL
Re
Pir Cx
mVm
vmH
V
Otic
SubM
H
Oc Cx
RS
LP
dLGN
VPL
VPM
Te Cx
CA1
CA3
Ent Cx
H
PMCo
pit
V
I
Oc Cx
RS
PoT
MGN
Te Cx
PreS
SC
Sub
Ent Cx
CA1
SN
pit
V
J
Oc Cx
Te Cx
PreS
SC
PaG
Ent Cx
ParaS
Po n
K
SC
PaG
RF
SO
VIII
SCG
L
IC
Cb n
Cb
Cb Cx
mVe
spVe
ntSol
Prep
nV
RF
IO

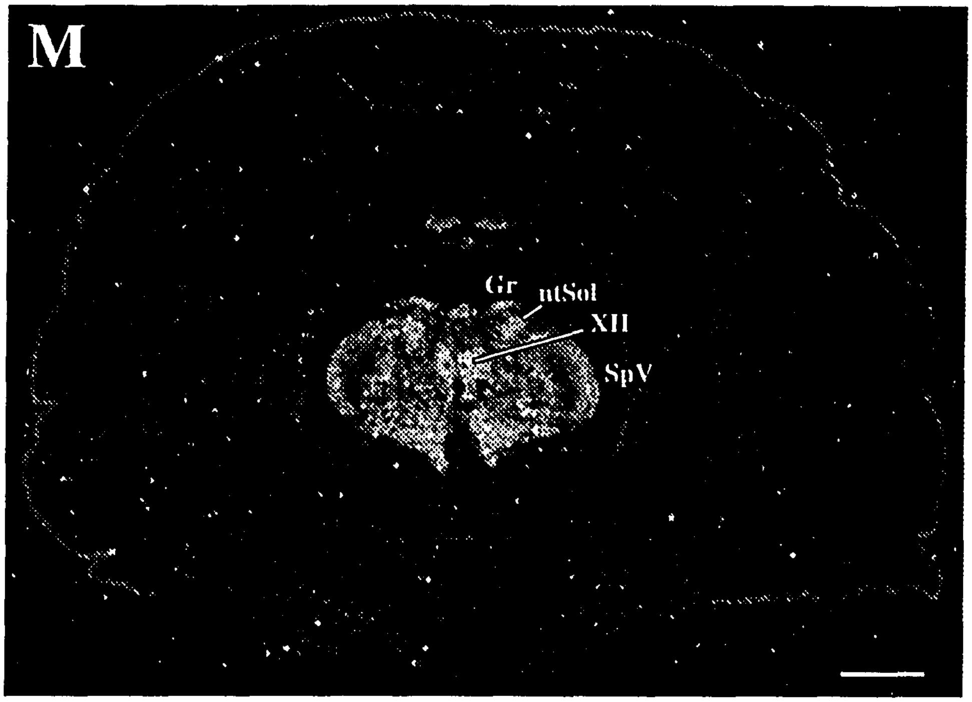
M
Gr
ntSol
XII
SpV

Figure 25: VGF mRNA expression in selected regions of the neonatal rat head at higher magnification. *A* & *A'*: coronal section through the olfactory bulb; in bright and dark field emulsion autoradiographs respectively. *B:* retina in coronal section; dark field. C & C': bright and dark field images of developing pituitary in coronal section.

For abbreviations see list p. xviii. Scale bars: *A*, 250 µm; *B*, 100 µm; *C*, 250 µm.

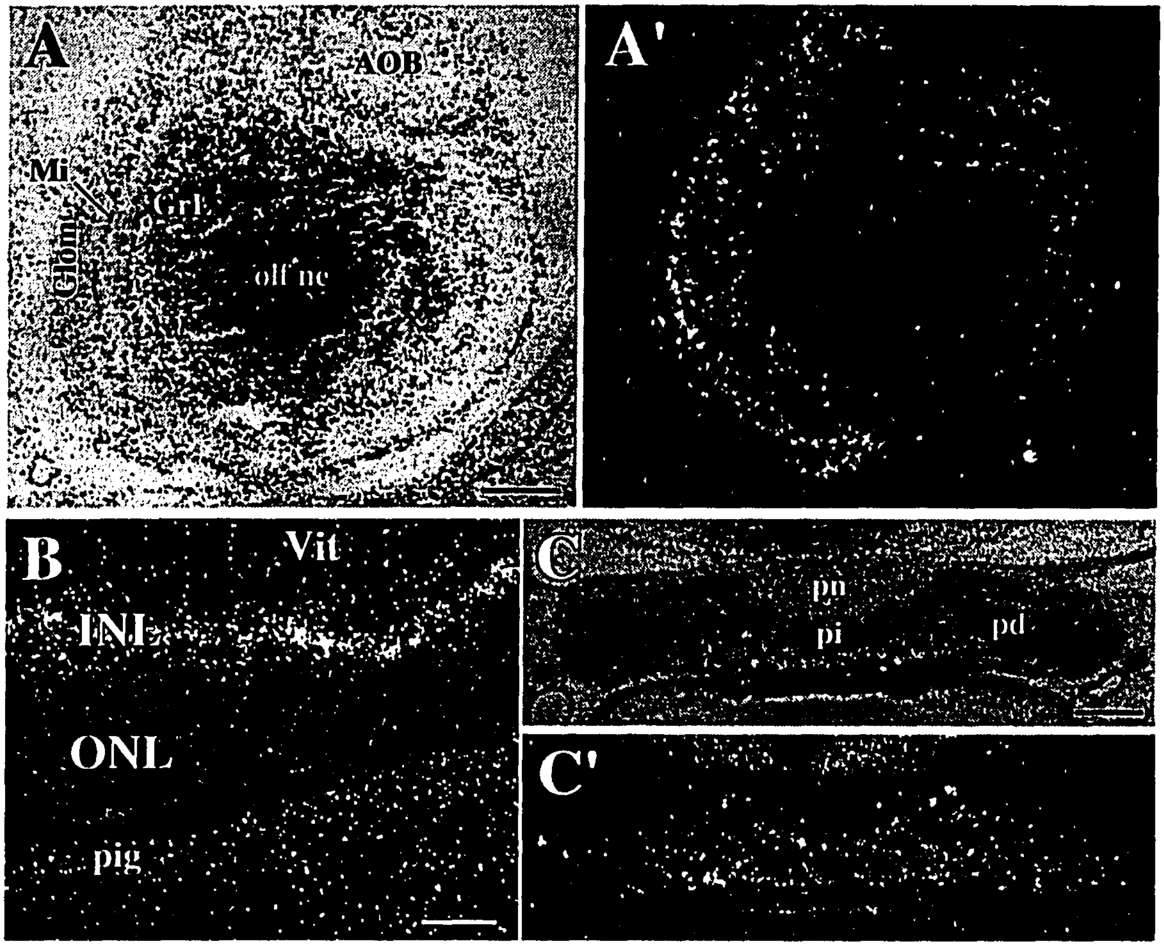
A
AOB
Mi
Glom
GrL
olf nc
A'
B
Vit
INL
ONL
pig
C
pn
pi
pd
C'

Figure 26: Dark field film and emulsion autoradiographs showing VGF mRNA expression in coronal sections of the P5 rat brain. *A-K*: rostral to caudal.

For abbreviations see list p. xviii. Scale bars: *A*, 500 µm; *B*, 750 µm; *C-K*, 1 mm.

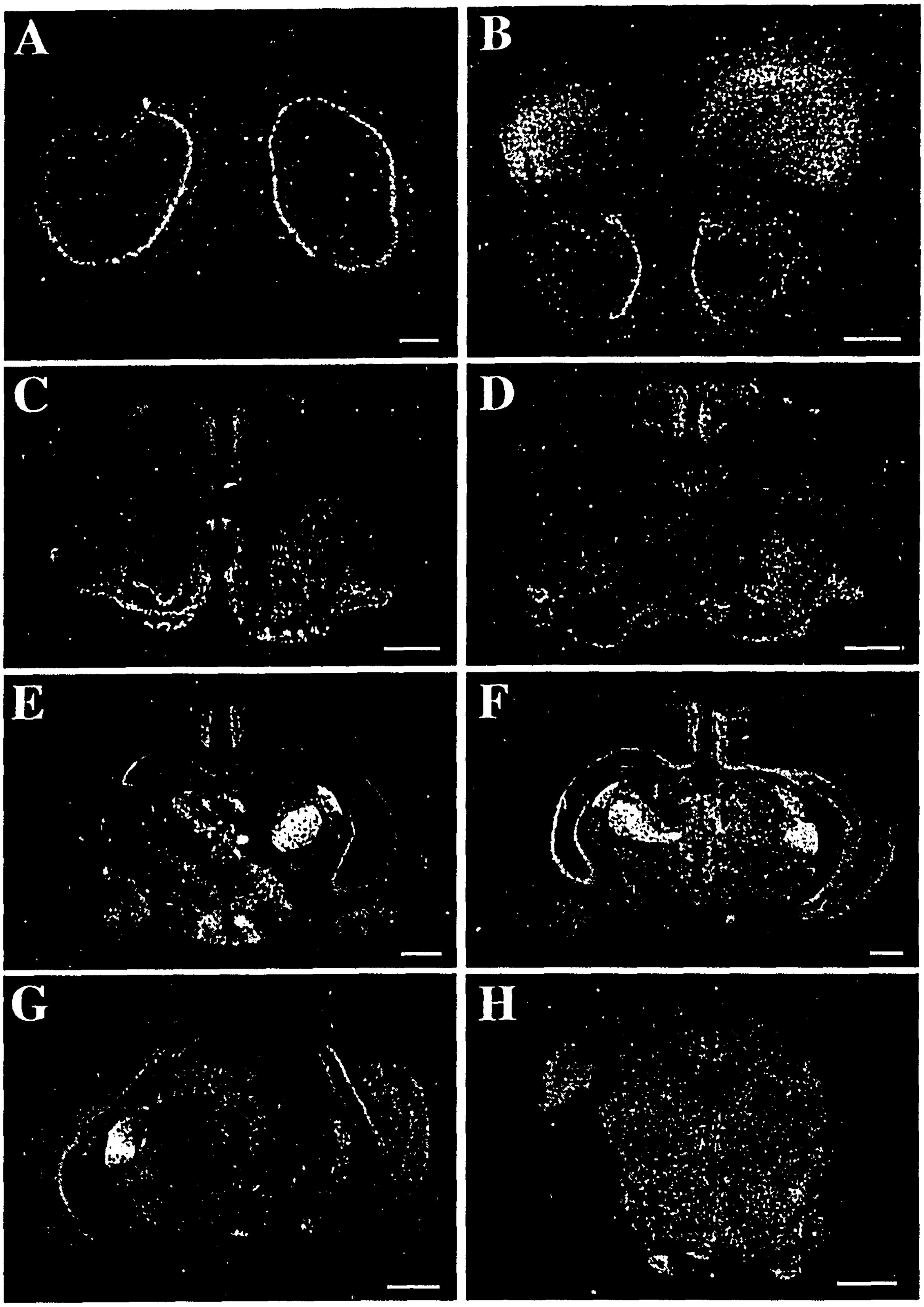
A
B
C
D
E
F
G
H

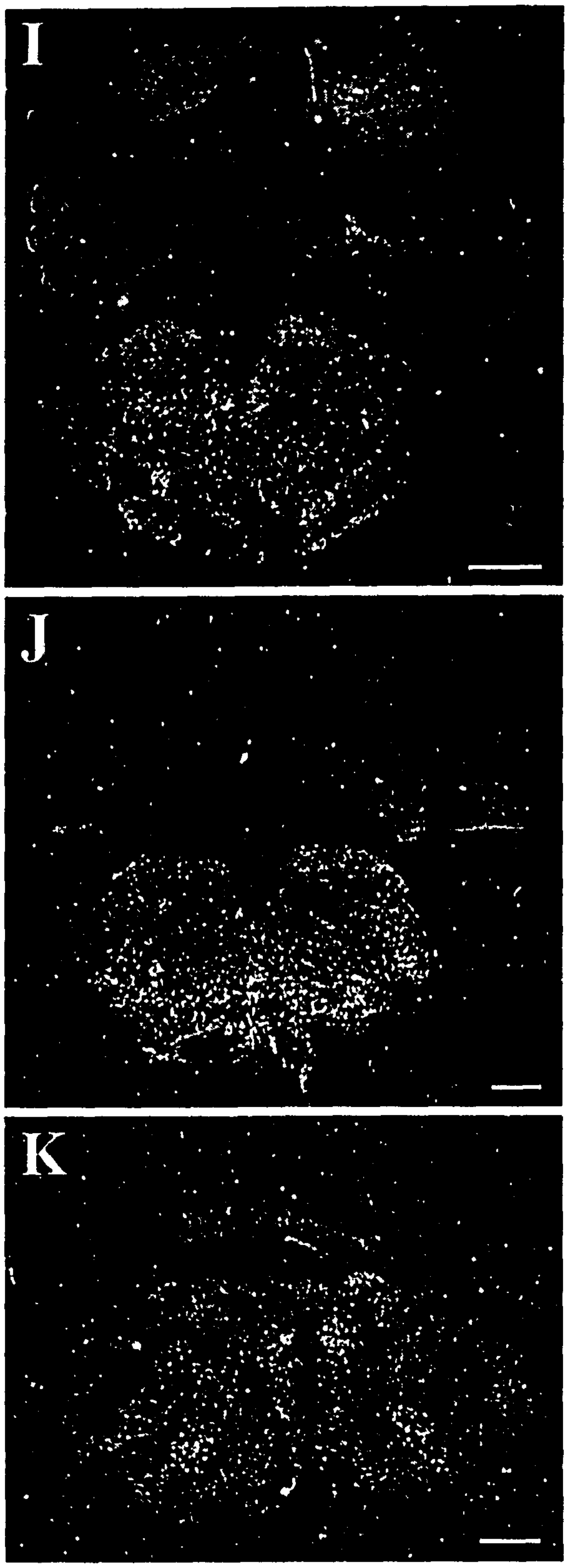
I
J
K

Figure 27: Dark field film autoradiographs (*A-H*) showing VGF mRNA expression in a dorsoventral series of transverse sections of the P5 rat brain. For abbreviations see list p. xviii. Scale bars, 1 mm.

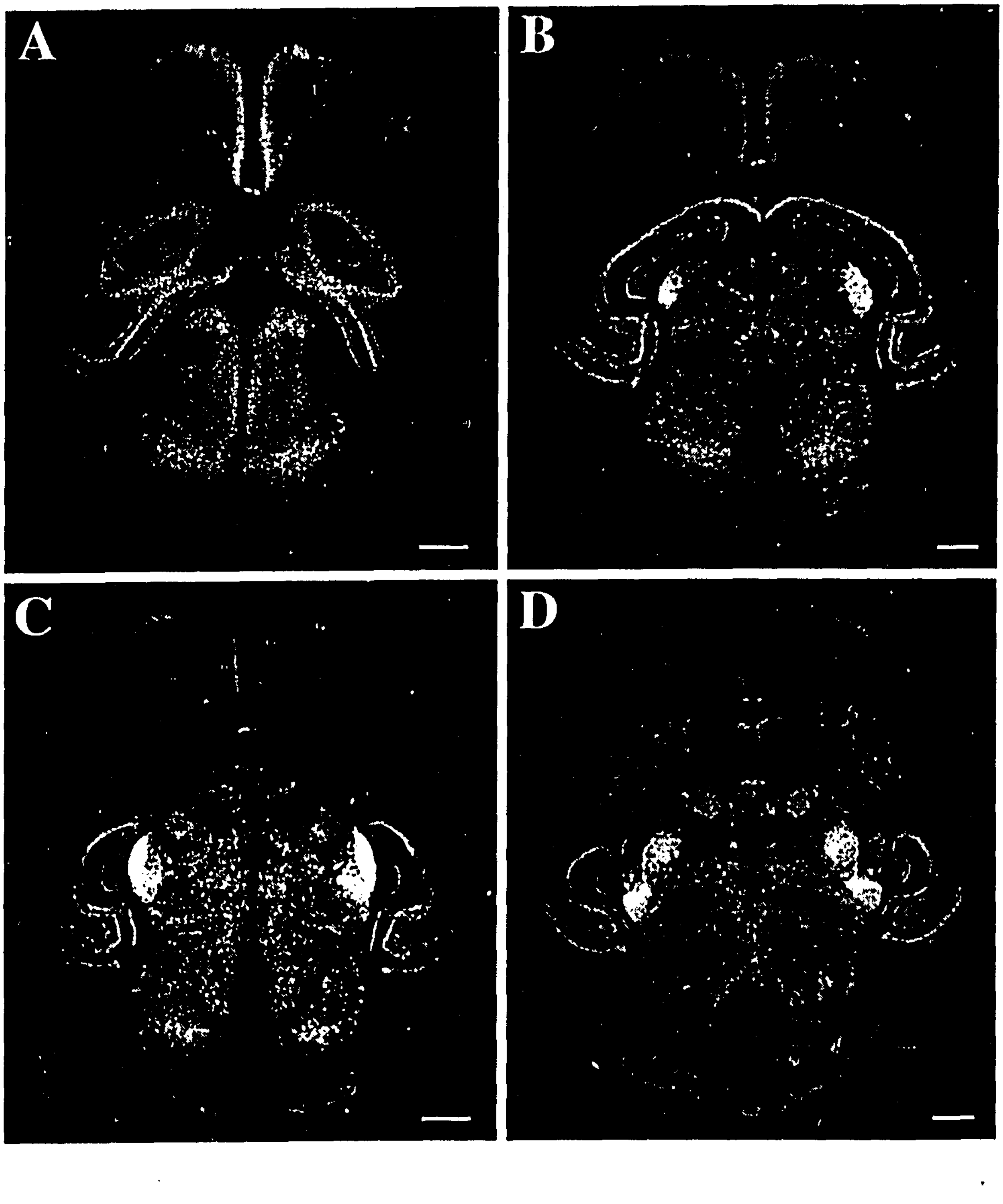
A
B
C
D

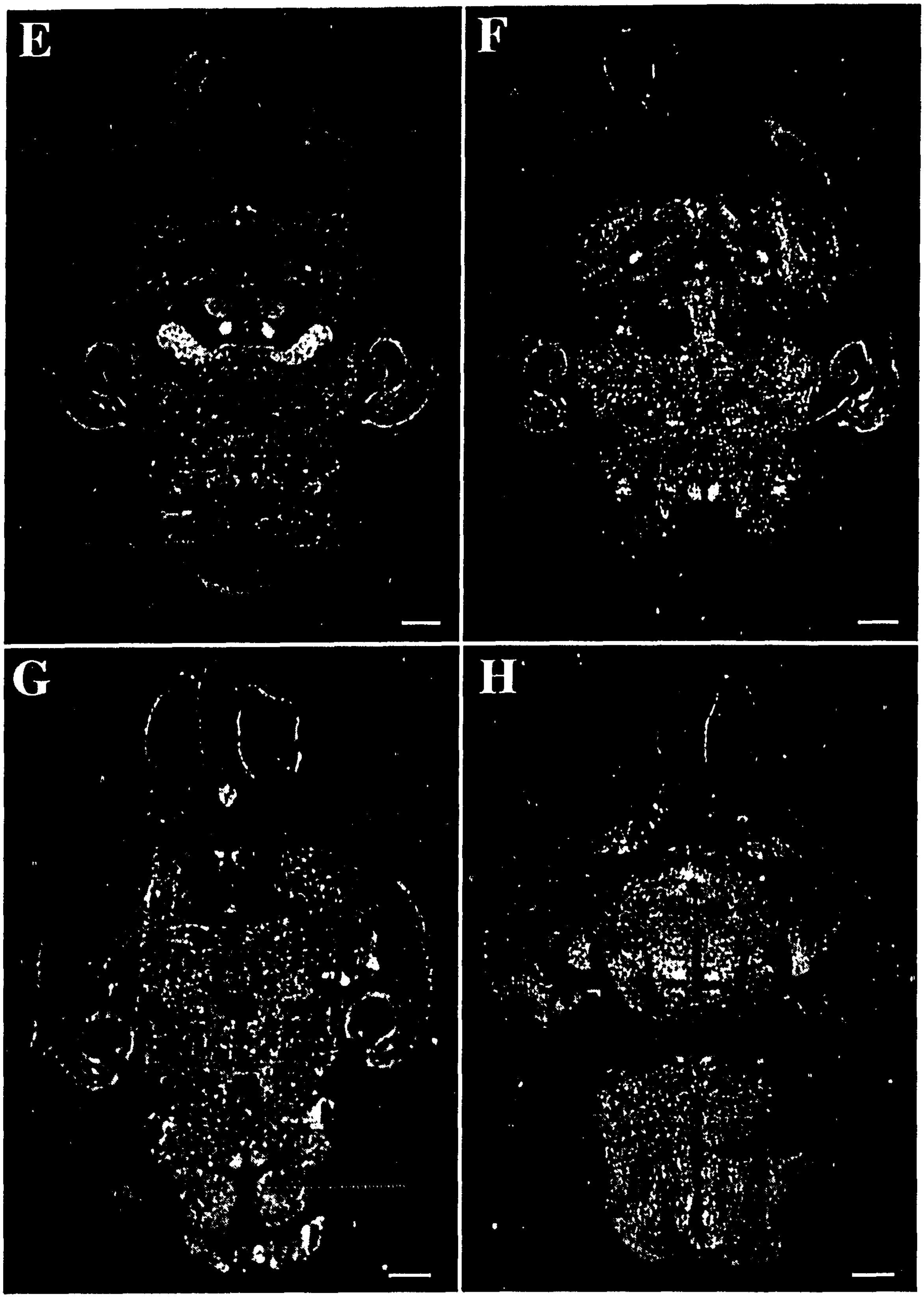
E
F
G
H

Figure 28: Dark field film and emulsion autoradiographs showing VGF mRNA expression in parasagittal sections of the P5 rat brain.
For abbreviations see list p. xviii. Scale bars, 1 mm.

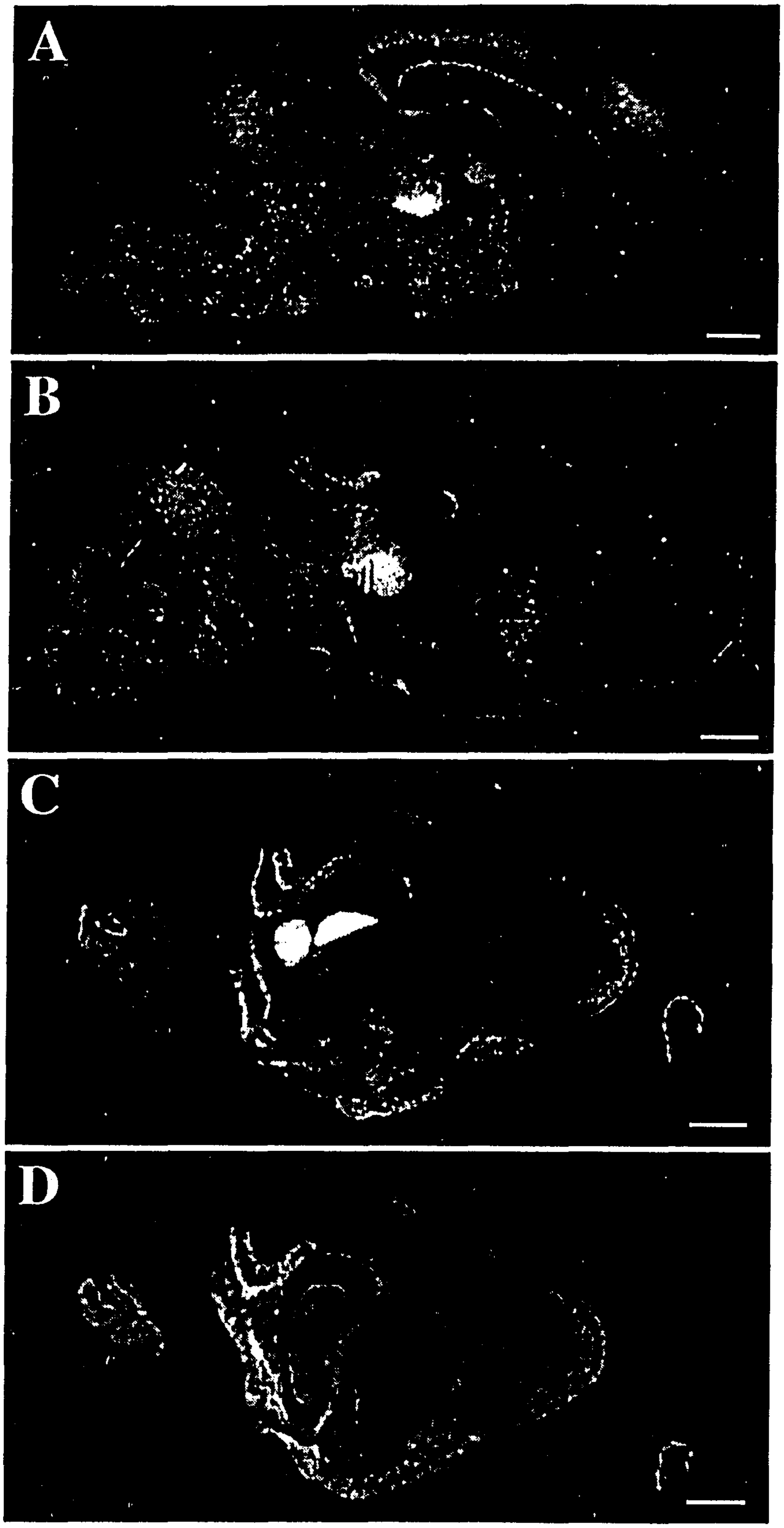
A
B
C
D

Figure 29: Dark field film and emulsion autoradiographs showing VGF mRNA expression in parasagittal sections of the P10 rat brain.

For abbreviations see list p. xviii. Scale bars, 1 mm.

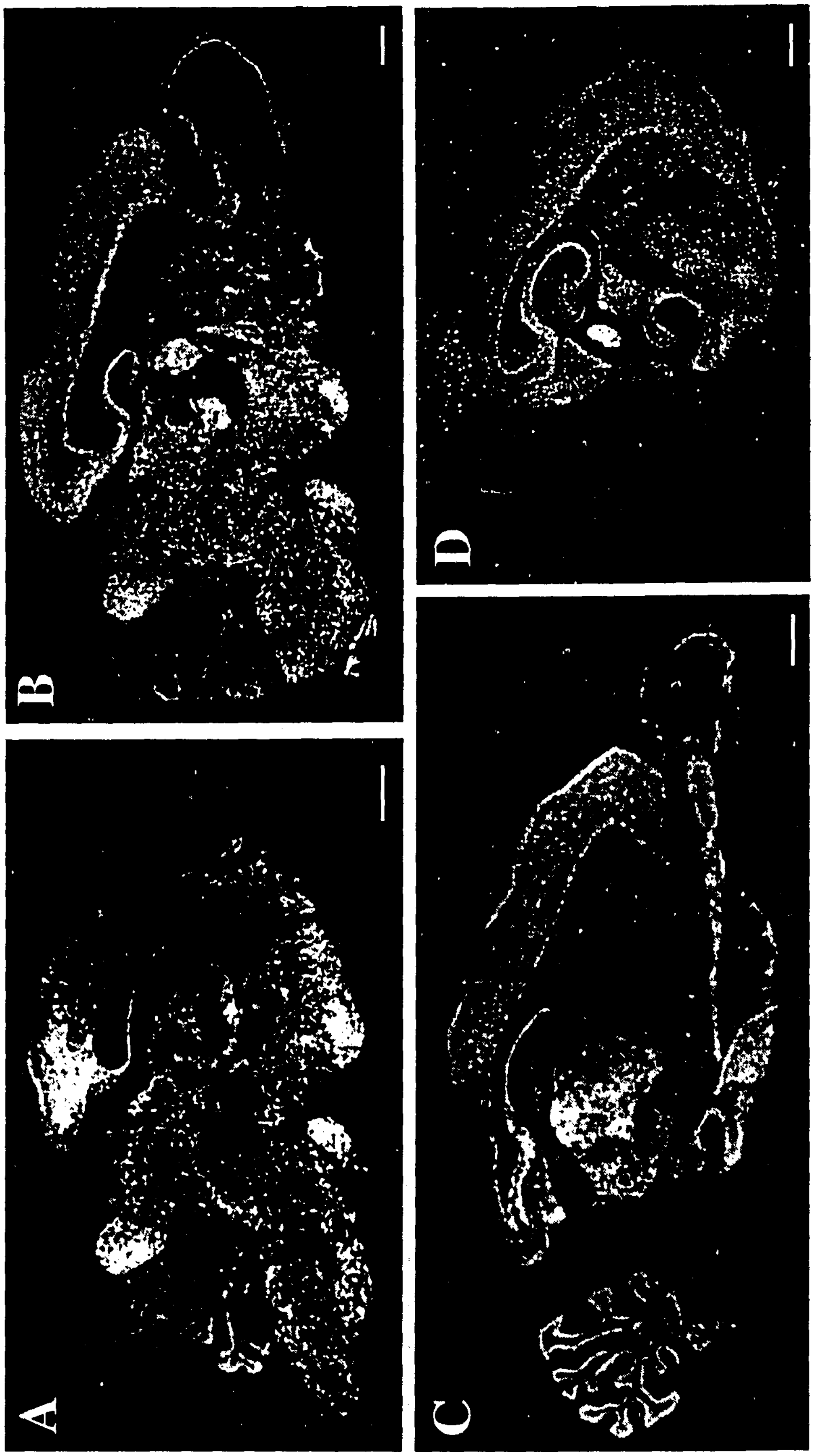
A
B
C
D

Figure 30: Dark field film autoradiographs showing VGF mRNA expression in horizontal sections of the P10 rat brain. *A* is more dorsal and *B* more ventral. For abbreviations see list p. xviii. Scale bars, 2 mm.

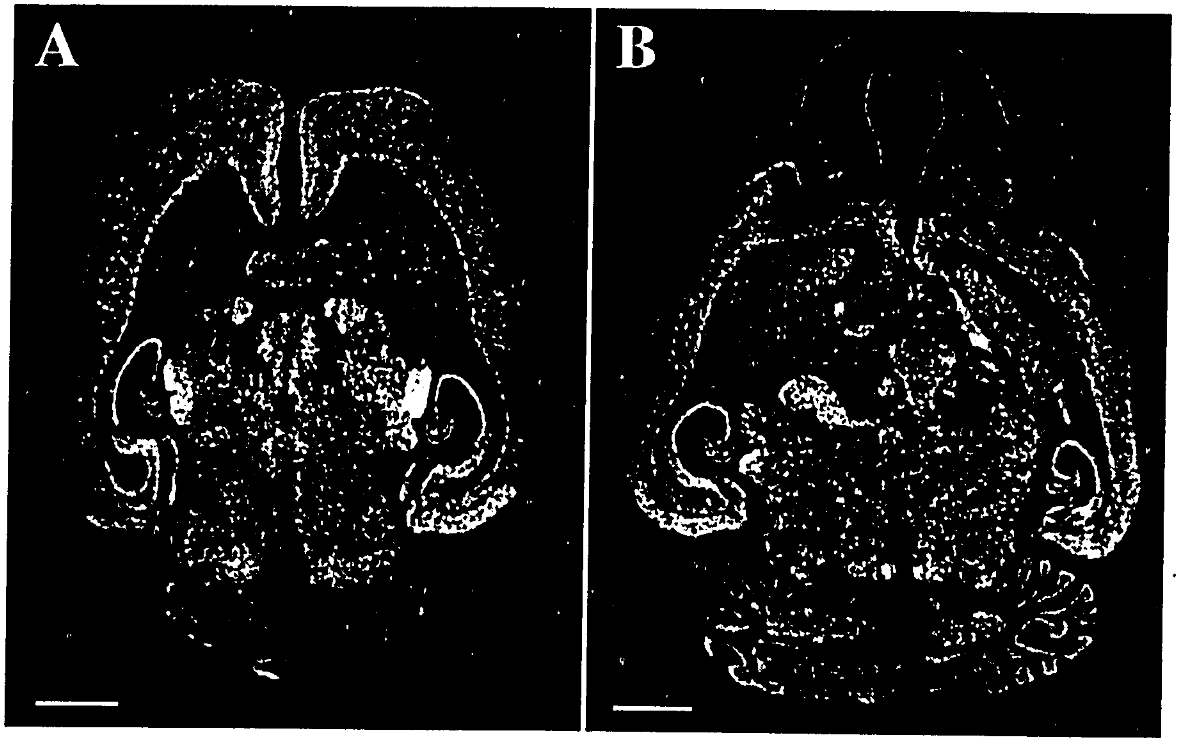
A
B

Figure 31: Dark field film autoradiographs showing VGF mRNA expression in coronal sections of the P10 rat brain.

For abbreviations see list p. xviii. Scale bars, 1 mm.

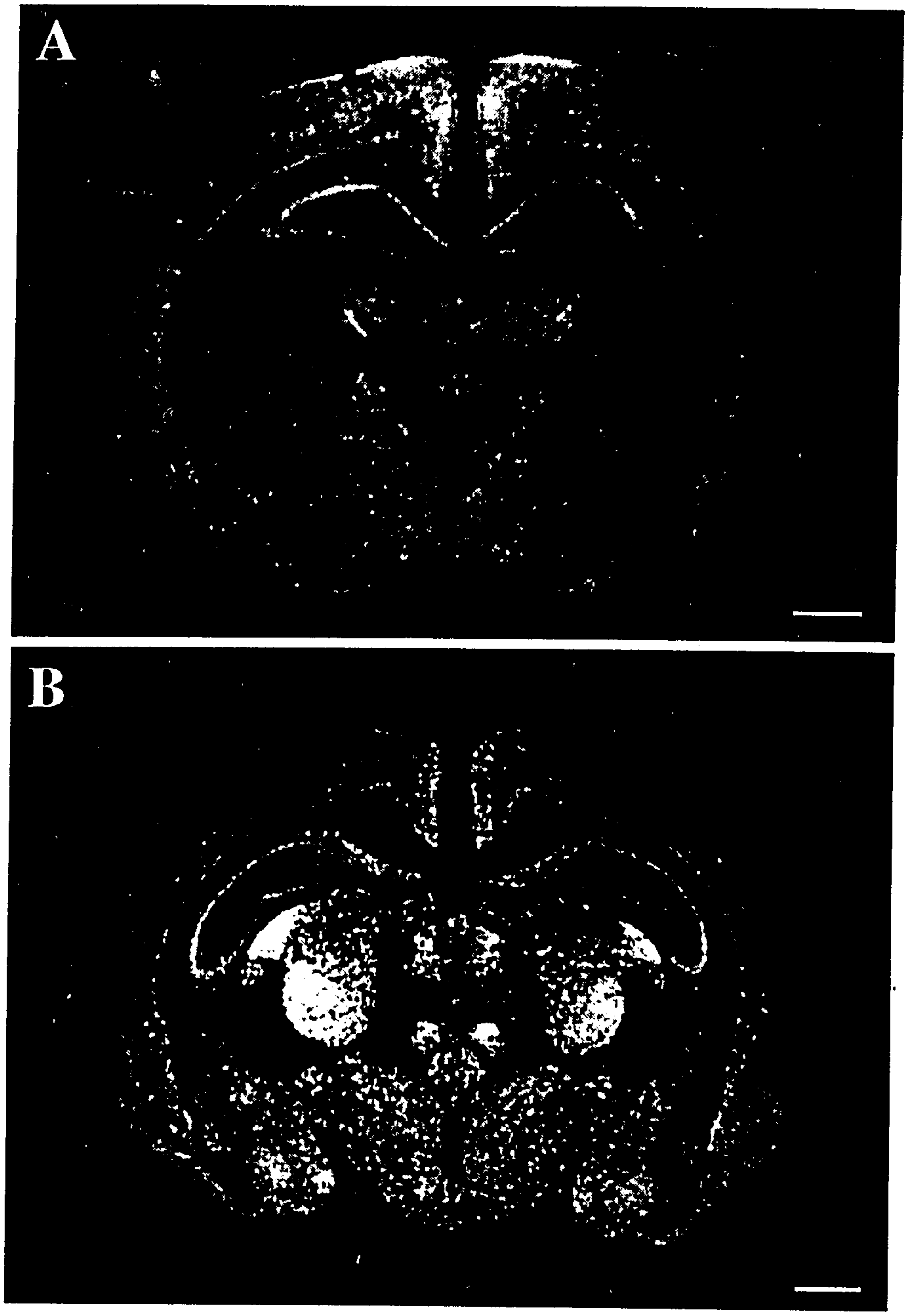
A
B

Figure 32: Dark field autoradiographs depicting the pattern of VGF mRNA expression throughout cerebellar development. *A*: E17.5 parasagittal, emulsion. *B*: E19.5 parasagittal, emulsion. *C*: P0 parasagittal, film. *D*: P5 coronal, emulsion. *E*: P10 horizontal, emulsion. *F*: Adult horizontal, film.

For abbreviations see list p. xviii. Scale bars: *A*-*C*, 100 µm; *D*-*F*, 500 µm.

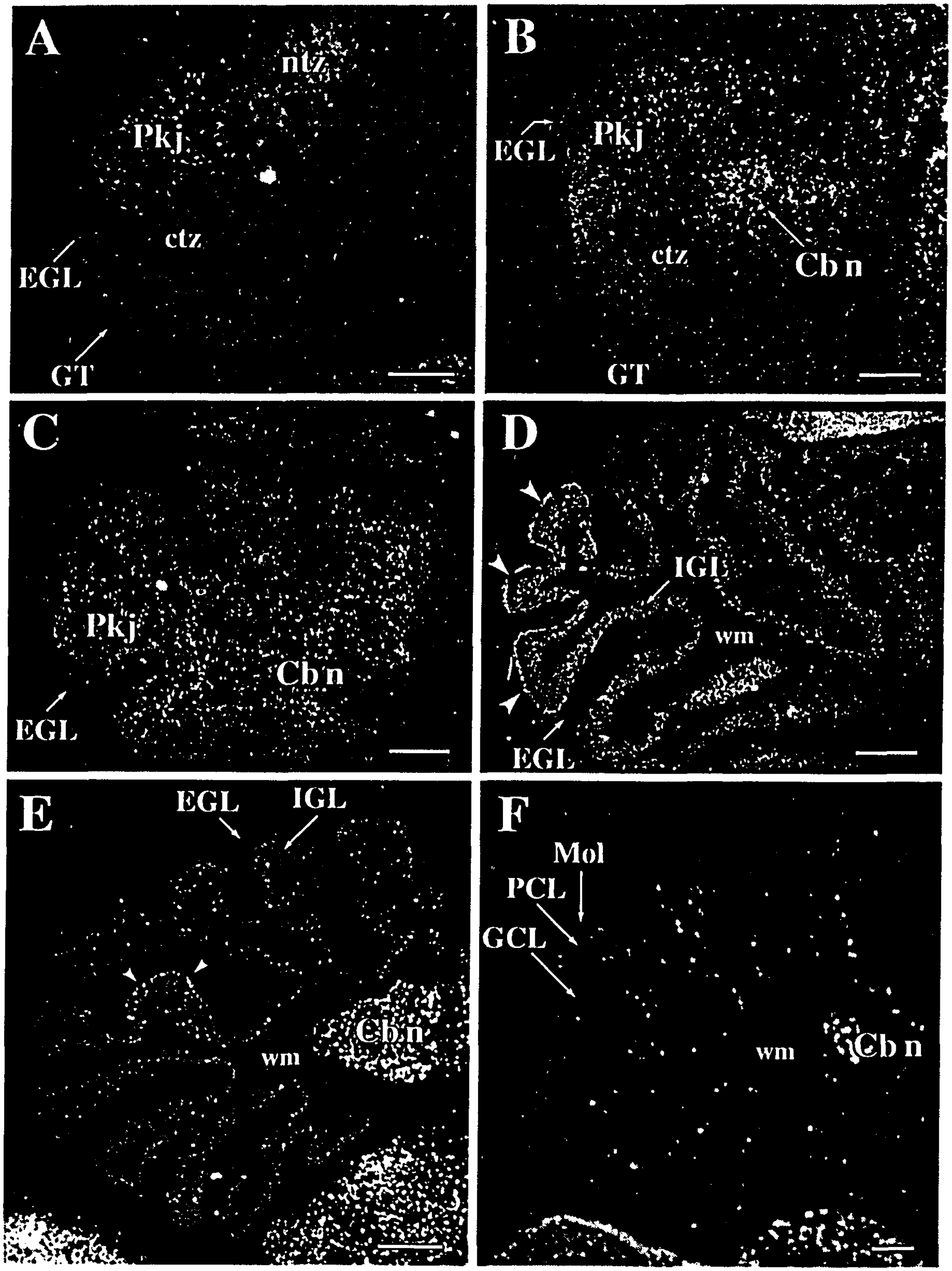
A
ntz
Pkj
ctz
EGL
GT
B
EGL
Pkj
ctz
Cb n
GT
C
Pkj
Cb n
EGL
D
IGL
wm
EGL
E
EGL
IGL
Cb n
wm
F
Mol
PCL
GCL
wm
Cb n

Figure 33: Dark field autoradiographs of VGF mRNA expression throughout hippocampal development. *A*: E17.5 parasagittal, emulsion. *B*: E19.5 parasagittal, emulsion. *C*: P0 parasagittal, emulsion. *D*: P5 parasagittal, emulsion. *E*: P10 parasagittal, emulsion. *F*: Adult horizontal, film.

For abbreviations see list p. xviii. Scale bars: *A*, 200 µm; *B*, 250 µm; *C*, 200 µm ; *D*, 250 µm; *E-F*, 500 µm.

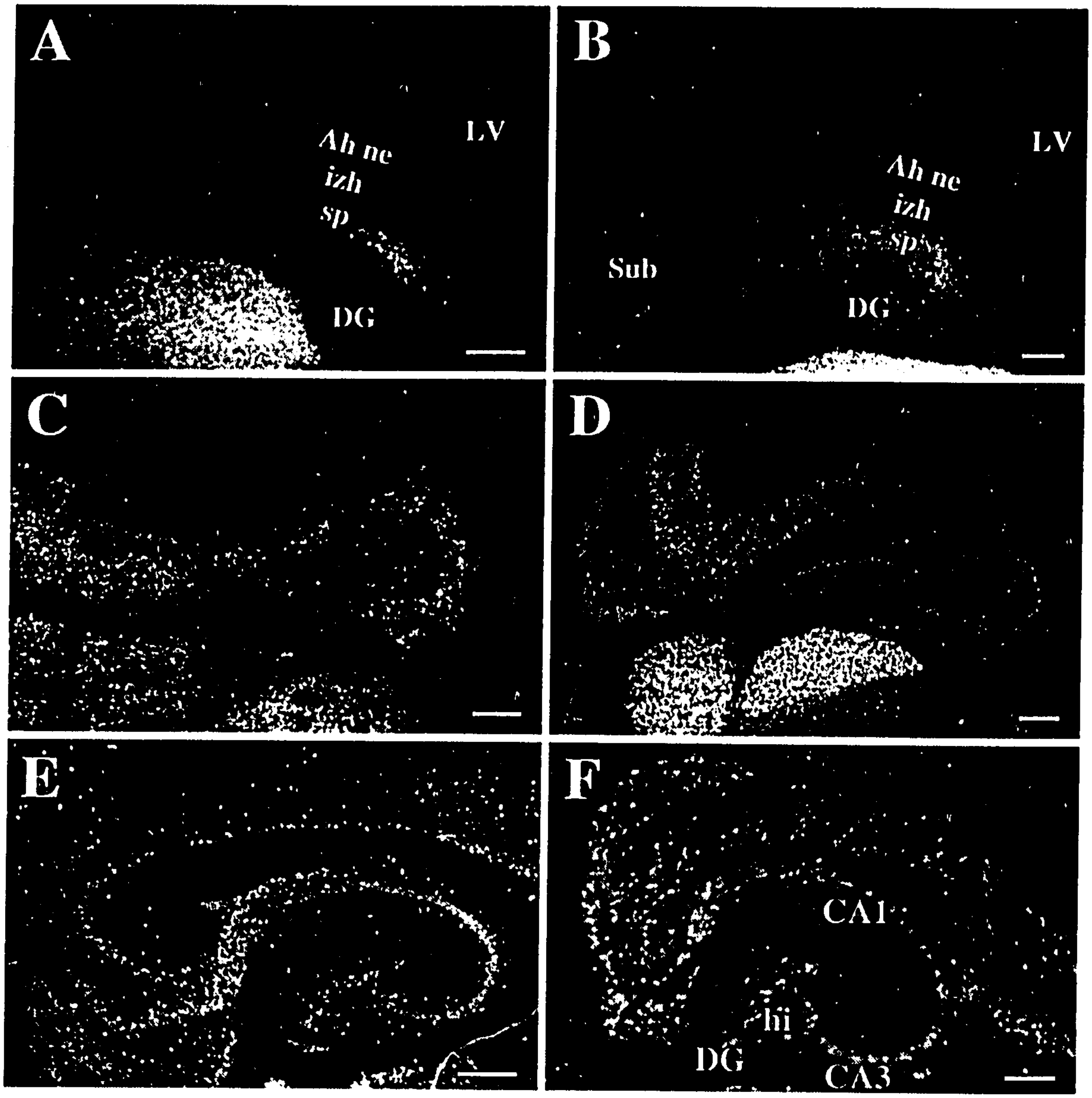
A
Ah ne
izh
sp
LV
DG
B
Ah ne
izh
sp
LV
Sub
DG
C
D
E
F
CA1
hi
DG
CA3

Figure 34: Ontogeny of VGF mRNA expression in parasagittal sections through the pituitary gland. *A* & *A'*: E15.5. *B* & *B'*: E17.5. *C* & *C'*: E19.5. *D* & *D'*: P0. Each bright and dark field respectively.

For abbreviations see list p. xviii.

Scale bars, 250 μm.

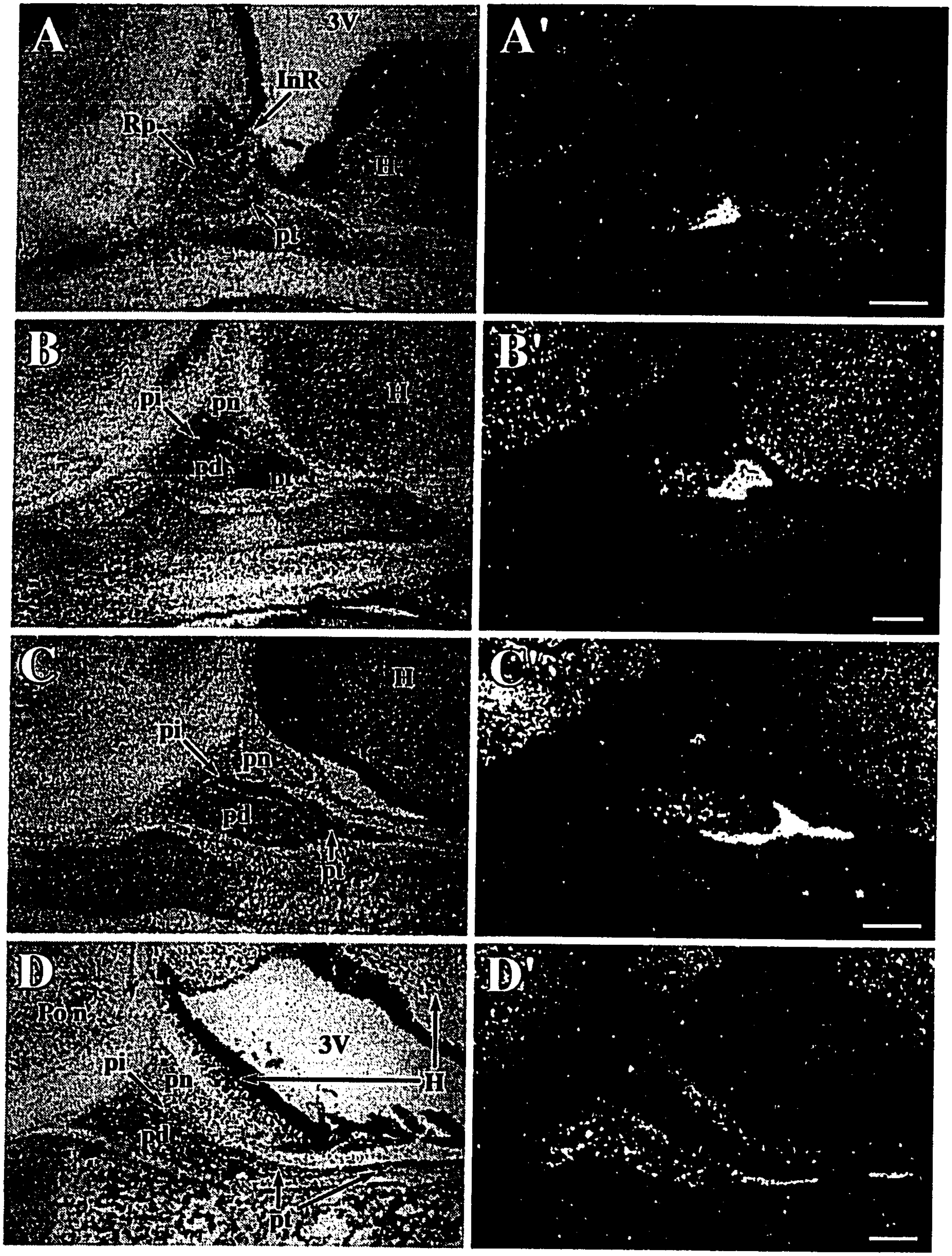
A
3V
InR
Rp
H
pt
A'
B
pi
pn
H
pd
pt
B'
C
H
pi
pn
pd
pt
C'
D
Pon
pi
pn
3V
H
pd
pt
D'

Discussion

Previous studies had examined only the gross regional distribution of VGF mRNA expression in the nervous systems of developing animals or in adults (Salton *et al.* 1991). Although one detailed immunohistochemical localization of VGF had been performed in the adult brain (van den Pol *et al.* 1994), most studies were largely restricted to hypothalamus, and little information on developing animals was available (van den Pol *et al.* 1989). In the hope that a more thorough knowledge of the anatomic localization of VGF production during neuroontogeny would aid in understanding the developmental role of VGF, I used *in situ* hybridization histochemistry to localize VGF mRNA throughout the rat embryo and postnatal rat head.

The data shown and described herein demonstrate that VGF mRNA expression begins much earlier in embryogenesis than previously believed. Whereas RNase protection studies performed in our laboratory had not been able to detect VGF mRNA in brain until E18 (Salton *et al.* 1991), I have found that moderate levels of VGF message occur in discrete regions of the brain as early as E13.5, and in the primordia of the dorsal root, cranial, and sympathetic ganglia, as well as what appear to be migrating crest cells fated to become enteric ganglia, as early as E11.5. It is possible that the initial onset of VGF expression may be even earlier, but in preliminary studies of E9.5 embryos no VGF riboprobe hybridization was appreciated (data not shown). It is between these two ages that the neural crest cells comprising the DRG and cranial ganglion anlage accumulate in their mature positions and begin to differentiate.

The age of onset of VGF expression I have shown here also significantly predates that proposed in a recent paper which reported some limited data describing VGF localization by *in situ* hybridization and immunohistochemistry in the developing rat (Lombardo *et al.* 1995). In that study, VGF mRNA was not detected until E16, when low levels were seen in the dLGN. By E19, they reported hybridization in the MGN, VPM and VPL nuclei of the thalamus as well. At P7, VGF labeling was seen in the thalamus, hypothalamus, amygdala, cingulate, and entorhinal cortex, and hybridization expanded and decreased into an adult-like pattern by P45. Generally, VGF immunoreactivity in a given structure appeared two days after the mRNA became detectable. While not in conflict with the data reported here, in that I observed VGF mRNA hybridization in these regions at similar stages, the pattern of VGF mRNA expression reported by Lombardo *et al.* is a subset of that which I have detected in the current study. For example, by E19.5 I have shown extensive labeling with the VGF probe not only in the thalamic nuclei, but also throughout other portions of the CNS and PNS including parts of the telencephalon, most of the diencephalon and brainstem, the pituitary, spinal cord, sensory and autonomic ganglia, and the myenteric plexus. While some of these differences may be due to technical differences of strain or sensitivity between the two studies, the remainder may easily be attributed to the fact that Lombardo *et al.* were focusing on the development of the thalamus and were not attempting to provide a detailed account of developmental VGF expression throughout the nervous system as was the goal of the current study. Both studies have noted, however, that VGF mRNA expression in the brain begins in restricted regions and gradually expands into more and more brain structures as development progresses.

A general temporal correlation between the onset of VGF mRNA production and very early neuronal differentiation of expressing cell populations was noted. Hybridization to the VGF probe was not seen in zones of active proliferation, nor was expression generally strong in many regions known to contain streams of young cells migrating away from the germinal matrices, such as the intermediate zone of the cortical plate. Thus, initial expression of VGF mRNA did not seem to occur at the time of commitment to the neuronal lineage. Rather, VGF message expression tended to appear in developing neurons as they reached their initial target locations and began to differentiate—as was seen in the neurons of the developing hippocampus, the developing Purkinje cells, and young motor neurons in the ventrolateral spinal cord among many others—and argues for an early role for VGF in neuronal differentiation *in vivo.*

That VGF mRNA hybridization was found at quite high levels throughout most of the brain by birth implies that significant expression of VGF mRNA precedes the bulk of synaptogenesis in many of the regions in which it is expressed (Jacobson 1991). However, since many neuronal populations establish sets of early "pioneer" synapses which can precede the peak of synaptogenesis by several days, and VGF mRNA synthesis must by necessity precede protein generation, direct involvement of VGF peptides in the process of synaptogenesis, a process critical to the course of neuronal differentiation, is not precluded. In fact, Lombardo *et al.* (1995) have recently shown that the appearance of VGF immunoreactive neurons in the thalamus and of VGF immunoreactive nerve fibers in the cortical subplate and subsequently in the cortical plate itself, coincide precisely with the location and timetable of synaptogenesis of the incoming thalamocortical afferent connections. Additional detailed studies of VGF mRNA and protein expression during development in specific regions of the brain should help to determine how general the association between VGF and synaptogenesis is. Furthermore, examination of mice carrying a targeted disruption of the VGF gene, which have recently been generated in our laboratory, should shed light on how critical VGF is in brain development in general and synaptogenesis in particular.

With regard to the VGF expression observed in the developing cerebellum, several different patterns were seen. The developing Purkinje cells, born between E12 and E15, began to express VGF mRNA after they had migrated out of the cortical transitory zone and settled in their target area below the path of the developing EGL. Expression in the Purkinje neurons increased in the first week of life, and decreased thereafter, displaying only weak VGF mRNA hybridization in the adult (see Chapter 3). Neurons of the deep cerebellar nuclei, on the other hand, express VGF mRNA from their settling in the nuclear transitory zone during embryogenesis, and continue to express high levels of VGF message into adulthood. It is not known whether granule cells ever express VGF mRNA: the proliferative EGL does not, nor do adult granule neurons. However, as these cells are born between P8 and P15, their major period of differentiation was not studied here, and remains to be investigated. An intriguing burst of strong expression in what appeared to be either the consolidating Purkinje cell layer or the inner portion of the primitive molecular layer, and seemed to occur in a developmental wave, was observed from P0-P10. During this period, a number of events are ongoing in this region including a profusion of Purkinje cell/climbing fiber synaptogenesis, the birth and differentiation of Golgi neurons (E19-P2), and the birth of basket and stellate cells (from P4-P7 and P9-P10 respectively), obscuring the interpretation of the significance of this wave of strong VGF hybridization. More detailed work will be needed to determine the precise nature of this phenomenon. Lastly, what appear to be Golgi neurons strongly express VGF mRNA in the adult cerebellum, but there is little known about the migration and differentiation of these cells during development. The punctate staining in the IGL at P10 may represent this population.

In the pituitary, VGF expression was observed at very high levels in the primordial pars tuberalis from E15.5 onward, decreasing to simply high levels by the day of birth. How long expression in this poorly understood lobe continues into postnatal life and whether changes occur at puberty remain to be determined. The onset of expression in the pars tuberalis seemed to occur simultaneously throughout, just at the time these cells are differentiating. By E15.5, the cells of the developing pars tuberalis have been shown to have become non-mitotic—it is not until E18 that evidence of further cell division is seen—and to possess a differentiated secretory morphology, making this the earliest differentiating lobe of the adenohypophysis (Stoeckel *et al.* 1973, 1993). Yet throughout both the non-mitotic differentiation and proliferative periods, intense *in situ* hybridization for the glycoprotein hormone α-subunit has been described in the pars tuberalis and pars distalis, in a nearly identical pattern to that seen for VGF hybridization in the current study, except that the α-subunit was shown to be expressed in Rathke's pouch as early as E12 (Stoeckel *et al.* 1993). Furthermore, immunoreactivity for the adrenal and gonadal stimulating hormones of the pars distalis has also been described by E15 in the pars tuberalis, one day earlier than the onset of similar expression in the pars distalis; however, with the exception of thyroid stimulating hormone-β (TSH-β) expression which has been seen by several groups, this has only been reported by one of the many groups studying pituitary glycoprotein hormone expression (Nemeskéri *et al.* 1988; Japon *et al.* 1994). Calbindin immunoreactivity has also been reported in the pars tuberalis by E16 (Abe *et al.* 1990). Moreover, melatonin receptors have been shown to be expressed in the pars tuberalis by E14 as well. Interestingly, the only other brain structures which contain high affinity receptors for this pineal hormone are the suprachiasmatic nuclei, which also exhibited exceptionally high VGF mRNA hybridization. This implies that VGF may play a specific downstream role in creating the circadian and seasonal physiological rhythms controlled by melatonin and these two neuroendocrine structures. Recently, the primate pars tuberalis and the other lobes of the adenohypophysis have been shown to express neurotrophin and $p75^{NTR}$ immunoreactivity during development and in the adult (Borson *et al.* 1994), so even here it is possible that the expression of VGF may be linked to neurotrophin activity.

From E17.5 onward, scattered cells in the pars distalis also displayed strong VGF mRNA expression; and at P0, hybridization could be seen in the pars intermedia. Immunohistochemical studies have found VGF immunostaining in occasional anterior pituitary lactotrophs in adult males, and in gonadotrophs and a few lactotrophs in adult females, the levels of which vary with the estrous cycle (Ferri 1995). Further studies to determine the expression pattern of VGF mRNA in the juvenile and adult rat should provide an interesting comparison with the immunohistochemical studies which have already been done. Furthermore, the population of cells in the pars distalis which expresses neurotrophin appears not to contain any of the classical adenohypophyseal hormones, and may thus constitute a novel cell type. It will be interesting to see in future studies what relationship exists between these cells and those expressing VGF.

Lastly, it warrants mention that VGF expression was also observed just outside the trophoblast in the wall of the gravid uterus at midgestation, implying a potential neural or neuroendocrine role for VGF in the maintenance of pregnancy. Further investigations will be necessary to determine whether this expression pattern uniquely occurs during pregnancy and if so what its timecourse and function might be. Alternately, it may be found that VGF expression in this region is part of the normal anatomy of the uterus; for example, this ring of cells could prove to be intramural postganglionic parasympathetic neurons.

Chapter 5: Regulation of VGF mRNA in the Adult Rat Brain by Neuronal Activity, Seizure and Lesion

Abstract

To gain further insight into the possible functions and regulation of VGF *in vivo*, I characterized the expression of VGF messenger RNA (mRNA) by *in situ* hybridization, during development and in adult brain, and compared it to the distributions of mRNAs encoding neurotrophin receptors TrkA, TrkB, and TrkC. Significant overlap in VGF and *trk* mRNA expression exists, and though no *trk* mRNA was exclusively colocalized with VGF message, a good correlation was found between the distributions of the VGF and *trk*B kinase mRNAs. VGF expression peaks during critical periods in the developing peripheral and central nervous systems (PNS and CNS), and I have found it to be regulated in the CNS by experimental manipulations that affect electrical activity and by lesion. Inhibition of retinal electrical activity during the critical period of visual development rapidly repressed VGF mRNA in the lateral geniculate (dLGN). In the adult, kainate-induced seizures transiently induced VGF in dentate, hippocampal, and cortical neurons within hours. Direct cortical lesion strongly induced VGF mRNA in ipsilateral cortex within hours, and strongly repressed expression in ipsilateral striatum. Ten days later, following normalization of ipsilateral cortical VGF expression, I observed delayed induction of VGF mRNA in a portion of deafferented striatum where compensatory cortical sprouting has been detected. VGF is, therefore, induced by *in vivo* paradigms which lead to neurotrophin induction and synaptic remodeling.

Introduction

Elucidation of the role of neurotrophic factors in nervous system development has been aided by study of neuronal differentiation *in vitro*. The PC12 pheochromocytoma cell line (Greene and Tischler 1976) is widely used to study the mechanism(s) of action of nerve growth factor (NGF) (reviewed by Halegoua *et al.* 1990). Treating PC12 cells with NGF initiates a signaling cascade downstream of the TrkA receptor tyrosine kinase, resulting in differentiation into neurite-bearing cells sharing many properties with sympathetic neurons (Loeb *et al.* 1991; Marshall 1995). VGF (the non-acronymous accepted name of this gene previously designated VGF8a, NGF33.1, and a2) is one of only a few genes rapidly regulated in PC12 cells much more robustly by NGF than epidermal growth factor (EGF) (Salton *et al.* 1991) which, despite activating similar signaling pathways, does not cause neuronal differentiation (Bartel *et al.* 1989; Qiu and Green 1992; Marshall 1995). VGF mRNA induction by NGF and by depolarization is rapid, peaking after 3-6 hours and returning to baseline by 48 hours, results from increased VGF gene transcription, and is partially independent of new protein synthesis (Levi *et al.* 1985; Salton 1991; Salton *et al.* 1991; Baybis and Salton 1992; Possenti *et al.* 1992). Furthermore, deprivation and readdition of NGF to neuronally-differentiated PC12 cells reinduces VGF mRNA (Salton *et al.* 1991). VGF mRNA is expressed in the PNS and CNS, peaking during the first two weeks of rat postnatal development (Salton *et al.* 1991), suggesting that increased VGF expression might be associated with synaptogenesis and/or synaptic remodeling *in vivo*. VGF polypeptide, identified in neurons in adult brain (van den Pol *et al.* 1989, 1994) and in neurosecretory cells in the adrenal medulla and pituitary (Ferri *et al.* 1992), is released from large dense-core vesicles through the regulated pathway (Possenti *et al.* 1989) and contains several putative sites of proteolytic cleavage which appear to be differentially processed by neuronal versus neuroendocrine cells (Possenti *et al.* 1989, 1994; Salton *et al.* 1991; Trani *et al.* 1995). Another study has identified a VGF-derived 30 amino acid carboxy-terminal peptide in bovine posterior pituitary (Liu *et al.* 1994), and salt-loading, adrenalectomy, and septohippocampal cholinergic damage have been shown to up-regulate VGF levels in hypothalamic neurosecretory cells (Mahata *et al.* 1993a,b,c).

Expression of Trk receptors in embryonic, postnatal and adult rat CNS and PNS, and targeted gene 'knockouts' of them, suggest that neurotrophin receptors and their ligands play critical roles in the developing and adult nervous system (reviewed in Klein 1994). Specific neurotrophins, and probably a subset of gene products regulated by them, contribute to the formation of synaptic connections during development (Cabelli *et al.* 1995) and following injury (reviewed in Longo *et al.* 1993). Since NGF, brain-derived neurotrophic factor (BDNF), and neurotrophin-3 (NT-3) all induce VGF gene expression *in vitro* (Levi *et al.* 1985; Salton *et al.* 1991; Bonni *et al.* 1995), I compared the distributions of the mRNAs encoding their receptors with that of VGF, and investigated whether VGF expression might be regulated *in vivo* by experimental manipulations, including intraocular tetrodotoxin (TTX) injection, cortical injury, and seizure, which all affect neuronal activity and/or neurotrophin expression in specific brain regions. My results demonstrate that VGF mRNA is rapidly regulated by these paradigms, that induction in the brain is likely to be triggered largely by activation of the TrkB receptor, and that VGF expression is dramatically increased in a region of the striatum where compensatory axonal sprouting is known to be occurring approximately ten days following cortical injury. VGF or VGF-derived peptides may, therefore, be involved in synaptogenesis and/or synaptic reorganization in response to injury.

Results

Comparison of VGF to trkA, B, & C mRNA distributions during development and in the adult rat brain

Expression of VGF and *trk* mRNAs was evaluated by *in situ* hybridization, and results are shown in Figure 35. The *trk* probes used are complementary to the regions of the mRNAs which encode the extracellular domains of the Trk receptors and, therefore, detect both full-length and noncatalytic truncated splice variant *trk* mRNAs (Middlemas *et al.* 1991). Control sense strand probes hybridized to adjacent tissue sections produced no specific hybridization signal as is shown in Figure 35*A*. Panels *B-E* show adjacent parasagittal sections of an E13.5 embryo hybridized with antisense cRNA probes specific for VGF, *trk*A, *trk*B, and *trk*C mRNAs respectively. In this plane of section, VGF and all three *trk* mRNAs were expressed quite strongly in the developing DRGs. Additionally, the *trk*B and *trk*C messages were also detected in the neuroepithelium of the brain, particularly the telencephalon, while the *trk*B alone appeared along the great vessels, and in the cervical sympathetic ganglia, the pancreatic primordium, and the ovary. At E13.5, moderate-high VGF mRNA expression was also found in developing cranial ganglia (*e.g.*, trigeminal (V), facial (VII), and vestibular (VIII)), sympathetic ganglia, and the ventrolateral mantle layer of the developing spinal cord, with low levels in the remainder of the neuroepithelium of the brain and spinal cord (Figure 35*B*, Figure 37*A*, and Chapter 4; a detailed description of VGF mRNA expression in the adult CNS and during development were presented in Chapters 3 and 4 respectively). Figure 35*F-I* show the distribution of VGF and the *trk* messages I found in the cranial region of parasagittal sections of an E19.5 embryo. By this point in late fetal life, VGF mRNA was expressed at moderate to high levels in much of the brain, particularly in the thalamus, hypothalamus, and brainstem, in the pituitary, and also continued to be expressed in the cranial, sympathetic, and sensory ganglia (Figure 35*F* and Chapter 4). *Trk*A message (Figure 35G) was seen in a few cells at the base of the forebrain, and in the trigeminal and cervical sympathetic ganglia, while *trk*B and *trk*C mRNAs (Figure 35*H* and *I*) were detectable not only in these ganglia, but throughout the brain.

By postnatal day 10 (P10), although some neurons are still being born (*e.g.*, in the olfactory system, dentate gyrus, and cerebellum), most regions are actively involved in differentiation and myelination. The distribution of VGF mRNA signal I observed clearly overlapped extensively with those of the *trks*, yet corresponded directly with none (Figure 35*J-M*). For example, VGF, *trk*B, and *trk*C were all found at high levels in the anteroventral nucleus of the thalamus, yet unlike *trk*B and *trk*C, VGF was not found at high levels in the cerebellum, and it was quite prevalent in the hypothalamus and brainstem while *trk*C was not. In general, in P10 sections, VGF signal was strongest in several of the thalamic nuclei, but was clearly expressed throughout the brain, including the neocortex. At this age, *trk*A was expressed in an extremely limited population of cells, in the striatum, basal forebrain, and brainstem. Conversely, *trk*B was widely distributed in the P10 brain and was expressed at much higher levels than the other neurotrophin receptor messages, particularly in areas such as the cortex, olfactory bulb, internal granule cell layer of the cerebellum, and the anteroventral nucleus of the thalamus, and unlike the other *trk* mRNAs, was found in fiber tracts and the proliferating subependymal zone. *Trk*C, on the other hand, showed low levels of hybridization throughout most of the brainstem and hypothalamus, moderately high levels in the cortex, olfactory bulb, basal ganglia, and tectum, and high levels in the hippocampal formation, anteroventral nucleus of the thalamus, internal granule cell layer of the cerebellum, pituitary, and olfactory tubercle.

The distribution of these messages in adjacent horizontal sections of an adult female rat brain is shown in Figure 35*N*-*Q*. The expression of VGF mRNA throughout the adult rat brain varied dramatically, from very high levels detected in several hypothalamic nuclei, for example, to very low levels in the cerebellum (see Chapter 3). VGF mRNA was expressed in at least a subset of neurons in nearly every region of the brain, however, as has been observed previously in immunohistochemical studies (van den Pol *et al.* 1994), there was no detectable VGF mRNA in non-neuronal cells of the CNS. The distributions of all three *trk* mRNAs overlapped in distinct regions with that of VGF, but each showed distinct differences as well. For example, although *trk*A (Figure 35*O*) mRNA was detected in areas of the brain that also expressed VGF, such as the medial septal nucleus, the vertical limb of the diagonal band, in scattered cells throughout the striatum, and several brainstem nuclei, its pattern was severely restricted compared to that of VGF. *Trk*B, on the other hand, although its distribution also overlapped with that of VGF, was expressed at high levels in many regions that did not express much VGF, such as white matter, the dentate gyrus, and the cerebellum (Figure 35*P*). Although like VGF, the distribution of *trk*C is neither as global as that of *trk*B nor as restricted as that of *trk*A, it too showed regions of similarity and dissimilarity with VGF expression (Figure 35*Q*). For example, both messages were broadly expressed in the cortex, striatum, and olfactory bulb, however, there was extremely strong *trk*C hybridization in the cerebellum and dentate granule layer and low levels of VGF, while there was a distinct lack of *trk*C in the portions of the thalamus where VGF levels were quite high.

Expression of VGF and the *trk* mRNAs in several areas of the nervous system is shown at higher magnification in Figure 36. Panels *A*-*D* show hybridization to transverse sections through the E13.5 spinal cord and DRGs. Although all four genes were clearly expressed in the developing DRGs, in the spinal cord VGF was only expressed in ventrolateral portion of the basal plate, a portion of the mantle layer which also expressed *trk*B and *trk*C mRNA, while the *trk*A hybridization signal was restricted to a narrow band in the ventromedial portion of the developing cord. In examples from P10 brain, there was again significant expression of VGF in areas not expressing *trk*A but containing *trk*B and *trk*C mRNA, as in the hippocampal formation *(E-H)*, where VGF mRNA was abundant in the CA fields including the dentate hilus, in scattered cells of the stratum oriens and the apical molecular layers, and in the subiculum, and was found at lower levels in the dentate granule layer. *Trk*B was expressed in all of these regions, in both neurons and glial cells, and in the ventricular ependyma, while *trk*C mRNA was restricted to the stratum pyramidale of CA1-3 and the dentate granule cell layer, in which it was particularly abundant, but which contained little VGF. In the thalamus *(I-L)*, VGF hybridization was strong in the anteroventral nucleus (AV) and the ventral group, modest in several other nuclei, and completely absent from some regions. *Trk*A was undetectable, while *trk*B was found at fairly uniform levels throughout, enhanced somewhat in VGF-expressing nuclei. *Trk*C was expressed at quite high levels in the AV where VGF mRNA was abundant, but was low in the ventral group which contained high levels of VGF message, and moderate in more posterior nuclei which displayed little VGF expression. Examination of the adult basal ganglia *(M-P)* revealed a diffuse, low *trk*B hybridization signal in the globus pallidus, while the *trk*C and VGF probes labeled scattered cells, and *trk*A was not expressed at all. In the striatum and nucleus basalis magnocellularis, all four mRNAs were expressed: *trk*B gave the most dense signal in the striatum, while *trk*A labeled the fewest cells, however, in the nucleus basalis VGF and *trk*A displayed the most prominent labeling of the four probes. In the septal region (*Q-T*) a similar pattern arose, with *trk*B displaying high but diffuse expression including labeling of the ependyma and fornix. VGF and *trk*C were both expressed throughout the septum, but in the nearby thalamic nuclei VGF expression was much higher than that of *trk*C. *Trk*A was expressed in fewer cells, and was restricted to the medial septal nucleus and anterior paraventricular nuclei of the thalamus. Overall, these data support the general relationships between VGF and *trk* expression observed at low magnification: *trk*A expressing regions were a subset of the VGF expressing ones; while the patterns of VGF and *trk*C mRNA expression overlapped, they correlated poorly overall (some areas with high VGF expressed little *trk*C and vice versa); finally, VGF expressing areas seemed to be a subset of those expressing *trk*B, particularly the neuronal sites of *trk*B expression.

The *trk*B probe used above hybridizes to mRNAs encoding both the truncated non-catalytic isoforms, expressed primarily by astrocytes, oligodendrocytes, and cells of the ependyma and choroid plexus, and the full-length catalytic kinase forms of Trk, expressed exclusively by neurons (Frisen *et al.* 1993; Altar *et al.* 1994). So, to further examine this apparent relationship between VGF and *trk*B expression, I compared the VGF *in situ* hybridization pattern with that generated using a probe specific for mRNA encoding the exclusively neuronal catalytic kinase form(s) of TrkB (*trk*BK probe). Although differences in distribution were apparent, most obviously in the cerebellum where *trk*BK hybridization was abundant while VGF levels were particularly low, and in the thalamic and brainstem nuclei, where VGF showed a broad range of expression levels whereas hybridization of the *trk*BK probe was more uniform, the patterns of expression of mRNAs encoding VGF and the catalytic form of TrkB were otherwise quite similar to one another (Figure 37).

Changes in VGF mRNA expression in the dorsal lateral geniculate nucleus following unilateral intraocular TTX injections

Unilateral intraocular injection of the sodium channel blocker TTX was performed on postnatal day 23 during the critical period of visual system development. As shown in Figure 38, this blockade of retinal electrical activity resulted in a rapid and substantial down-regulation of VGF mRNA in the geniculate fields corresponding to the injected eye: the large crossed retinal terminal field comprising most of the contralateral dLGN and the small uncrossed field in the ipsilateral dLGN both showed down-regulation of VGF message. No change was seen in animals injected only with vehicle (C and D), nor was any change observed at 1 hour after TTX injection (E and F). By 6 hours after injection, however, a decrease in VGF mRNA hybridization was detectable (G and H). This effect was most marked at 12 (I and J) and 24 hours (K and L), and was still apparent at 48 hours after TTX injection (M and N). No changes in VGF mRNA expression were detected in either the superior colliculus, the other major target of retinal axons, or the visual cortex at any of these time points (data not shown).

Changes in VGF mRNA expression following kainate-induced seizures

Moderate VGF mRNA hybridization was seen over the pyramidal cell layer of the CA regions of the normal adult rat hippocampal formation, while low levels were observed over the dentate gyrus granule cells. As seen in Figure 39, after a seizure-inducing intraperitoneal injection of kainic acid there was an increase in VGF mRNA in the stratum granulosum of the dentate gyrus, barely detectable at 1 hour (Figure 39*B*) but clearly visible by 3 hours (Figure 39*C*). Maximum induction in the dentate to over 700% of control levels was observed at 12 hours postinjection (Figure 39*E*), and had decreased to nearly control levels by 48 hours (Figure 39*G*). VGF mRNA expression also increased in the hippocampal CA fields (Figure 39; 370% maximum), the neocortex (250% maximum), and the piriform cortex (Figure 40; 450% maximum), all clearly apparent by 3-6 hours postinjection. However, unlike the case in the dentate gyrus, VGF mRNA levels in these regions remained elevated at 48 hours postinjection, the latest time point examined. The relative levels of these VGF mRNA changes are plotted in Figure 42.

In the neocortex, the laminar distribution of VGF mRNA expression changed transiently as a result of kainate injection (Figure 41). In control animals, layer V displayed the heaviest VGF labeling, with moderate signal in layer II, and light labeling of layers III, IV, and VI, while only the rare cell in neuron-sparse layer I displayed detectable hybridization. However, by 3 hours following kainate injection, hybridization of the VGF probe over layer II had increased, and by 12 hours, the signal in layer V had begun to decrease—until, by 24 hours hybridization in layer II had become stronger than that in layer V, and additionally, strong expression in layer VI was now apparent. By 48 hours, the distribution of VGF mRNA in the cortical layers was returning toward its normal pattern, with labeling predominantly in layers II and V, although the level of labeling remained higher than in control animals appearing similar to that seen at the 3 hour timepoint.

Changes in VGF mRNA expression following unilateral cortical lesion

Unilateral cortical lesion produced a complex pattern of changes in VGF mRNA expression in the rat brain. In the intact animal, moderate levels of VGF were detected by *in situ* hybridization in most neurons of the forebrain (Figure 43A). No significant changes in VGF mRNA levels were seen at 1 hour after cortical lesioning (Figure 43B). However, by 3 hours I observed a striking increase in autoradiographic labeling of the entire remaining ipsilateral cortex (Figure 43C). This induction, which lasted through at least 24 hours after lesioning (Figure 43D-F), extended throughout the rostrocaudal extent of the neocortex, the cingulate cortex, the orbital, agranular insular, infralimbic, perirhinal, piriform, and entorhinal cortices, the claustrum and the amygdalo-piriform transition area (Figure 44 and data not shown). This robust induction was also seen throughout the anterior olfactory and posteromedial cortical amygdaloid nuclei. No increase was seen in the ventral retrosplenial cortex, the hippocampal formation, or any other structures examined. In this region of ipsilateral cortical induction (shown at higher magnification in Figure 45), VGF mRNA expression was significantly increased in all cortical layers, with levels over 200% of control when averaged across the full depth of the cortex. However, whereas in the intact animal the strongest neocortical VGF expression was found in layer V, following the cortical lesion expression was particularly intense over the cells of layers II/III where levels reached at least 1400% of control. On the side contralateral to the cortical lesion, a subtle decrease in VGF mRNA hybridization in the entire hemisphere was observed beginning by 3 hours postlesion (Figure 43), reaching a nadir of less than 50% of control levels between 6 and 24 hours, and recovering to normal levels by 10 days.

By 3 hours postlesion, in addition to the increased ipsilateral cortical labeling and contralateral repression noted above, repression of VGF mRNA expression in the ipsilateral dorsolateral striatum became detectable (Figure 43*D*). This striatal down-regulation steadily became more apparent from 6 hours following the lesion onward (Figure 43*E-G*). At 3 days postlesion, while the ipsilateral striatum was nearly devoid of VGF expression, displaying less than 20% of control hybridization, the ipsilateral cortical induction seen earlier was gone and the contralateral hemisphere was beginning to recover its expression

(Figure 43*G*). By 10 days following the lesion, although VGF expression in the bulk of the dorsolateral striatum on the side of the lesion remained depressed, there was a striking induction of VGF hybridization in a restricted rostrodorsal region to levels at least 160% of those in control striatum and well over 550% of the hybridization levels in the surrounding repressed area (Figure 43*H*). Figure 46 shows at higher magnification the repression and subsequent localized induction of VGF mRNA in this region of the striatum across time. Quantitative analysis of the VGF mRNA changes described above are plotted in Figure 47.

Figure 35: Comparison of VGF (*B, F, J, N*), *trk*A (*C, G, K, O*), *trk*B (*D, H, L, P*), and *trk*C (*E, I, M, Q*) mRNA expression in the embryo (E13.5, *A-E*), fetal head (E19.5, *F-I*), postnatal brain (P10, *J-M*), and adult brain (*N-Q*) of the rat. *A* demonstrates the lack of specific hybridization of control VGF sense strand riboprobe to a parasagittal section of the E13.5 embryo. All other control hybridizations produced a comparable lack of signal. All sections are parasagittal except the adult sections which were cut in the horizontal plane. Dark field emulsion and inverted film autoradiograms are shown. Abbreviations: *bs*, brainstem; *Cbm*, cerebellum; *Cx*, cortex; *DRGs*, dorsal root ganglia; *fb*, forebrain; *hb*, hindbrain; *Hippo*, hippocampal formation; *OB*, olfactory bulb; *S*, septum; *Str*, striatum; *TriG*, trigeminal ganglion. Scale bars: *A*, 1 mm; *B-E*, 1 mm; *F-I*, 2 mm; *J-M*, 2 mm; *N-Q*, 2 mm.

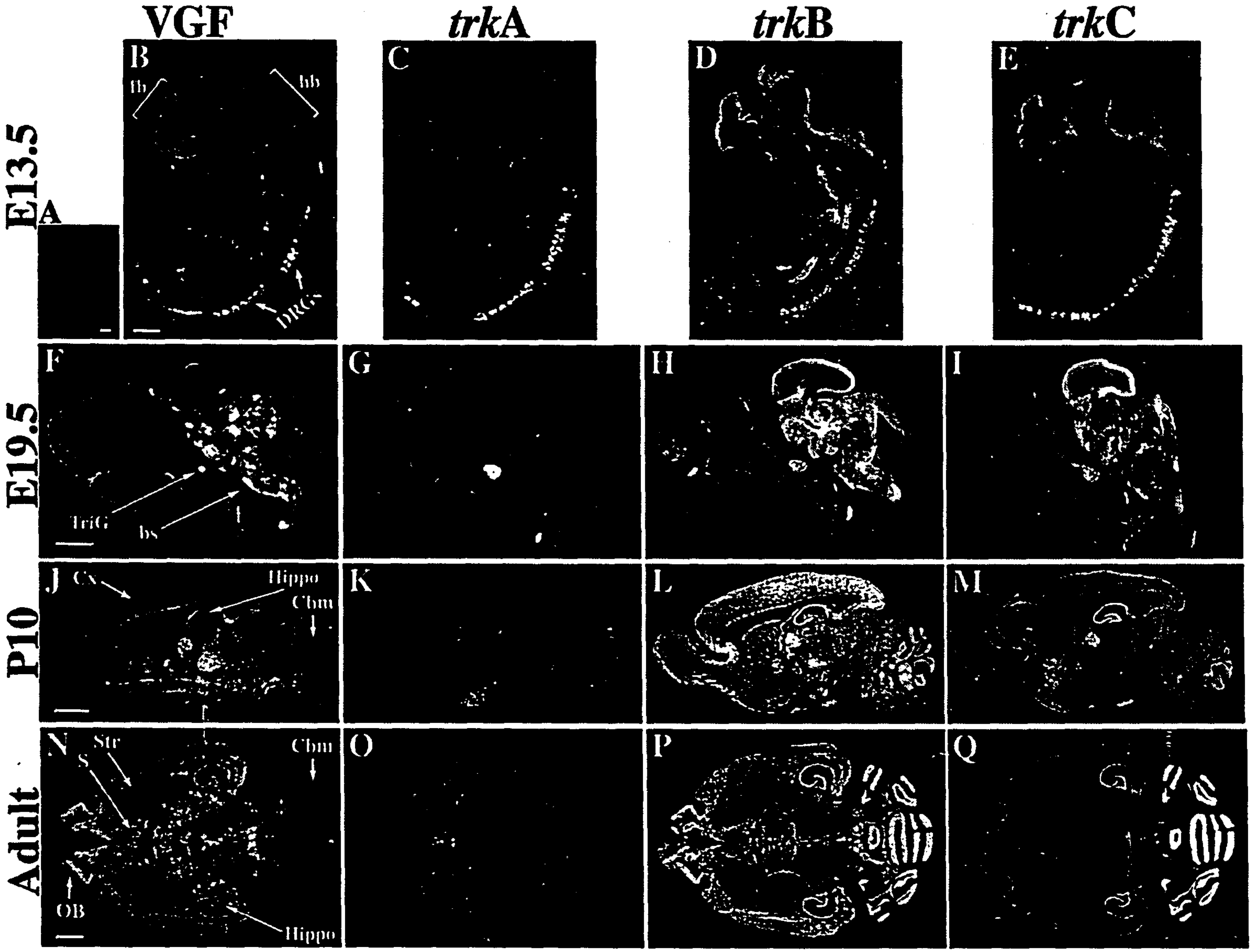
VGF
trkA
trkB
trkC
E13.5
E19.5
P10
Adult
A
B
fb
hb
DRGs
C
D
E
F
TriG
bs
G
H
I
J
Cx
Hippo
Cbm
K
L
M
N
S
Str
Cbm
OB
Hippo
O
P
Q

Figure 36: Dark field emulsion autoradiograms comparing VGF (*A, E, I, M, Q*), *trk*A (*B, F, J, N, R*), *trk*B (*C, G, K, O, S*), and *trk*C (*D, H, L, P, T*) mRNA expression at higher magnification in transverse sections through E13.5 spinal cord and DRGs (*A-D*), the hippocampus (*E-H*) and thalamus (*I-L*) in parasagittal section at P10, and the striatum (*M-P*) and septal region (*Q-T*) in horizontal section in adulthood. Abbreviations: *alar,* alar plate; *AV,* anteroventral nucleus of the thalamus; *basal,* basal plate; *DG,* dentate gyrus; *DRG,* dorsal root ganglion; *fx,* fornix; *GP,* globus pallidus; *LS,* lateral septum; *mantle,* mantle layer; *MS,* medial septum; *nbM,* nucleus basalis magnocellularis; *pvn,* periventricular nucleus of the thalamus; *Str,* striatum; *V,* ventral nuclei of the thalamus; *vz,* ventricular zone. Scale bars: *A-D,* 100 µm; *E-H,* 250 µm; *I-L,* 500 µm; *M-P,* 100 µm; *Q-T,* 200 µm.

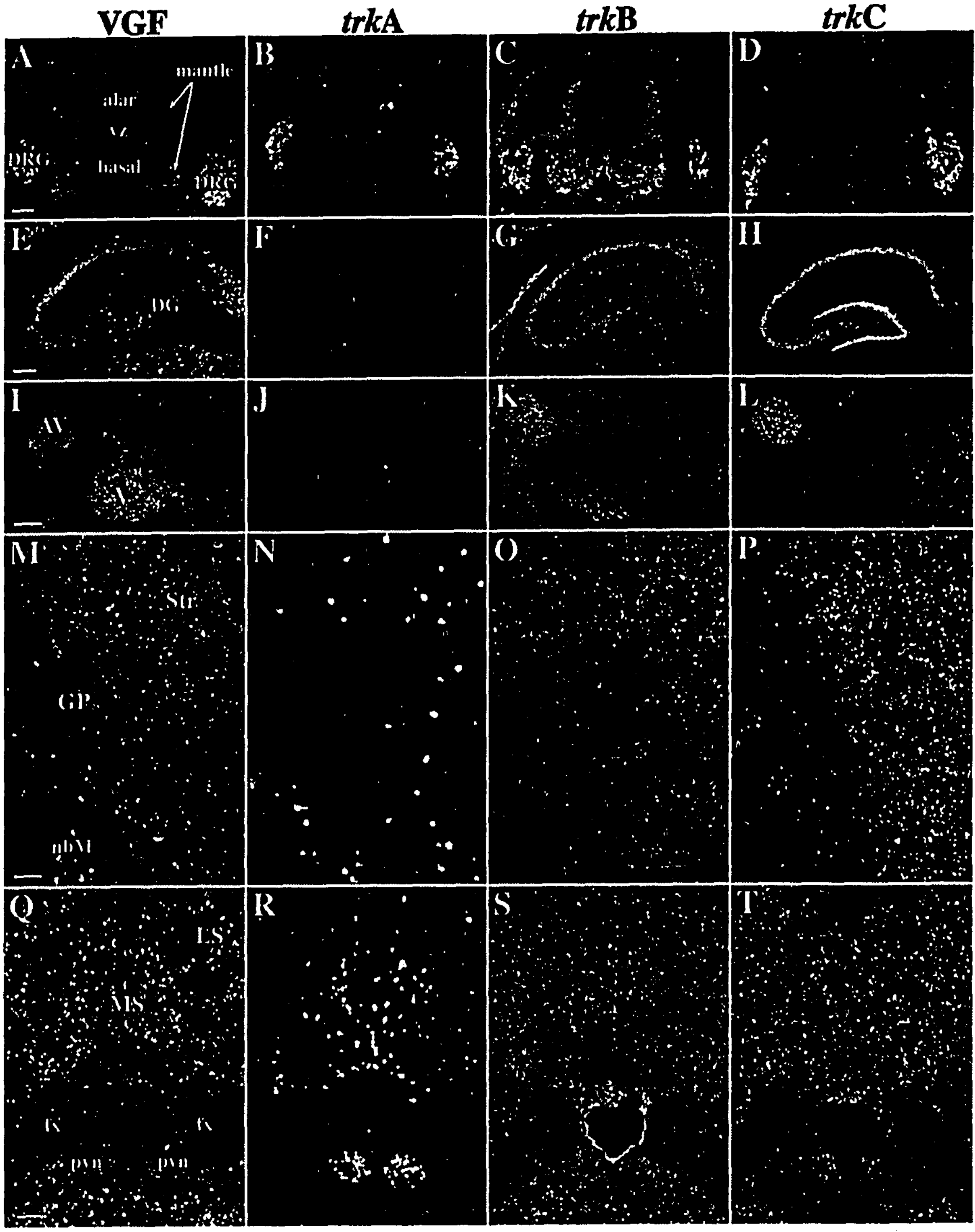
VGF
*trk*A
*trk*B
*trk*C
A
mantle
alar
vz
DRG
basal
DRG
B
C
D
E
DG
F
G
H
I
AV
V
J
K
L
M
Str
GP
nbM
N
O
P
Q
LS
MS
fx
fx
pvn
pvn
R
S
T

Figure 37: Film autoradiograms comparing VGF (*A*) and *trk*B kinase (*B*) mRNA expression in horizontal sections of adult rat brain. Scale bar, 2 mm.

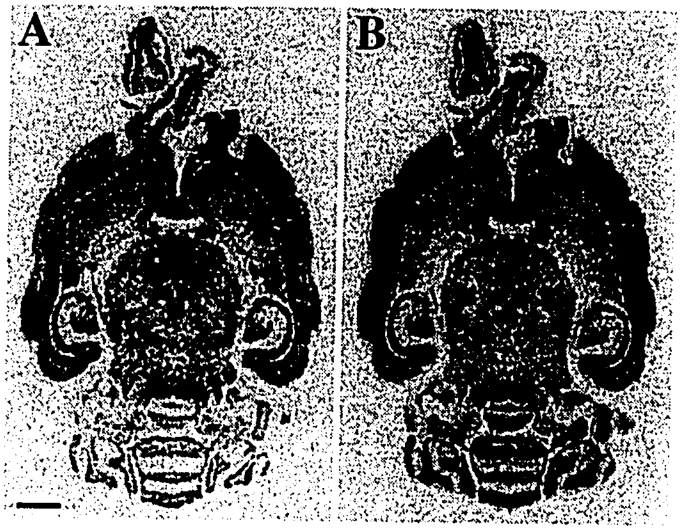
A
B

Figure 38: Effect of unilateral intraocular TTX injection during the critical period of visual development on the expression of VGF mRNA in the dLGN of the thalamus. The schematic diagrams in *A* and *B* indicate the regions of the dLGN containing cells receiving input from *crossed* and uncrossed (*uncr.*) retinal fibers. Other abbreviations: *Hippo Pyr,* a portion of the hippocampal pyramidal cell layer of CA3; *PBS,* phosphate buffered saline. Scale bar, 200 μm.

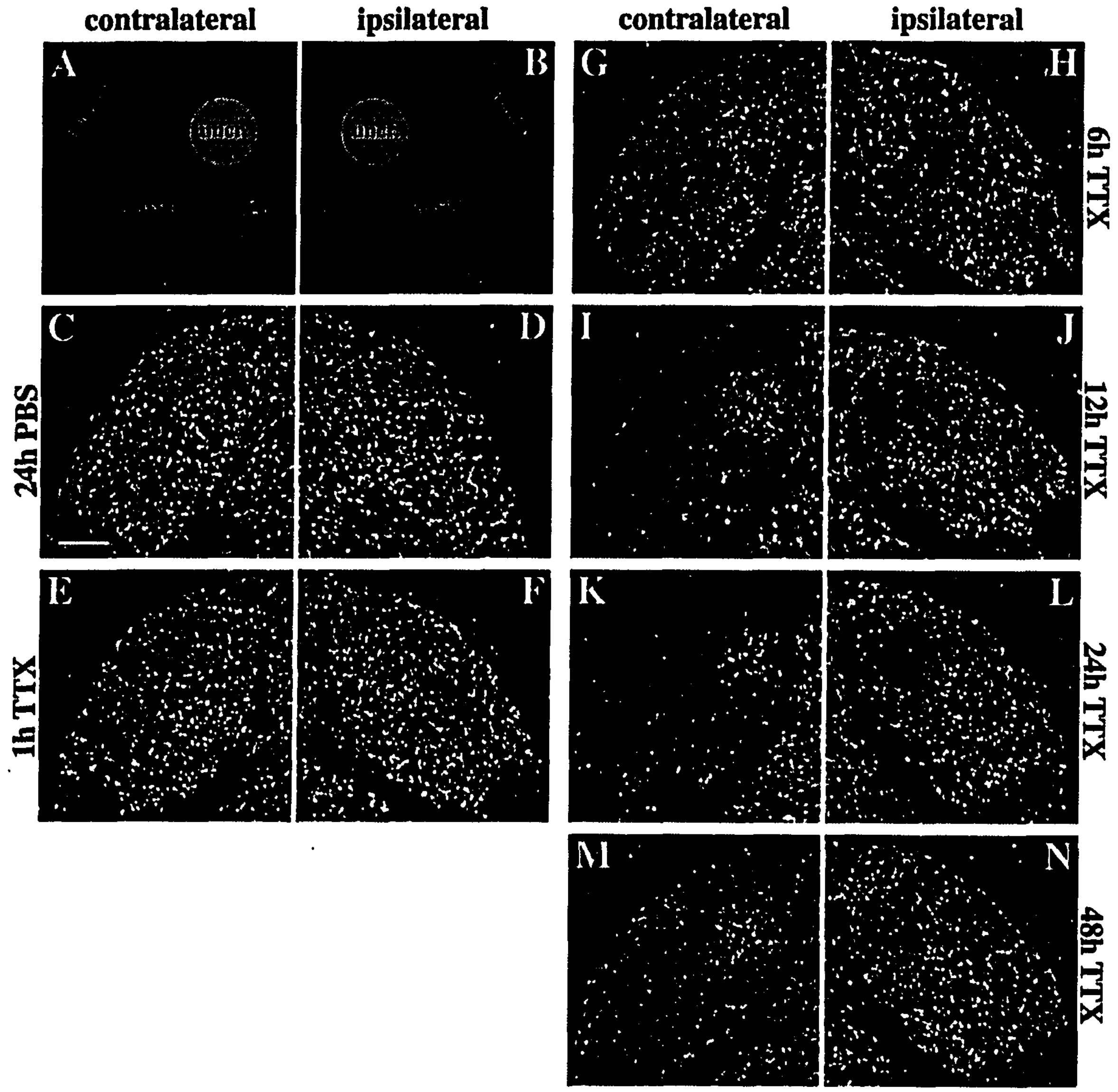
contralateral
ipsilateral
contralateral
ipsilateral
A
B
G
H
6h TTX
C
D
24h PBS
I
J
12h TTX
E
F
1h TTX
K
L
24h TTX
M
N
48h TTX

Figure 39: Dark field emulsion autoradiograms showing rapid induction of VGF mRNA in the dentate gyrus granule cell layer relative to control (*A*), at 1 (*B*), 3 (*C*), 6 (*D*), 12 (*E*), 24 (*F*), and 48 hours (*G*) following i.p. kainic acid injection. Sections were cut in the coronal plane. Scale bar, 600 µm.

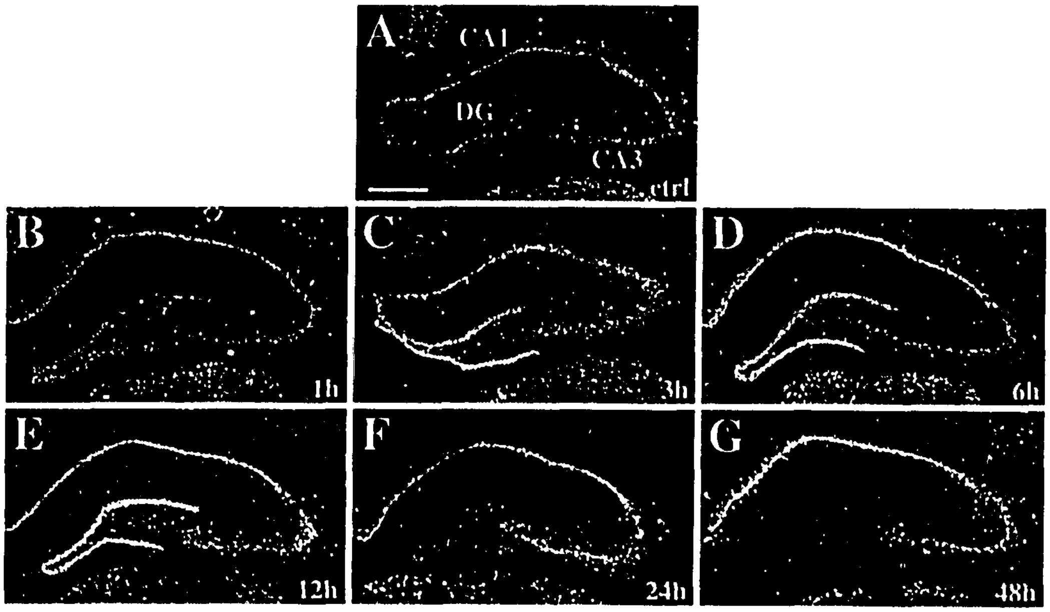
A
CA1
DG
CA3
ctrl
B
1h
C
3h
D
6h
E
12h
F
24h
G
48h

Figure 40: Dark field emulsion autoradiograms showing rapid induction of VGF mRNA in piriform cortex in a control animal (*A*) and 12 hours (*B*) following i.p. kainic acid injection. Scale bar, 500 µm.

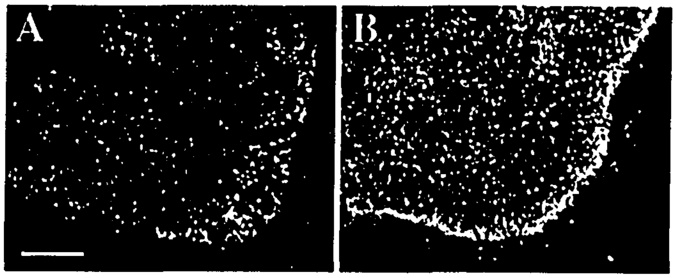
A
B

Figure 41: Dark field emulsion autoradiograms showing changes in the laminar distribution of VGF mRNA in cortex relative to control (*A*), at 3 (*B*), 12 (C), 24 (*D*), and 48 hours (*E*) following i.p. kainic acid injection. Cortical layers are indicated by the Roman numerals *I-VI*. Scale bar, 100 μm.

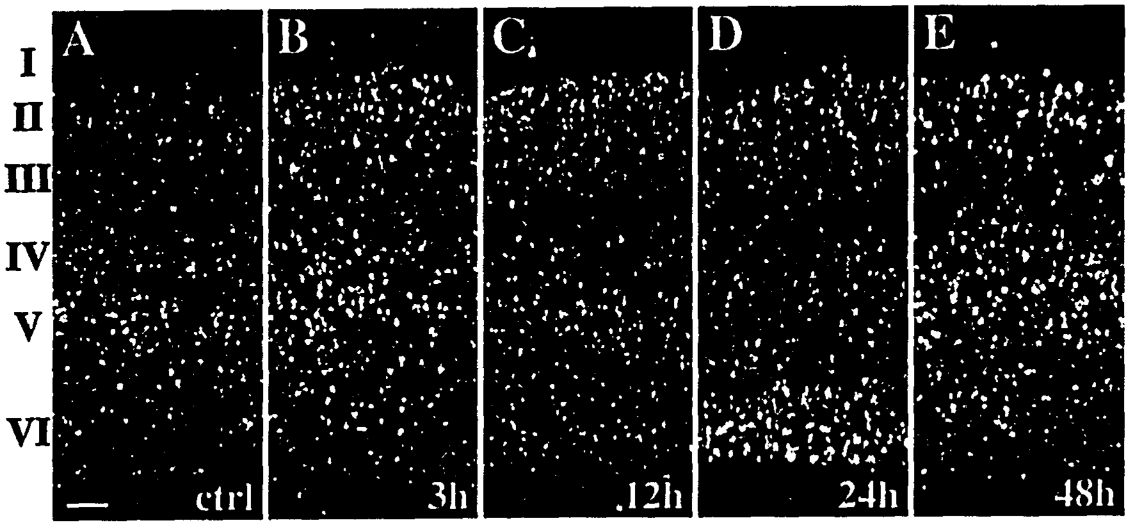
I
II
III
IV
V
VI
A
B
C
D
E
ctrl
3h
12h
24h
48h

Figure 42: Quantitative analysis of changes in VGF mRNA expression in the hippocampal formation, neocortex, and piriform cortex at various times following kainic acid-induced seizure. Values significantly different from those in control animals are marked with *asterisks* (*, p <0.001; ANOVA). Results are given as means ± SEM.

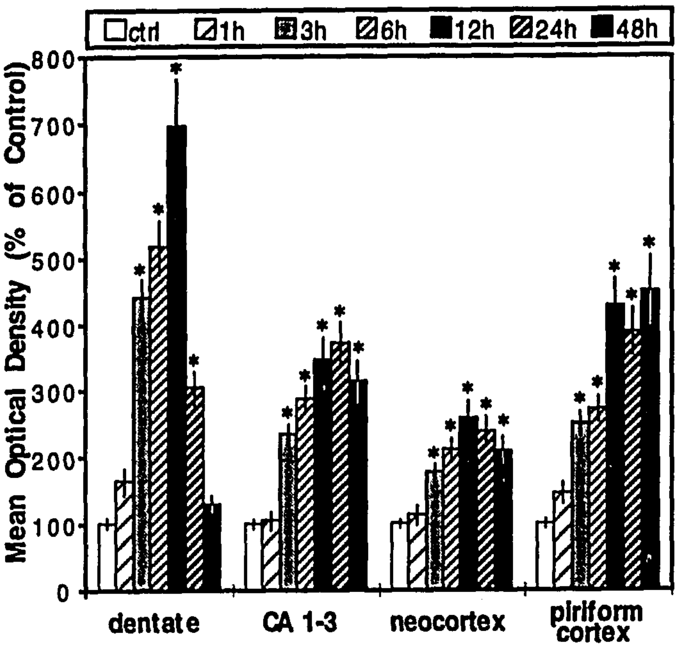
☐ctrl
▨1h
▨3h
▨6h
■12h
▨24h
■48h
Mean Optical Density (% of Control)
800
700
600
500
400
300
200
100
0
*
dentate
CA 1-3
neocortex
piriform cortex

Figure 43: Effect of unilateral cortical lesion on the expression of VGF mRNA in the adult rat brain. Film autoradiograms of coronal sections of control (*A*), and lesioned brains 1 (*B*), 3 (C), 6 (*D*), 12 (*E*), and 24 hours (*F*), 3 days (G), and 10 days (*H*) after lesion are shown. Area of lesion is indicated by *asterisks*. *Area boxed* in *A* is that shown at higher magnification in Figure 13, and where delayed induction is seen at 10 days postlesion (*arrow* in *H*). Scale bar, 2 mm.

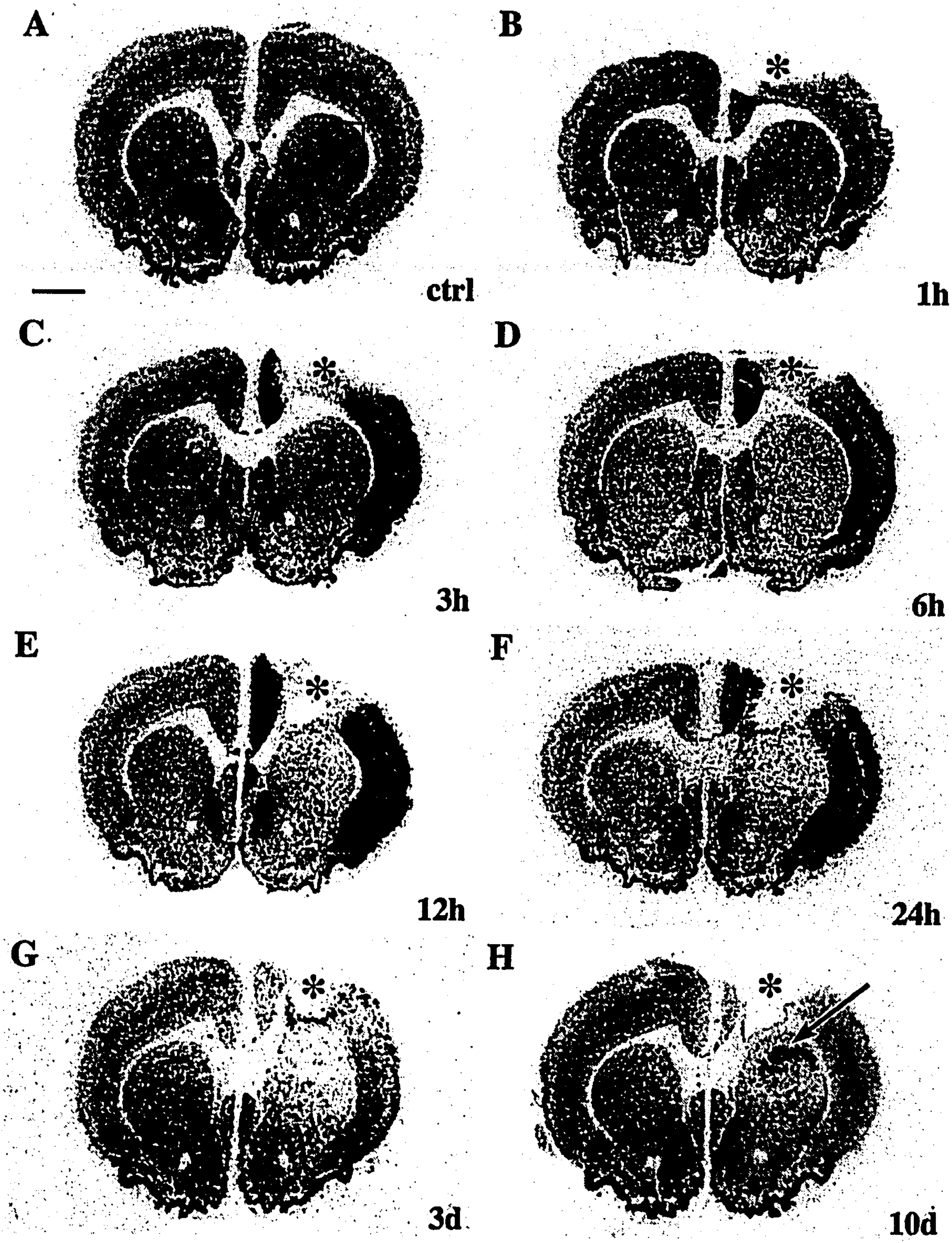
A
ctrl
B
*
1h
C
*
3h
D
*
6h
E
*
12h
F
*
24h
G
*
3d
H
*
10d

Figure 44: Film autoradiograms of coronal sections through a rat brain 12 hours after a unilateral cortical lesion, demonstrating the broad extent of the ipsilateral cortical induction of VGF mRNA. More rostral sections are toward the bottom of the page. Area of lesion is indicated by *asterisks*. Scale bar, 1.5 mm.

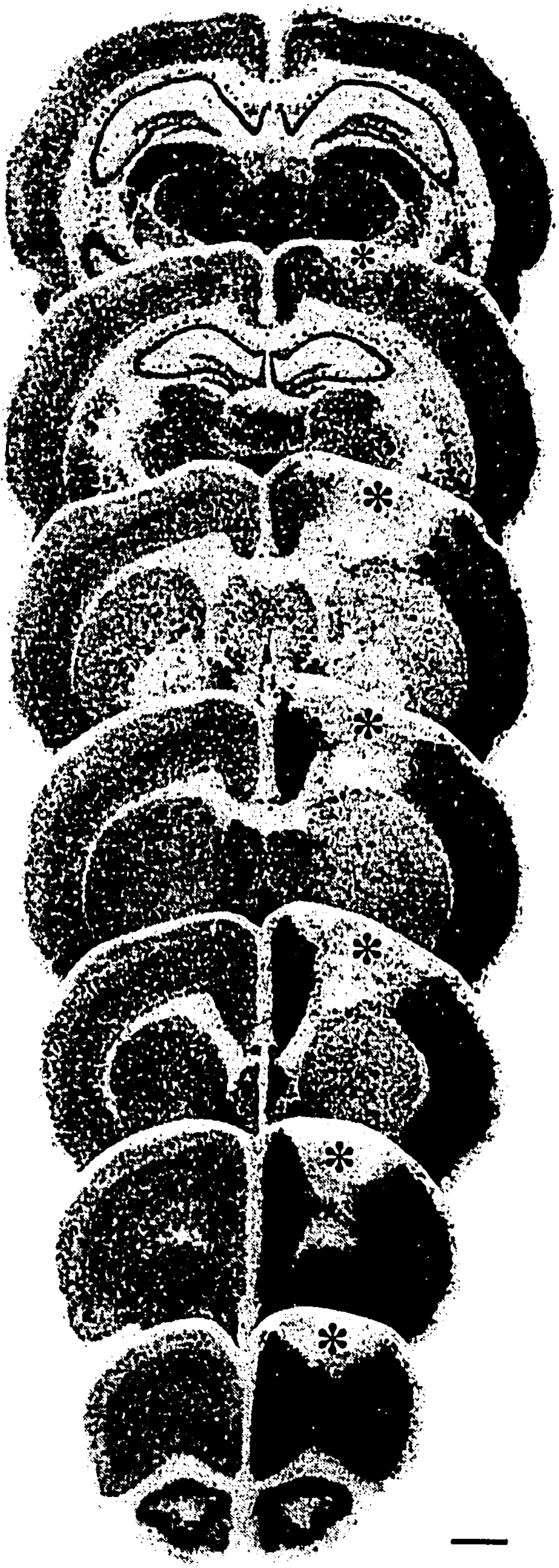

Figure 45: Dark field emulsion autoradiograms showing changes in the laminar distribution of VGF mRNA in cortex relative to control (*A*), at 3 (*B* and C), and 24 hours (D and *E*), and 10 days (*F* and *G*) following unilateral cortical lesion. Note that the laminar distribution of VGF expression remained very similar to that of control cortex on the side contralateral to the lesion (*B, D, F*), while changing on the ipsilateral side (*C, E, G*). Cortical layers are indicated by the Roman numerals *I-VI*. Scale bar, 250 μm.

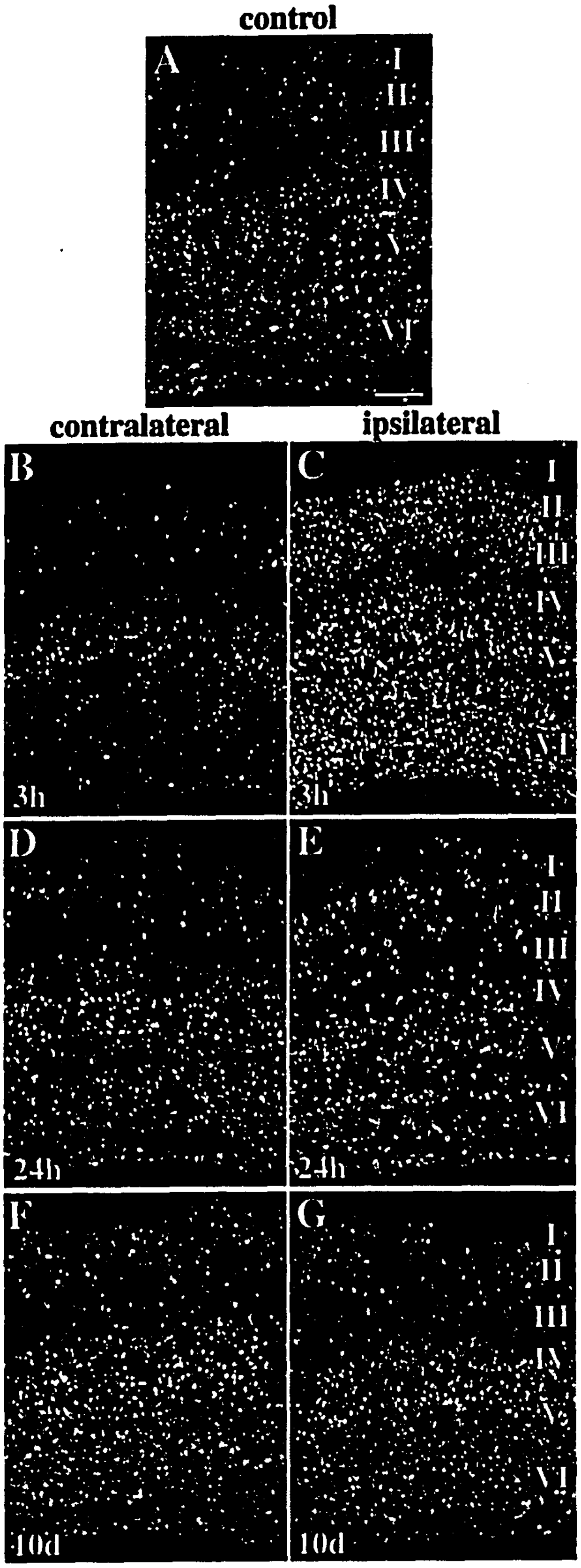
control
A
I
II
III
IV
V
VI
contralateral
ipsilateral
B
3h
C
I
II
III
IV
V
VI
3h
D
24h
E
I
II
III
IV
V
VI
24h
F
10d
G
I
II
III
IV
V
VI
10d

Figure 46: Dark field emulsion autoradiograms showing, at higher magnification, the repression and subsequent localized induction of VGF mRNA in the rostrodorsal region of the striatum following unilateral cortical lesion. (*A*) control, and (*B*) 1, (*C*) 3, (*D*) 6, (*E*) 12, and (*F*) 24 hours, (*G*) 3 days, (*H*) and 10 days after lesion. Scale bar, 400 µm.

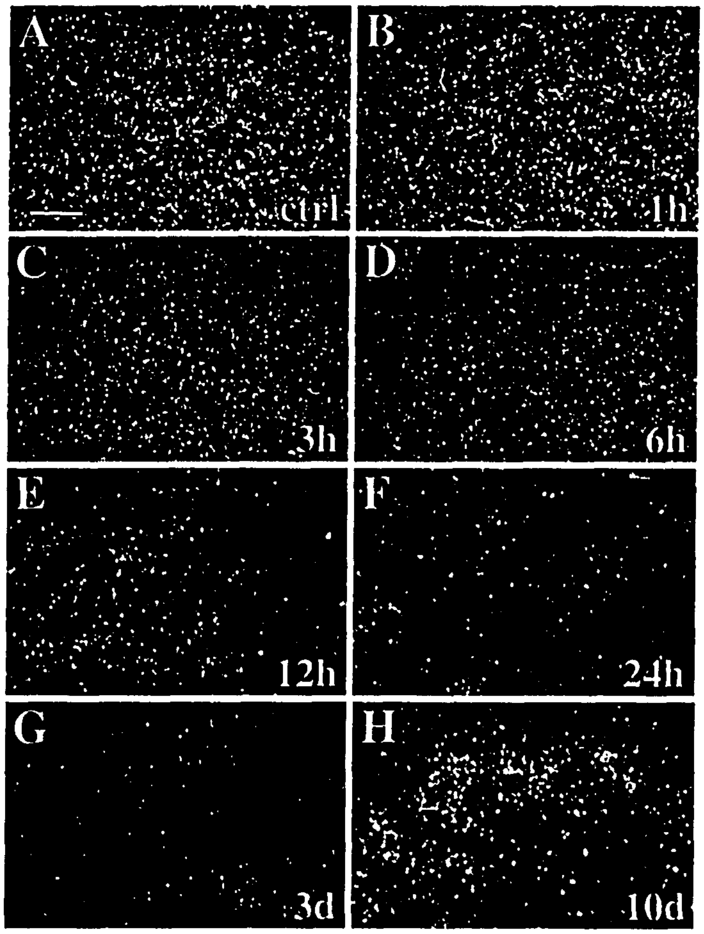
A
ctrl
B
1h
C
3h
D
6h
E
12h
F
24h
G
3d
H
10d

Figure 47: Quantitative analysis of changes in VGF mRNA expression in the neocortex and dorsolateral striatum contralateral and ipsilateral to and at various timepoints following a unilateral cortical lesion. In the ipsilateral striatum at 10 days postlesion, separate evaluation of the localized region of VGF mRNA induction and the surrounding striatum was done, and the results are expressed as two separate bars labeled *region of sprouting* and *bulk of striatum* respectively. Values significantly different from those in control animals are marked with *asterisks* (*, $p<0.05$; **, $p<0.01$; ***, $p<0.001$; ANOVA). Results are given as means ± SEM.

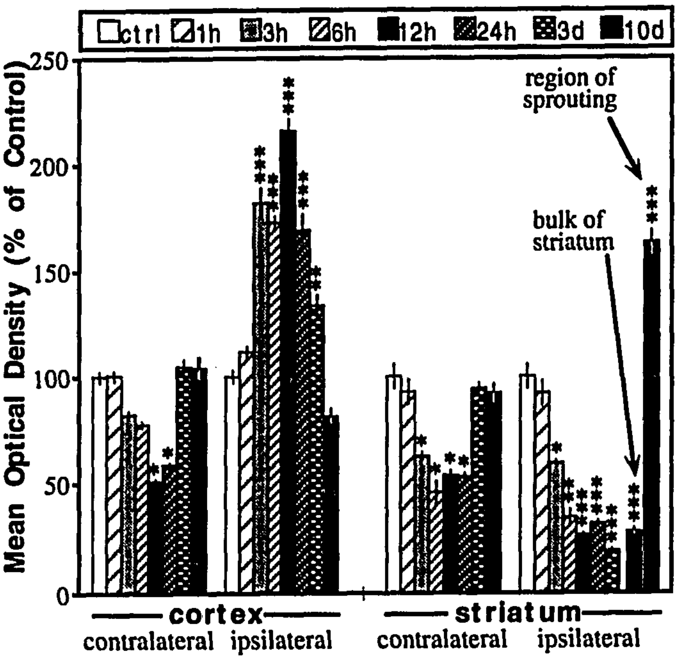
ctrl
1h
3h
6h
12h
24h
3d
10d
Mean Optical Density (% of Control)
250
200
150
100
50
0
region of sprouting
bulk of striatum
cortex
contralateral
ipsilateral
striatum
contralateral
ipsilateral

Discussion

This study briefly demonstrates widespread distribution of VGF mRNA in the developing and adult rat nervous systems. VGF mRNA expression was shown in CNS and PNS by E13.5, three days earlier than previously reported (Lombardo *et al.* 1995), and was more extensive at all ages than described before, perhaps due to methodological or strain differences between the studies. The apparently more restricted distribution of VGF polypeptide in adult brain (van den Pol *et al.* 1994) in comparison to widespread VGF mRNA expression may result from low VGF protein levels, but given recent findings describing the cleavage of VGF into secreted peptides (Liu *et al.* 1994; Possenti *et al.* 1994; Trani *et al.* 1995), it is more likely that posttranslational processing may have limited the observable immunoreactivity. In agreement with earlier studies, however, my data indicate that in the CNS, VGF is only synthesized by neurons (van den Pol *et al.* 1989; Ferri *et al.* 1992).

Further, this study provides the first direct comparison of the VGF mRNA distribution with those of the neurotrophin receptors, TrkA, TrkB, and TrkC. Although many reports describe *trk* expression in developing and adult animals (reviewed in Barbacid 1994), and limited VGF *in situ* data demonstrating expression during development or in extrahypothalamic regions of adult brain exist (Snyder *et al.* 1992; Lombardo *et al.* 1995), comparison has been difficult because of differences in developmental ages examined. My findings demonstrate significant overlap in the expression patterns of these genes, but no absolute correlation of VGF and any single *trk* message. The *trk*A and *trk*C mRNA distributions are more restricted than that of VGF, implying that although NGF and/or NT-3 may participate in VGF induction *in vivo*, neither can account for the entire range of VGF expression. In a related comparison, van den

Pol *et al.* (1994) demonstrated lack of overlap between immunostaining for VGF and the p75 neurotrophin receptor in the septum, and suggested that their data imply NGF is unlikely to be responsible for VGF expression in the brain. However, since TrkA alone can transduce a signal in response to NGF (Ibanez *et al.* 1992; Ip *et al.* 1993), and *trk*A mRNA is found in areas expressing VGF, NGF may regulate VGF in these small populations of neurons. Conversely, *trk*B expression is more extensive than that of VGF. However, several TrkB isoforms exist: exclusively neuronal catalytic tyrosine kinase form(s), and truncated variants expressed predominantly in glia, but also in ependyma, choroid, and some neurons (Frisen *et al.* 1993; Altar *et al.* 1994). Using a catalytic kinase-specific probe, I found a close correlation between the distributions of the exclusively neuronal VGF and *trk*B kinase mRNAs. Furthermore, recent work has shown that in addition to being NGF-inducible, VGF is highly inducible by BDNF and NT-3 (endogenous ligands of TrkB and TrkC respectively) in primary CNS neuronal cultures (Bonni *et al.* 1995). Given these data, and localization of catalytic TrkB-encoding mRNA in all regions expressing VGF, and *trk*C mRNA in many of them, it is likely that BDNF, neurotrophin-4/5 (NT-4/5, which also binds TrkB), and/or NT-3 are the predominant neurotrophic factors responsible for regulating VGF expression in brain. My data do not preclude the possibility that VGF may be subject to regulation by all four neurotrophins, NGF, BDNF, NT-3, and NT-4/5, and may be a vital element mediating their actions.

Depolarization of PC12 cells also rapidly induces VGF transcription (Salton *et al.* 1991; Baybis and Salton 1992), and stimulates secretion of VGF protein (Possenti *et al.* 1989). Having observed abundant VGF mRNA in the brain during peak periods of synaptogenesis (Salton *et al.* 1991), which in many systems is regulated by neural activity, I began my examination of VGF regulation *in vivo* in the visual system, where this phenomenon is best documented. During early postnatal life, geniculate terminals representing each eye segregate into alternating regions within visual cortex by an activity-dependent competitive mechanism. Inhibition of input from one eye during the critical period disrupts formation of these ocular dominance columns (reviewed in Goodman and Shatz 1993). Furthermore, this system is highly sensitive to modulation by neurotrophins: cortical NGF infusion prevents monocular deprivation-induced pathology (Domenici *et al.* 1991; Maffei *et al.* 1992), and excess BDNF or NT-4/5 can perturb normal ocular dominance column development (Cabelli *et al.* 1995). Results of my study using TTX to block retinal activity indicate that VGF expression in dLGN is dependent upon afferent electrical activity during the critical period, extending a study which appeared while this paper was being prepared (Lombardo *et al.* 1995) by demonstrating that the effect occurs very rapidly: decreased VGF mRNA is evident by 6 hours following TTX injection. In contrast to their findings, my data show that VGF levels, while beginning to recover, are still depressed 48 hours postinjection, perhaps due to differences in dosage or mode of TTX administration between the studies. Lombardo *et al.* proposed that following activity-dependent secretion from synaptic terminals VGF may act as an anterograde factor in the developing visual system. Taking together the results of these monocular deprivation experiments, the expression of both VGF and TrkB in the dLGN during the critical period (Ringstedt *et al.* 1993), and induction of VGF by BDNF *in vitro* (Bonni *et al.* 1995), I further suggest these secreted VGF peptides may mediate the combinatorial response of neurons in the developing visual system to neurotrophins and activity.

My finding that kainate-induced seizures produce rapid and transient up-regulation of VGF message in hippocampus and cortex, provides further evidence of the powerful influence neuronal electrical activity has on the expression of this gene. Indeed, seizure activity has been shown to rapidly induce the immediate-early gene products NGFI-A and NGFI-C in hippocampus and cortex (Crosby *et al.* 1992; Dragunow *et al.* 1992; Gass *et al.* 1993; Mack *et al.* 1995), transcription factors either or both of which amplify VGF induction in PC12 cells (D'Arcangelo *et al.* 1996). Kainate-induced seizures also rapidly up-regulate mRNAs encoding NGF, BDNF, and both catalytic and truncated forms of TrkB in hippocampus and cortex (Zafra *et al.* 1990; Gall *et al.* 1991; Dugich-Djordjevic *et al.* 1992, 1995; Merlio *et al.* 1993). In turn, neurotrophin stimulation of Trk receptors produces prolonged phosphorylation and thus activation of the cAMP/Ca^{+2} response element-binding protein CREB, required for VGF induction by neurotrophins (Hawley *et al.* 1992; Bonni *et al.* 1995; D'Arcangelo *et al.* 1996). These early changes in gene expression probably result from the global increase in electrical activity which is characteristic of seizures. Kainate-induced seizures also rapidly produce long-lasting changes in the hippocampus, including neuronal degeneration in CA1 and CA3, and sprouting of mossy fibers (Tauck and Nadler 1985), which are accompanied by a prolonged increase in neurotrophin activity and increased expression of glial non-catalytic TrkB (Dugich-Djordjevic *et al.* 1992, 1995; Lowenstein *et al.* 1993).

Although we have not yet examined regulation of VGF during the later period of synaptic reorganization days to weeks after cessation of seizure activity, I did examine the longer-term effects of striatal deafferentation by unilateral cortical lesion on VGF expression. Massive VGF induction in the entire ipsilateral cortex, particularly the superficial layers, lasting from 3 to at least 24 hours post-lesion was the earliest change observed. Induction may have resulted from acute hyperactivity of this remaining cortex, and/or the response of axotomized corticocortical neurons to direct injury. This was followed by a substantial decrease of VGF labeling throughout the dorsolateral striatum, which is deafferented by this lesion, beginning within hours and lasting at least 10 days. Similar ipsilateral cortical up-regulation and striatal down-regulation in this paradigm have been reported for the δ-9-tetrahydrocannabinol receptor gene (Mailleux and Vanderhaeghen 1994), and changes in glutamate receptor subunits in the striatum have also been described (Wüllner *et al.* 1994). A more modest decrease throughout the entire contralateral hemisphere, perhaps resulting from spreading depression, also began within hours, recovering by 10 days. Lastly, I observed intense induction of VGF in part of the dorsolateral striatum at 10 days, coinciding with reactive astrocytosis and sprouting of homotopic contralateral corticostriatal afferents to synapse with deafferented medium spiny neurons (Cheng *et al.* 1988, 1995b). Interestingly, the mRNA encoding the neuronal growth-associated protein SCG-10 is also up-regulated in association with this sprouting response, but in the sprouting contralateral cortical neurons rather than in the denervated striatum (Cheng *et al.* 1995a). Since VGF polypeptide is not synthesized by astrocytes, and reactive astrocytes at sites of direct lesion do not express VGF mRNA (Snyder *et al.* 1996) my results provide the first evidence that VGF is regulated by and/or may play a role in axonal sprouting and synaptic reorganization. Whether this VGF induction involves the participation of neurotrophins is still unknown but seems likely.

Chapter 6: Conclusions

As discussed in Chapter 1, until very recently the vast majority of investigations studying the expression and/or regulation of VGF had either been done in PC12 cells or had focused predominantly on VGF in the hypothalamus. The little work which involved other regions of the nervous system was done by northern or RNase protection analysis, and thus while it clearly showed that VGF mRNA is expressed in the brain, spinal cord, and peripheral ganglia, but not most non-neuronal tissues, and that it is regulated during development, no detail was provided regarding the regional or cellular distribution of VGF.

The data presented in Chapters 3 and 4 of this dissertation provide the first comprehensive detailed analysis of the anatomical localization of VGF mRNA in the adult rat central nervous system and throughout the developing animal. In the adult, I showed that VGF mRNA is expressed in at least a subset of neurons in nearly every region of the brain and spinal cord. VGF mRNA expression was not found in astrocytes, oligodendrocytes, choroid plexus, ependymal cells, or capillaries. These data confirm and extend earlier studies detailing the distribution of VGF mRNA and immunoreactivity in the hypothalamus (van den Pol *et al.* 1989; Mahata *et al.* 1993a,b,c). Furthermore, my results are supported by a more recent study by van den Pol *et al.* (1994) describing the distribution of VGF expression in the adult brain, in that the neuronal populations they found to contain VGF immunoreactivity were a clear subset of those in which I demonstrated VGF mRNA hybridization. As discussed in detail in Chapter 3, the difference between the two reported distributions is most likely due to the inability of the antisera used by van den Pol *et al.* to detect carboxy-terminal derived VGF peptides, the major secreted forms, and therefore probably the major functional forms, of VGF in the brain

(Trani *et al.* 1995). Others have very recently shown some data demonstrating VGF mRNA and protein in the adult brain, particularly the cortex, thalamus, and hippocampus which though more limited in scope, correspond quite well to the data I have shown here (Lombardo *et al.* 1995).

I have also shown the first evidence that VGF mRNA is expressed by the retinal ganglion cells and neurons of the inner nuclear layer of the adult retina where bipolar, horizontal, and amacrine cells reside. Taken together these data imply that VGF plays a role in the normal function of the entire visual system, from retina to cortex and colliculus.

Additionally, as discussed in detail in Chapter 3, I have demonstrated that VGF message is expressed in the adult adrenal medulla, agreeing with the work of Laslop *et al.* (1994) who reported detecting VGF mRNA in the chromaffin and ganglion cells of the adrenal medulla, both derived from the neural crest. They also found that VGF levels in the medulla could be further induced by stimulation of the medulla with reserpine. In light of recent studies showing that the VGF polypeptide is not processed into small peptides in the adrenal as it is in neurons (Trani *et al.* 1995), it is likely that the functions subserved by VGF in the adrenal are quite different from those in the nervous system.

In a series of experiments reported in Chapter 4, I investigated the development of VGF mRNA expression from the time of neural tube closure through the first 10 days of postnatal life. This is the most detailed description of VGF localization in the developing animal available to date. In light of the neural specificity, developmental regulation, and NGF inducibility of VGF, as well as early work by Possenti *et al.* demonstrating that the VGF protein is secreted by both the constitutive and regulated pathways, it was tantalizing to speculate that VGF might play a role in nervous system development, particularly with regard to neuronal differentiation. Yet at the outset of this project, the only histological localization of VGF in the developing animal had been a brief description of VGF immunoreactivity in the thalamus, suprachiasmatic nucleus, and hippocampus of a P4 rat brain (van den Pol *et al.* 1989). In the intervening time, the only other report of VGF expression in development failed to demonstrate VGF mRNA before E16 in the rat (Lombardo *et al.* 1995), whereas I was able to show that VGF message is expressed in developing cranial, dorsal root, and sympathetic ganglia as early as E11.5. Again, the locations of VGF hybridization reported in their study constitute a subset of those I have described herein, partially because their investigation focused on thalamocortical development and was not intended to be comprehensive. My results and those of Lombardo *et al.* agree substantially in that both studies showed a gradual increase in the number of VGF mRNA expressing structures in the brain across development, with the overall intensity of expression peaking in the first 2 weeks of life and decreasing somewhat by adulthood. My data further show that this expansion occurred in a roughly caudal-to-rostral and ventral-to-dorsal direction, corresponding to the very general pattern of maturation in the CNS. Importantly, the onset of VGF mRNA expression in a given region seems to correlate with the onset of neuronal differentiation, implying that VGF may play a role in neurotrophin-mediated differentiation and support of developing neurons. Obviously, a critical event in the maturation of a neuron is the development and maintenance of synaptic connections with other neurons, a process also strongly influenced by the neurotrophins. Given the secretory nature of VGF and the timing and distribution of its expression, it is likely that VGF may play a role in synaptogenesis in the developing nervous system. This assertion is supported by interesting new data presented by Lombardo *et al.* (1995) which shows VGF immunoreactivity in the somata of thalamic sensory relay nuclei and immunoreactive fibers at the cortical subplate, then invading the cortical plate, which coincide exactly with the known timing and location of the development of thalamocortical afferent connections.

I also presented data in Chapter 5 which demonstrate that significant overlap between the expression pattern of VGF mRNA and those of the Trk neurotrophin receptors exists, and further, that there is a particularly close, though not perfect, correlation between the distributions of the mRNAs encoding VGF and the catalytic kinase form of TrkB. These data imply that the mechanisms exist to allow neurotrophin regulation of VGF *in vivo* and further, that BDNF and/or NT-4/5 are likely to be responsible for a large portion of any such regulation.

I further demonstrated in Chapter 5 that VGF mRNA can be regulated by neuronal electrical activity *in vivo* by showing rapid down-regulation of VGF mRNA levels in the neurons of the dLGN following intraocular TTX injection during the visual critical period. This work is supported by the results of similar experiments conducted by Lombardo *et al.* (1995) which showed a decrease of VGF mRNA in the dLGN 24 hours following TTX injection. My data showed that this effect can be appreciated as soon as 6 hours post-injection. Additionally, Lombardo *et al.* found that eyelid suture and dark-rearing did not produce the same effect, implying that basal spontaneous electrical activity is sufficient to maintain VGF expression. Lombardo *et al.* proposed that following activity-dependent secretion from synaptic terminals VGF may act as an anterograde factor in the developing visual system. Taking together the results of these monocular deprivation experiments, the expression of both VGF and TrkB in the dLGN during the critical period, the ability of BDNF to induce VGF, and a number of studies showing neurotrophins to be critical in the development of geniculocortical connections, I further suggest that secreted VGF-derived peptides may mediate the combinatorial response of neurons in the developing visual system to neurotrophins and activity. I would further extend this thought and hypothesize that this dependence upon the coordination of neurotrophin support and neuronal activity probably underlies the normal development of many regions of the nervous system, certainly other sensory systems, and perhaps other systems as well.

Additional data I have presented here (also in Chapter 5), support this notion, showing for the first time that kainate-induced seizures produce rapid and transient up-regulation of VGF message in hippocampus and cortex. This provides further evidence of the powerful influence neuronal electrical activity has on VGF expression, in a system known to affect and be affected by neurotrophin activity, and to result in long-term changes in synaptic circuitry and efficacy.

Lastly, I have also reported in Chapter 5 the rapid, dramatic and multiple effects unilateral cortical lesion has on VGF mRNA expression in the brain. Massive ipsilateral cortical VGF mRNA induction, a more subtle contralateral cortical repression, and a substantial decrease of VGF labeling in the deafferented striatum, occur within hours, the repression lasting at least 10 days. Interestingly, I also observed intense induction of VGF 10 days post-lesion, in a region of the deafferented striatum where reactive astrocytosis and sprouting are known to be occurring. This is the first report studying VGF expression in response to brain injury.

In addition to their role in the differentiation and survival of neurons, and recovery from injury, neurotrophins may also participate in the normal functioning of adult brain. All three experimental paradigms described above, in which VGF expression is rapidly regulated, involve gross perturbations of normal physiologic neuronal activity, are known to result in changes in neurotrophin and Trk receptor expression, and lead to synaptic reorganization. Recent studies have shown not only that physiologic neuronal activity can regulate Trks and neurotrophins (Castrén *et al.* 1992; Kesslak *et al.* 1995; Neeper *et al.* 1995), but also that neurotrophins, acting through their Trk receptors, can regulate synaptic activity (Frostig *et al.* 1995; Kang and Schuman 1995; Levine *et al.* 1995; Patterson *et al.* 1995). The rapidity with which VGF mRNA can be induced or repressed by variation in neuronal electrical activity in the paradigms used herein strongly suggests that VGF or the peptides derived from it may play a critical role in the synaptogenesis and synaptic reorganization which often result from changing afferent input both during development and in the adult, in both physiological and pathological conditions. I postulate that throughout the brain, the regulation of VGF, and secretion of peptides derived from it, most likely occurs as a result of the combinatorial and interdependent effects of neurotrophin action and modulation by neuronal electrical activity, the association of which appears to be a fundamental element in brain function. Furthermore, it is possible that secreted VGF (or any of its constituent peptides) may be a necessary effector in the pathway leading from neurotrophin action and neuronal activity to the genesis, strengthening, or reorganization of synapses. The events occurring downstream of VGF release remain to be elucidated.

References

Abe H., Amano O., Yamakuni T., Takahashi Y., and Kondo H. (1990) Localization of spot 35-calbindin (rat cerebellar calbindin) in the anterior pituitary of the rat: developmental and sexual differences. *Arch. Histol. Cytol.* **53**: 585-591.

Aloe L. and Levi-Montalcini R. (1979) Nerve growth factor-induced transformation of immature chromaffin cells *in vivo* into sympathetic neurons: Effects of antiserum to nerve growth factor. *Proc. Natl. Acad. Sci. U.S.A.* **76**: 1246-1250.

Altar C. A., Siuciak J. A., Wright P., Ip N. Y., Lindsay R. M., and Wiegand S. J. (1994) In situ hybridization of trkB and trkC receptor mRNA in rat forebrain and association with high-affinity binding of [^{125}I]BDNF, [^{125}I]NT-4/5 and [^{125}I]NT-3. *Eur. J. Neurosci.* **6**: 1389-1405.

Altman J. (1972a) Postnatal development of the cerebellar cortex in the rat. I. The external germinal layer and the transitional molecular layer. *J. Comp. Neurol.* **145**: 353-398.

Altman J. (1972b) Postnatal development of the cerebellar cortex in the rat. II. Phases in the maturation of Purkinje cells and of the molecular layer. *J. Comp. Neurol.* **145**: 399-464.

Altman J. (1972c) Postnatal development of the cerebellar cortex in the rat. III. Maturation of the components of the granular layer. *J. Comp. Neurol.* **145**: 465-513.

Altman J. and Bayer S. A. (1990a) Migration and distribution of two populations of dentate granule cell precursors during the perinatal and postnatal periods. *J. Comp. Neurol.* **301**: 365-381.

Altman J. and Bayer S. A. (1990b) Prolonged sojourn of developing pyramidal cells in the intermediate zone of the hippocampus and their settling in the stratum pyramidale. *J. Comp. Neurol.* **301**: 343-364.

Altman J. and Bayer S. A. (1995) *Atlas of Prenatal Rat Brain Development*. Boca Raton, FL: CRC Press.

Altman J. and Das G. D. (1965) Autoradiographic and histological evidence of postnatal hippocampal neurogenesis in rats. *J. Comp. Neurol.* **124**: 319-336.

Arenas E. and Persson H. (1994) Neurotrophin-3 prevents the death of adult central noradrenergic neurons in vivo. *Nature* **367**: 368-371.

Barbacid M. (1994) The Trk family of neurotrophin receptors. *J. Neurobiol.* **25**: 1386-1403.

Bartel D. P., Sheng M., Lau M. F., and Greenberg M. E. (1989) *Genes Dev.* **3**: 304-313.

Basi G. S., Jacobson R. D., Virag I., Schilling J., and Skene J. H. P. (1987) Primary structure and transcriptional regulation of GAP-43, a protein associated with nerve growth. *Cell* **49**: 785-791.

Baybis M. and Salton S. R. J. (1992) Nerve growth factor rapidly regulates VGF gene transcription through cycloheximide sensitive and insensitive pathways. *FEBS Lett.* **308**: 202-206.

Bayer S. A. (1980a) Development of the hippocampal region in the rat. I. Neurogenesis examined with ^{3}H-thymidine autoradiography. *J. Comp. Neurol.* **190**: 87-114.

Bayer S. A. (1980b) Development of the hippocampal region in the rat. II. Morphogenesis during embryonic and early postnatal life. *J. Comp. Neurol.* **190**: 115-134.

Bayer S. A. and Altman J. (1974) Hippocampal development in the rat: Cytogenesis and morphogenesis examined with autoradiography and low-level X-irradiation. *J. Comp. Neurol.* **158**: 55-80.

Berkemeier L. R., Winslow J. W., Kaplan D. R., Nikolics K., Goeddel D. V., and Rosenthal A. (1991) Neurotrophin-5: a novel neurotrophic factor that activates *trk* and *trkB*. *Neuron* **7**: 857-866.

Bonni A., Ginty D. D., Dudek H., and Greenberg M. E. (1995) Serine 133-phosphorylated CREB induces transcription via a cooperative mechanism that may confer specificity to neurotrophin signals. *Mol. Cell. Neurosci.* **6**: 168-183.

Borson S., Schatteman G., Claude P., and Bothwell M. (1994) Neurotrophins in the developing and adult primate adenohypophysis: a new pituitary hormone system? *Neuroendocrinology* **59**: 466-76.

Brugg B., Michel p. P., Agid Y., and Ruberg M. (1996) Ceramide induces apoptosis in cultured mesencephalic neurons. *J. Neurochem.* **66**: 733-739.

Cabelli R. J., Hohn A., and Shatz C. J. (1995) Inhibition of ocular dominance column formation by infusion of NT-4/5 or BDNF. *Science* **267**: 1662-1666.

Castrén E., Zafra F., Thoenen H., and Lindholm D. (1992) Light regulates expression of brain-derived neurotrophic factor mRNA in visual cortex. *Proc. Natl. Acad. Sci. U.S.A.* **89**: 9444-9448.

Chandler C. E., Parsons L. M., Hosang M., and Shooter E. M. (1984) A monoclonal antibody modulates the interaction of nerve growth factor with PC12 cells. *J. Biol. Chem.* **259**: 6882-6889.

Chao M. V. (1994) The p75 neurotrophin receptor. *J. Neurobiol.* **25**: 1373-1385.

Chao M. V. and Hempstead B. L. (1995) p75 and Trk: a two-receptor system. *Trends Neurosci.* **18**: 321-326.

Cheng H.-W., Anavi Y., Coshgarian H., McNeill T. H., and Rafols J. A. (1988) Loss and recovery of striatal dendritic spines following lesions in the cerebral cortex of adult and aged mice. *Soc. Neurosci. Abstr.* **14**: 1292.

Cheng H.-W., Mori N., and McNeill T. H. (1995a) Differential regulation of growth associated protein mRNAs in the contralateral cortex after a striatal deafferentation lesion in adult rats. *J. Neurosci.* (submitted).

Cheng H.-W., Rafols J. A., Gashgarian H. G., and McNeill T. H. (1995b) Synapse replacement in the striatum of adult mice following a unilateral cortex lesion: An ultrastructural study. *Exp. Neurol.* (submitted).

Chong J. A., Tapia-Ramirez J., Kim S., Toledo-Aral J. J., Zheng Y., Boutros M. C., Altshuller Y. M., Frohman M. A., Kraner S. D., and Mandel G. (1995) REST: a mammalian silencer protein that restricts sodium channel gene expression to neurons. *Cell* **80**: 949-957.

Chun L. L. Y. and Patterson P. H. (1977a) Role of nerve growth factor in the development of rat sympathetic neurons *in vitro*. I. Survival, growth and differentiation of catecholamine production. *J. Cell Biol.* **75**: 694-704.

Chun L. L. Y. and Patterson P. H. (1977b) Role of nerve growth factor in the development of rat sympathetic neurons *in vitro*. II. Developmental studies. *J. Cell Biol.* **75**: 705-711.

Chun L. L. Y. and Patterson P. H. (1977c) Role of nerve growth factor in the development of rat sympathetic neurons *in vitro*. III. Effect on acetylcholine production. *J. Cell Biol.* **75**: 712-718.

Conover J. C., Erickson J. T., Katz D. M., Bianchi L. M., Poueymirou W. T., McClain J., Pan L., Helgren M., Ip N. Y., Boland P., *et al.* (1995) Neuronal deficits, not involving motor neurons, in mice lacking BDNF and/or NT4. *Nature* **375**: 235-238.

Crespo D., Stanfield B. B., and Cowan W. M. (1986) Evidence that late-generated granule cells do not simply replace earlier formed neurons in the rat dentate gyrus. *Exp. Brain Res.* **62**: 541-548.

Crosby S. D., Veile R. A., Donis-Keller H., Baraban J. M., Simburger K. S., and Milbrandt J. (1992) Neural-specific gene expression, genomic structure and chromosomal localization of the gene encoding the zinc-finger transcription factor NGFI-A. *Proc. Natl. Acad. Sci. U.S.A.* **89**: 4739-4743.

Crowley C., Spencer S. D., Nishimure M. C., Chen K. S., Pitts-Meek S., Armanini M. P., Ling L. H., McMahon S. B., Shelton D. L., Levinson A. D., and Phillips H. S. (1994) Mice lacking nerve growth factor display perinatal loss of sensory and sympathetic neurons yet develop basal forebrain cholinergic neurons. *Cell* **76**: 1001-1011.

Curtis R., Adryan K. M., Stark J. L., Park J. S., Compton D. L., Weskamp G., Huber L. J., Chao M. V., Jaenisch R., Lee K.-F., Lindsay R. M., and DiStefano P. S. (1995) Differential role of the low affinity neurotrophin receptor (p75) in retrograde axonal transport of the neurotrophins. *Neuron* **14**: 1201-1211.

D'Arcangelo G., Habas R., Wang S., Halegoua S., and Salton S. R. J. (1996) Activation of co-dependent transcription factors is required for transcriptional induction of the *vgf* gene by NGF and Ras. *Mol. Cell. Biol.* (in revisions).

Davies A. M., Thoenen H., and Barde Y.-A. (1986) The response of chick sensory neurons to brain-derived neurotrophic factor. *J. Neurosci.* **6**: 1897-1904.

de Olmos J., Hardy H., and Heimer L. (1978) The afferent connections of the main and the accessory olfactory bulb formations in the rat: An experimental HRP study. *J. Comp. Neurol.* **181**: 213-224.

Domenici L., Berardi N., Carmignoto G., Vantini G., and Maffei L. (1991) Nerve growth factor prevents the amblyopic effects of monocular deprivation. *Proc. Natl. Acad. Sci. U.S.A.* **88**: 8811-8815.

Doupe A. J., Landis S. C., and Patterson P. H. (1985) Environmental influences in the development of neural crest derivatives: glucocorticoids, growth factors, and chromaffin cell plasticity. *J. Neurosci.* **5**: 2119-2142.

Dragunow M., Yamada N., Bilkey D. K., and Lawlor P. (1992) Induction of immediate-early gene proteins in dentate granule cells and somatostatin interneurons after hippocampal seizures. *Mol. Brain Res.* **13**: 119-126.

Drubin D. G., Feinstein S. C., Shooter E. M., and Kirschner M. W. (1985) Nerve growth factor-induced neurite outgrowth in PC12 cells involves the coordinate induction of microtubule assembly and assembly-promoting factors. *J. Cell Biol.* ?: ?

Dubrowsky R. T., Jenkins G. M., and Hannun Y. A. (1995) Neurotrophins induce sphingomyelin hydrolysis. Modulation by co-expression of p75NTR with Trk receptors. *J. Biol. Chem.* **270**: 22135-22142.

Dubrowsky R. T., Werner M. H., Castelino A. M., and Chao M. V. (1994) Activation of the sphingomyelin cycle through the low-affinity neurotrophin receptor. *Science* **265**: 1596-1599.

Dugich-Djordjevic M. M., Ohsawa F., Okazaki T., Mori N., Day J. R., Beck K. D., and Hefti F. (1995) Differential regulation of catalytic and non-catalytic trkB messenger RNAs in the rat hippocampus following systemic administration of kainate. *Neuroscience* **66**: 861-877.

Dugich-Djordjevic M. M., Tocco G., Lapchak P. A., Pasinetti G. M., Najm I., Baudry M., and Hefti F. (1992) Regionally specific and rapid increases in brain-derived neurotrophic factor messenger RNA in the adult rat brain following seizures induced by systemic administration of kainic acid. *Neuroscience* **47**: 303-315.

Ernfors P., Lee K., and Jaenisch R. (1994a) Mice lacking brain-derived neurotrophic factor develop with sensory deficits. *Nature* **368**: 147-150.

Ernfors P., Lee K. F., Kucera J., and Jaenisch R. (1994b) Lack of neurotrophin-3 leads to deficiencies in the peripheral nervous system and oss of limb proprioceptive afferents. *Cell* **77**: 503-512.

Feinstein S. C., Dana S. L., McConlogue L., Shooter E. M., and Coffino P. (1985) Nerve growth factor rapidly induces ornithine decarboxylase mRNA in PC12 rat pheochromocytoma cells. *Proc. Natl. Acad. Sci. U.S.A.* **82**: 5761-5765.

Ferri G.-L. (1995) Differential processing of the neuro-endocrine protein "VGF" in mammalian hypophysis. *Soc. Neurosci. Abstr.* **21**(3): 1628.

Ferri G.-L., Levi A., and Possenti R. (1992) A novel neuroendocrine gene product: selective VGF8a gene expression and immuno-localisation of the VGF protein in endocrine and neuronal populations. *Mol. Brain Res.* **13**: 139-143.

Frisen J., Verge V. M., Fried K., Risling M., Persson H., Trotter J., Hokfelt T., and Lindholm D. (1993) Characterization of glial trkB receptors: differential response to injury in the central and peripheral nervous systems. *Proc. Natl. Acad. Sci. U.S.A.* **90**: 4971-4975.

Frostig R. D., Prakash N., and Cohen-Cory S. (1995) BDNF rapidly modifies activity-dependent responses to tactile stimulation in the adult rat somatosensory cortex. *Soc. Neurosci. Abstr.* **21**(1): 114.

Funakoshi H., Belluardo N., Arenas E., Yamamoto Y., Casabona A., Persson H., and Ibanez C. F. (1995) Muscle-derived neurotrophin-4 as an activity-dependent trophic signal for adult motor neurons. *Science* **268**: 1495-1499.

Gall C. and Lauterborn J. (1992) The dentate gyrus: a model system for studies of neurotrophin regulation. *Epilepsy Res. Suppl.* **7**: 171-185.

Gall C., Murray K., and Isackson P. J. (1991) Kainic acid-induced seizures stimulate increased expression of nerve growth factor mRNA in rat hippocampus. *Mol. Brain Res.* **9**: 113-123.

Gao W. Q., Zheng J. L., and Karihaloo M. (1995) Neurotrophin 4/5 (NT-4/5) and brain-derived neurotrophic factor (BDNF) act at later stages of cerebellar granule cell development. *J. Neurosci.* **15**: 2656-2667.

Gass P., Herdegen T., Bravo R., and Kiessling M. (1993) Spatiotemporal induction of immediate early genes in the rat brain after limbic seizures: effects of NMDA receptor antagonist MK-801. *Eur. J. Neurosci.* **5**: 933-943.

Goodman C. S. and Shatz C. J. (1993) Developmental mechanisms that generate precise patterns of neuronal connectivity. *Cell* **72**: 77-98.

Gorin P. D. and Johnson E. M. (1979) Experimental autoimmune model of nerve growth factor deprivation: Effects on developing peripheral sympathetic and sensory neurons. *Proc. Natl. Acad. Sci. U.S.A.* **76**: 5382-5386.

Gotz R., Koster R., Winkler C., Raulf F., Lottspeich F., Schartl M., and Thoenen H. (1994) Neurotrophin-6 is a new member of the nerve growth factor family. *Nature* **372**: 266-269.

Greenberg M. E., Greene L. A., and Ziff E. B. (1985) Nerve growth factor and epidermal growth factor induce rapid transient changes in proto-oncogene transcription in PC12 cells. *J. Biol. Chem.* **260**: 14101-14110.

Greene L. A. (1977a) Quantitative in vitro studies on the nerve growth factor (NGF) requirement of neurons. I. Sympathetic neurons. *Dev Biol* **58**: 96-105.

Greene L. A. (1977b) Quantitative in vitro studies on the nerve growth factor (NGF) requirement of neurons. II. Sensory neurons. *Dev Biol* **58**: 106-13.

Greene L. A. and Tischler A. S. (1976) Establishment of a noradrenergic clonal line of rat adrenal pheochromocytoma cells which respond to nerve growth factor. *Proc. Natl. Acad. Sci. U.S.A.* **73**: 2424-2428.

Halegoua S., Armstrong R. C., and Kremer N. E. (1990) Dissecting the mode of action of a neuronal growth factor. *Curr. Top. Microbiol. Immunol.* **165**: 119-170.

Hallböök F., Ibáñez C. F., and Persson H. (1991) Evolutionary studies of the nerve growth factor reveal a novel member abundantly expressed in the *Xenopus* ovary. *Neuron* **6**: 845-858.

Hawley R. J., Scheibe R. J., and Wagner J. A. (1992) NGF induces the expression of the VGF gene through a cAMP response element. *J. Neurosci.* **12**: 2573-2581.

Hebel R. and Stromberg M. W. (1986) *Anatomy and Embryology of the Laboratory Rat*. Wörthsee, Germany: Biomed Verlag.

Heumann R. (1994) Neurotrophin signalling. *Curr. Opin. Neurobiol.* **4**: 668-679.

Hohn A., Leibrock J., Bailey K., and Barde Y.-A. (1990) Identification and characterization of a novel member of the nerve growth factor/brain-derived neurotrophic factor family. *Nature* **344**: 339-341.

Hyman C., Hofer M., Barde Y.-A., Juhasz M., Yancopoulos G. D., Squinto S. P., and Lindsay R. M. (1991) BDNF is a neurotrophic factor for the dopaminergic neurons of the substantia nigra. *Nature* **350**: 230-232.

Hynes M. A., Poulsen K., Armanini M., Berkemeier L., Phillips H., and Rosenthal A. (1994) Neurotrophin-4/5 is a survival factor for embryonic midbrain dopaminergic neurons in enriched cultures. *J. Neurosci. Res.* **37**: 144-154.

Ibanez C. F., Ebendal T., Barbany G., Murrary-Rust J., Blundell T. L., and Persson H. (1992) Disruption of the low affinity receptor-binding site in NGF allows neuronal survival and differentiation by binding to the trk gene product. *Cell* **69**: 329-341.

Ip N. Y., Stitt T. N., Tapley P., Klein R., Glass D. J., Fandl J., Greene L. A., Barbacid M., and Yancopoulos G. D. (1993) Similarities and differences in the way neurotrophins interact with the Trks in neuronal and non-neuronal cells. *Neuron* **10**: 137-149.

Jacobson M. (1991) *Developmental Neurobiology.* New York, NY: Plenum Press.

Japon M. A., Rubinstein M., and Low M. J. (1994) In situ hybridization analysis of anterior pituitary hormone gene expression during fetal mouse development. *J. Histochem. Cytochem.* **42**: 1117-1125.

Jelsma T. N. and Aguayo A. J. (1994) Trophic factors. *Curr. Opin. Neurobiol.* **4**: 717-725.

Johnson E. M., Gorin P. D., Brandeis L. D., and Pearson J. (1980) Dorsal root ganglion neurons are destroyed by exposure *in utero* to maternal antibody to nerve growth factor. *Science* **210**: 916-918.

Johnson J. E., Barde Y.-A., Schwab M., and Thoenen H. (1986) Brain-derived neurotrophic factor supports the survival of cultured rat retinal ganglion cells. *J. Neurosci.* **6**: 3031-3038.

Johnston M. V., Rutkowski L. J., Wainer B. H., Long J. B., and Mobley W. C. (1987) NGF effects on developing forebrain cholinergic neurons are regionally specific. *Neurochem. Res.* **12**: 985-994.

Jones K. R., Farinas I., Backus C., and Reichardt L. F. (1994) Targeted disruption of the BDNF gene perturbs brain and sensory neuron development but not motor neuron development. *Cell* **76**: 989-999.

Kanemasa K., Okamura H., Kodama T., and Ibata Y. (1995) Induction of VGF mRNA in neurons of the rat nucleus tractus solitarius and the dorsal motor nucleus of the vagus in duodenal ulceration by cysteamine. *Mol. Brain Res.* **32**: 55-62.

Kang H. and Schuman E. M. (1995) Long-lasting neurotrophin-induced enhancement of synaptic transmission in the adult hippocampus. *Science* **267**: 1658-1662.

Kaplan D. R., Hempstead B. L., Martin-Zanca D., Chao M. V., and Parada L. F. (1991a) The *trk* proto-oncogene product: a signal transducing receptor for nerve growth factor. *Science* **252**: 554-558.

Kaplan D. R., Martin-Zanca D., and Parada L. F. (1991b) Tyrosine phosphorylation and tyrosine kinase activity of the *trk* proto-oncogene product induced by NGF. *Nature* **354**: 411-414.

Kaufman M. H. (1992) *The Atlas of Mouse Development.* San Diego, CA: Academic Press.

Kesslak J. P., Gómez-Pinilla F., So V., Choi J., and Cotman C. W. (1995) Increased expression of NGF and BDNF mRNA associated with learning. *Soc. Neurosci. Abstr.* **21**(1): 36.

Kim H. G., Wang T., Olafsson P., and Lu B. (1994) Neurotrophin 3 potentiates neuronal activity and inhibits gamma-aminobutyratergic synaptic transmission in cortical neurons. *Proc. Natl. Acad. Sci. U.S.A.* **91**: 12341-12345.

Klein R. (1994) Role of neurotrophins in mouse neuronal development. *FASEB J.* **8**: 738-744.

Klein R., Jing S., Nanduri V., O'Rourke E., and Barbacid M. (1991a) The trk proto-oncogene encodes a receptor for nerve growth factor. *Cell* **65**: 189-197.

Klein R., Lamballe F., Bryant S., and Barbacid M. (1992) The trkB tyrosine protein kinase is a receptor for neurotrophin-4. *Neuron* **8**: 947-956.

Klein R., Nanduri V., Jing S., Lamballe F., Tapley P., Bryant S., Cordon-Cardo C., Jones K. R., Reichardt L. F., and Barbacid M. (1991b) The trkB tyrosine protein kinase is a receptor for brain-derived neurotrophic factor and neurotrophin-3. *Cell* **66**: 395-403.

Klein R., Silos-Santiago I., Smeyne R. J., Lira S. A., Brambilla R., Bryant S., Zhang L., Snider W. D., and Barbacid M. (1994) Disruption of the neurotrophin-3 receptor gene *trkC* eliminates Ia muscle afferents and results in abnormal movements. *Nature* **368**: 249-251.

Klein R., Smeyne R. J., Wurst W., Long L. K., Auerbach B. A., Joyner A. L., and Barbacid M. (1993) Targeted disruption of the *trkB* neurotrophin receptor gene results in nervous system lesions and neonatal death. *Cell* **75**: 113-122.

Knüsel B., Burton L. E., Longo F. M., Mobley W. C., Koliatsos V. E., Price D. L., and Hefti F. (1990) Trophic actions of recombinant human nerve growth factor on cultured rat embryonic CNS cells. *Exp. Neurol.* **110**: 274-283.

Knüsel B., Winslow J. W., Rosenthal A., Burton L. E., Seid D. P., Kikolics K., and Hefti F. (1991) Promotion of central cholinergic and dopaminergic neuron differentiation by brain-derived neurotrophic factor but not neurotrophin-3. *Proc. Natl. Acad. Sci. U.S.A.* **88**: 961-965.

Koliatsos V. E., Applegate M. D., Knüsel B., Junard E. O., Burton L. E., Mobley W. C., Hefti F., and Price D. L. (1991) Recombinant human nerve growth factor prevents retrograde degeneration of axotomized basal foregrain cholinergic neurons in the rat. *Exp. Neurol.* **112**: 161-173.

Koliatsos V. E., Cayouette M. H., Berkemeier L. R., Clatterbuck R. E., Price D. L., and Rosenthal A. (1994) Neurotrophin 4/5 is a trophic factor for mammalian facial motor neurons. *Proc. Natl. Acad. Sci. U.S.A.* **91**: 3304-3308.

Koliatsos V. E., Nauta H. J., Clatterbuck R. E., Holtzman D. M., Mobley W. C., and Price D. L. (1990) Mouse nerve growth factor prevents degeneration of axotomized basal foregrain cholinergic neurons in the monkey. *J. Neurosci.* **10**: 3801-3818.

Lainé J. and Axelrad H. (1994) The candelabrum cell: a new interneuron in the cerebellar cortex. *J. Comp. Neurol.* **339**: 159-173.

Lamballe F., Klein R., and Barbacid M. (1991) *trk*C, a new member of the *trk* family of tyrosine protein kinases, is a receptor for neurotrophin-3. *Cell* **66**: 967-979.

Landis D. M. D. and Patterson P. H. (1981) Neural crest cell lineages. *Trends Neurosci.* **4**: 172-175.

Laslop A., Mahata S. K., Wolkersdorfer M., Mahata M., Srivastava M., Seidah N. G., Fischer-Colbrie R., and Winkler H. (1994) Large dense-core vesicles in rat adrenal after reserpine: levels of mRNAs of soluble and membrane-bound constituents in chromaffin and ganglion cells indicate a biosynthesis of vesicles with higher secretory quanta. *J. Neurochem.* **62**: 2448-2456.

LeDouarin N. M. (1980) The ontogeny of the neural crest in avian embryo chimeras. *Nature* **286**: 663-669.

Lee K. F., Bachman K., Landis S. C., and Jaenisch R. (1994a) Dependence on p75 for innervation of some sympathetic targets. *Science* **263**: 1447-1449.

Lee K. F., Davies A. M., and Jaenisch R. (1994b) p75-deficient embryonic dorsal root sensory and neonatal sympathetic neurons display a decreased sensitivity to NGF. *Development* **120**: 1027-1033.

Lee K. F., Li E., Huber L. J., Landis S. C., Sharpe A. H., Chao M. V., and Jaenisch R. (1992) Targeted mutation of the gene encoding the low affinity NGF receptor p75 leads to deficits in the peripheral nervous system. *Cell* **69**: 737-749.

Leonard D. G., Gorham J. D., Cole P., Greene L. A., and Ziff E. B. (1988) A nerve growth factor-regulated messenger RNA encodes a new intermediate filament protein. *J. Cell Biol.* **106**: 181-193.

Leonard D. G., Ziff E. B., and Greene L. A. (1987) Identification and characterization of mRNAs regulated by nerve growth factor in PC12 cells. *Mol. Cell. Biol.* **7**: 3156-3167.

Levi A., Canu N., Trani E., Benedetti M., and Possenti R. (1991) VGF: a tissue specific protein and a marker of NGF-induced neuronal differentiation. In Bagnoli P. and Hodos W. (eds): *The Changing Visual System.* New York: Plenum Press, pp. 319-332.

Levi A., Eldridge J. D., and Paterson B. M. (1985) Molecular cloning of a gene sequence regulated by nerve growth factor. *Science* **229**: 393-395.

Levi-Montalcini R. and Angeletti P. U. (1963) Essential role of the nerve growth factor in the survival and maintenance of dissociated sensory and sympathetic embryonic nerve cells *in vitro*. *Dev. Biol.* **7**: 653-659.

Levi-Montalcini R. and Angeletti P. U. (1966) Immunosympathectomy. *Pharmacol. Rev.* **18**: 619-628.

Levi-Montalcini R. and Booker B. (1960) Destruction of the sympathetic ganglia in mammals by an antiserum to a nerve-growth protein. *Proc. Natl. Acad. Sci. U.S.A.* **46**: 384-391.

Levi-Montalcini R. and Hamburger V. (1951) Selective growth-stimulation effects of mouse sarcoma on the sensory and sympathetic nervous system of the chick embryo. *J. Exp. Zool.* **116**: 321-362.

Levi-Montalcini R., Meyer H., and Hamburger V. (1954) *In vitro* experiments on the effects of mouse sarcomas 180 and 37 on the spinal and sympathetic ganglia of the chick embryo. *Cancer Res.* **14**: 49-57.

Levine E. S., Dreyfus C. F., Black I. B., and Plummer M. R. (1995) Brain-derived neurotrophic factor rapidly enhances synaptic transmission in hippocampal neurons via post-synaptic tyrosine kinase receptors. *Proc. Natl. Acad. Sci. U.S.A.* **92**: 8074-8077.

Lindenbaum M. H., Carbonetto S., Grosveld F., Flavell D., and Mushynski W. E. (1988) Transcriptional and post-transcriptional effects of nerve growth factor on expression of the three neurofilament subunits in PC12 cells. *J. Biol. Chem.* **263**: 5662-5667.

Lindsay R. M., Barde Y.-A., Davies A. M., and Rohrer H. (1985) Differences and similarities in the neurotrophic growth factor requirements of sensory neurons derived from neural crest and neural placode. *J. Cell. Sci. Suppl.* **3**: 115-129.

Lindvall O., Kokaia Z., Bengzon J., Elmér E., and Kokaia M. (1994) Neurotrophins and brain insults. *Trends Neurosci.* **17**: 490-496.

Liu J.-W., Andrews P. C., Mershon J. L., Yan C., Allen D. L., and Ben-Jonathan N. (1994) Peptide V: a VGF-derived neuropeptide purified from bovine posterior pituitary. *Endocrinology* **135**: 2742-2748.

Liu X., Ernfors P., Wu H., and Jaenisch R. (1995) Sensory but not motor neuron deficits in mice lacking NT4 and BDNF. *Nature* **375**: 238-241.

Loeb D. M., Maragos J., Martin-Zanca D., Chao M. V., Parada L. F., and Greene L. A. (1991) The *trk* proto-oncogene rescues NGF responsiveness in mutant NGF-nonresponsive PC12 cell lines. *Cell* **66**: 961-966.

Lombardo A., Rabacchi S. A., Cremisi F., Pizzorusso T., Cenni M. C., Possenti R., Barsacchi G., and Maffei L. (1995) A developmentally regulated nerve growth factor-inducible gene, VGF, is expressed in geniculocortical afferents during synaptogenesis. *Neuroscience* **65**: 997-1008.

Longo F., Holtzman D., Grimes M., and Mobley W. (1993) Nerve growth factor: actions in the peripheral and central nervous systems. In Loughlin S. and Fallon J. (eds): *Neurotrophic Factors.* San Diego, CA: Academic Press, pp. 209-256.

Lowenstein D. H., Seren M. S., and Longo F. M. (1993) Prolonged increases in neurotrophic activity associated with kainate-induced hippocampal synaptic reorganization. *Neuroscience* **56**: 597-604.

Mack K. J., Yi S. D., Chang S., Millan N., and Mack P. (1995) NGFI-C expression is affected by physiological stimulation and seizures in the somatosensory cortex. *Mol. Brain Res.* **29**: 140-146.

Maffei L., Berardi N., Domenici L., Parisi V., and Pizzorusso T. (1992) Nerve growth factor (NGF) prevents the shift in ocular dominance distribution of visual cortical neurons in monocularly deprived rats. *J. Neurosci.* **12**: 4651-4662.

Mahata M., Hortnagl H., Mahata S. K., Fischer-Colbrie R., and Winkler H. (1993a) Messenger RNA levels of chromogranin B, secretogranin II, and VGF in rat brain after AF64A-induced septohippocampal cholinergic lesions. *J. Neurochem.* **61**: 1648-1656.

Mahata S. K., Mahata M., Fischer-Colbrie R., and Winkler H. (1993b) In situ hybridization: mRNA levels of secretogranin II, VGF and peptidylglycine alpha-amidating monooxygenase in brain of salt-loaded rats. *Histochemistry* **99**: 287-293.

Mahata S. K., Mahata M., Hortnag H., Fischer-Colbrie R., Steiner H. J., Dietze O., and Winkler H. (1993c) Concomitant changes of messenger ribonucleic acid levels of secretogranin II, VGF, vasopressin and oxytocin in the paraventricular nucleus of rats after adrenalectomy and during lactation. *J. Neuroendo.* **5**: 323-330.

Mailleux P. and Vanderhaeghen J.-J. (1994) Glutamatergic regulation of cannabinoid receptor gene expression in the caudate-putamen. *Eur. J. Pharm.* **266**: 193-196.

Maisonpierre P. C., Belluscio L., Squinto S., Ip N. Y., Furth M. E., Lindsay R. M., and Yancopoulos G. D. (1990) Neurotrophin-3: A neurotrophic factor related to NGF and BDNF. *Science* **247**: 1446-1451.

Marshall C. J. (1995) Specificity of receptor tyrosine kinase signaling: Transient versus sustained extracellular signal-regulated kinase activation. *Cell* **80**: 179-185.

Merlio J.-P., Ernfors P., Kokaia Z., Middlemas D. S., Bengzon J., Kokaia M., Smith M.-L., Siesjö B. K., Hunter T., Lindvall O., and Persson H. (1993) Increased production of the TrkB protein tyrosine kinase receptor after brain insults. *Neuron* **10**: 151-164.

Middlemas D. S., Lindberg R. A., and Hunter T. (1991) trkB, a neural receptor protein-tyrosine kinase: evidence for a full-length and two truncated receptors. *Mol. Cell. Biol.* **11**: 143-153.

Milbrandt J. (1987) A nerve growth factor-induced gene encodes a possible transcriptional regulatory factor. *Science* **238**: 797-799.

Mugnaini E. and Floris A. (1994) The unipolar brush cell: a neglected neuron of the mammalian cerebellar cortex. *J. Comp. Neurol.* **339**: 174-180.

Neeper S. A., Gómez-Pinilla F., Choi J., and Cotman C. W. (1995) Physical activity up-regulates BDNF and NGF mRNA in the rat brain. *Soc. Neurosci. Abstr.* **21**(1): 296.

Nemeskéri A., Sétáló G., and Halász B. (1988) Ontogenesis of the three parts of the fetal rat adenohypophysis: a detailed immunocytochemical analysis. . *Neuroendocrinology* **48**: 534-543.

Okamura N., Miyatake Y., Takao T., Tamaru T., Nagai K., Okada M., and Nakagawa H. (1994) *Neurosci. Lett.*

Patterson S. L., Abel T., Ernfors P., Jaenisch R., and Kandel E. R. (1995) Deficits in short-term plasticity and LTP in hippocampal slices from BDNF knockout mice. *Soc. Neurosci. Abstr.* **21**(1): 35.

Paxinos G. (1995) *The Rat Nervous System.* San Diego, CA: Academic Press.

Paxinos G., Törk I., Tecott L. H., and Valentino K. L. (1991) *Atlas of the Developing Rat Brain.* San Diego, CA: Academic Press.

Paxinos G. and Watson C. (1986) *The Rat Brain in Stereotaxic Coordinates.* San Diego: Academic Press.

Possenti R., Di Rocco G., Nasi S., and Levi A. (1992) Regulatory elements in the promoter region of vgf, a nerve growth factor-inducible gene. *Proc. Natl. Acad. Sci. U.S.A.* **89**: 3815-3819.

Possenti R., Eldridge J. D., Paterson B. M., Grasso A., and Levi A. (1989) A protein induced by NGF in PC12 cells is stored in secretory vesicles and released through the regulated pathway. *EMBO J.* **8**: 2217-2223.

Possenti R., Rinaldi A. M., Canu N., Levi A., Ferri G.-L., and Trani E. (1994) Neuronal specific processing of VGF protein leads to the production and regulated secretion of peptides derived from its carboxi-terminal. *Soc. Neurosci. Abstr.* **20**

Qiu M.-S. and Green S. H. (1992) PC12 cell neuronal differentiation is associated with prolonged $p21^{ras}$ activity and consequent prolonged ERK activity. *Neuron* **9**: 705-717.

Rabizadeh S., Oh J., Zhong L., Yang J., Bitler C. M., Butcher L., and Bredesen D. E. (1993) Induction of apoptosis by the low-affinity NGF receptor. *Science* **261**: 345-348.

Ringstedt T., Lagercrantz H., and Persson H. (1993) Expression of members of the *trk* family in the developing postnatal rat brain. *Dev. Brain Res.* **72**: 119-131.

Rydel R. E. and Greene L. A. (1987) Acidic and basic fibroblast growth factors promote stable neurite outgrowth and neuronal differentiation in cultures of PC12 cells. *J. Neurosci.* **7**: 3639-3653.

Salton S. R. J. (1991) Nucleotide sequence and regulatory studies of VGF, a nervous system-specific mRNA that is rapidly and relatively selectively induced by nerve growth factor. *J. Neurochem.* **57**: 991-996.

Salton S. R. J., Fischberg D. J., and Dong K.-W. (1991) Structure of the gene encoding VGF, a nervous system-specific mRNA that is rapidly and selectively induced by nerve growth factor in PC12 cells. *Mol. Cell. Biol.* **11**: 2335-2349.

Salton S. R. J., Richter L. C., Greene L. A., and Shelanski M. L. (1983a) Nerve growth factor-inducible large external (NILE) glycoprotein: studies of a central and peripheral neuronal marker. *J. Neurosci.* **3**: 441-454.

Salton S. R. J., Shelanski M. L., and Greene L. A. (1983b) Biochemical properties of the nerve growth factor-inducible large external (NILE) glycoprotein. *J. Neurosci.* **3**: 2420-2430.

Sambrook J., Fritsch E. F., and Maniatis T. (1989) *Molecular Cloning: A Laboratory Manual*. Cold Spring Harbor, NY: Cold Spring Harbor Laboratory Press.

Saria A., Troger J., Kirchmair R., Fischer-Colbrie R., Hogue-Angeletti R., and Winkler H. (1993) Secretoneurin releases dopamine from rat striatal slices: biological effect of a peptide derived from secretogranin II (chromogranin C). *Neuroscience* **54**: 1-4.

Satoh T., Nakamura S., Taga T., Matsuda T., Hirano T., Kishimoto T., and Kaziro Y. (1988) Induction of neuronal differentiation in PC12 cells by B-cell stimulatory factor 2/interleukin-6. *Mol. Cell. Biol.* **8**: 3546-3549.

Schambra U. B., Lauder J. M., and Silver J. (1992) *Atlas of the Prenatal Mouse Brain*. San Diego, CA: Academic Press.

Schlessinger A. R., Cowan W. M., and Gottlieb E. I. (1975) An autoradiographic study of the time of origin and the pattern of granule cell migration in the dentate gyrus of the rat. *J. Comp. Neurol.* **159**: 149-176.

Schlessinger A. R., Cowan W. M., and Swanson L. W. (1978) The time of origin of neurons in Ammon's horn and associated retrohippocampal fields. *Anat. Embryol.* **154**: 153-173.

Schlessinger J. and Ullrich A. (1992) Growth factor signaling by receptor tyrosine kinases. *Neuron* **9**: 383-391.

Sherwood N. M. and Timiras P. S. (1970) *A Stereotaxic Atlas of the Developing Rat Brain*. Berkeley, CA: University of California Press.

Smith M. A., Makino S., Altemus M., Michelson D., Hong S. K., Kvetnansky R., and Post R. M. (1995) Stress and anti-depressants differentially regulate neurotrophin 3 mRNA expression in the locus coeruleus. *Proc. Natl. Acad. Sci. U.S.A.* **92**: 8788-8792.

Snyder S. E., Li J., Schauwecker P. E., McNeill T. H., and Salton S. R. J. (1996) Comparison of RPTPζ/β, phosphacan, and trkB mRNA expression in the developing and adult rat nervous system, and induction of RPTPζ/β and phosphacan mRNA following brain injury. *Mol. Brain Res.* (in press).

Snyder S. E., Streck R. D., Pintar J. E., and Salton S. R. J. (1992) Distribution of VGF mRNA in the postnatal rat brain. *Soc. Neurosci. Abstr.* **18**: 1291.

Sohrabji F., Miranda R. C., and Toran-Allerand C. D. (1995) Identification of a putative estrogen response element in the gene encoding brain-derived neurotrophic factor. *Proc. Natl. Acad. Sci. U.S.A.* **92**: 11110-11114.

Soppet D., Escandon E., Maragos J., Middlemas D. S., Reid S. W., Blair J., Burton L. E., Stanton B. R., Kaplan D. R., Hunter T., *et al.* (1991) The neurotrophic factors brain-derived neurotrophic factor and neurotrophin-3 are ligands for the *trkB* tyrosine kinase receptor. *Cell* **65**: 895-903.

Squinto S. P., Stitt T. N., Aldrich T. H., Davis S., Bianco S. M., Radziejewski C., Glass D. J., Masiakowski P., Furth M. S., Valenzuela D. M., *et al.* (1991) *trkB* encodes a functional receptor for brain-derived neurotrophic factor and neurotrophin-3 but not nerve growth factor. *Cell* **65**: 885-893.

Stoeckel M. E., Hindelang C., Klein M.-J., Poissonnier M., and Félix J.-M. (1993) Early expression of the glycoprotein hormone alpha-subunit in the pars tuberalis of the rat pituitary gland during ontogenesis. *Neuroendocrinology* **58**: 616-624.

Stoeckel M. E., Porte A., Hindelang-Gertner C., and Dellmann H.-D. (1973) A light and electron microscopic study of the pre- and postnatal development and secretory differentiation of the pars tuberalis of the rat hypophysis. *Z. Zellforsch* **142**: 347-365.

Swanson L. W. (1992) *Brain Maps: Structure of the Rat Brain*. New York: Elsevier.

Tauck D. L. and Nadler J. V. (1985) Evidence of functional mossy fiber sprouting in hippocampal formation of kainic acid-treated rats. *J. Neurosci.* **5**: 1016-1022.

Tessarollo L., Vogel K. S., Palko M. E., Reid S. W., and Parada L. F. (1994) Targeted mutation in the neurotrophin-3 gene results in loss of muscle sensory neurons. *Proc. Natl. Acad. Sci. U.S.A.* **91**: 11844-11848.

Togari A., Dickens G., Kuzuya H., and Guroff G. (1985) The effect of fibroblast growth factor on PC12 cells. *J. Neurosci.* **5**:

Trani E., Ciotti T., Rinaldi A. M., Canu N., Ferri G. L., Levi A., and Possenti R. (1995) Tissue-specific processing of the neuroendocrine protein VGF. *J. Neurochem.* **65**: 2441-2449.

Tuszynski M. H., U H. S., Amaral D. G., and Gage F. H. (1990) Nerve growth factor in the primate brain reduces lesion-induced cholinergic neuronal degeneration. *J. Neurosci.* **10**: 3604-3614.

van den Pol A. N., Bina K., Decavel C., and Ghosh P. (1994) VGF Expression in the Brain. *J. Comp. Neurol.* **347**: 455-469.

van den Pol A. N., Decavel C., Levi A., and Paterson B. (1989) Hypothalamic expression of a novel gene product, VGF: immunocytochemical analysis. *J. Neurosci.* **9**: 4122-4137.

Ventimiglia R., Mather P. E., Jones B. E., and Lindsay R. M. (1995) The neurotrophins BDNF, NT-3, and NT-4/5 promote survival and morphological and biochemical differentiation of striatal neurons in vitro. *Eur. J. Neurosci.* **7**: 213-222.

Winkler H. and Fischer-Colbrie R. (1992) The chromogranins A and B: the first 25 years and future perspectives. *Neuroscience* **49**: 497-528.

Wolf D. E., McKinnon C. A., Daou M. C., Stephens R. M., Kaplan D. R., and Ross A. H. (1995) Interaction with TrkA immobilizes gp75 in the high affinity nerve growth factor receptor complex. *J. Biol. Chem.* **270**: 2133-2138.

Wu B.-Y., Fodor E. J. B., Edwards R. H., and Rutter W. J. (1989) Nerve growth factor induces the proto-oncogene c-jun in PC12 cells. *J. Biol. Chem.* **264**: 9000-9003.

Wüllner U., Standaert D. G., Testa C. M., Landwehrmeyer G. B., Catania M. V., Penney J. B., Jr and Young A. B. (1994) Glutamate receptor expression in rat striatum: effect of deafferentation. *Brain Res.* **647**: 209-219.

Yan Q., Elliott J. L., Matheson C., Sun J., Zhang L., Mu X., Rex K. L., and Snider W. D. (1993) Influences of neurotrophins on mammalian motoneurons *in vivo*. *J. Neurobiol.* **24**: 1555-1577.

Zafra F., Hengerer B., Leibrock J., and Thoenen H. (1990) Activity dependent regulation of BDNF and NGF mRNAs in the rat hippocampus is mediated by non-NMDA glutamate receptors. *EMBO J.* **9**: 3545-3550.

Zheng J. L., Stewart R. R., and Gao W. Q. (1995) Neurotrophin 4/5 enhances survival of cultured spiral ganglion neurons and protects them from cisplatin neurotoxicity. *J. Neurosci.* **15**: 5079-5087.

Zheng M. and Pintar J. E. (1995) Analysis of ontogeny of processing enzyme gene expression and regulation. *Methods Neurosci.* **23**: 45-64.